ON NEW AND IMPROVED SEMI-NUMERICAL TECHNIQUES FOR SOLVING NONLINEAR FLUID FLOW PROBLEMS

A THESIS SUBMITTED IN FULFILLMENT OF THE ACADEMIC REQUIREMENTS FOR THE DEGREE OF DOCTOR OF PHILOSOPHY IN THE FACULTY OF SCIENCE AND AGRICULTURE

By

Zodwa Gcinaphi Makukula

School of Mathematical Sciences

University of KwaZulu Natal, Pietermaritzburg

February 2012

Dedication

To my two God sent Angels, Busizizwe and Lesihle Malaza.

Acknowledgment

This study was funded by the German Academic Exchange Service (Deutscher Akademischer Austauchdienst, DAAD) under grant A/08/13658.

First and foremost, I would like to thank God Almighty for the gift of life and for His wonderful guidance in the past three decades of my life.

To my supervisors Prof. Precious Sibanda and Prof. Sandile Motsa, I am grateful for your support and guidance throughout this project. Thank you so much for shaping my future with evidently open and keen hearts.

Special thanks to my loving family, my parents, my brothers and sister in-law for their emotional support. I would not have managed to carry on with my studies without their encouragements and for being there for my children.

To my colleagues, Pedro, Faiz, Medard, Makhala, Olina, Hloniphile, Ayoub, Thekiso, Mahesha and Ahmed, thank you for making me feel at home away from home. I wish you all the best in your future endeavours.

The writing of the thesis has been made easier with the help of Shaun Moodley and the school's Administrative Assistant Faith Nzimande. Thank you so much guys for being there for me whenever I encountered difficulties with my computer. Your input is greatly treasured.

Declaration

I hereby declare that this thesis is my original work and effort. It was carried out under the supervision of Prof. P. Sibanda and Prof. S. S. Motsa in the School of Mathematical Sciences, University of KwaZulu-Natal, Pietermaritzburg. It has not been submitted to any University or institution for any qualification. Contributions of others or any other sources of information have been clearly acknowledged throughout this work.

February, 2012.

Student: _____ _____

Zodwa Gcinaphi Makukula Date

Supervisor: _____ _____

Prof. P. Sibanda Date

Abstract

Most real world phenomena is modeled by ordinary and/or partial differential equations. Most of these equations are highly nonlinear and exact solutions are not always possible. Exact solutions always give a good account of the physical nature of the phenomena modeled. However, existing analytical methods can only handle a limited range of these equations. Semi-numerical and numerical methods give approximate solutions where exact solutions are impossible to find. However, some common numerical methods give low accuracy and may lack stability. In general, the character and qualitative behaviour of the solutions may not always be fully revealed by numerical approximations, hence the need for improved semi-numerical methods that are accurate, computational efficient and robust.

In this study we introduce innovative techniques for finding solutions of highly nonlinear coupled boundary value problems. These techniques aim to combine the strengths of both analytical and numerical methods to produce efficient hybrid algorithms. In this work, the homotopy analysis method is blended with spectral methods to improve its accuracy. Spectral methods are well known for their high levels of accuracy. The new spectral homotopy analysis method is further improved by using a more accurate initial approximation to accelerate convergence. Furthermore, a quasi-linearisation technique is introduced in which spectral methods are used to solve the linearised equations. The new techniques were used to solve

mathematical models in fluid dynamics.

The thesis comprises of an introductory Chapter that gives an overview of common numerical methods currently in use. In Chapter 2 we give an overview of the methods used in this work. The methods are used in Chapter 3 to solve the nonlinear equation governing two-dimensional squeezing flow of a viscous fluid between two approaching parallel plates and the steady laminar flow of a third grade fluid with heat transfer through a flat channel. In Chapter 4 the methods were used to find solutions of the laminar heat transfer problem in a rotating disk, the steady flow of a Reiner-Rivlin fluid with Joule heating and viscous dissipation and the classical von Kármán equations for boundary layer flow induced by a rotating disk. In Chapter 5 solutions of steady two-dimensional flow of a viscous incompressible fluid in a rectangular domain bounded by two permeable surfaces and the MHD viscous flow problem due to a shrinking sheet with a chemical reaction, were solved using the new methods.

Contents

Preface

The work in this thesis has been published or accepted for publication as follows;

Chapter 3;

(i) Z. G. Makukula, S. S. Motsa and P. Siband (2010). On a new solution for the visco-elastic squeezing flow between two parallel plates. *Journal of Advanced Research in Applied Mathematics* 2(4):31–38.

(ii) S. S. Motsa, Z. G. Makukula and P. Sibanda (2012). A spectral-homotopy analysis method for heat transfer flow of a third grade fluid between parallel plates. *International Journal of Numerical Methods for Heat & Fluid Flow* 22(1):4-23 (Impact factor; 1.058).

(iii) Z. G. Makukula, P. Sibanda and S. S. Motsa (2010). On new solutions for heat transfer in a visco-elastic fluid between parallel plates. *International Journal of Mathematical Models and Methods in Applied Sciences* 4(4):221–230.

Chapter 4;

(i) Z. G. Makukula, P. Sibanda and S. S. Motsa (2010). A note on the solution of the von Kármán equations using series and Chebyshev spectral methods. *Boundary Value Problems* Volume 2010, Article ID 471793, 17 pages doi:10.1155/2010/471793 (Impact

factor; 1.047).

(ii) Z. G. Makukula, P. Sibanda and S. S. Motsa (2010). On a quasilinearisation method for the von Kármán flow problem with heat transfer. Accepted for publication in *Latin American Applied Research*, http://www.laar.uns.edu.ar (Impact factor; 0.16).

(iii) S. S. Motsa, Z. G. Makukula and P. Sibanda (2010). On a linearisation method for Reiner-Rivlin swirling flow. Accepted for publication in the *Journal of Computational and Applied Mathematics*, http://www.journals.elsevier.com/journal-of-computational-and-applied-mathematics/ (Impact factor; 1.029).

Chapter 5;

(i) Z. G. Makukula, S. S. Motsa and P. Sibanda (2010). A novel numerical technique for two-dimensional laminar flow between two moving porous walls. *Mathematical Problems in Engineering* Volume 2010, Article ID 528956, 15 pages doi:10.1155/2010/528956 (Impact factor; 0.689).

(ii) Z. G. Makukula, P. Sibanda, S. S. Motsa and S. Shateyi (2011). On new numerical techniques for the MHD flow past a shrinking sheet with heat and mass transfer in the presence of a chemical reaction. *Journal of Mathematical Problems in Engineering*, Volume 2011, Article ID 489217, 19 pages doi:10.1155/2011/489217 (Impact factor; 0.689).

1

Introduction

Most real world phenomena is modeled using partial and/or ordinary differential equations. Solutions of differential equations are important in predicting the future states of the phenomena under study (Hale and Moore, 2008). Such physical phenomena include the motion of planets, nonlinear optics, oceanography, meteorology, projectiles, fluid dynamics and population dynamics to mention just a few (Hale and Moore, 2008). Most of these equations are highly nonlinear and exact solutions are not always possible. For those cases where exact solutions are not possible, numerical methods often provide approximate solutions (Nayfeh, 1973). Both numerical and analytical methods have their advantages and drawbacks. This study sought to introduce new and improved semi-numerical techniques for solving nonlinear equations. These techniques aim to combine the strengths of both numerical and analytical methods.

1.1. Numerical methods for fluid flow problems

The process of modeling physical phenomena results in equations that may have variable coefficients and nonlinear boundary conditions (Nayfeh, 1973). This makes it difficult or

even impossible to find exact analytical solutions. Modelers often resort to various forms of approximations such as using perturbation or numerical methods or a combination of both. Since the invention of high speed digital computers in the late twentieth century, the study of different phenomena in science and engineering has been made easier and more efficient by the application of numerical simulation techniques (Toro, 1999). The basis of any numerical technique is the discretization of the time and space variables in the governing equations (Geiser, 2005). The discretization process approximates the differential equation by a system of algebraic equations (Steinhauser, 2008). Hence approximate solutions are obtained at distinct positions in space and time (Ferzinger and Perić, 2002). Numerical methods may be used to solve problems defined in complex geometries and are thus applicable to a wider range of problems compared to analytical methods (Fletcher, 1988; Tu et al., 2008). However, this advantage often comes at the expense of accuracy (Kikani, 1989). The discretization process differs from one numerical approach to the other. Each numerical scheme will be particular in the way it approximates derivatives and the way it represents the solution (Moczo et al., 2004). Brief descriptions of a few common numerical methods is given in the sections that follow.

1.1.1 Discretization approaches

There are many different types of discretization schemes currently in use by researchers in applied mathematics, engineering and other fields of science. In this section we discuss some of the common approaches. These include finite differences, finite element, finite volume and boundary element methods.

The finite difference method (FDM) is believed to have been first used in 1768 by Euler.

At that time it was used to find numerical solutions of differential equations using pen and paper (Tu et al., 2008). In the late 1950s a new version was proposed and applied to partial differential equations (Ampadu, 2007). The FDM belongs to the so-called grid-point methods where a computational domain is covered by a space-time grid (Moczo et al., 2004). Taylor series expansions are then used to compute finite-difference approximations to the partial derivatives of the governing equations at each nodal point of the grid (Tandjiria, 1999). There are three different kinds of FDMs, namely the explicit FDM, the implicit FDM and the Crank-Nicolson FDM (Geiser, 2005). The FDM has been applied to, *inter alia*, geothermal engineering problems (Kikani, 1989; Tandjiria, 1999), financial mathematics (Duffy, 2004; Ekström et al., 2009), HIV transmission dynamics (Ampadu, 2007), seismology and earthquake ground motion modeling (Moczo et al., 2004; Rinehart, 2011) and fluid dynamics (Ferzinger and Perić, 2002; Tu et al., 2008). The finite difference schemes have been improved extensively in the works of Patidar and his co-works to to be applicable to singularly perturbed two-point boundary value problems (Kadalbajoo and Patidar, 2001, 2002, 2006; Lubuma and Patidar, 2006; Bashier and Patidar, 2011). The FDM has great flexibility in handling problems that are defined in complex geometries (Kikani, 1989). For example, the FDM has been applied to automobile transmission development where the domain changes (Ampadu, 2007). Tandjiria (1999) noted that finite difference schemes are relatively easy to implement and are computationally efficient. However they also suffer from inherent discretization errors which may lead to poor accuracy (Ferzinger and Perić, 2002).

Unlike the FDM, in the finite element method (FEM) the computational domain is viewed as a collection of simple geometric shapes called finite elements (Reddy and Gartling, 1994). The FEM is a generalization of the classical variational and weighted residual methods. For two- and three-dimensional domains, these elements are usually triangles or quadrilaterals

and tetrahedra or hexahedra respectively (Ferzinger and Perić, 2002). On each local element a piecewise polynomial approximating function to the governing equation is generated by any of the variational and weighted residual methods. These polynomials are zero on all other elements except on the element where they are defined (Kikani, 1989). This leads to a sparse matrix which makes the computational work easy (Thomée, 1984).

The history of the FEM dates back to the beginning of the twentieth century. In the early 1940s, Hrennikov and Courant laid the mathematical foundations of the FEM (Elishakoff and Ren, 2003). In the 1950s the FEM became prominent in the engineering literature as an informal procedure for formulating matrix solutions to stress and displacement calculations (Fletcher, 1988). The name finite element was first used by Clough in 1960 (Thomée, 1984). Some of the pioneering work using the FEM is reported to have been done by Turner, Martin, Zienkiewicz and Cheung in the mid 1960s (Thomée, 1984).

Like the FDM, the FEM is efficient in solving problems with complex geometries and boundary conditions (Ferzinger and Perić, 2002; Steinhauser, 2008). This is because the meshes created can easily be adapted to almost any type of domain. However, the FEM also suffers from low accuracy (Schuberth, 2003). Mistakes by users including, for example the use of wrong or distorted elements, may lead to very serious errors (de Weck and Kim, 2004). The FEM uses a variational formulation that automatically accommodates the boundary conditions (Thomée, 1984).

The finite volume method (FVM) was introduced in the early 1970s by McDonald in 1971 and MacCormark and Pillay in 1972 for the solution of the two-dimensional time dependent Euler equations (Tu et al., 2008). The method was extended to three-dimensional flows in the 1973s. In the FVM the computational domain is subdivided into a grid of a finite number of adjacent control volumes (Steinhauser, 2008). In each control volume the conservation equations are

applied (Ferzinger and Perić, 2002). The centroid of each control volume is a computational node where values of the variable are to be computed (Ashgriz and Mostaghimi, 2001). Interpolation is then applied to express in terms of the nodal values, the variable values and the resulting surface and volume integrals are approximated by suitable quadrature formulae (Barth and Ohlberger, 2004). Evaluation of the integrals results in an algebraic equation at each control volume (Ashgriz and Mostaghimi, 2001).

Since the FVM can use both structured and unstructured meshes, the method can handle complex geometries. Boundary conditions are easily applied since the variables are known at all the control volume boundaries (Karim et al., 2011). Also, unlike in the case of the FDM, the transformation of the equations in terms of body-fitted coordinate systems is not required (Tu et al., 2008). However, extending the FVM to three-dimensions for higher order difference approximations becomes difficult (Ferzinger and Perić, 2002). This difficulty is associated with the structure of the FVM algorithm. It involves three levels of approximations, interpolation, differentiation and integration (Barth and Ohlberger, 2004). In recent studies, the FVM has been used for studies in rheology (Pinho, 2001), fluid mechanics (Steinhauser, 2008), biological sciences (Ludwig et al., 2008), and in water flow simulations (Abedini and Ghiassi, 2010).

The mathematical foundation of the boundary element method (BEM) is the method of integral equations (Sato, 1992; Grecu et al., 2009). The solution of Fredholm integral equations by Kellog in 1929 led to the development of the indirect BEM, while the application of the Green's theorem as an alternative to the derivation of the integral equation led to the development of the direct BEM, (Katsikadelis, 2002; Watson, 2003).

Unlike the FDM and FEM, the BEM is a boundary-oriented method. The governing PDEs are transformed into integral equations relating to the boundary values only (Eldho and Young,

2001; El-Bashir, 2006). Values at interior points may be calculated from the boundary data (El-Bashir, 2006). The numerical approximations in this method occur at the boundaries, as a result reducing the problem dimension by one (Grecu et al., 2009). It has been used to solve the heat diffusion equations, flows in porous media, biological flows, and environmental problems such as the circulation in human bodies and in weather predictions (Sato, 1992; El-Bashir, 2006; Muhammad et al., 2009). Kikani (1989) used the BEM to investigate the effects of reservoir geometry and heterogeneity of the flow field in underground reservoirs. Lough et al. (1998) solved boundary integral equations modeling the flow through a fractured porous media using the BEM. Florez et al. (2003) used the BEM to find solutions of a non-Newtonian flow problem.

The reduction in the dimensionality of a boundary value problem has made the BEM more advantageous over the FEM and FDM (Muhammad et al., 2009), making the method economical and time saving since there is less data analyzed. The method is also appropriate for complicated and unbounded domain problems (Mushtaq et al., 2010). However the requirement of a suitable fundamental solution when using the BEM brings a major drawback to the method. Such solutions are not readily available for all types of problems (Katsikadelis, 2002). Eldho and Young (2001) proposed a dual reciprocity boundary element method (DRBEM) to overcome the dependance on finding a fundamental solution. The DRBEM was used successfully to find solutions of the Laplace equation by Eldho and Young (2001).

The BEM however cannot be applied to non-homogeneous nonlinear flow problems (Muhammad et al., 2009). It becomes numerically unstable at high Renolds or Rayleigh numbers and leads to non-symmetric and fully populated matrices which increase the computational work (Dargush and Grigoriev, 2000). However the method is still useful for laminar flows, flows in finite and infinite fields and incompressible flows (Kikani, 1989).

1.1.2 Runge-Kutta schemes

Runge-Kutta methods comprise a class of so-called step-by-step methods (Ferracina, 2005). The origins of the Runge-Kutta method (RKM) can be traced back to the late eighteenth and early nineteenth centuries. In 1895, Kutta extended the Euler method so it can allow multiple evaluations of the derivative at each time-step. Several contributions were made by Heun in 1900 and Kutta in 1901 that lead to the development of the fifth order Runge-Kutta method (Butcher, 1987; Segawa, 2011). The sixth order Runge-Kutta methods were proposed in 1925 by Nyström and by Huta in 1956 and further developments of methods were made by Gill in 1951, Merson in 1957 and Butcher in 1963 Segawa (2011).

Runge-Kutta methods are well known for their stability. However more computational effort is required when using Runge-Kutta methods compared to other numerical schemes, for example, the Euler's method, (Prokopakls and Selder, 1981). However, discretization errors are greatly reduced compared to the Euler method. The explicit Runge-Kutta methods are much simpler than the implicit Runge-Kutta methods. Nonetheless, explicit Runge-Kutta methods have very small regions of stability compared to implicit Runge-Kutta methods (Collin and Schett, 1983; Wolke and Knoth, 2000). In addition, implicit Runge-Kutta methods are capable of handling stiff ODEs while the former can not. As a result, much attention has been dedicated to the improvement and application of implicit Runge-Kutta methods to, for example, stiff ODEs (Cash, 1996).

A compound form of the Runge-Kutta method for solving nonlinear stiff dynamical systems was presented by Zhang and Li (2011). Prokopakls and Selder (1981) proposed an adaptative semi-implicit RKM to integrate linear and nonlinear stiff systems with and without oscillations. An improved version of the approximate Newton method for implicit RKMs was

presented by Xie (2011). Wolke and Knoth (2000) studied the relationship between explicit Runge-Kutta methods and the implicit integrator and used these methods to integrate atmospheric chemistry-transport-models. Alvarez and Rojo (2003) introduced an improved class of generalized Runge-Kutta methods for stiff problems. However explicit methods have not been completely abandoned. Alvarez and Rojo (2004) proposed and tested a new family of explicit methods of order four with two evaluations per step on special second-order differential equations. The numerical solutions of age-structured population models were generated by Abia and López-Marcos (1995) using a difference scheme based on RKMs. Haelterman et al. (2009) developed a new formulation of the RKM that handles large algebraic systems.

1.1.3 The Keller-box scheme

Proposed by Keller in the early 1970s, the Keller box scheme is an implicit finite difference scheme for finding numerical approximate solutions of differential equations. Also named the Preissman box scheme, the Keller box scheme is a deviation from the finite volume approach in which the derivatives or unknowns are stored at control volume faces rather than at the conventional cell centers. The unknowns, in space and time, are placed at the corners of the space-time control volume, which is a box in one dimension on a stationary mesh (Perot and Subramanian, 2007).

Originally devised to find solutions of diffusion equations, the Keller box method has been used to solve a wide range of fluid flow problems. It has been used to find solutions of wave equations (Perot and Subramanian, 2007), convection flows, jet flows and separating flows (Shu and Wilks, 1995), turbulent flows (Cebeci and Shao, 2003) and free and forced convection flows (Salleh et al., 2009).

Meek and Norbury (1984) modified the Keller box method into a second-order, two-stage, two-level finite difference scheme and used it to find solutions of a nonlinear diffusion equation. The normal central difference approximation used in the Keller box method was found to sometimes bring about large and bounded oscillations in the numerical solutions (Kafoussias et al., 1999). They used a backward difference scheme to eliminate the oscillations in the solutions. However the solutions obtained using this modification were only first-order accurate. Shu and Wilks (1995) used a combination of merging and reduction processes to handle multi-layer and integral operators in the governing equations. This approach was successfully used by Shu and Wilks (2009) for solutions of the heat transfer problem from a draining sheet.

1.1.4 WENO schemes

Weighted essentially non-oscillatory (WENO) schemes are a modification of the original essentially non-oscillatory (ENO) schemes. They are reconstruction finite volume schemes used together with suitable time-step discretizations and applicable to hyperbolic conservation laws (Aboiyar et al., 2006). The idea behind ENO schemes is to first select a set of stencils for each cell of the finite volume discretization (Shu, 1997, 2001). Each set of stencils consists of a set of neighboring cells (Aboiyar et al., 2006). A recovery polynomial is used to interpolate cell averages in the stencil. A suitable oscillator indicator is used to ensure that only a smooth (least oscillatory) polynomial is used (Balsara, 2009). The order of the ENO schemes depends on the order of the polynomial used.

In the case of WENO schemes, the whole set of stencils and their equivalent polynomials are used to estimate the solution over a control volume as opposed to using the least oscillatory polynomial (Shu, 2001). The WENO schemes improved the robustness, smoothness of the

numerical fluxes, convergence properties and computational efficiency of the ENO schemes. However WENO schemes are usually not optimal for computing turbulent flows and other flows with fluctuations (Capdeville, 2008). To this end, a number of improvements to WENO schemes have been proposed. Shi et al. (2002) developed WENO schemes suitable for problems with negative weights. Qiu and Shu (2005) proposed a class of WENO schemes based on Hermite polynomials (HWENO) which further improved the compactness of the WENO schemes. The HWENO schemes were used to find solutions of the Hamilton-Jacobi equations by Qiu and Shu (2005). To avoid numerical instabilities and reduce computational complexity, Aboiyar et al. (2006), proposed WENO schemes that use polyharmonic splines rather than polynomials. This scheme gave not only numerically stable results but also proved to be more flexible. Qiu (2007) proposed Lax-Wendroff time discretization for WENO schemes (WENO-LW) to find solutions of Hamilton-Jacobi equations. To improve the convergence order and decrease dissipation near discontinuities, Zahran (2009) proposed a combination of the central WENO schemes with smoothness indicators. A fourth order divergence-free WENO scheme for MHD flow problems was proposed by Balsara (2009). This version was an improvement form the second order accurate schemes.

WENO schemes have been applied to diffusion equations in thin film flows (Ha et al., 2008), incompressible flows (Yang et al., 1998), underwater blast-wave focusing (Liang and Chen, 1999), wave propagation equations (Noelle, 2000), Navier-Stokes equations with high Reynolds number (Zhang et al., 2003) and free shear layer equations (Cheng and Lee, 2005) amongst many other problems.

1.1.5 The bvp4c algorithm

Kierzenka and Shampine (2001) developed a finite difference code that implements the three-stage Lobatto formula, the bvp4c, for boundary value problems (BVPs). The bvp4c is an implicit Runge-Kutta method with a continuous extension and uses Simpson's formula as its basic discretization scheme (Kierzenka and Shampine, 2001; Shampine et al., 2003).

The error control approach used in the bvp4c tends to deal robustly with poor guesses to the mesh and the procedure can handle problems with non-separated boundary conditions (Shampine et al., 2005; Hale and Moore, 2008). The bvp4c can also be viewed as a residual control based adaptive mesh solver with the advantage of low computational and storage costs while allowing control of the grid resolution (Hale, 2006). Zhao (2011) compared the performance of the bvp4c with two shooting methods in solving a cavity expansion problem.

The bvp4c was found to be robust and consistent, showing superiority over the other numerical methods. Nonetheless, BVP solvers rely on a good initial guess for their performance and the bvp4c is no exception. It may fail if a poor guess is used and it works better for systems involving relatively few equations, (Shampine et al., 2005). Wang (2001) found that for piecewise continuous optimal control problems, the bvp4c fails at the discontinuous points.

Shampine (2003) modified the original bvp4c so that it could be applied to a class of singular ODEs. This extension was termed the sbvp4c. Hale (2006) developed the bvp6c as an extension to the bvp4c of Kierzenka and Shampine (2001). In this solver, for the interpolant, a sixth-order solver is implemented instead of the fourth-order one that is used in the bvp4c (Zhao, 2011). The bvp6c improves the accuracy and efficiency of the former whilst retaining its generality (Hale, 2006). Hale and Moore (2008) showed that the new modification has the

same level of robustness as the bvp4c but superior for most problems as it uses fewer internal mesh points and takes less time to achieve the same level of accuracy.

Kierzenka and Shampine (2008) introduced the bvp5c which functions exactly like the bvp4c but differs in the way error tolerances are defined. The bvp4c indirectly controls the true error whilst the bvp5c is able to directly control the true error of a solution (Hollborn, 2011).

The bvp4c has been used successfully to solve BVPs from different models in science and engineering. For example, the bvp4c was used by Budd et al. (2006) to find self-similar blow-up solutions of certain nonlinear partial differential equations. Harley and Momoniat (2008) were able to estimate integrals and bifurcations of Lane-Emden equations of the second kind using the bvp4c. Numerical solutions for a model of non-isothermal free surface flows were found using the bvp4c by Zhmayev et al. (2008). Thomé et al. (2010) investigated a model describing the dynamics of mosquito populations under certain conditions. The steady axisymmetric mixed convection boundary layer flow past a thin vertical cylinder placed in a water-based copper nanofluid was investigated by Grosan and Pop (2011).

1.1.6 The shooting method

The shooting method is a BVP solver that works by converting the BVP into an initial value problem. The starting point is an assumed condition for the unknown initial condition. The guess is improved through an iterative process until a solution that satisfies all the given boundary conditions is achieved, (Ha, 2001; El-Gebeily and Attil, 2003).

Successful applications and extensions of the shooting method have been documented over the years. The Falkner-Skan equation was solved by El-Hawary (2001) using a shooting method.

El-Gebeily and Attil (2003) coupled the shooting method with an iterative method to find numerical solutions of a certain class of singular two-point BVPs. Makinde (2009a) investigated the hydromagnetic mixed convection flow of an incompressible viscous electrically conducting fluid and mass transfer over a vertical porous plate with constant heat flux embedded in a porous medium using the Newton-Raphson shooting method along with fourth-order RungeKutta integration algorithm. Ribeiro (2004) investigated the geometrically nonlinear periodic vibrations of elastic and isotropic, beams and plates by the shooting method. A shooting method for porous catalysts was developed by Lee and Kim (2005). Yang (2006) used the shooting method to find numerical solutions of controllability problems constrained by linear and semi-linear wave equations with locally distributed controls. Chih-Wen et al. (2006) proposed a Lie-group shooting method to solve the Falkner-Skan and Blasius equations. Their approach involved integrating the IVPs using group preserving scheme (GPS) developed earlier by Liu (2001). Multiple solutions of the Falkner-Skan and Blasius equations under suction-injection conditions were studied by Liu and Chang (2008) using a new extension of the shooting method. In their approach the governing equation was transformed into a nonlinear second-order boundary value problem and then solved using the Lie-group shooting method. The numerical solution of a special class of fractional boundary value problems of second order was investigated by Al-Mdallal et al. (2010) using a conjugating collocation and spline analysis technique combined with the shooting method.

In summary, shooting methods are quite general and applicable to a wide variety of differential equations (Ha, 2001; Lebedev and Lovtsov, 2002). They are quite robust as they can be used to solve various types of BVPs (Asai, 2006). However, they may fail to converge for problems sensitive to initial conditions and also lack stability in relation to the perturbation of

parameters (Lebedev and Lovtsov, 2002). For some problems, shooting methods are sensitive to modest changes in the initial conditions which may give rise to numerical difficulties in the computations (Ha, 2001).

1.1.7 Spectral methods

The idea in spectral methods is to approximate functions using truncated series of orthogonal polynomials or functions (Mantzaris et al., 2001; Gheorghiu, 2007; van de Vosse and Minev, 2002). These polynomials are global, meaning that they are defined over the whole domain of a particular problem (Mantzaris et al., 2001). For this reason spectral methods are sometimes referred to as global methods. Spectral methods can further be viewed as expansions of the method of weighted residuals (MWR), a class of discretization schemes for differential equations (van de Vosse and Minev, 2002; Babolian et al., 2007). In the MWR, the approximating functions are known as trial functions. These trial functions are used as basis functions of a truncated series expansion of the solution, (Babolian et al., 2007). The orthogonal functions used in spectral methods include Fourier series, Chebyshev and Legendre polynomials (Gheorghiu, 2007). Fourier series are used for periodic problems while Chebyshev and Legendre polynomials are used in non-periodic problems. In addition, Hermite polynomials are preferable for approximations on the real line, and Laguerre polynomials for approximations on the half line (Gheorghiu, 2007).

Depending on the choice of trial functions, there are three different types of spectral methods, namely Galerkin, Tau and collocation or psuedospectral methods. The major difference between these methods is that Galerkin and Tau methods are applied in terms of expansion coefficients while collocation methods are applied in terms of the physical space values of the

unknown function and trial functions are used to evaluate spatial derivatives (Mantzaris et al., 2001; Babolian et al., 2007). The major difference between the Tau and Galerkin methods is that each of the trial functions used in the Galerkin methods must satisfy the boundary conditions and yet in Tau methods this is not necessarily the case. The major drawback of Galerkin and Tau methods is that they require substantial CPU time when dealing with higher-dimensional approximate solutions (Mantzaris et al., 2001).

Spectral methods have been used successfully in many different fields in the sciences and engineering because of their ability to give accurate solutions of differential equations. These fields include fluid flows (Hussaini and Zang, 1987; Grandclément and Novak, 2009), geophysics, meteorology and climate modeling (Canuto et al., 2007; Grandclément and Novak, 2009), magnetohydrodynamics (MHD) (Shan et al., 1991; Shan, 1994), electrodynamics (Belgacem and Grundmann, 1998) and in quantum mechanics (Canuto et al., 2007; Hesthaven et al., 2007).

Besides giving highly accurate results, spectral methods have several other advantages over other numerical methods. Spectral methods generally converge to the true solution faster than any finite power of $1/N$ (N, the dimension of the reduced order model) (Juang and Kanamitsu, 1994; Mantzaris et al., 2001; Cueto-Felgueroso and Juanes, 2009). They produce more accurate results than finite differences (Trefethen and Trummer, 1987; Juang and Kanamitsu, 1994). There is freedom to choose the appropriate basis functions for a particular problem when using spectral methods (Juang and Kanamitsu, 1994).

Spectral methods work under specific domains called spectral domains. Occasionally, it may be more difficult to solve a problem in its original domain than in the spectral domain. However, on the downside, spectral methods are not easy to implement and for problems with singularities in a complex plane close to the spectral domain, convergence of spectral methods

is decelerated (Cueto-Felgueroso and Juanes, 2009). Discretization of large systems of partial differential equations using spectral methods gives rise to full matrices and problems with complex computational domains and rigorous nonlinearities cannot be handled efficiently by spectral methods (Juang and Kanamitsu, 1994; Mantzaris et al., 2001). The stability of spectral methods for initial value problems is also not proven (Trefethen and Trummer, 1987).

Moves to overcome some of the limitations of spectral methods have been made. For instance, the spectral element method (SEM) was developed by Patera (1984) to overcome the weakness of spectral methods in handling problems in complex geometries. The SEM merges the accuracy of spectral methods with the flexibility of the finite element method (van de Vosse and Minev, 2002). Raspo (2003) developed a direct domain decomposition method coupled with the Chebyshev collocation method for the solutions of incompressible Navier-Stokes equations. Based on Hermite-Fourier expansions Korostyshevskiy and Wanner (2007) proposed a spectral method for the computation of homoclinic orbits in ordinary differential equations. The list is not exhaustive, there are indeed many more applications and improvements that have been made to spectral methods over the years.

1.2. Perturbation methods

Perturbation methods are an alternative to numerical methods and are useful for finding approximate analytic solutions of differential equations. Nonetheless, literature reveals that the use of perturbation techniques in fluid dynamics has somewhat declined since the advent of high-speed digital computers.

A non-exhaustive list of perturbation methods include the method of averaging, the method of strained coordinates, Struble's technique, the method of variation of parameters, the method

of multiple scales (Bellman, 1966; Nayfeh, 1973; von Dyke, 1975), the δ-expansion method (Bender et al., 1989) and Lyapunov's artificial small parameter method (Lyapunov, 1992), to mention but just a few. Perturbation techniques in general construct the solution for a problem involving a small parameter ϵ, the perturbation parameter (von Dyke, 1975; Bellman, 1966; Holmes, 1995). The perturbation quantity may either be part of the differential equation, the boundary conditions or both (Nayfeh, 1973; Liao, 2003a). In general, the solution of the differential equation at $\epsilon = 0$ should be known (Bellman, 1966; Kevorkian and Cole, 1981). The approximate solutions are then generated using asymptotic expansions of suitable sequences of the perturbation parameter (Bellman, 1966). The accuracy of perturbation approximations does not depend on the value of the independent variable but on the perturbation parameter (Liao, 2003b,a). For smaller values of ϵ, the accuracy of perturbation methods tends to improve (Nayfeh, 1973).

The analytic solutions obtained through perturbation methods are often more useful than numerical results as they provide a more qualitative and quantitative representation of the solution compared to numerical solutions (Liao, 2003b). They often provide a clearer meaning of the physical parameters contained in the solutions (Liao, 2003a). However, their reliance on small perturbation quantities makes them subject to several constraints (Liao, 2003b). Not all nonlinear equations have such parameters. Consequently, for some problems the perturbation quantities have to be artificially introduced which may lead to erroneous or even incorrect results (Holmes, 1995). Kevorkian and Cole (1981) show that perturbation techniques may not work for the whole computational domain for some problems. Choosing suitable sequences of the perturbation parameter requires previous knowledge of the general nature of the solution (Nayfeh, 1973). This introduces a major drawback because such knowledge can be difficult to have, especially for complicated problems.

Perturbation methods can be trusted to work for problems with weak nonlinearity (Kevorkian and Cole, 1981; Liao, 2003b). Some perturbation methods may fail for expansions near an irregular point and so render complete analysis of the solution impossible (Kevorkian and Cole, 1981). Nayfeh (1973) further showed that if the perturbation parameter multiplies the highest derivative term, incorrect results may be obtained. This is because the first approximation will be governed by a lower order equation which may not satisfy all the given initial boundary conditions (Nayfeh, 1973).

1.3. Non-perturbation methods

Non-perturbation techniques have been developed to avoid the dependence on perturbation parameters. Existing techniques include the Adomian decomposition method (ADM), the differential transform method (DTM), the variational iteration method (VIM), the homotopy analysis method (HAM) and the homotopy perturbation method (HPM).

1.3.1 Adomian decomposition method

The Adomian decomposition method was developed by Adomian (Adomian, 1976, 1994, 1991). The idea is to split the given equation into its linear and nonlinear parts. The highest derivative of the linear part is then inverted on both sides of the equation (Adomian, 1976). The initial approximate solution of the ADM comprises of the initial and/or boundary conditions together with terms involving the independent variables only (Chen and Lu, 2004). The unknown function is then decomposed into a series whose components are to be determined. Special polynomials called Adomian polynomials are used to decompose the nonlinear function (Allan, 2007). Using a recurrent relation in terms of the Adomian polynomials, successive terms of

the series solution are generated (Allan, 2007; Bratsos et al., 2008).

The ADM solutions are closed form making it a quantitative rather than a qualitative approach. It is analytic and requires neither linearization nor resort to discretization (Allan, 2007; Bratsos et al., 2008). Consequently, the ADM gives the true solution of the problem and is not affected by discretization errors. The method has been shown to give reliable analytical approximations that converge rapidly for nonlinear equations (Chen and Lu, 2004). It is valid for strongly nonlinear ordinary differential equations or partial differential equations with or without small/large parameters (Pamuk, 2005; Basak et al., 2009).

The ADM has been used successfully to solve a wide range of linear and nonlinear equations in science and engineering. These include fourth-order parabolic partial differential equations (Wazwaz, 2001a), heat diffusion equations (Arslanturk, 2005; Hashim, 2006b), generalized Burgers-Huxely equation (Hashim, 2006a), Lorenz system (Hashim et al., 2006), nonlinear fractional boundary value problems (Jafari and Daftardar-Gejji, 2006), SIR epidemic model (Makinde, 2007), Klein-Gordon equation (Basak et al., 2009), Falkner-Skan equation (Alizadeh et al., 2009), and many other applications of the ADM cited in the literature.

The ADM suffers from a number of limitations. The approximate solutions given by the ADM often contain polynomials with small convergence regions. It also does not provide the freedom to choose efficient base functions other than the power series which is usually inefficient to approximate some nonlinear problems (Liao, 2003b). This is because convergence of the approximation series used is not always guaranteed. The ADM's stability in other applications can be lower than that of other numerical methods such as collocation methods (Aminataei and Hosseini, 2007). To improve the applicability of the ADM, a number of modifications to the standard ADM have been suggested. Wazwaz (1999b) proposed a modification of

the Adomian decomposition method (MADM) that accelerates the convergence of the series solution. This modified version has been widely used to solve boundary value problems and higher-order integro-differential equations (Wazwaz, 2001d). It has been applied to sixth-order boundary value problems (Wazwaz, 2001c), mixed Volterra-Fredholm integral equations (Wazwaz, 2002b) and to third-order dispersive partial differential equations (Wazwaz, 2003).

Padé approximants were used in conjunction with the ADM for the solution of boundary layer equations in unbounded domains (Wazwaz, 2006). The use of Padé approximants helped to achieve better accuracy, increase the convergence region and rates of the truncated series produced by the ADM. The ADM-Padé has been used to solve Burger's equation (Abassy et al., 2007; Dehghan et al., 2007; Alharbi and Fahmy, 2010), linear and nonlinear systems of Volterra functional equations (Dehghan et al., 2009), MHD flow problem over a stretching sheet (Hayat et al., 2009), and differential-difference equations (Wang et al., 2011) amongst other applications.

Wazwaz (2002a) proposed yet another modification of the ADM. This version is particulary useful for singular initial boundary value problems where the ADM would at times fail to converge. Wazwaz and Khuri (1996) used the new modification to solve weakly singular second-kind Volterra-type integral equations, the Thormas-Fermi equation (Wazwaz, 1999a) and differential equations of Lane-Emden type (Wazwaz, 2001b), amongst other applications. Hosseini (2006) introduced a modification of the ADM that uses Chebyshev polynomials. Zhang et al. (2006) proposed a two-step Adomian decomposition method (TSADM), for systems of inhomogeneous differential equations, hyperbolic partial differential equations and for singular initial value problems. Legendre polynomials in combination with the ADM were used by Liu (2009). Abassy (2010a) proposed the improved Adomian decomposition method

(IADM), which is based on a new formulation of the Adomian polynomials to accelerate the convergence of the ADM. Further modifications of the ADM may be found in the literature.

1.3.2 The differential transform method

The differential transform method, was first introduced by Zhou in 1986. It is a semi-analytical-numerical technique that has been successfully used in electrical circuit studies to solve linear and nonlinear initial value problems (Ayaz, 2003). Taylor series expansions are used to construct analytical solutions in polynomial form (Catal, 2008; Jang, 2010). The traditional Taylor series method requires symbolic computation of the derivatives of the data functions and requires more computation time for large orders while the DTM iteratively obtains analytic Taylor series solutions of differential equations (Ayaz, 2003). Compared to the Taylor series, the DTM can easily handle highly nonlinear problems (Ayaz, 2003).

The main advantage of the DTM, like the ADM, is that it can be used directly to solve nonlinear ordinary and partial differential equations without the need for linearization, discretization or perturbation (Ebaid, 2010). The DTM is thus also free of discretization errors and yields closed form solutions.

Applications of the DTM to various problems in the sciences and engineering fields include solutions of the Blasius and difference equations (Arikoglu and Ozkol, 2005, 2006), vibration equations (Catal, 2008), singular two-point boundary value problems (Kanth and Aruna, 2008), convective straight fin problem with temperature-dependent thermal conductivity (Joneidi et al., 2009) and the fractional modified KdV equation by Kurulay and Bayram (2010), amongst others.

There are two major drawbacks of the DTM. Firstly, the truncated series solution obtained by the DTM suffers from small convergence regions (Odibat and Momani, 2008; Rashidi, 2009; Gökdoğan et al., 2011). Secondly, the truncated series does not reveal any periodic behaviour that maybe associated with oscillator systems (Gökdoğan et al., 2011). Padé approximants and Laplace transforms have been extensively used together with the DTM in attempts to overcome the limitations of the DTM. Momani and Ertürk (2008) proposed the modified differential transform method (MDTM), that uses Laplace transforms and Padé approximants. This version successfully extended the convergence regions of the DTM and also captured the periodic behavior of solutions. Gökdoğan et al. (2011) successfully used the MDTM to find solutions of Genesio systems.

Another modification of the DTM based on Laplace transforms and Padé approximants is the DTM-Padé. Rashidi (2009) proposed the DTM-Padé to solve MHD boundary-layer equations. The DTM-Padé mainly extended the convergence region of the DTM. The DTM-Padé was used by Rashidi et al. (2010) to solve the convection fin problem about an inclined flat plate embedded in porous media. Solutions of the Camassa-Holm equation were obtained using the DTM-Padé by Zou et al. (2009). However, the DTM-Padé has been reported by Ebaid (2011) to significantly increase computational work and that difficulties associated with finding the inverse Laplace transform may arise. Ebaid (2011) proposed an after-treatment technique for obtaining periodic solutions that avoids the use of both the Laplace transforms and the Padé approximants. Odibat et al. (2010) proposed and used yet another modification of the DTM, the multi-step DTM, to extend convergence regions.

1.3.3 The variational iteration method

Ji-Huan He (He, 1999a,c) proposed the variational iteration method. The basic idea is to construct a correction functional by means of a general Lagrange multiplier. The Lagrange multiplier is chosen such that its correction solution is superior to the initial approximate solution (He, 1999a). The initial approximate solution is chosen to satisfy the boundary conditions of the problem. The VIM, like the ADM and DTM needs no discretization, linearization, or transformation (Soltani and Shirzadi, 2010). It has been proven in many applications to be an effective, easy to use and accurate method for finding solutions of many classes of linear and nonlinear problems (Biazar and Aminikhah, 2009).

Moghimi and Hejazi (2007) used the VIM to find solutions of the generalized Burger-Fisher and Burger equations. Wazwaz (2007) used the VIM to find rational solutions of the KdV, $K(2,2)$, Burgers and cubic Boussinesq equations. Wazwaz (2008) solved linear and nonlinear Schrödinger equations and Inc (2008), the space- and time-fractional Burgers equations using the VIM. Dehghan and Shakeri (2008b,a) used the VIM to solve the Lane-Emden equation and the Cauchy reaction-diffusion problem. Ganji et al. (2009) and Yıldırım and Öziş (2009) used the VIM to find solutions of the Jefferey-Hamel flow problem and singular initial value problems of the Lane-Emden type respectively. Makinde and Charles (2010) used the VIM to investigate the hydromagnetic stagnation flow of an incompressible viscous, electrically conducting fluid, towards a stretching sheet. The delay logistic problem was solved by Dehghan and Salehi (2010) using the VIM. Hassan and Alotaibi (2010) used the VIM to solve the improved KdV equation.

However, users have reported some weaknesses of the VIM. Amongst these weaknesses, is the

small convergence region of the VIM solutions (Abassy et al., 2007c; Geng, 2010). It also has been reported that the accuracy of the VIM is greatly compromised by unneeded noise terms that usually crop up in the computations (Abassy et al., 2007d; Abassy, 2010b). These terms tend to unnecessarily consume computational time further decelerating convergence rates.

Many researchers have worked on modifications of the VIM to overcome its inadequacies. Abassy and his co-workers extensively worked on improving the VIM in 2007. They introduced enhancements using Padé approximants (Abassy et al., 2007c) to extend the convergence region of the VIM. They further enhanced the method using Laplace transforms (Abassy et al., 2007a). An adjustment to get rid of the unneeded term was introduced by (Abassy et al., 2007d) who further modified the VIM to be applicable to a certain class of partial differential equations (Abassy et al., 2007b).

A version suitable for nonlinear integral-differential equations was introduced by Biazar and Aminikhah (2009). Ghorbani and Saberi-Nadjafi (2009) proposed a modified VIM that was based on using an improved initial approximation to accelerate the accuracy of the method. A piecewise-truncated VIM algorithm to overcome the unneeded terms was initiated by (Ghorbani and Momani, 2010). Geng (2010) introduced a modification of the VIM whose aim was to extend the convergence region of the solutions. This approach introduced a convergence controlling parameter. These modifications amongst others, have made the VIM a useful tool applicable to a wide variety of problems.

1.3.4 The homotopy analysis method

A homotopy analysis method was proposed by Liao (1992) in his PhD thesis. The HAM is a non-perturbation method that is valid for strongly nonlinear problems with or without

small/large parameters. The HAM contains an artificial parameter $\hbar$ used to adjust the convergence rate and the region of convergence (Liao, 2003b). It offers great freedom to express solutions of a given problem using a set of base functions (Liao, 2003b). The central design of the HAM is to replace a nonlinear equation by a system of ordinary differential equations (ODEs) that can easily be solved with the help of symbolic computation software such as Mathematica and Maple. The solution of system of ODEs forms a convergent series that approximates the solution of the nonlinear equation (Liao, 1992, 2003b). A detailed description of the HAM can be found in Liao's book (Liao, 2003b).

The HAM has been successfully used by several researchers in science and engineering to find solutions of different types of nonlinear equations. In particular one may draw attention to the works of Hayat and his collaborators on the solution of non-Newtonian fluid problems (Hayat et al., 2007; Hayat and Sajid, 2007b,a; Hayat et al., 2007). Abbasbandy (2006a, 2007b) and Sajid and Hayat (2008) used the HAM to solve nonlinear heat transfer problems. The KdV type of equations were studied by Abbasbandy (2008, 2007a) and Song and Zhang (2007). A more comprehensive list of the applications of the HAM can be found in Liao (2009).

However, like many other similar methods, the HAM suffers from a number of deficiencies. In his book, Liao (Liao, 2003b, ch. 5), discusses some of these as well as its strengths. One of the main limitations of the HAM is the requirement that the solution sought ought to conform to some pre-set rules. The so-called rule of solution expression and the rule of coefficient ergodicity provide a guide on how to choose the appropriate initial approximations, the auxiliary linear operators and the auxiliary functions. These parameters are conveniently chosen to ensure that the resulting higher order deformation equations that are used to obtain the approximate series solutions can be easily integrated using symbolic computation software

(van Gorder and Vajravelu, 2009). Complicated initial approximations and linear operators could lead to difficult or even impossible to integrate higher order deformation equations. The restriction on the choice of the initial guess might lead to the use of poor initial guesses which may compromise convergence rates as well as the accuracy of the results.

The so-called $\hbar$-curves used for finding suitable values of the convergence controlling parameter do not give the optimal $\hbar$ value, but a range of values. This makes finding the optimal convergence controlling parameter a trial and error process (van Gorder and Vajravelu, 2009). This further compromises the accuracy of the results if any other value besides the optimal value is used.

There has been improvements and adjustments made to the HAM. Yabushita et al. (2007) made an attempt to correct the limitations of the HAM in obtaining the optimal value of the convergence controlling parameter. They introduced an extra convergence controlling parameter instead of using the so-called $\hbar$-curves. Marinca et al. (2008), introduced the optimal homotopy analysis method (OHAM) where more than two convergence parameters were used in the algorithm. Ali et al. (2010) and Esmaeilpour and Ganji (2010) used the OHAM to solve multi-point boundary value problems including the Jeffery-Hamel flow problem. In their findings they note that the OHAM is a straight forward and reliable approach. Also, it converges for larger physical domains compared to the HAM. Idrees et al. (2010) also successfully applied the OHAM to the squeezing flow problem, Iqbal et al. (2010) to the linear and nonlinear Klein-Gordon equations and Iqbal and Javed (2011) to singular Lane-Emden type equations. However, Liao (2010) suggests that the development by Marinca et al. (2008) is time-consuming and has been occasionally reported to fail for complicated nonlinear problems.

Liao (2010) presented a new version of the OHAM in which three convergence controlling

parameters are used at each iteration step. This accelerated the convergence and improved the accuracy of the HAM. Niu and Wang (2010) proposed a one-step OHAM based on the Taylor series expansion to improve the computational efficiency of the HAM. Bataineh et al. (2009) presented yet a new modified homotopy analysis method, the MHAM, that was able to avoid the uncontrollability problems of the non-zero endpoint conditions that are usually encountered in using the original HAM. One further modification of special interest in this work is by Motsa et al. (2010). Based on the use of spectral methods, this modification aims to improve the choice of the initial guesses and basis functions used in the HAM algorithm, and consequently increase the convergence rates and accuracy of the HAM. The HAM is discussed in greater depth in Chapter 2.

1.3.5 The homotopy perturbation method

He (1999b, 2003) developed the homotopy perturbation method, which unlike traditional perturbation methods, does not require the presence of a small parameter in an equation, (He, 1999b). Instead it couples the traditional perturbation method and the homotopy in topology to construct a homotopy with an embedding parameter $p \in [0, 1]$ (Ghorbani and Saberi-Nadjafi, 2008; Yusufoğlu, 2009). As p gradually increases from 0 to 1, the homotopy deforms the nonlinear equation from its initial approximation to the required results (He, 1999b). The perturbation technique is then used to solve the equation with the series solution expressed in terms of p (Abbasbandy, 2006b). The HPM is flexible in that it can be used for both analytical and numerical purposes (Chowdhury et al., 2010). It has been shown also that it avoids some of the problems encountered when applying the ADM (Ariel, 2009; Ariel et al., 2006; Ariel, 2007a; Chowdhury et al., 2010).

The HPM has been widely used by He to solve algebraic, nonlinear ODEs, bifurcation problems and PDEs amongst other applications (He, 1997, 1998b,a, 2004, 2005b,a, 2006). Other applications include the solution of the quadratic Ricatti differential equation (Abbasbandy, 2006b), Fredholm integral equations (Javidi and Golbabai, 2007; Biazar et al., 2011), integro differential equations (Golbabai and Javidi, 2007; Ghasemi et al., 2007), nonlinear heat transfer equations (Ganji, 2006; Domairry and Nadim, 2008), wave equations (Chun et al., 2009), Klein-Gordon and sine-Gordon equations Chowdhury and Hashim (2009a) and the reaction diffusion Brusselator model (Chowdhury et al., 2010).

One inadequacy of the HPM reported in recent studies (Ariel et al., 2006; Ariel, 2007a,b, 2009), is that the solution is limited to only one correction term. The possibility of occurrence of secular terms may also be unavoidable when using the HPM (Ariel, 2009). To avoid the appearance of secular terms, Ariel (2009) extended the HPM by stretching the independent variable in the problem by a scaling parameter that incorporated the homotopy parameter p. To accelerate convergence, Sweilam and Khader (2009) combined the method with Laplace transforms, Padé approximations and the Taylor series method. Their approach did not only improve the convergence rate of the HPM, but also proved to be suitable for highly nonlinear coupled systems of PDEs. Instead of the Padé approximation, Khan and Wu (2011) combined the Laplace transform method and He's polynomials with the HPM to accelerate convergence rates of the HPM.

Another approach introduced to accelerate convergence, is the use of accelerating parameters. This approach was used by Ghorbani and Saberi-Nadjafi (2008) and Yusufoğlu (2009) among others. Odibat (2007) introduced a new approach that aids convergence of the HPM. This version was used by Siddiqui et al. (2009) to solve the equations associated with the flow of

a third grade fluid. Hashim et al. (2008) implemented ideas from the ADM and formulated a multistage homotopy perturbation method (MHPM) to improve on the global convergence of the HPM. The MHPM was successfully used by Chowdhury and Hashim (2009b) to solve nonlinear chaotic and non-chaotic systems of ordinary differential equations.

1.4. Objectives of this study

Analytical methods can be used to find solutions to a limited range of problems as seen above, while numerical methods can be used to solve a wider range of problems in fluid dynamics. However, the solutions obtained using numerical methods are only approximations. Most physical characteristics of the flow cannot be revealed by these solutions. However, these solutions are still important in cases where exact solutions cannot be generated hence the need to develop improved semi-numerical or numerical methods. It is well known that the convergence of an approximate solution greatly relies on the initial guess solution used. In this study therefore we;

- introduce a new improvement of the homotopy analysis method using spectral methods (Motsa et al., 2010),
- introduce a successive linearisation method which uses spectral methods to solve the resulting higher order deformation equations,
- introduce an improvement to the spectral homotopy analysis method, which blends ideas from both the spectral homotopy analysis method and the successive linearisation method,
- use the three new methods to solve fluid flow problems (i) between parallel plates

(Makukula et al., 2010d; Sibanda et al., 2012; Makukula et al., 2010a), (ii) rotating disk flows (Makukula et al., 2010b, 2011a; Motsa et al., 2010) and, (iii) flows through porous media (Makukula et al., 2010c, 2011b).

1.5. Thesis outline

The organization of the thesis is as follows;

- In Chapter 2 we review the homotopy analysis method and describe the new methods, the algorithms and strengths and weaknesses.
- In Chapter 3 we use the methods to solve viscous incompressible fluid flow problems occurring between parallel plates.
- In Chapter 4 we use the methods to solve rotating disk flow problems.
- In Chapter 5 we use the methods to solve fluid flow problems in porous media.
- A conclusion of the thesis is given in Chapter 6 with a list of references at the end.

2

On hybrid semi-analytical methods for boundary value problems

In this Chapter we describe recent hybrid semi-numerical methods for solving boundary value fluid flow problems. It is necessary in the first instance to give a brief overview of the homotopy analysis method since the first hybrid method builds on this method and serves to improve the accuracy of the HAM. The spectral-homotopy analysis method refines the HAM by using a more accurate initial approximate solution and by solving the higher order deformation equations using spectral methods, known for high accuracy. The algorithm formulation, its strengths and weaknesses are discussed. In Section 2.3 we introduce a successive linearisation method which reduces the nonlinear BVP into a series of linear equations that are then solved using spectral methods. The formulation of the successive linearisation method for nonlinear equations is given together with the strengths and weaknesses of the method. In Section 2.4 we introduce an improvement of the spectral-homotopy analysis method which blends together ideas from the successive linearisation approach and the spectral-homotopy analysis method. In this approach, a more convergent initial approximation is used, further improving

the accuracy of the spectral-homotopy analysis method.

2.1. Review of the homotopy analysis method

The homotopy analysis method was first proposed by Liao in 1992 in his PhD thesis (Liao, 1992). The HAM constructs a sequence which continuously deforms from an initial guess of the solution of a differential equation to the exact solution. To construct such a homotopy, one needs an initial approximation, an auxiliary linear operator, $\mathcal{L}$, a non zero auxiliary function, $H(x)$, and a non zero convergence controlling parameter $\hbar$. These parameters allow the user of the HAM to effectively control the region and rate of convergence of the series solution. There is also a great freedom in the choice of the initial guess, the auxiliary linear operator and the auxiliary function with useful guidelines on how to chose these functions (van Gorder and Vajravelu, 2009; Liao, 2003b). Following Liao (2003b), let us consider a nonlinear equation of the form;

$$\mathcal{N}[f(x,t)] = 0, \qquad t > 0, \tag{2.1}$$

where $\mathcal{N}$ is a nonlinear operator and $f(x,t)$ is an unknown function of the independent variables x and t. The homotopy, also referred to as the *zeroth* order deformation equation is constructed by setting;

$$(1-q)\mathcal{L}[F(x,t;q) - f_0(x,t)] = q\hbar H(x,t)\mathcal{N}[F(x,t;q)], \quad q \in [0,1], \tag{2.2}$$

where q is an embedding parameter, $\hbar$ is an auxiliary parameter, $H(x,t)$ is a nonzero auxiliary function, $\mathcal{L}$ is an auxiliary linear operator, $f_0(x,t)$ is an initial guess to the solution $f(x,t)$ and $F(x,t;q)$ is an unknown mapping function. When $q = 0$ and $q = 1$ we have that

$$F(x,t;0) = f_0(x,t), \qquad F(x,t;1) = f(x,t). \tag{2.3}$$

Hence from equation (2.3), $F(x,t;q)$ maps continuously from the initial guess $f_0(x,t)$ to the exact solution $f(x,t)$ as q varies from 0 to 1.

Definition 2.1. *Let ϕ be a function of the homotopy parameter q, then*

$$D_m\phi = \frac{1}{m!}\frac{\partial^m \phi}{\partial q^m}\bigg|_{q=0}$$

is called the mth order homotopy derivative of ϕ where $m \geq 0$ is an integer (Liao, 2003b).

Liao (2003b) expanded $F(x,t;q)$ using the Taylor series to get

$$F(x,t;q) = f_0(x,t) + \sum_{m=1}^{\infty} f_m(x,t)q^m, \tag{2.4}$$

with

$$f_m(x,t) = \frac{1}{m!}\frac{\partial^m F(x,t;q)}{\partial q^m}\bigg|_{q=0}. \tag{2.5}$$

The convergence of the series in equation (2.4) is controlled by $\hbar$ in equation (2.2). When suitable choices of $\hbar$, $\mathcal{L}$ and $f_0(x,t)$ are made such that the series (2.4) converges when $q = 1$, then, (2.4) yields the exact solution $f(x,t)$ as simply

$$f(x,t) = f_0(x,t) + \sum_{m=1}^{\infty} f_m(x,t). \tag{2.6}$$

Differentiating the *zeroth* order deformation equation (2.2) m times with respect to the embedding parameter q, setting $q = 0$ and then dividing by $m!$, gives the mth order deformation equation,

$$\mathcal{L}[f_m(x,t) - \chi_m f_{m-1(x,t)}] = \hbar H(x,t) R_m(\vec{f}_{m-1}(x,t)), \tag{2.7}$$

where

$$R_m(\vec{f}_{m-1}) = \frac{1}{(m-1)!}\frac{\partial^{m-1}\mathcal{N}[F(x,t;q)]}{\partial q^{m-1}}\bigg|_{q=0}, \tag{2.8}$$

$$\vec{f}_m = \{f_0(x,t),\ f_1(x,t),\ f_2(x,t),\ \ldots,\ f_m(x,t)\}, \tag{2.9}$$

and

$$\chi_m = \begin{cases} 0, & m \leq 1, \\ 1, & m > 1. \end{cases}$$

For any $\mathcal{L}$ and $\mathcal{N}$, solving the mth order deformation equation (2.7) yields solutions of the form (2.6). Symbolic software like Maple and Mathematica may be used to solve equation (2.7).

The fundamental rules to consider when using the HAM are the rule of solution expression, the rule of coefficient egordicity and the rule of solution existence (Liao, 2003b). These rules provide guidelines on how to choose the initial guess, the auxiliary linear operator and the auxiliary function, all used in the formulation of the zeroth-order deformation equations. Each fundamental rule is briefly discussed below. A full exposition can be found in, for example, van Gorder and Vajravelu (2009) and Liao (2003b).

The rule of solution expression is important in the selection of the initial guess, auxiliary linear operator and the auxiliary function. Liao (2003b) notes that this rule is formulated from two main facts about an individual problem. Firstly, the solution of a nonlinear problem can be expressed using a variety of base functions. Secondly, such base functions are possible to determine from the physical properties of the problem and from its initial and/or boundary conditions. Hence for any given nonlinear problem, one can establish the rule of solution expression. For the initial guess to satisfy the requirements of the rule of solution expression, it must be expressed by a sum of the base functions. The auxiliary function must be chosen to guarantee that the higher order deformation equations are expressed by a sum of the base functions. The linear operator has to be chosen to ensure that the solution of

$$\mathcal{L}[f(x,t)] = 0, \tag{2.10}$$

may be expressed as a sum of the basis functions.

Together with the rule of solution expression, the rule of coefficient egordicity helps to uniquely define the auxiliary function (Liao, 2003b). The rule ensures that as the order of approximation approaches infinity, each base function appears in the solution expression.

The rule of solution existence is derived from the fact that if the original problem has a solution, then the subproblems that arise from the higher order deformation equation should have solutions. This further restricts the choice of the initial guess, the auxiliary linear operator and the auxiliary function. Together, the three rules provide a useful guideline that makes the use of the HAM possible.

A key parameter in the HAM is the non-zero convergence controlling auxiliary parameter $\hbar$ (van Gorder and Vajravelu, 2009; Liao, 2003b). This parameter controls the convergence region and rate of the series solution. Such regions are determined using the so-called $\hbar$-curves, where a physical quantity (such as the velocity or skin friction) is plotted against values of $\hbar$ (see for example Liao (2003b) and Sibanda et al. (2012)). The valid values of $\hbar$ are those that correspond to the horizontal part of the graph. However, it has not been determined how to select the best value of $\hbar$, which is found by trial and error (van Gorder and Vajravelu, 2009).

2.1.1 Strengths and weaknesses of the HAM

The HAM is a powerful tool for solving nonlinear problems. Liao (2003b, chap. 5) discusses the advantages of the HAM over other techniques. These include the freedom to choose different base functions, the ability to control the rate of convergence of the series solution and the ability to handle efficiently both weakly and strongly nonlinear problems with or without embedded small or large quantities. Other methods such as Adomian's decomposition method,

Lyapunov's artificial small parameter method and the δ-expansion method are special cases of the HAM (Liao, 2003b).

Nonetheless, Liao (2003b) shows that even with such great freedom to choose the base functions, for a meaningful solution, it is important for the user to have some prior-knowledge of the physics of the problem. This is a disadvantage since this is not always possible, especially with completely new problems. Also, the rules offer general guidelines on how to choose the initial guess, the auxiliary linear operator and the auxiliary function, there are however no systematic theories to direct such choices (Liao, 2003b). Furthermore, the choice of the initial guess is restricted to convenient and useful functions (van Gorder and Vajravelu, 2009). Such functions include polynomials, exponentials, trigonometric functions, rational functions or products of such functions, functions that are generally easy to integrate. Complicated base functions may make it difficult or even impossible to integrate the higher order deformation equations. Such a restriction then impairs the choice of the initial guess and forces the user to use just an adequate initial guess instead of the best possible initial guess (van Gorder and Vajravelu, 2009).

It has been pointed out earlier that there is no fail safe guide to aid the choice of the optimal $\hbar$. The so-called $\hbar$-curves only provide a range of possible $\hbar$ values. This is also a disadvantage of the method as a user might end up not using the best possible value of $\hbar$. Despite its many acknowledged successes, the HAM is not guaranteed to solve nonlinear problems with chaotic solutions (Liao, 2003b).

2.2. The spectral-homotopy analysis method

The speed of convergence of an approximate method is highly dependent on the initial guess. If the initial approximation is a poor guess, the method might take too long or may even fail to converge to the accurate result. As we have seen above, the homotopy analysis method suffers from a number of limitations, principally the fact that the solution sought ought to satisfy the rule of solution expression, the rule of coefficient egordicity and the rule of solution existence. In this section we introduce an innovation aimed at improving the accuracy of the initial guess used in the homotopy analysis method. Complicated base functions that are avoided when using the standard HAM can be used here as long as they satisfy the initial conditions. In addition, the higher order deformation equations are solved using the Chebyshev spectral collocation method, known for its accuracy (Canuto et al., 2007; Hesthaven et al., 2007).

2.2.1 Construction of the SHAM algorithm

Consider a nonlinear equation of the form

$$\mathcal{N}[f(x)] = g(x), \tag{2.11}$$

subject to the boundary conditions

$$B[f(x), f'(x), \dots] = 0, \qquad x \in [a, b], \tag{2.12}$$

where $\mathcal{N}[f(x)]$ stands for the nonlinear operator, $g(x)$ a source term, $f(x)$ is an unknown function, x an independent variable and $[a, b]$ is the domain of the problem. Equation (2.11) is decomposed into its linear and nonlinear parts as

$$\mathcal{L}_1[f(x)] + \mathcal{N}_1[f(x)] = g(x), \tag{2.13}$$

with $\mathcal{L}_1$ and $\mathcal{N}_1$ representing the linear and nonlinear operators respectively. The initial guess is the solution of the equation

$$\mathcal{L}_1[f_0(x)] = g(x), \tag{2.14}$$

with boundary conditions

$$B[f_0(x), f_0'(x), \dots] = 0, \qquad x \in [a, b]. \tag{2.15}$$

We note that in using the HAM, the initial guess is chosen to satisfy the boundary conditions and must be expressed as a sum of basis functions. The solution to equation (2.14) is generally a "better" choice compared to the one chosen to satisfy the boundary conditions only. It is only if the solution to equation (2.14) is zero or does not exist that the initial guess is chosen arbitrarily to simply satisfy the boundary conditions. To ensure homogeneous boundary conditions, the following transformation is introduced

$$u(x) = f(x) - f_0(x). \tag{2.16}$$

It is useful to note that originally, the transformation (2.16) was not made in the SHAM algorithm. This was made at a later stage (see Sibanda et al. (2012) in Chapter 3) in the modified spectral-homotopy analysis method (MSHAM). In recent studies the MSHAM has been used but called the SHAM instead of the MSHAM.

Substituting equation (2.16) into equation (2.13) yields

$$\mathcal{L}_2[u(x)] + \mathcal{N}_2[u(x)] = \psi(x), \tag{2.17}$$

subject to

$$B[u(x), u'(x), \dots] = 0, \qquad x \in [a, b], \tag{2.18}$$

where $\mathcal{L}_2$ and $\mathcal{N}_2$ are the adapted linear and nonlinear operators respectively and

$$\psi(x) = g(x) - \mathcal{L}_1[f_0(x)] - \mathcal{N}_1[f_0(x)].$$

At this stage, the solution procedure is similar to that of the HAM algorithm. We formulate zeroth-order deformation equations as;

$$(1-q)\mathcal{L}_2[U(x;q)-u_0(x)] = q\hbar\{\mathcal{L}_2[U(x;q)]+\mathcal{N}_2[U(x;q)]-\psi(x)\}, \quad q\in[0,1]. \tag{2.19}$$

We note again that, unlike in the case of the HAM the auxiliary function $H(x)$ is not necessary as there is no need for the solution of the higher order deformation equation to conform to some rule of solution expression. q and $\hbar$ are the embedding and convergence controlling parameters respectively, and $U(x;q)$ is an unknown function. The initial approximation $u_0(x)$ is the solution of the equation

$$\mathcal{L}_2[u_0(x)] = \psi(x), \tag{2.20}$$

with boundary conditions

$$B[u_0(x), u_0'(x), \dots] = 0, \qquad x\in[a,b]. \tag{2.21}$$

From the zeroth-order deformation equation (2.19), it can be shown that at $q=0$ and at $q=1$,

$$U(x;0) = u_0(x), \quad \text{and} \quad U(x;1) = u(x). \tag{2.22}$$

Consequently, as q increases from 0 to 1, the unknown function $U(x;q)$ varies from the initial approximation $u_0(x)$ to the solution $u(x)$. Using the Taylor series to expand $U(x;q)$ about q gives

$$U(x;q) = u_0(x) + \sum_{m=1}^{\infty} u_m(x)q^m, \quad u_m(x) = \frac{1}{m!}\frac{\partial^m U(x;q)}{\partial q^m}\bigg|_{q=0}, \tag{2.23}$$

where $\hbar$ is chosen such that the series (2.23) converges at $q=1$. Hence from equation (2.22) we obtain solutions of the form

$$u(x) = u_0(x) + \sum_{m=1}^{\infty} u_m(x). \tag{2.24}$$

Following the HAM procedure, we formulate the higher order deformation equations by differentiating the zeroth-order deformation equation m times with respect to q then dividing by $m!$ to get

$$\mathcal{L}_2[u_m(x) - (\chi_m + \hbar)u_{m-1}(x)] = \hbar R_m(x), \tag{2.25}$$

with

$$R_m(x) = \frac{1}{(m-1)!}\frac{\partial^{m-1}}{\partial q^{m-1}}\{\mathcal{N}_2[U(x;q)] - \psi(x)\}\bigg|_{q=0}, \tag{2.26}$$

and

$$\chi_m = \begin{cases} 0, & m \leq 1, \\ 1, & m > 1. \end{cases}$$

Nonetheless comparing the higher order deformation equations, for the SHAM,

$$\mathcal{L}_2[u_m(x) - (\chi_m + \hbar)u_{m-1}(x)] = \hbar R_m(x), \tag{2.27}$$

and for the HAM (2.7)

$$\mathcal{L}[f_m(x) - \chi_m f_{m-1}(x)] = \hbar H(t) R_m(x), \tag{2.28}$$

it is clear that the difference between (2.27) and (2.28) is the extra term $\hbar u_{m-1}$ which is assumed to be finite.

In solving the higher order deformation equations (2.25), the Chebyshev spectral collocation method (Boyd, 2000; Canuto et al., 1988, 2007; Hesthaven et al., 2007; Trefethen, 2000) is used. In the collocation method, the unknown functions $u_m(\xi)$ are approximated as truncated series of Chebyshev polynomials of the form

$$u_m(\xi) \approx \sum_{k=0}^{N} \hat{u}_k T_k(\xi_j), \quad j = 0, 1, 2, \ldots, N, \tag{2.29}$$

where T_k denotes the kth Chebyshev polynomial defined by

$$T_k(\xi_j) = \cos[k \cos^{-1}(\xi_j)], \tag{2.30}$$

$\hat{u}_k$ are coefficients and $\xi_0, \xi_1, \xi_2, \ldots, \xi_N$ are Gauss-Lobatto points defined by

$$\xi_j = \cos\frac{\pi j}{N}, \qquad j = 0, 1, \ldots, N, \tag{2.31}$$

where $N+1$ is the total number of collocation points. The physical domain $[a, b]$ is mapped by an appropriate change of variable to the spectral domain $[-1, 1]$ where the Chebyshev spectral method may be applied. The derivatives of the functions $u_m(\xi)$ are expressed in terms of the Chebyshev spectral differentiation matrix $\mathcal{D}$ (Canuto et al., 1988, 2007; Hesthaven et al., 2007; Trefethen, 2000) as

$$\frac{d^r u_m}{d\xi^r} = \sum_{k=0}^{N} \mathcal{D}_{kj}^r u_m(\xi_j), \tag{2.32}$$

where r denotes the order of differentiation. The entries of the matrix $\mathcal{D}$ are defined as

$$\mathcal{D}_{kj} = \begin{cases} \frac{c_j}{c_k}\frac{(-1)^{j+k}}{\xi_j - \xi_k}, & j \neq k, \\ -\frac{\xi_k}{2(1-\xi_k^2)}, & 1 \leq j = k \leq N-1, \\ \frac{2N^2+1}{6}, & j = k = 0, \\ -\frac{2N^2+1}{6}, & j = k = N, \end{cases}$$

where

$$c_j = \begin{cases} 2, & j = 0, N, \\ 1, & 1, 2, \ldots, N-1. \end{cases}$$

Applying the Chebyshev approximations (2.29) - (2.32) to the higher order deformation equations (2.25) results in a matrix equation of the form

$$\mathbf{A}\mathbf{U}_m = (\chi_m + \hbar)\mathbf{A}\mathbf{U}_{m-1} + \hbar\ \mathbf{Q}_{m-1}. \tag{2.33}$$

$\mathbf{A}$ and $\mathbf{Q}_{m-1}$ are matrices obtained after applying the Chebyshev transformations to $\mathcal{L}_2$ and R_m respectively, $\mathbf{U}_m = [u_m(\xi_0), u_m(\xi_1), u_m(\xi_2), \ldots u_m(\xi_N)]^T$, where T stands for the transpose. The boundary conditions are then imposed on the matrix equation (2.33), and making $\mathbf{U}_m$

the subject yields

$$\mathbf{U}_m = (\chi_m + \hbar)\mathbf{A}^{-1}\tilde{\mathbf{A}}\mathbf{U}_{m-1} + \hbar\mathbf{A}^{-1}\tilde{\mathbf{Q}}_{m-1}, \tag{2.34}$$

where $\tilde{\mathbf{A}}$ and $\tilde{\mathbf{Q}}_{m-1}$ are matrices obtained after applying the boundary conditions to the right hand side of equation (2.33). Equation (2.34) gives a recursive formula that is used to find solutions of the higher order approximations $u_m(x)$, $(m \geq 1)$. The recursive formula for the HAM involves a series of ordinary differentiation equations, equation (2.34) gives a series of algebraic equations, and as Boyd (2000) points out, it is easier to evaluate a function than to integrate a differential equation.

2.2.2 Convergence theorem for the SHAM

Unless the series (2.24) converges, the results obtained by this method cannot be regarded as useful. The functions $u_m(x)$ are governed by the higher order deformation equation (2.25). As suggested earlier, this approach serves to remove some limitations of the HAM. There is a very slight difference between the higher order deformation equations found using the SHAM and those found using the HAM. Liao (2003b, ch. 3) proved the convergence of the series (2.24). Proof of convergence of the series (2.4) associated with equation (2.28) is given in Liao (2003b, ch. 3);

Theorem 2.1. *As long as the series*

$$f_0(x,t) + \sum_{m=1}^{\infty} f_m(x,t) \tag{2.35}$$

is convergent, where $f_m(x,t)$ is governed by the high-order deformation equation (2.7), it must be a solution of equation (2.1).

Proof. See Liao (2003b, ch. 3). ■

This theorem also guarantees convergence of the SHAM series.

2.2.3 Strengths and weaknesses of the SHAM

The strengths and weaknesses of the SHAM will be discussed relative to the HAM since this method is an improvement to the HAM. We start with the strengths of the method. In finding the initial approximation more information about the governing equation is used as opposed to the boundary conditions only. The initial guess obtained is therefore a better function than in the case of the HAM. There is no restriction on the nature of the initial guess as long as it exists and is nontrivial. In the case of the HAM, the initial guess has to be expressed as a sum of basis functions which are conveniently chosen to be easy to integrate (van Gorder and Vajravelu, 2009). This restriction is unnecessary in relation to the SHAM.

In using the HAM, an auxiliary function $H(x)$ is chosen to force all coefficients of the higher order deformation to be expressed by the basis functions (van Gorder and Vajravelu, 2009; Liao, 2003b). This is done to ensure that the higher order deformation equations are possible to integrate. The SHAM algorithm does not require an $H(x)$ and gives a series of algebraic equations as opposed to ordinary differential equations. This makes it possible for the SHAM to handle problems with complicated initial guesses and linear operators.

The method gives fast converging solutions with high accuracy (Makukula et al., 2010b; Motsa et al., 2010; Motsa and Shateyi, 2010; Motsa and Sibanda, 2011). The use of a spectral method to solve the higher order deformation equations further accelerates the convergence of the SHAM. The method uses the default value $\hbar = -1$ to give good results except when the equation is strongly nonlinear or has special functions that increase its complexity. Nonethe-

less, finding the right number of collocation points to use for a particular problem is not straightforward, although experience in application of the method makes it easier. The choice becomes more crucial if the problem domain is unbounded at one or both ends. The domain truncation procedure (Boyd, 2000) allows the use of a scaling parameter L to invoke the boundary conditions at the free end. It is also not obvious which combination of N and L would give optimal performance of the SHAM for a particular problem.

2.3. The successive linearisation method

In the successive linearisation method (SLM) one assumes that the error in an approximate solution decreases with an increase in the number of iterations. In the sections that follow, the theoretical foundation of the method is explained. The method is used to solve nonlinear equations and nonlinear systems of ordinary differential equations (ODEs).

2.3.1 The SLM for nonlinear ODEs in one variable

Consider a general nth-order nonlinear ODE represented by a nonlinear boundary value problem of the form

$$\mathcal{L}[y(x), y'(x), \ldots, y^{(n)}(x)] + \mathcal{N}[y(x), y'(x), \ldots, y^{(n)}(x)] = 0, \quad x \in [a, b], \tag{2.36}$$

subject to the boundary conditions

$$y(a) = y_a, \qquad y(b) = y_b, \tag{2.37}$$

where $y(x)$ is an unknown function, x is an independent variable and the primes denote ordinary differentiation with respect to x, $\mathcal{L}$ and $\mathcal{N}$ represent the linear and nonlinear components of the governing equation and y_a and y_b are given constants. As an initial guess of the solution of (2.36), we propose as a guide a function that satisfies the boundary conditions (2.37). Thus a polynomial function (in this case a straight line) that satisfies the boundary conditions is considered as a suitable initial guess solution, denoted by $y_0(x)$. We define a function $Y_1(x)$ to represent the vertical difference between $y(x)$ and the initial guess $y_0(x)$, shown in Figure 2.1, that is

$$Y_1(x) = y(x) - y_0(x), \quad \text{or} \quad y(x) = y_0(x) + Y_1(x). \tag{2.38}$$

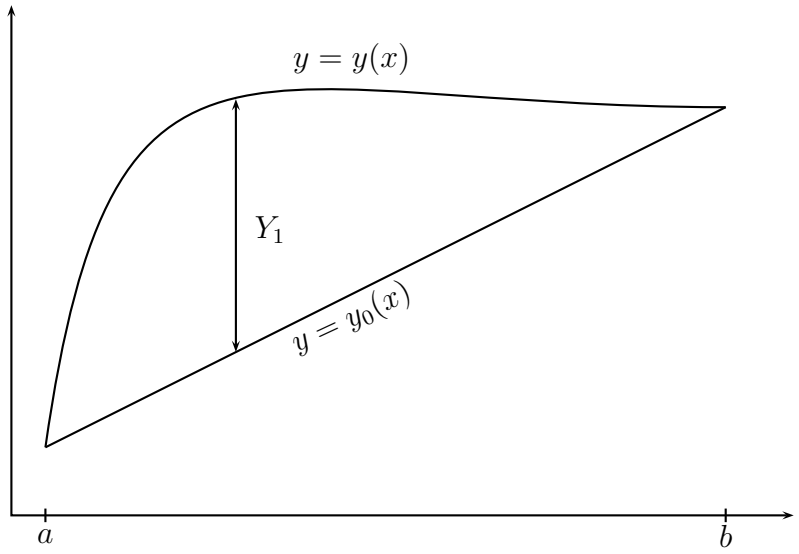

Figure 2.1: *Geometric representation of* $Y_1(x)$

Substituting equation (2.38) in (2.36) gives

$$\mathcal{L}[Y_1, Y_1', \ldots, Y_1^{(n)}] + \mathcal{N}[y_0 + Y_1, y_0' + Y_1', \ldots, y_0^{(n)} + Y_1^{(n)}] = -\mathcal{L}[y_0, y_0', \ldots, y_0^{(n)}]. \tag{2.39}$$

Since $y_0(x)$ is known, solving equation (2.39) would yield an exact solution for $Y_1(x)$. However, since the equation is nonlinear, it may not be possible to find an exact solution. We therefore seek an approximate solution which is obtained by solving the linear part of the equation and assuming that $Y_1(x)$ and its derivatives are small. If $Y_1(x)$ is the solution of equation (2.39) we let $y_1(x)$ denote the solution of the linear part of (2.39) which takes the following composite form

$$a_{0,0}y_1^{(n)} + a_{1,0}y_1^{(n-1)} + \cdots + a_{n-1,0}y_1' + a_{n,0}y_1 = r_0(x), \tag{2.40}$$

subject to the boundary conditions

$$y_1(a) = 0, \quad y_1(b) = 0. \tag{2.41}$$

The coefficients $a_{k,0}$, $k = 0, 1, \ldots, n$ are functions of the initial guess and its derivatives, that

is $a_{k,0} = a_{k,0}(y_0, y_0', \ldots y_0^{(n)})$ and

$$r_0(x) = -\left(\mathcal{L}[y_0, y_0', y_0'', \ldots, y_0^{(n)}] + \mathcal{N}[y_0, y_0', y_0'', \ldots, y_0^{(n)}]\right).$$

Since the left hand side of equation (2.40) is linear and the right hand side is known, a solution for $y_1(x)$ can be found. From this the first order approximation of the solution $y(x)$ can be written as

$$y(x) \approx y_0(x) + y_1(x). \tag{2.42}$$

Since $y_1(x)$ is an approximate solution of $Y_1(x)$, we can improve the solution by defining a new *slack* function $Y_2(x)$ and add it to $y_1(x)$ as shown in Figure 2.2, to have

$$Y_1(x) = y_1(x) + Y_2(x). \tag{2.43}$$

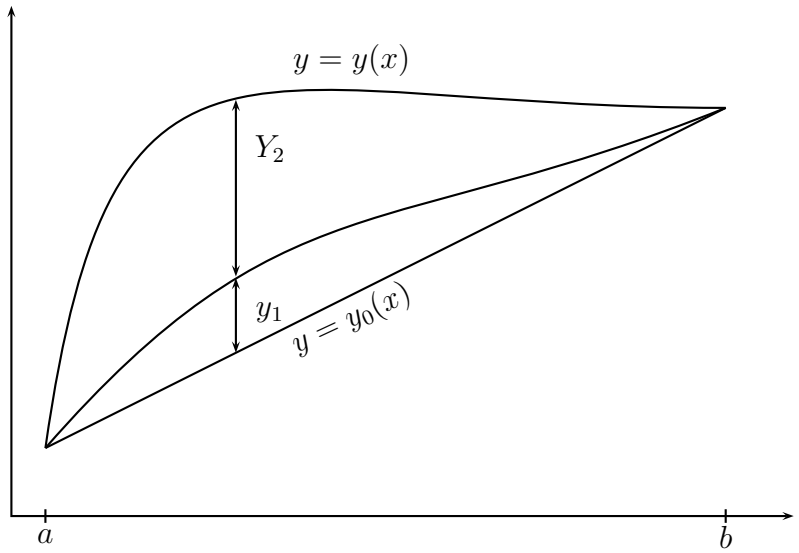

Figure 2.2: *Geometric representation of* Y_2

Equation (2.38) then takes the form

$$y(x) = y_0(x) + y_1(x) + Y_2(x). \tag{2.44}$$

Substituting equation (2.43) into (2.39) yields

$$\begin{aligned}\mathcal{L}[Y_2, Y_2', Y_2'', \ldots, Y_2^{(n)}] &+ \mathcal{N}[y_0 + y_1 + Y_2, y_0' + y_1' + Y_2', y_0'' + y_1'' + Y_2'', \\ &\quad \ldots, y_0^{(n)} + y_1^{(n)} + Y_2^{(n)}] \\ &= -\mathcal{L}[y_0 + y_1, y_0' + y_1', y_0'' + y_1'', \ldots, y_0^{(n)} + y_1^{(n)}].\end{aligned} \tag{2.45}$$

Equation (2.45) is nonlinear in $Y_2(x)$ and so an exact solution might not be possible. We solve the linear part and denote its solution by $y_2(x)$ so that $Y_2(x) \approx y_2(x)$. This will give rise to the new form

$$a_{0,1}y_2^{(n)} + a_{1,1}y_2^{(n-1)} + \cdots + a_{n-1,1}y_2' + a_{n,1}y_2 = r_1(x), \tag{2.46}$$

subject to the boundary conditions

$$y_2(a) = 0, \quad y_2(b) = 0. \tag{2.47}$$

The coefficients $a_{k,1}$ are now functions of $y_0(x)$ and $y_1(x)$ and their derivatives, $a_{k,1} = a_{k,1}(y_0 + y_1, y_0' + y_1', y_0'' + y_1'', \ldots, y_0^{(n)} + y_1^{(n)})$ and the right hand side

$$r_1(x) = -\left(\mathcal{L}[y_0 + y_1, y_0' + y_1', \ldots, y_0^{(n)} + y_1^{(n)}] + \mathcal{N}[y_0 + y_1, y_0' + y_1', \ldots, y_0^{(n)} + y_1^{(n)}]\right).$$

After solving equation (2.46), the 2nd order estimate of the solution $y(x)$ is given by

$$y(x) \approx y_0(x) + y_1(x) + y_2(x). \tag{2.48}$$

as suggested by equation (2.44). To again improve this solution, a new *slack* function $Y_3(x)$ is defined, shown in Figure 2.3, such that

$$Y_2(x) = y_2(x) + Y_3(x). \tag{2.49}$$

Equation (2.49) is substituted in the nonlinear equation (2.45) and the linear part of the equation solved. This is repeated for $m = 3, 4, 5, ...i$ to give the general form

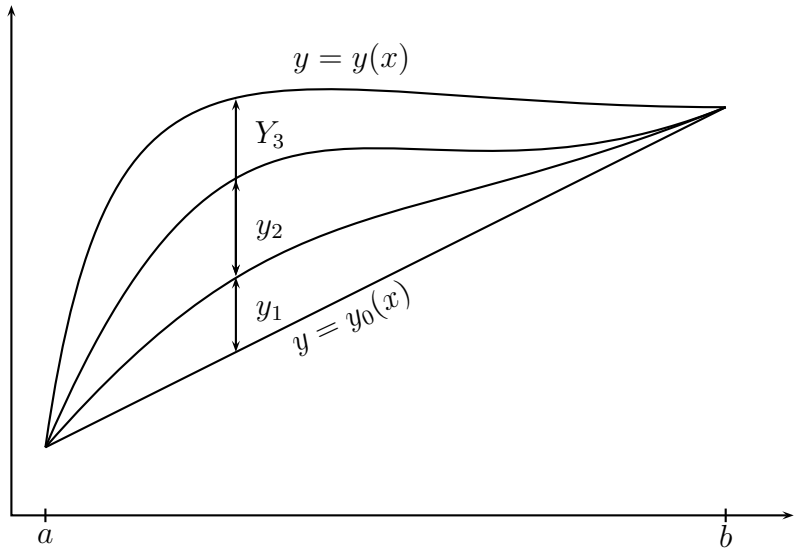

Figure 2.3: *Geometric representation of* Y_3

$$Y_i(x) = y_i(x) + Y_{i+1}(x). \tag{2.50}$$

The solution $y(x)$ is obtained as

$$\begin{aligned} y(x) &= y_0(x) + Y_1(x), && (2.51)\\ &= y_0(x) + y_1(x) + Y_2(x), && (2.52)\\ &= y_0(x) + y_1(x) + y_2(x) + Y_3(x), && (2.53)\\ &\vdots \\ &= y_0(x) + y_1(x) + y_2(x) + \ldots y_i(x) + Y_{i+1}(x) && (2.54)\\ &= \sum_{m=0}^{i} y_m(x) + Y_{i+1}(x).. && (2.55) \end{aligned}$$

We note that $Y_{i+1}(x)$ becomes increasingly small as i increases, that is

$$\lim_{i\to\infty} Y_{i+1} = 0.$$

The ith order solution $y(x)$ is then approximated by

$$y(x) = \sum_{m=0}^{i} y_m(x) = \sum_{m=0}^{i-1} y_m(x) + y_i(x). \tag{2.56}$$

Starting from the initial guess $y_0(x)$, the solutions $y_i(x)$ are obtained by successively linearising equation (2.36) and solving the resulting linear equation. The general form of the linearised equation that is successively solved for $y_i(x)$ is given by

$$a_{0,i-1}y_i^{(n)} + a_{1,i-1}y_i^{(n-1)} + \cdots + a_{n-1,i-1}y_i' + a_{n,i-1}y_i = r_{i-1}(x), \tag{2.57}$$

subject to the boundary conditions

$$y_i(a) = 0, \quad y_i(b) = 0, \tag{2.58}$$

where

$$a_{k,i-1} = a_{k,i-1}\left(\sum_{m=0}^{i-1} y_m(x), \sum_{m=0}^{i-1} y_m'(x), \sum_{m=0}^{i-1} y_m''(x), \ldots, \sum_{m=0}^{i-1} y_m^{(n)}(x)\right), \tag{2.59}$$

$$k = 0, 1, 2, \ldots n,$$

$$r_{i-1}(x) = -\mathcal{L}\left[\sum_{m=0}^{i-1} y_m(x), \sum_{m=0}^{i-1} y_m'(x), \sum_{m=0}^{i-1} y_m''(x), \ldots, \sum_{m=0}^{i-1} y_m^{(n)}(x)\right] \tag{2.60}$$

$$- \mathcal{N}\left[\sum_{m=0}^{i-1} y_m(x), \sum_{m=0}^{i-1} y_m'(x), \sum_{m=0}^{i-1} y_m''(x), \ldots, \sum_{m=0}^{i-1} y_m^{(n)}(x)\right]. \tag{2.61}$$

2.3.2 The SLM for systems of nonlinear ODEs

In this section we describe the SLM for nonlinear systems of ODEs. Consider a general nth-order nonlinear system represented by a nonlinear boundary value problem of the form

$$\mathbf{L}[Y(x), Y'(x), Y''(x), \ldots, Y^{(n)}] + \mathbf{N}[Y(x), Y'(x), Y''(x), \ldots, Y^{(n)}] = 0, \tag{2.62}$$

where $Y(x)$ represents a vector of unknown functions, x is the independent variable and the primes denote ordinary differentiation with respect to x, $\mathbf{L}$ and $\mathbf{N}$ are vector functions

representing the linear and nonlinear parts of the system of equations respectively. These are defined as follows;

$$\mathbf{L} = \begin{bmatrix} L_1\left(y_1, y_2, \ldots, y_k; y_1', y_2', \ldots, y_k'; \ldots; y_1^{(n)}, y_2^{(n)}, \ldots, y_k^{(n)}\right) \\ L_2\left(y_1, y_2, \ldots, y_k; y_1', y_2', \ldots, y_k'; \ldots; y_1^{(n)}, y_2^{(n)}, \ldots, y_k^{(n)}\right) \\ \vdots \\ L_k\left(y_1, y_2, \ldots, y_k; y_1', y_2', \ldots, y_k'; \ldots; y_1^{(n)}, y_2^{(n)}, \ldots, y_k^{(n)}\right) \end{bmatrix}, \tag{2.63}$$

$$\mathbf{N} = \begin{bmatrix} N_1\left(y_1, y_2, \ldots, y_k; y_1', y_2', \ldots, y_k'; \ldots; y_1^{(n)}, y_2^{(n)}, \ldots, y_k^{(n)}\right) \\ N_2\left(y_1, y_2, \ldots, y_k; y_1', y_2', \ldots, y_k'; \ldots; y_1^{(n)}, y_2^{(n)}, \ldots, y_k^{(n)}\right) \\ \vdots \\ N_k\left(y_1, y_2, \ldots, y_k; y_1', y_2', \ldots, y_k'; \ldots; y_1^{(n)}, y_2^{(n)}, \ldots, y_k^{(n)}\right) \end{bmatrix}, \tag{2.64}$$

$$Y(x) = \begin{bmatrix} y_1(x) \\ y_2(x) \\ \vdots \\ y_k(x) \end{bmatrix}, \tag{2.65}$$

$$\tag{2.66}$$

where $y_1, y_2, \ldots, y_k$ are the unknown functions. An initial guess $Y_0(x)$ is defined by

$$Y_0(x) = \begin{bmatrix} y_{1,0}(x) \\ y_{2,0}(x) \\ \vdots \\ y_{k,0}(x) \end{bmatrix}. \tag{2.67}$$

For demonstration purposes, it is assumed that equation (2.62) is to be solved for $x \in [a, b]$ subject to the boundary conditions

$$Y(a) = Y_a, \qquad Y(b) = Y_b, \tag{2.68}$$

where Y_a and Y_b are given constants. An initial guess $Y_0(x)$ will consist of functions that satisfy the boundary conditions. A function $Z_1(x)$ is defined to represent the vertical difference between $Y(x)$ and $Y_0(x)$, that is

$$Z_1(x) = Y(x) - Y_0(x), \quad \text{or} \quad Y(x) = Y_0(x) + Z_1(x). \tag{2.69}$$

Consider for instance, the vertical displacement between the function $y_1(x)$ and its corresponding initial guess $y_{1,0}(x)$ to be $z_{1,1} = y_1(x) - y_{1,0}(x)$. This is shown in Figure 2.4. Substituting

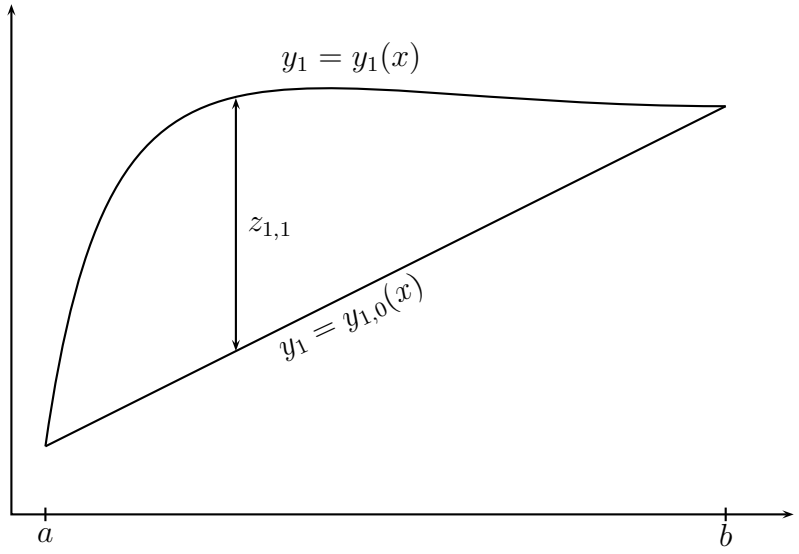

Figure 2.4: *Geometric representation of* $z_{1,1}(x)$

equation (2.69) in (2.62) gives

$$\mathbf{L}[Z_1, Z_1', \ldots, Z_1^{(n)}] + \mathbf{N}[Y_0 + Z_1, Y_0' + Z_1', \ldots, Y_0^{(n)} + Z_1^{(n)}] = -\mathcal{L}[Y_0, Y_0', \ldots, Y_0^{(n)}]. \tag{2.70}$$

Since $Y_0(x)$ is a known function, solving equation (2.70) would in theory yield an exact solution for $Z_1(x)$. An approximate solution is obtained by solving the linear part of the equation (2.70) assuming that Z_1 and its derivatives are small. If $Z_1(x)$ is the solution of the full equation (2.70), we let $Y_1(x)$ denote the solution of the linear part of (2.70) thus assume $Z_1(x) \approx Y_1(x)$.

The linear part gives the equation

$$\mathbf{A}_{0,0}Y_1^{(n)} + \mathbf{A}_{1,0}Y_1^{(n-1)} + \cdots + \mathbf{A}_{n-1,0}Y_1' + \mathbf{A}_{n,0}Y_1 = \tag{2.71}$$
$$-\left(\mathbf{L}[Y_0, Y_0', \ldots, Y_0^{(n)}] + \mathbf{N}[Y_0, Y_0', \ldots, Y_0^{(n)}]\right),$$

with $\mathbf{A}_{k,0} = \mathbf{A}_{k,0}(Y_0, Y_0', Y_0'', \ldots, Y_0^{(n)}), k = 0, 1, 2, \ldots, n$. Since the right hand side of equation (2.71) is known and the left hand side is linear, the equation can be solved for $Y_1(x)$. The first order estimate of the solution $Y(x)$ is

$$Y(x) \approx Y_0(x) + Y_1(x). \tag{2.72}$$

To improve this solution, we define a *slack* function, $Z_2(x)$ such that (Figure 2.5)

$$Z_1(x) = Y_1(x) + Z_2(x). \tag{2.73}$$

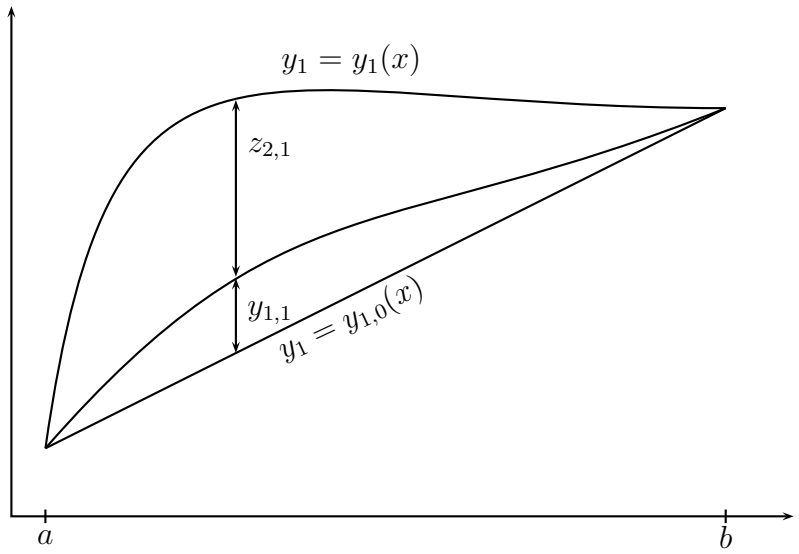

Figure 2.5: *Geometric representation of* $z_{2,1}$

Since $Y_1(x)$ is now known (as a solution of equation (2.71)), we substitute equation (2.73) in equation (2.70) to obtain

$$\begin{aligned}\mathbf{L}[Z_2, Z_2', \ldots, Z_2^{(n)}] \;+\; & \mathbf{N}[Y_0 + Y_1 + Z_2 +, Y_0' + Y_1' + Z_2', \ldots, Y_0^{(n)} + Y_1^{(n)} + Z_2^{(n)}] \\ = \; & -\mathcal{L}[Y_0 + Y_1, Y_0' + Y_1', \ldots, Y_0^{(n)} + Y_1^{(n)}]. \end{aligned} \tag{2.74}$$

Solving equation (2.74) would give in an exact solution for $Z_2(x)$. We solve the linear part of the equation and represent its solution by $Y_2(x)$. Setting $Z_2(x) = Y_2(x)$, substituting in equation (2.74) and assuming that $Y_2(x)$ and its derivatives are small, gives

$$\begin{aligned}&\mathbf{A}_{0,1}Y_2^{(n)} + \mathbf{A}_{1,1}Y_2^{(n-1)} + \cdots + \mathbf{A}_{n-1,1}Y_2' + \mathbf{A}_{n,0}Y_1 = \\ &-\Big(\mathbf{L}[Y_0 + Y_1, Y_0' + Y_1', \ldots, Y_0^{(n)} + Y_1^{(n)}] + \mathbf{N}[Y_0 + Y_1, Y_0' + Y_1', \ldots, Y_0^{(n)} + Y_1^{(n)}]\Big),\end{aligned} \tag{2.75}$$

where

$$\mathbf{A}_{k,1} = \mathbf{A}_{k,1}(Y_0 + Y_1, Y_0' + Y_1', Y_0'' + Y_1'', \ldots, Y_0^{(n)} + Y_1^{(n)}), \quad k = 0, 1, 2, \ldots, n.$$

After solving (2.75), the second order estimate of the solution $Y(x)$ is now

$$Y(x) \approx Y_0(x) + Y_1(x) + Y_2(x). \tag{2.76}$$

This process is repeated for $m = 2, 3, 4, 5, \ldots, i$. In general, it can be shown that

$$Z_i(x) = Z_{i+1}(x) + Y_i(x). \tag{2.77}$$

Thus, $Y(x)$ is obtained as

$$\begin{aligned} Y(x) &= Y_0(x) + Z_1(x), && (2.78)\\ &= Y_0(x) + Y_1(x) + Z_2(x), && (2.79)\\ &= Y_0(x) + Y_1(x) + Y_2(x) + Z_3(x), && (2.80)\\ &\vdots \\ &= Y_0(x) + Y_1(x) + Y_2(x) + Y_3(x) + \ldots + Y_i(x) + Z_{i+1}(x), && (2.81)\\ &= \sum_{m=0}^{i} Y_m(x) + Z_{i+1}(x). && (2.82) \end{aligned}$$

The procedure for obtaining each $Z_i(x)$ is illustrated in Figures 2.4 and 2.5 respectively for $i = 1, 2$. We note that when i is large, Z_{i+1} is small, hence for large i, we can approximate the ith order solution of $Y(x)$ by

$$Y(x) = \sum_{m=0}^{i} Y_m(x) = \sum_{m=0}^{i-1} Y_m(x) + Y_i(x). \tag{2.83}$$

Starting from a known initial guess $Y_0(x)$, the solutions $Y_i(x)$ $(i \geq 2)$ can be obtained by successively solving the resulting linear part of the governing equation (2.62) for $Y_i(x)$. The general form of the linear part of the equation to be solved for $Y_i(x)$ is given by

$$\mathbf{A}_{0,i-1}Y_i^{(n)} + \mathbf{A}_{1,i-1}Y_i^{(n-1)} + \ldots + \mathbf{A}_{n-1,i-1}Y_i' + \mathbf{A}_{n,i-1}Y_i = \mathbf{r}_{i-1}(x), \tag{2.84}$$

where for $k = 0, 1, \ldots, n$;

$$\begin{aligned} \mathbf{A}_{k,i-1}(x) &= \mathbf{A}_{k,i-1}(x)\left(\sum_{m=0}^{i-1} Y_m, \sum_{m=0}^{i-1} Y_m', \sum_{m=0}^{i-1} Y_m'', \ldots, \sum_{m=0}^{i-1} Y_m^{(n)}\right), && (2.85)\\ \mathbf{r}_{i-1}(x) &= -\mathbf{L}\left(\sum_{m=0}^{i-1} Y_m, \sum_{m=0}^{i-1} Y_m', \sum_{m=0}^{i-1} Y_m'', \ldots, \sum_{m=0}^{i-1} Y_m^{(n)}\right) \\ &\quad -\mathbf{N}\left(\sum_{m=0}^{i-1} Y_m, \sum_{m=0}^{i-1} Y_m', \sum_{m=0}^{i-1} Y_m'', \ldots, \sum_{m=0}^{i-1} Y_m^{(n)}\right). && (2.86) \end{aligned}$$

The recursive equations (2.57) and (2.84) are solved using the Chebyshev spectral collocation method.

2.3.3 Strengths and weaknesses of the SLM

The SLM inherits the fast convergence and accuracy of the Chebyshev spectral collocation method. In Makukula et al. (2010c) (see Chapter 5) the SLM is shown to give converging results after a few iterations. It has been used successfully to solve a limited range of nonlinear ODEs of varying complexity. The SLM algorithm is not purely numerical, it can be modified to generate analytical results. Choosing N is however still a trial an error exercise. Using the SLM on irregular domains might cause loss of accuracy. The mathematical foundation for this method is yet to be established. It is essential to develop general theorems and mathematical guidelines for the SLM.

2.4. Improved spectral homotopy analysis method

In the improved spectral homotopy analysis method (ISHAM) the main innovation is the further improvement of the initial approximation used in the spectral homotopy analysis method. A more convergent form of the initial solution is used in the higher order deformation equations. This new approach merges ideas from both the SLM and the SHAM. The initial approximate solution takes the form of a general SLM solution and is then used in the SHAM algorithm.

For a nonlinear equation

$$\mathcal{N}[f(x)] = g(x), \tag{2.87}$$

the following transformation is made

$$f(x) = f_i(x) + \sum_{n=0}^{i-1} f_n(x). \tag{2.88}$$

We note that equation (2.88) takes the general form of an SLM solution. The series (2.88) is substituted into (2.87) and starting with an initial guess $f_0(x)$, the resulting equation is solved using the standard SHAM. The zeroth order deformation equations now takes the form

$$(1-q)\mathcal{L}[F_i(x;q) - f_{i,0}(x)] = q\hbar\{\mathcal{N}[f_i(x;q)] - r_{i-1}(x)\}, \quad q \in [0,1]. \tag{2.89}$$

The higher order deformation equations take the form (see equation (2.25)

$$\mathcal{L}[f_{i,m}(x) - (\chi_m + \hbar) f_{i,m-1}(x)] = \hbar R_{i,m}(x), \tag{2.90}$$

where the solution f_i is given by

$$f_i = f_{i,0} + f_{i,1} + f_{i,2} + f_{i,3} + \cdots + f_{i,m}. \tag{2.91}$$

The solution for $f(x)$ is then given by

$$f(x) = f_i + \sum_{n=0}^{i-1} f_n(x). \tag{2.92}$$

3

Fluid flow between parallel plates

Fluid flow between two parallel surfaces has received much attention because of its importance in many fields of science and engineering. Such areas include electrostatic precipitation, polymer technology, petroleum industry (Attia, 2005), food and pharmaceutical industries (Iqbal et al., 2011). Many experimental and theoretical studies have been documented in the literature where means of optimizing the desired products were sought.

In this Chapter we investigated two fluid flow problems between parallel plates using the successive linearisation method, the spectral homotopy analysis method and the improved spectral homotopy analysis method. The successive linearisation method was used to solve the fourth order nonlinear equation governing a two-dimensional constant speed squeezing flow of a viscous fluid between two approaching parallel plates in Section 3.1. A comparison between results obtained using the successive linearisation method and those in the literature, and the numerical solution in terms of accuracy and efficiency of the method. The comparison revealed the efficiency and accuracy of the method compared to the homotopy analysis method. Its efficiency was not compromised by increasing parameter values in the equation. The spectral homotopy analysis method, the successive linearisation method and the im-

proved spectral homotopy analysis method were used to study the steady laminar flow of a pressure driven third-grade fluid with heat transfer in a horizontal channel in Sections 3.2 and 3.3. The computational efficiency and accuracy of the spectral-homotopy analysis method was demonstrated by comparing the results with those obtained using the homotopy analysis method. Results obtained using the improved spectral homotopy analysis method and the successive linearisation method showed that both methods converged rapidly to the exact solution. However, the ISHAM converged much more rapidly than the SLM. Convergence to the exact solution was achieved by both methods for all parameter values, with the ISHAM showing better convergence for larger parameter values. The results were also consistent with results from earlier findings.

3.1. On a new solution for the visco-elastic squeezing flow between two parallel plates [1]

Corrigenda

The following corrections and further explanations have been made to the published work in Section 3.1.

(i) Problem geometry

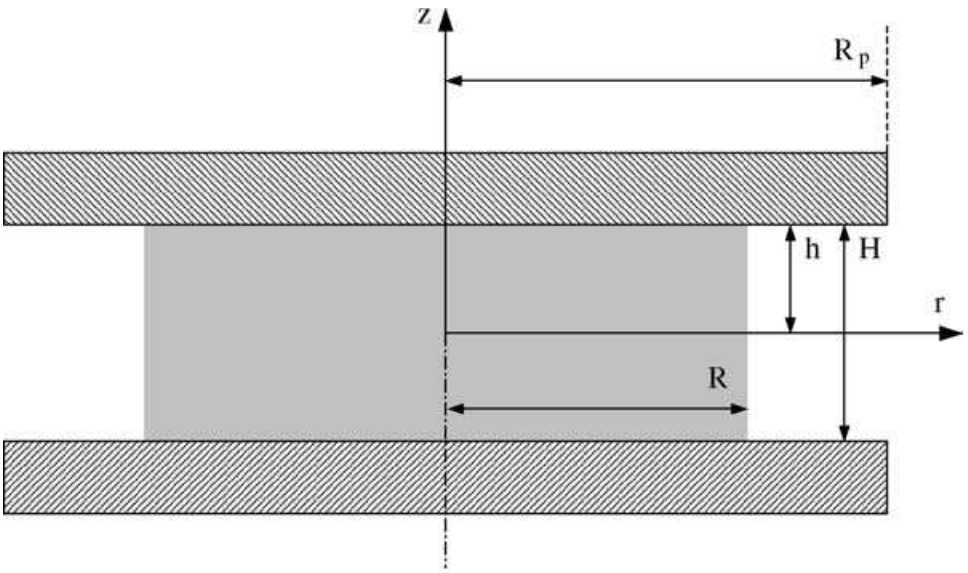

Figure 3.1: *Coordinate system and basic dimensions used to describe axisymmetric squeeze flows (Engmann et al., 2005).*

(ii) On page 33, a different parameter M_1 should have been used to represent the SLM order.

[1] Z. G. Makukula, S. S. Motsa and P. Sibanda (2010). *Journal of Advanced Research in Applied Mathematics* 2(4):31–38.

(iii) On page 34 equation (3.14) is incorrect. The correct equation is

$$\frac{d^a f_i}{dz^a} = \sum_{k=0}^{N} D_{kj}^a f_i(x_k), \quad j = 0, 1, ..., N.$$

Further explanations:

(i) On page 35 the results were generated using $N = 40$. The tolerance used with the bvp4c was 1×10^{-9} and eight decimal places were used with the SLM results while five decimal places were used for the HAM solutions.

(ii) The HAM failed to converge even at the $50th$ order for $M = 10$ as noted in reference [14]. In Table 3 the SLM gives convergent results at the sixth order for large values of M.

Journal of Advanced Research in Applied Mathematics

Vol. 2, Issue. 4, 2010, pp. 31-38
Online ISSN: 1942-9649

On a new solution for the viscoelastic squeezing flow between two parallel plates

Makukula Zodwa[1], Motsa Sandile[2,*], Sibanda Precious[1]

[1] *School of Mathematical Sciences, University of KwaZulu Natal,Private Bag X01, Scottsville 3209, Pietermaritzburg, South Africa.*
[2] *Department of Mathematics, University of Swaziland, P/Bag 4, Kwaluseni, Swaziland.*

Abstract. A newly developed successive linearization method for nonlinear problems in engineering and science is used to solve the nonlinear equation governing two-dimensional constant speed squeezing flow of a viscous fluid between two approaching parallel plates. The results obtained using the SLM were compared with those in the literature and against the numerical solution in terms of accuracy and efficiency of the method. The findings from the comparisons prove that the SLM is powerful, more efficient yet simple to use than the HAM and is independent of the size of parameter values used in the problem.

Keywords: Squeezing flow; Linearization method; Spectral method; Nonlinear equations.

Mathematics Subject Classification 2010: 34B15,65L10,76A10,76M25.

1 Introduction

Squeezing flow occurs when a fluid, particularly a viscoelastic fluid, is constrained in the gap between two parallel plates or coaxial disks resulting in both shear and longitudinal deformation. Such flows occur in many practical applications such as in polymer extrusion and compression moulding processes in industry as well as in lubrication theory where a thin film of oil prevents contact between metal surfaces. Due to the changing geometry, squeezing flows are inherently transient and inhomogeneous [4,7,9,13,14]. Various aspects of squeeze flows have been studied theoretically and experimentally by previous researchers [7,14]. In most of these studies perturbation techniques have been used to solve the governing nonlinear equations. The homotopy analysis method (HAM) has been used recently by Ran et al [14] to find analytical solutions of the equations for squeezing flow between two infinite plates. However, as shown by Motsa et al [11,12], the HAM has a number of limitations and in this paper, we solve the problem in [14] using a new method, hereinafter referred to as the successive linearization method (SLM).

*Correspondence to: Motsa Sandile, Department of Mathematics, University of Swaziland, P/Bag 4, Kwaluseni, Swaziland. Email: sandilemotsa@gmail.com
†Received: 3 June 2010, accepted: 26 July 2010.

2 Governing equations

The problem under consideration is that of a two-dimensional quasi-steady axisymmetric flow of an incompressible viscous fluid between two infinite parallel plates as in [14]. The velocity is $\mathbf{u} = [u_r(r,z,t), 0, u_z(r,z,t)]$ and the governing equations can be expressed as

$$\frac{\partial p}{\partial r} + \frac{\rho}{r}\frac{\partial^2 \psi}{\partial t \partial z} - \rho \frac{\partial \psi}{\partial r}\frac{E^2\psi}{r^2} - \frac{\mu}{r}\frac{\partial E^2 \psi}{\partial z} = 0, \tag{2.1}$$

$$\frac{\partial p}{\partial r} - \frac{\rho}{r}\frac{\partial^2 \psi}{\partial t \partial z} - \rho \frac{\partial \psi}{\partial z}\frac{E^2\psi}{z^2} + \frac{\mu}{r}\frac{\partial E^2 \psi}{\partial z} = 0, \tag{2.2}$$

where r and z are the radial and axial coordinates respectively, ρ is the fluid density, μ is the coefficient of kinematic viscosity, p is the pressure and $\psi(r,z)$ is the Stokes stream function given by

$$u_r(r,z,t) = \frac{1}{r}\frac{\partial \psi}{\partial z}, \quad u_z(r,z,t) = -\frac{1}{r}\frac{\partial \psi}{\partial r} \quad \text{and} \quad E^2 = \frac{\partial^2}{\partial r^2} - \frac{1}{r}\frac{\partial}{\partial r} + \frac{\partial^2}{\partial z^2}. \tag{2.3}$$

Upon eliminating the generalized pressure p in (2.1 - 2.2) we get

$$\rho\left[\frac{1}{r}\frac{\partial E^2 \Psi}{\partial t} - \frac{\partial(\Psi, \frac{E^2\Psi}{r^2})}{\partial(r,z)}\right] = \frac{\mu}{r}E^4\Psi. \tag{2.4}$$

For small values of the approach velocity v of the two plates, the gap $2H$ changes slowly with time and can be assumed to constant, hence from (2.4) we write

$$-\rho\left[\frac{\partial(\psi, \frac{E^2\psi}{r^2})}{\partial(r,z)}\right] = \frac{\mu}{r}E^4\psi, \tag{2.5}$$

with the boundary conditions

$$\begin{aligned} u_r &= 0, \quad u_z = -V \quad \text{at} \quad z = H, \\ u_z &= 0, \quad \frac{\partial u_r}{\partial z} = 0 \quad \text{at} \quad z = 0. \end{aligned} \tag{2.6}$$

Using the stream function

$$\psi(r,z) = r^2 F(z), \tag{2.7}$$

and introducing the non-dimensional parameters

$$F^* = \frac{F}{V/2}, \quad Z^* = \frac{Z}{H}, \quad M = \frac{\rho H}{\mu/V}, \tag{2.8}$$

equation (2.5) and boundary conditions (2.6) become

$$F^{(iv)}(z) + MF(z)F'''(z) = 0, \tag{2.9}$$

and

$$\begin{aligned} F(0) = 0, \quad F''(0) = 0, \\ F(1) = 1, \quad F'(1) = 0. \end{aligned} \tag{2.10}$$

The nonlinear equation (2.9) with boundary conditions (2.10) is solved in the section that follows using the SLM.

3 Successive linearization method (SLM)

The main assumption made with the SLM is that the unknown function $F(z)$ can be expanded as

$$F(z) = F_i(z) + \sum_{m=0}^{i-1} f_m(z), \quad i = 1, 2, 3, \ldots, \tag{3.1}$$

where F_i, are unknown functions and f_m, $(m \geq 1)$ are approximations which are obtained by recursively solving the linear part of the equation that results from substituting (3.1) in the governing equation (2.9). Substituting (3.1) in the governing equation gives

$$F_i^{(iv)} + a_{1,i-1} F_i''' + a_{2,i-1} F_i + M F_i F_i''' = r_{i-1}, \tag{3.2}$$

where the coefficient parameters $a_{k,i-1}$, $(k = 1, 2)$, r_{i-1} are defined as

$$a_{1,i-1} = M \sum_{m=0}^{i-1} f_m, \quad a_{2,i-1} = M \sum_{m=0}^{i-1} f_m''', \tag{3.3}$$

$$r_{i-1} = -\left(\sum_{m=0}^{i-1} f_m^{(iv)} + M \sum_{m=0}^{i-1} f_m \sum_{m=0}^{i-1} f_m''' \right). \tag{3.4}$$

The SLM algorithm starts from the initial approximation

$$f_0(z) = \frac{1}{2}(3z - z^3), \tag{3.5}$$

which is chosen to satisfy the boundary conditions (2.10). The subsequent solutions for f_m , $m \geq 1$ are obtained by successively solving the linearized form of equation (3.2) and which is given as

$$f_i^{(iv)} + a_{1,i-1} f_i''' + a_{2,i-1} f_i = r_{i-1}, \tag{3.6}$$

subject to the boundary conditions

$$f_i(0) = 0, \quad f_i''(0) = 0, \quad f_i(1) = 1, \quad f_i'(1) = 0. \tag{3.7}$$

Once each solution for f_i, $(i \geq 1)$ has been found from iteratively solving equations (3.6) for each i, the approximate solution for $F(z)$ is obtained as

$$F(z) \approx \sum_{m=0}^{M} f_m(z), \tag{3.8}$$

where M is the order of SLM approximation. In coming up with (3.8), it is assumed that Fi become increasingly smaller when i becomes large, that is

$$\lim_{i \to \infty} F_i = 0. \tag{3.9}$$

Since the coefficient parameters and the right hand side of equations (3.6), for $i = 1, 2, 3, \ldots$, are known from previous iterations, equation (3.6) can easily be solved using analytical means or any numerical methods such as finite differences, finite elements, Runge-Kutta based shooting

methods or collocation methods. In this work, equations (3.6) is solved using the Chebyshev spectral collocation method. This method is based on approximating the unknown function by the Chebyshev interpolating polynomials in such a way that it is collocated at the Gauss-Lobatto points defined as

$$x_j = \cos\frac{\pi j}{N}, \quad j = 0, 1, \ldots, N, \tag{3.10}$$

where N is the number of collocation points used (see for example [2,3,15]). In order to implement the method, the physical region $[0, 1]$ is transformed into the region $[-1, 1]$ using the domain truncation technique. This leads to the mapping

$$z = \frac{x+1}{2}, \quad -1 \leq x \leq 1. \tag{3.11}$$

The unknown function f_i is approximated at the collocation points by

$$f_i(x) \approx \sum_{k=0}^{N} f_i(x_k) T_k(x_j), \; j = 0, 1, \ldots, N, \tag{3.12}$$

where T_k is the kth Chebyshev polynomial defined as

$$T_k(x) = \cos[k \cos^{-1}(x)]. \tag{3.13}$$

The derivatives of $f_i(z)$ at the collocation points are represented as

$$\frac{d^a f_i}{dz^a} = \sum_{k=0}^{N} \mathbf{D}^r_{kj} f_i(x_k), \; j = 0, 1, \ldots, N, \tag{3.14}$$

where a is the order of differentiation and $\mathbf{D} = 2\mathcal{D}$ with $\mathcal{D}$ being the Chebyshev spectral differentiation matrix (see for example, [2,15]). Substituting equations (3.11 - 3.12) in (3.6) leads to the matrix equation given by

$$\mathbf{A}\mathbf{Y}_i = \mathbf{R}_{i-1}, \tag{3.15}$$

in which $\mathbf{A}$ is an $(N+1) \times (N+1)$ square matrix and $\mathbf{Y}$ and $\mathbf{R}$ are $(N+1) \times 1$ column vectors defined by

$$\mathbf{A} = \mathbf{D}^4 + \mathbf{a}_{1,i-1}\mathbf{D}^3 + \mathbf{a}_{2,i-1}, \tag{3.16}$$

$$\mathbf{Y}_i = \mathbf{F}_i, \tag{3.17}$$

$$\mathbf{R}_{i-1} = \mathbf{r}_{i-1} \tag{3.18}$$

with

$$\mathbf{F}_i = [f_i(x_0), f_i(x_1), \ldots, f_i(x_{N-1}), f_i(x_N)]^T, \tag{3.19}$$

$$\mathbf{r}_{i-1} = [r_{i-1}(x_0), r_{i-1}(x_1), \ldots, r_{i-1}(x_{N-1}), r_{i-1}(x_N)]^T, \tag{3.20}$$

In the above definitions, $\mathbf{a}_{k,i-1}$, $(k = 1, 2)$ are diagonal matrices of size $(N+1) \times (N+1)$. After modifying the matrix system (3.15) to incorporate boundary conditions, the solution is obtained as

$$\tilde{\mathbf{Y}}_i = \mathbf{A}^{-1}\mathbf{R}_{i-1}. \tag{3.21}$$

4 Results and Discussion

In Table 1 we compare the solution of $F'''(0)$ from the SLM and the HAM in [14] against the bvp4c numerical solution when $M = 2$. Clearly, the SLM is computationally much more effective than the HAM since convergence to the numerical solution is achieved at the 3rd order of approximation while convergence of the HAM solution is achieved at the sixth order. The level of accuracy is also significantly better using the SLM at seven decimal places compared to five for the HAM solution.

Table 1: Comparison of $F'''(0)$ obtained at different orders for the SLM, HAM solution of [14] and bvp4c numerical solution when $M = 2$.

Present Results		Reference [14]		
Order	SLM	Order	HAM	bvp4c
2	-3.8447033	5	-3.84525	-3.8452065
3	-3.8452065	6	-3.84521	
4	-3.8452065	7	-3.84521	
5	-3.8452065	8	-3.84521	

Table 2 gives a comparison of the solutions of $F(z)$ obtained by the SLM against the bvp4c numerical solutions when $M = 2$. The SLM solutions converge to the numerical solutions with eight decimal place accuracy at 3rd order, which is remarkably very efficient.

In Table 3, the flexibility and strength of the method is demonstrated by its ability to converge for large parameter values used in the problem. The solution of $F'''(0)$ by the SLM is converging to the numerical solution at the 5th order of approximation for values of M as large $M = 50$. Previous studies have proved that the general weakness of most perturbation methods is their inability to converge when dealing with problems where large parameter values are involved.

Figures 1 - 2 show that the SLM approximate solutions to $F(z)$ and $F'(z)$ converge uniformly to the numerical solution at the 3rd order approximation for different values of M. This again demonstrate the reliability and robustness of the SLM to give accurate solutions for all parameter values.

Table 2: Comparison of $F(z)$ obtained at different orders of the SLM and the bvp4c numerical solution when $M = 2$.

z	2nd order	3rd order	4th order	5th order	6th order	bvp4c
0.1	0.15562079	0.15558330	0.15558330	0.15558330	0.15558330	0.15558330
0.2	0.30742785	0.30735107	0.30735107	0.30735107	0.30735107	0.30735107
0.3	0.45171816	0.45160336	0.45160336	0.45160336	0.45160336	0.45160336
0.4	0.58500183	0.58485835	0.58485835	0.58485835	0.58485835	0.58485835
0.5	0.70408538	0.70393178	0.70393178	0.70393178	0.70393178	0.70393178
0.6	0.80612744	0.80598750	0.80598750	0.80598750	0.80598750	0.80598750
0.7	0.88866331	0.88855853	0.88855853	0.88855853	0.88855853	0.88855853
0.8	0.94960079	0.94954223	0.94954223	0.94954223	0.94954223	0.94954223
0.9	0.98719348	0.98717592	0.98717592	0.98717592	0.98717592	0.98717592

Table 3: Comparison of the numerical results against the SLM approximate solutions for $F'''(0)$ for different values of M.

M	2nd order	3rd order	4th order	5th order	6th order	bvp4c
0	-3.000000	-3.000000	-3.000000	-3.000000	-3.000000	-3.000000
5	-5.058677	-5.071647	-5.071652	-5.071652	-5.071652	-5.071652
10	-6.848982	-6.852014	-6.853093	-6.853093	-6.853093	-6.853093
15	-8.434877	-8.312561	-8.344057	-8.344075	-8.344075	-8.344075
20	-9.772070	-9.631868	-9.635779	-9.635779	-9.635779	-9.635779
30	-12.040575	-11.834878	-11.837532	-11.837533	-11.837533	-11.837533
40	-14.225703	-13.700807	-13.712302	-13.712307	-13.712307	-13.712307
50	-15.845775	-15.366708	-15.372253	-15.372254	-15.372254	-15.372254

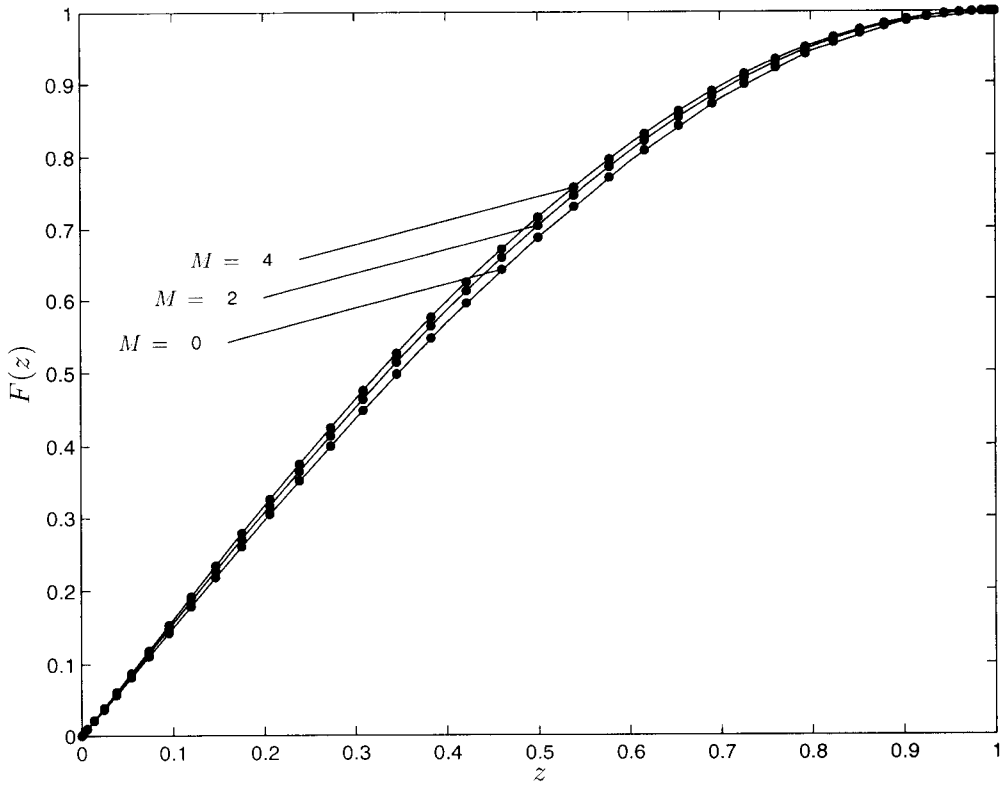

Figure 1: Comparison of $F(z)$ obtained from the 3rd order SLM approximate solution (filled circles) with the numerical solution (solid line) at different values of M.

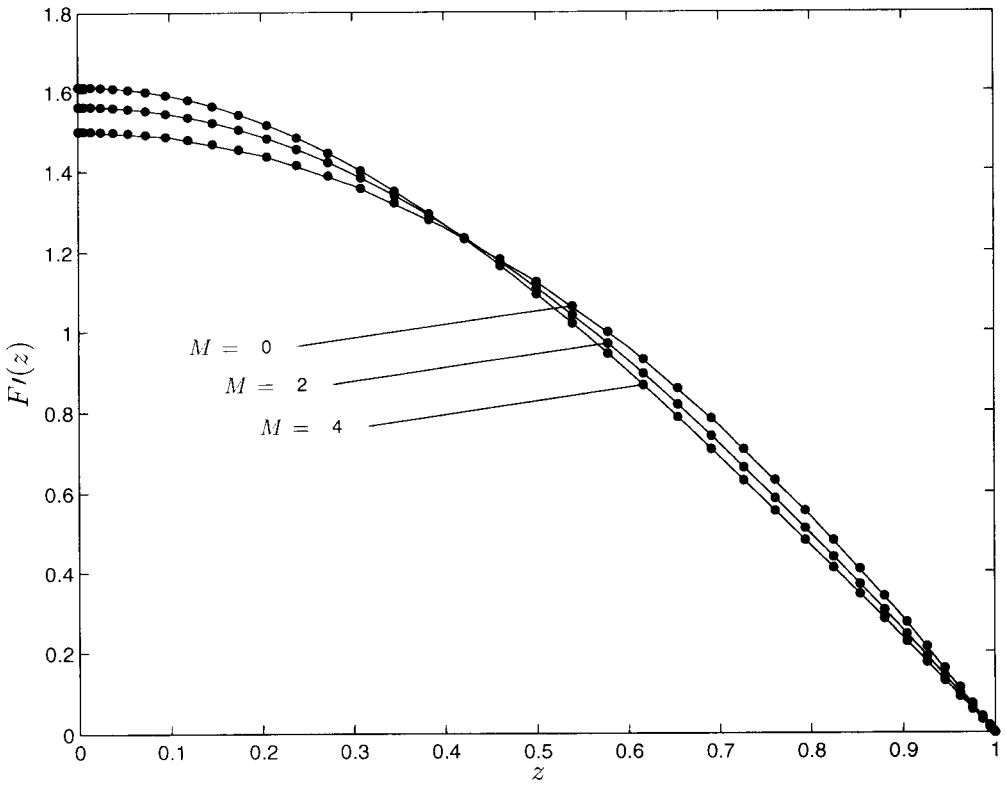

Figure 2: Comparison of $F'(z)$ obtained from the 3rd order SLM approximate solution (filled circles) with the numerical solution (solid line) at different values of M.

5 Conclusion

The nonlinear differential equation governing the squeezing flow between two infinite plates has been successfully solved in this work using a new algorithm for nonlinear problems. The SLM results were compared against those previously obtained using the HAM from [14] and the numerical results from the bvp4c solver. Both tabulated results (as shown in tables 1 - 2 and Figs 1 - 2) show that the SLM converges faster and is computationally more efficient than the HAM. The efficiency of the method is not compromised by the size of parameters inherent in the problem. It converges at low orders of approximation even for large parameter values. Hence we conclude that the SLM is a method that can be used to solve nonlinear systems occurring in science and engineering.

Acknowledgments

The authors wish to acknowledge financial support from the University of Kwa-Zulu Natal and the National Research Foundation (NRF).

References

[1] A. S. Burbidge, C. Servais. Squeeze flows of apparently lubricated thin films. J. Non-Newtonian Fluid Mech., 2004, 124: 115 - 127.

[2] C. Canuto, M.Y. Hussaini, A. Quarteroni, T.A. Zang. Spectral Methods in Fluid Dynamics. Springer-Verlag, Berlin, 1988.

[3] W.S. Don, A. Solomonoff. Accuracy and speed in computing the Chebyshev Collocation Derivative. SIAM J. Sci. Comput., 1995, 16(6): 1253 - 1268.

[4] M. Fang, R.P. Gilbert, X.-G. Liu. A squeeze flow problem with a Navier slip conditions. Mathematical and Computer Modelling, 2010, doi:10.1016/j.mcm.2010.02.024

[5] A.G. Gibson, S. Toll. Mechanics of the squeeze flow of planar fibre suspensions. J. Non-Newtonian Fluid Mech., 1999, 82: 1 - 24.

[6] A. P. Jackson, Xiao-Lin Liu, R. Paton. Squeeze flow characterisation of thermoplastic polymer. Composite Structures, 2006, 75: 179 - 184.

[7] J. Engmann, C. Servais, A.S. Burbidge. Squeeze flow theory and applications to rheometry: A review. J. Non-Newtonian Fluid Mech., 2005, 132: 1 27.

[8] G. Karapetsas, J. Tsamopoulos. Transient squeeze flow of viscoplastic materials. J. Non-Newtonian Fluid Mech., 2006, 133: 35 - 56.

[9] G. Lian, Y. Xub, W. Huang, M.J. Adams. On the squeeze flow of a power-law fluid between rigid spheres. J. Non-Newtonian Fluid Mech., 2001, 100: 151 - 164.

[10] S.J. Liao. The proposed homotopy analysis technique for the solution of nonlinear problems. PhD thesis, Shanghai Jiao Tong University, 1992.

[11] S.S. Motsa, P. Sibanda, S. Shateyi. A new spectral-homotopy analysis method for solving a nonlinear second order BVP. Commun. Nonlinear Sci. Numer. Simulat., 2010, 15: 2293 - 2302.

[12] S.S. Motsa, P. Sibanda, F.G. Awad, S. Shatey. A new spectral-homotopy analysis method for the MHD Jeffery-Hamel problem. Computer & Fluids, 2010, 39: 1219 - 1225

[13] G.H. Meeten. Effects of plate roughness in squeeze-flow rheometry. J. Non-Newtonian Fluid Mech., 2004, 124: 51 - 60.

[14] X.J. Ran, Q.Y. Zhu, Y. Li. An explicit series solution of the squeezing flow between two infinite plates by means of the homotopy analysis method. Commun. Nonlinear Sci. Numer. Simulat., 2009, 14: 119 - 132.

[15] L.N. Trefethen. Spectral Methods in MATLAB. SIAM, 2000.

[16] Shi-Pu Yang, Ke-Qin Zhu. Analytical solutions for squeeze flow of Bingham fluid with Navier slip condition. J. Non-Newtonian Fluid Mech., 2006, 138: 173 - 180.

3.2. A spectral-homotopy analysis method for heat transfer flow of a third grade fluid between parallel plates [2]

Corrigenda

The following corrections and further explanations were made to the published work in Section 3.2.

(i) Schematic diagram representing the flow (Makinde, 2009b)

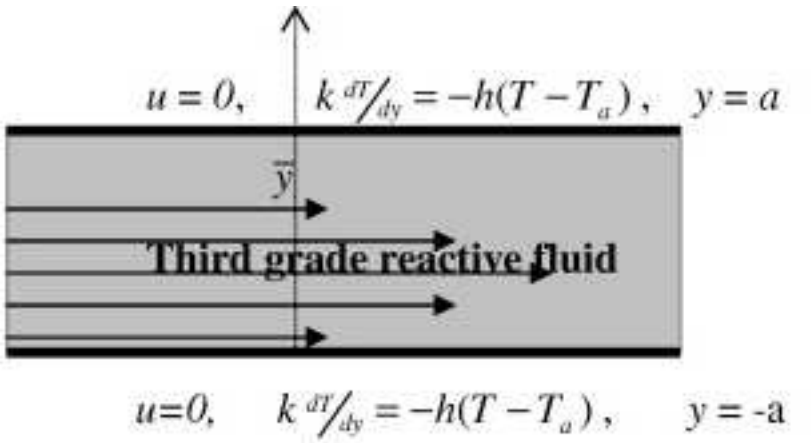

Figure 3.2: *Geometrical presentation of the problem.*

(ii) On page 15, Section 5, the correct caption for Table 2 is "Comparison of the values of the HAM and SHAM approximate solutions for $u_0(1)$ with the numerical solution for various values of B when $\beta = 1$".

[2] S. S. Motsa, Z. G. Makukula and P. Sibanda (2012). *International Journal of Numerical Methods for Heat & Fluid Flow* 22(1):4–23 (Impact factor; 1.058).

Further explanations:

(i) The MSHAM was not introduced in a formal section like the other methods but mentioned in passing on page 40. This is because it is only a minor modification of the SHAM. The slight modification was made after the first published article, and it was decided to retain the original name.

(ii) All results in the paper were generated using parameter values guided by the value of the critical point of $u'(1)$ on page 9 of the paper found to be

$$\beta = -\frac{2}{27B^2}.$$

A spectral-homotopy analysis method for heat transfer flow of a third grade fluid between parallel plates

Precious Sibanda
School of Mathematical Sciences, University of KwaZulu-Natal, Pietermaritzburg, South Africa
Sandile Motsa
Mathematics Department, University of Swaziland, KwaLuseni, Swaziland, and
Zodwa Makukula
School of Mathematical Sciences, University of KwaZulu-Natal, Pietermaritzburg, South Africa

Abstract

Purpose – The purpose of this paper is to study the steady laminar flow of a pressure driven third-grade fluid with heat transfer in a horizontal channel. The study serves two purposes: to correct the inaccurate results presented in Siddiqui et al., where the homotopy perturbation method was used, and to demonstrate the computational efficiency and accuracy of the spectral-homotopy analysis methods (SHAM and MSHAM) in solving problems that arise in fluid mechanics.

Design/methodology/approach – Exact and approximate analytical series solutions of the non-linear equations that govern the flow of a steady laminar flow of a third grade fluid through a horizontal channel are constructed using the homotopy analysis method and two new modifications of this method. These solutions are compared to the full numerical results. A new method for calculating the optimum value of the embedded auxiliary parameter $\sim$ is proposed.

Findings – The "standard" HAM and the two modifications of the HAM (the SHAM and the MSHAM) lead to faster convergence when compared to the homotopy perturbation method. The paper shows that when the same initial approximation is used, the HAM and the SHAM give identical results. Nonetheless, the advantage of the SHAM is that it eliminates the restriction of searching for solutions to the nonlinear equations in terms of prescribed solution forms that conform to the rule of solution expression and the rule of coefficient ergodicity. In addition, an alternative and more efficient implementation of the SHAM (referred to as the MSHAM) converges much faster, and for all parameter values.

Research limitations/implications – The spectral modification of the homotopy analysis method is a new procedure that has been shown to work efficiently for fluid flow problems in bounded domains. It however remains to be generalized and verified for more complicated nonlinear problems.

Originality/value – The spectral-HAM has already been proposed and implemented by the authors in a recent paper. This paper serves the purpose of verifying and demonstrating the utility of the new spectral modification of the HAM in solving problems that arise in fluid mechanics. The MSHAM is a further modification of the SHAM to speed up converge and to allow for convergence for a much wider range of system parameter values. The utility of these methods has not been tested and verified for systems of nonlinear equations. For this reason as much emphasis has been placed on proving the reliability and validity of the solution techniques as on the physics of the problem.

Keywords Heat transfer, Laminar flow, Spectral homotopy analysis method, Analytical results, Third grade fluid

Paper type Research paper

International Journal of Numerical Methods for Heat & Fluid Flow
Vol. 22 No. 1, 2012
pp. 4-23

0961-5539
DOI 10.1108/09615531211188766

Nomenclature

α = auxiliary parameter
Θ = fluid temperature
Θ_0 = lower plate temperature
λ = Brinkman number
ρ = fluid density
B = pressure gradient term
c_p = specific heat
h = half channel width
$\mathbf{T}$ = Cauchy stress tensor
$\mathbf{v}$ = fluid velocity
x = streamwise coordinate
β = material moduli
κ = thermal conductivity,
Θ_1 = upper plate temperature
μ = dynamic viscosity
ϕ = variable parameter
$\mathbf{b}$ = body force
Ec = Eckert number
$\hbar$ = auxiliary parameter
U = characteristic velocity
u = streamwise velocity component
y = normal coordinate

1. Introduction

Interest in the study of non-Newtonian fluids is driven as much by the many interesting mathematical features presented by the equations governing the flow as by the technological significance of such flows (Ariel, 2003; Asghar *et al.*, 2004). One of the main challenges in studying viscoelastic flows is that the viscoelasticity leads to an increase in the order of the differential equations that characterize the flow. There is as yet no satisfactory extra boundary condition to give unique solutions to such viscoelastic flows. For this reason, and the fact that the governing equations are non-linear, there is a paucity of exact solutions of equations that govern non-Newtonian fluid flows (Hayat *et al.*, 2008a, b). There is currently a large body of literature on studies on non-Newtonian fluids that include, among others, Benharbit and Siddiqui (1992), Dunn and Rajagopal (1995), Hayat *et al.* (1998) and Akçay and Yukselen (1999) and the survey article by Rajagopal (1993). Third-grade non-Newtonian fluid flow between two heated horizontal parallel plates in particular has been studied by Szeri and Rajagopal (1985), Siddiqui *et al.* (2008) and Makinde (2009). Exact solutions of the thin-film flow problem for a third-grade fluid on an inclined plane have been found by Hayat *et al.* (2008a, b). The recent study by Ellahi and Afzal (2009) deals with the flow of temperature-dependent non-Newtonian fluids in a porous medium. Series solutions of the velocity and temperature were obtained by the homotopy analysis method (HAM) for temperature-dependent viscosity.

This investigation closely follows the studies by Siddiqui *et al.* (2008) and Makinde (2009) where the flow and heat transfer in a third-grade fluid in a channel was considered. The governing non-linear differential equations were solved using the homotopy perturbation method (HPM) and Hermite-Padé approximations, respectively. In previous studies various perturbation techniques such as the Adomian decomposition method (Adomian, 1991), the HPM (He, 1999, 2000) and the Hermite-Padé approximations (Guttamann, 1989; Tourigny and Drazin, 2000) have been used to study non-linear problems that arise in fluid flow and heat transfer problems. However, as pointed out by Liao (2009), most of these perturbation techniques cannot guarantee the convergence of the series solution and may, in fact, be only valid for weakly non-linear problems. The HAM has been applied to a wide range of non-linear problems in science and engineering, for example, to viscous flows of non-Newtonian fluids and to heat transfer problems. Recent studies that employ the HAM include, among others, Hayat *et al.* (2006, 2008b) and Dinarvand and Rashidi (2010). A more exhaustive list can be found in Liao (2009). Fakhar *et al.* (2008) used the HAM to find approximate solutions

for an unsteady flow of an incompressible third-grade fluid in an infinite porous channel. However, as shown by Motsa *et al.* (2010a), the HAM suffers from a number of limitations, for example, the requirement that the solution sought ought to conform to the so-called rule of solution expression and the rule of coefficient ergodicity that is central to choosing the appropriate initial approximation, the auxiliary linear operators and the auxiliary functions.

The key to the HAM is a generalized Taylor expansion and an embedded auxiliary parameter $\hbar$ that allows for the control of both the convergence rate and the region of convergence. It has been shown elsewhere (Liao, 2005), that the HPM is equivalent to the HAM when the auxiliary parameter $\hbar = -1$. In this study we show that $\hbar = -1$ is, in fact, outside the admissible values of $\hbar$ that lead to the convergence of the series solution. A consequence of this is that, by using $\hbar = -1$, the study by Roohi *et al.* (2009) is effectively equivalent to the HPM study by Siddiqui *et al.* (2008).

In this study we introduce novel modifications of the HAM and compare the results with the exact solutions and with results generated numerically. We use methods based on combining a Chebyshev pseudo-spectral method and the "standard" HAM to study the flow of a third-grade fluid in a channel with heat transfer. The rationale for this study is to correct the inaccurate results presented in Siddiqui *et al.* (2008) where the HPM was used, and to bring to the fore innovative new semi-analytical techniques for solving non-linear equations that give better accuracy and rapid convergence to the exact solution. The higher order deformation equations and the auxiliary linear operator are defined in terms of the Chebyshev spectral collocation differentiation matrix described. The advantage of this modification is that it eliminates the restriction associated with the HAM of searching for solutions that conform to a prescribed rule of solution and the rule of coefficient ergodicity. Any form of initial guess may be used as long as it satisfies the boundary conditions whereas with the HAM one is restricted to choosing an initial approximation that would make the integration of the higher order deformation equations possible. In addition, the spectral HAM (SHAM) is more flexible than HAM as it allows for a wider range of linear operators and the restriction to using the method of higher order differential mapping falls away. However, it should be noted that, theoretically, if the same initial approximation and linear operators are used, the solutions of the governing equations obtained using the HAM and SHAM should be fairly similar, although the SHAM should still converge much faster. This is so because, in this case, both the HAM and SHAM would be integrating the same differential equations under the same conditions.

In this study we test the conclusions presented in Motsa *et al.* (2010a, b) by applying two different versions of the spectral modification of the HAM along side the standard HAM to the problem of a third-grade fluid flow between two horizontal parallel plates. When using the same initial approximation and linear operators, we show that the two methods give the same results. We show that both the HAM and the SHAM results converge much faster than the HPM results presented in Siddiqui *et al.* (2008). The salient difference between the SHAM and the modified SHAM (MSHAM) is that the SHAM algorithm is applied to the original governing equation whereas the MSHAM is applied to a transformed version of the governing equation. In addition, instead of guessing the initial approximation to be used in implementing the higher order deformation equations (as is the case with the HAM/SHAM), the initial approximation is generated in a much more systematic way in the MSHAM. This simple change in

approach produces a computationally efficient algorithm that is more accurate and converges faster than the original form of the SHAM.

2. Mathematical formulation

We consider the flow of an incompressible third-grade fluid placed between two horizontal parallel impermeable plates with the x-axis parallel to the plate and the y-axis normal to it. The constitutive equation for the Cauchy stress tensor T and the associated Rivlin-Ericksen tensors for a third-grade fluid are given in Fosdick and Rajagopal (1980) as:

$$\mathbf{T} = -p\mathbf{I} + \mu\mathbf{A}_1 + \alpha_1\mathbf{A}_2 + \alpha_2\mathbf{A}_1^2 + \beta_1\mathbf{A}_3 + \beta_2[\mathbf{A}_1\mathbf{A}_2 + \mathbf{A}_2\mathbf{A}_1] + \beta_3(tr\mathbf{A}_1^2)\mathbf{A}_2, \quad (1)$$

with:

$$\mathbf{A}_1 = \nabla\mathbf{v} + (\nabla\mathbf{v})^T, \quad (2)$$

$$\mathbf{A}_n = \frac{d}{dt}(\mathbf{A}_{n-1}) + \mathbf{A}_{n-1}\nabla\mathbf{v} + (\nabla\mathbf{v})^T\mathbf{A}_{n-1}. \quad (3)$$

where p is the pressure; μ denotes the viscosity; α_1, α_2, β_1, β_2 and β_3 are the material moduli; d/dt is the material derivative; $\mathbf{v}$ denotes the velocity field; while $\mathbf{A}_1$, $\mathbf{A}_2$ and $\mathbf{A}_3$ are the first three Rivlin-Ericksen tensors. The equations of motion are given by Siddiqui *et al.* (2008):

$$\nabla\cdot\mathbf{v} = 0, \quad (4)$$

$$\rho\frac{d\mathbf{v}}{dt} = \nabla\cdot\mathbf{T} + \rho\mathbf{b}, \quad (5)$$

$$\rho c_p\frac{d\Theta}{dt} = \kappa\nabla^2\Theta + \mathbf{T}\cdot\nabla\mathbf{v}, \quad (6)$$

where ρ is the mass density, κ the thermal conductivity, c_p is the specific heat at constant pressure, $\mathbf{b}$ is a body force, $\mathbf{v}$ is the fluid velocity and Θ is the temperature. For a fluid confined between two parallel plates located at $y = -h$ and $y = h$ we assume that:

$$\mathbf{v} = (u(y), 0, 0) \quad \text{and} \quad \Theta = \Theta(y),$$

where, following Siddiqui *et al.* (2008), we assume that the temperature of the upper plate is maintained at Θ_1 and that of lower plate at Θ_0. The fluid motion is driven by a constant pressure gradient and, in the case of Couette flow, by the motion of the upper plate with a constant velocity. With these assumptions in mind, it has been shown (Makinde, 2009) that equations (4)-(6) reduce to:

$$\frac{d^2u}{dy^2} + 6\beta\left(\frac{du}{dy}\right)^2\frac{d^2u}{dy^2} = -B, \quad (7)$$

$$\frac{d^2\Theta}{dy^2} + \lambda\left(\frac{du}{dy}\right)^2 + 2\beta\lambda\left(\frac{du}{dy}\right)^4 = 0, \quad (8)$$

subject to the boundary conditions:

$$u(-1) = 0, \quad u(1) = 0 \tag{9}$$

$$\Theta(-1) = 0, \quad \Theta(1) = 1, \tag{10}$$

where:

$$\beta = \frac{(\beta_2 + \beta_3)U^2}{\mu h^2}, \quad \lambda = \frac{\mu U^2}{\kappa(\Theta_1 - \Theta_0)} = PrEc \quad \text{and} \quad B = -\frac{h^2}{\mu U}\frac{dp}{dx},$$

where U is a characteristic velocity, λ is the Brinkman number, Pr is the Prandtl number and Ec is the Eckert number.

3. Solution methods

The main aims of this study are to test the functionality, robustness and computational efficiency of a new quasi-linearisation technique, and two recent modifications of the HAM for solving non-linear equations. We however begin by finding exact solutions for the velocity and skin friction. In the case of Couette flow with zero pressure gradient, $B = 0$, the exact solutions to equations (7) and (8) that satisfy the appropriate boundary conditions are:

$$u(y) = \frac{1}{2}(1 + y), \tag{11}$$

$$\Theta(y) = \frac{\lambda}{8}\left(1 + \frac{1}{2}\beta\right)(1 - y^2) + \frac{1}{2}(1 + y). \tag{12}$$

This linear velocity profile is independent of the non-Newtonian parameter and similar to that of a Newtonian fluid. This anomaly has been attributed to the constant velocity boundary conditions by Lipscombe (2010) and Roohi *et al.* (2009).

3.1 Exact solution for the skin friction

For non-zero pressure gradient, we begin by finding an explicit analytical solution for $u'(y)$. Equation (7) is written in the form:

$$\frac{d}{du}\left[\frac{du}{dy} + 2\beta\left(\frac{du}{dy}\right)^3\right] = -B. \tag{13}$$

Integrating equation (13) with respect to y and making use of the symmetry boundary condition $u'(0) = 0$ gives:

$$2\beta\left(\frac{du}{dy}\right)^3 + \frac{du}{dy} + By = 0, \tag{14}$$

which is a third-order equation in the deformation rate $u'(y)$. The exact analytical solution of the above result is:

$$\frac{du}{dy} = \frac{1}{6\beta}[\psi(y)]^{1/3} - \frac{1}{[\psi(y)]^{1/3}}, \tag{15}$$

where:

$$\psi(y) = \left(-54By + 6\sqrt{\frac{6 + 81\beta By^2}{\beta}}\right)\beta^2. \tag{16}$$

An alternative but equivalent solution was obtained in terms of hyperbolic functions in Holmes (2002) and Lipscombe (2010) as:

$$\frac{du}{dy} = -\frac{1}{\sqrt{6\beta}}\sinh\left[\frac{1}{3}\sinh^{-1}\left(\frac{6^{3/2}By\sqrt{\beta}}{4}\right)\right]. \tag{17}$$

The analytical result (equation (15)) is important because, when evaluated at $y = 1$, it gives an explicit analytical expression for the skin friction coefficient C_f. It is worth noting, from equation (16) that $u'(1)$ has a critical point at:

$$\beta = -\frac{2}{27B^2}.$$

This critical point was reported as a bifurcation point in Makinde (2007) who used a Hermite Padé approach for the case when $B = 1$. This means that the shear stress term, and hence the solution $u(y)$, is only valid when:

$$\beta \geq -\frac{2}{27B^2}.$$

We note that when equation (14) is combined with equation (8), the temperature equation simplifies to:

$$\frac{d^2\Theta}{dy^2} - \lambda By\frac{du}{dy} = 0. \tag{18}$$

Thus, by making use of equation (15), we have:

$$\frac{d^2\Theta}{dy^2} = \phi(y), \tag{19}$$

where:

$$\phi(y) = \lambda By\left(\frac{1}{6\beta}[\psi(y)]^{1/3} - \frac{1}{[\psi(y)]^{1/3}}\right). \tag{20}$$

Since the right-hand side of equation (19) is a known function of y, the equation can easily be solved using any numerical method such as finite differences, Runge-Kutta-based shooting or spectral methods. Below we use the standard HAM, the SHAM and the MSHAM to find approximate analytical solutions to equations (7) and (8). The results are compared with the full numerical solution in order to show the computational efficiency and to validate these new solution techniques.

3.2 HAM solution of the problem

The solution of the governing equations (7)-(10) is obtained by applying the HAM to the momentum equation (7) to find the velocity field $u(y)$. The resulting solution $u(y)$ is then used to find the temperature distribution $\Theta(y)$ by integrating the energy equation (8) twice. For the HAM solution we look for base functions and an initial guess that satisfies the boundary conditions in the form:

$$u(y) = \sum_{n=0}^{+\infty} a_n y^n, \tag{21}$$

where a_n are coefficients to be determined, and equation (21) is the so-called rule of solution expression. We use the method of higher order differential mapping (van Gorder and Vajravelu, 2009) to choose the linear operator $\mathcal{L}$ and initial guess $u_0(y)$ as:

$$\mathcal{L}[\phi(y;q)] = \frac{\partial^2 \phi(y;q)}{\partial y^2}, \tag{22}$$

$$u_0(y) = \alpha(1 - y^2), \tag{23}$$

where α is an auxiliary parameter. The zero-order deformation equation for the problem is:

$$(1 - q)\mathcal{L}[\phi(y;q) - u_0(y)] = q\hbar\mathcal{N}[\phi(y;q)], \tag{24}$$

$$\phi(-1;q) = 0, \quad \phi(1;q) = 0, \tag{25}$$

where $q \in [0, 1]$ is an embedding parameter, $\hbar$ is a non-zero auxiliary parameter and $\phi(y;q)$ is an unknown function. The non-linear operator $\mathcal{N}$is defined by:

$$\mathcal{N}\phi(y;q) = \frac{\partial^2 \phi(y;q)}{\partial y^2} + 6\beta\left[\left(\frac{\partial \phi(y;q)}{\partial y}\right)^2 \frac{\partial^2 \phi(y;q)}{\partial y^2}\right] + B. \tag{26}$$

When $q = 0$ it is easy to show that:

$$\phi(y;0) = u_0(y), \tag{27}$$

and when $q = 1$ the zero-order deformation equation (24) is equal to the original governing equation (7), so that:

$$\phi(y;1) = u(y). \tag{28}$$

Expanding $\phi(y;q)$ in a Taylor series with respect to the embedding parameter q yields:

$$\phi(y;q) = u_0(y) + \sum_{m=1}^{+\infty} u_m(y) q^m, \tag{29}$$

where:

$$u_m(y) = \frac{1}{m!} \frac{\partial^m \phi(y;q)}{\partial q^m}\bigg|_{q=0}. \tag{30}$$

The convergence of the above series depends on the auxiliary parameter $\hbar$. The mathematical meaning of this parameter is explained in the recent paper by Liu (2010).

Assuming that $\hbar$ is carefully selected so that the above series is convergent when $q = 1$, then the series solution is:

$$u(y) = u_0(y) + \sum_{m=1}^{+\infty} u_m(y), \tag{31}$$

where $u_m(y)$ are unknown functions that are determined from higher order deformation equations. The higher order deformation equations are obtained by first differentiating the zero-order deformation equations (24) and (25) m times with respect to q and then dividing them by $m!$ and finally setting $q = 0$. This way, we obtain the following higher order deformation equations:

$$\mathcal{L}[u_m(y) - \chi_m u_{m-1}(y)] = \hbar R_m(y), \tag{32}$$

with the boundary conditions:

$$u_m(-1) = u_m(1) = 0, \tag{33}$$

where:

$$R_m(y) = u''_{m-1}(y) + (1 - \chi_m)B + 6\beta \sum_{n=0}^{m-1} u''_{m-1-n}(y) \sum_{i=0}^{n} u'_i(y) u'_{n-i}(y), \tag{34}$$

and:

$$\chi_m = \begin{cases} 0, & m \leq 1 \\ 1, & m > 1 \end{cases}. \tag{35}$$

The mth order deformation equations form a set of linear ordinary differential equations and can be easily solved, especially by means of symbolic computation software such as Maple, Mathematica, Matlab and others.

The analytical solution for the temperature distribution $\Theta(y)$ is then obtained by substituting the velocity $u(y)$ in the energy equation (8) and integrating the resulting equation twice with respect to y.

3.3 SHAM solution

In this section we present the SHAM for solving the non-linear equation (7) as described in Motsa *et al.* (2010a). The basic idea is to integrate the higher order deformation equations using spectral methods. This implicitly implies using Chebyshev polynomials as basis functions leading to relatively faster convergence of the method. We use the Chebyshev pseudo-spectral method to transform the higher order deformation equations (32) into the following set of equations:

$$\sum_{j=0}^{N} \mathcal{D}_{kj}^2[u_m(y_j) - \chi_m u_{m-1}(y_j)] = \hbar\left(\sum_{j=0}^{N} \mathcal{D}_{kj}^2 u_{m-1}(y_j) + (1-\chi_m)B + 6\beta\sum_{n=0}^{m-1} \mathcal{D}_{kj}^2 u_{m-1-n}(y_j)\sum_{i=0}^{n}[\mathcal{D}_{kj}u_i(y_j)][\mathcal{D}_{kj}u_{n-i}(y_j)]\right), \tag{36}$$

where $\mathcal{D}$ is the Chebyshev differentiation matrix with $N+1$ collocation points and $k = N/2+1, \ldots, N$, denotes the kth row of the differentiation matrix $\mathcal{D}$. The boundary equations become:

$$u_m(y_0) = u_m(y_N) = 0. \tag{37}$$

We employ the Gauss-Lobatto collocation (Canuto *et al.*, 1988) to define the Chebyshev nodes in $[-1, 1]$, namely:

$$y_j = cos\left(\frac{\pi j}{N}\right). \tag{38}$$

Following Don and Solomonoff (1995), we express the entries of the differentiation matrix $\mathcal{D}$ as:

$$\begin{aligned} \mathcal{D}_{kj} &= -\frac{1}{2}\frac{c_k}{c_j}\frac{(-1)^{k+j}}{\sin(\pi/2N)(j+k)\sin(\pi/2N)(j-k)}, \quad j \neq k, \\ \mathcal{D}_{kj} &= -\frac{1}{2}\frac{\cos(\pi k/N)}{\sin^2(\pi k/N)}, \quad k \neq 0 \\ \mathcal{D}_{00} &= -\mathcal{D}_{NN} = \frac{2N^2+1}{6}. \\ \text{and } \mathcal{D}_{kj} &= -\mathcal{D}_{N-k,N-j}, \end{aligned} \tag{39}$$

where $c_0 = c_N = 2$ and $c_j = 1$ with $1 \leq j \leq N-1$. Equation (36) can be written in matrix form as:

$$\mathcal{D}^2[u_m - (\chi_m + \hbar)u_{m-1}] = \hbar\left((1-\chi_m)B + 6\beta\sum_{n=0}^{m-1} \mathcal{D}^2 u_{m-1-n}\sum_{i=0}^{n}[\mathcal{D}u_i][\mathcal{D}u_{n-i}]\right). \tag{40}$$

This simplifies to the following recurrence relation for u_m:

$$u_m = (\chi_m + \hbar)u_{m-1} + (\mathcal{D}^2)^{-1}\hbar\left((1-\chi_m)B + 6\beta\sum_{n=0}^{m-1} \mathcal{D}^2 u_{m-1-n}\sum_{i=0}^{n}[\mathcal{D}u_i][\mathcal{D}u_{n-i}]\right). \tag{41}$$

Thus, starting from the initial approximation $u_0(y)$, we can use the recurrence formula (41) to successively obtain $u_m(y)$ for $m \geq 1$. To implement the boundary conditions (equation (37)), the derivative matrix $\mathcal{D}$ was evaluated when $j = k = 1, \ldots, N-1$. Once $u(y)$ has been obtained, we apply the Chebyshev pseudo-spectral collocation

method to the energy equation (8) to obtain the solution for the temperature distribution as:

$$\Theta = (\mathcal{D}^2)^{-1}[-\lambda(\mathcal{D}u)^2 - 2\beta\lambda(\mathcal{D}u)^4]. \tag{42}$$

The SHAM as given above was devised by Motsa *et al.* (2010a) and to give better convergence than the standard HAM. However, as shown in Motsa *et al.* (2010b), an alternative but much more efficient implementation of the SHAM is possible.

3.4 MSHAM solution

In this section we present the MSHAM for solving the governing non-linear equation (7). Implementation of the MSHAM involves simplifying the governing equations by making use of the following transformation:

$$U(y) = u(y) - u_0(y) \tag{43}$$

where $u_0(y)$ is the initial guess. Substituting equation (43) in the governing equation (7) gives:

$$a_1U'' + a_2U' + a_3(U')^2 + a_4U'U'' + 6\beta(U')^2U'' = \psi(y) \tag{44}$$

subject to the boundary conditions:

$$U(-1) = U(1) = 0, \tag{45}$$

where:

$$a_1 = 1 + 6\beta(U_0')^2, \quad a_2 = 12\beta U_0'U_0'', \quad a_3 = 6\beta U_0'', \tag{46}$$

$$a_4 = 12\beta U_0', \quad \psi(y) = -\left\{B + \left[1 + 6\beta(U_0')^2\right]U_0''\right\}. \tag{47}$$

The homotopy analysis theory, along the lines described in the last section, is then applied to equation (44). The initial approximation is obtained by solving the linear part of equation (44), given as:

$$a_1U_0'' + a_2U_0' = \psi(y) \tag{48}$$

subject to the boundary conditions:

$$U_0(-1) = U_0(1) = 0. \tag{49}$$

Applying the Chebyshev spectral collocation method on equation (48) gives the solution of $U_0(y)$ as:

$$\mathbf{U}_0 = \mathbf{A}^{-1}\mathbf{\Psi}, \tag{50}$$

where:

$$\mathbf{A} = \mathbf{a}_1\mathcal{D}^2 + \mathbf{a}_2\mathcal{D}, \tag{51}$$

$$\mathbf{\Psi} = [\psi(y_0), \psi(y_1), \ldots, \psi(y_{N-1}), \psi(y_N)]. \tag{52}$$

Importing the ideas of the HAM, we construct the zero-order deformation equations as:

$$(1 - q)\mathcal{L}_2[\tilde{U}(y;q) - U_0(y)] = q\hbar\{\mathcal{N}_2[\tilde{U}(y;q)] - \psi(y)\} \tag{53}$$

subject to:

$$\tilde{U}(1;q) = \tilde{U}(-1;q) = 0, \tag{54}$$

where:

$$\mathcal{L}_2[\tilde{U}(y;q)] = a_1 \frac{\partial^2 \tilde{U}}{\partial y^2} + a_2 \frac{\partial \tilde{U}}{\partial y}, \tag{55}$$

$$\mathcal{N}_2[\tilde{U}(y;q)] = \mathcal{L}_2[\tilde{U}(y;q)] + a_3 \left(\frac{\partial \tilde{U}}{\partial y}\right)^2 + a_4 \frac{\partial \tilde{U}}{\partial y}\frac{\partial^2 \tilde{U}}{\partial y^2} + 6\beta \frac{\partial^2 \tilde{U}}{\partial y^2}\left(\frac{\partial \tilde{U}}{\partial y}\right)^2. \tag{56}$$

The higher order deformation equation is given by:

$$\mathcal{L}_2[U_m(y) - (\chi_m + \hbar)U_{m-1}(y)] = \hbar R_m(y), \tag{57}$$

where:

$$R_m(y) = a_3 \sum_{n=0}^{m-1} U'_n U'_{m-1-n} + a_4 \sum_{n=0}^{m-1} U'_n U''_{m-1-n} + 6\beta \sum_{n=0}^{m-1} U''_{m-1-n} \sum_{i=0}^{n} U'_i U'_{n-i} - (1 - \chi_m)\psi(y). \tag{58}$$

Applying the Chebyshev spectral collocation method on equations (57) and (58) gives:

$$\mathbf{A}\mathbf{U}_m = (\chi_m + \hbar)\mathbf{A}\mathbf{U}_{m-1} - \hbar(1 - \chi_m)\mathbf{\Psi} + \hbar \mathbf{P}_{m-1}, \tag{59}$$

subject to the boundary conditions:

$$U_m(y_0) = U_m(y_N) = 0, \tag{60}$$

when $\mathbf{A}$ and Ψ are as defined in equations (51) and (52) and:

$$\mathbf{U}_m = [U_m(y_0), U_m(y_1), \ldots, U_m(y_{N-1}), U_m(y_N)], \tag{61}$$

$$\mathbf{P}_{m-1} = \mathbf{a}_3 \sum_{n=0}^{m-1} (\mathcal{D}\mathbf{U}_n)(\mathcal{D}\mathbf{U}_{m-1-n}) + \mathbf{a}_4 \sum_{n=0}^{m-1} (\mathcal{D}\mathbf{U}_n)(\mathcal{D}^2\mathbf{U}_{m-1-n}) + 6\beta \sum_{n=0}^{m-1} \mathcal{D}^2\mathbf{U}_{m-1-n} \sum_{i=0}^{n} (\mathcal{D}\mathbf{U}_i)(\mathcal{D}\mathbf{U}_{n-i}). \tag{62}$$

After incorporating the boundary conditions, equation (59) can be written as:

$$\mathbf{U}_m = (\chi_m + \hbar)\mathbf{U}_{m-1} + \mathbf{A}^{-1}\hbar[\mathbf{P}_{m-1} - (1 - \chi_m)\mathbf{\Phi}]. \tag{63}$$

Thus, starting from the initial approximation, which is obtained as a solution of equation (48), higher order approximations $U_m(y)$ for $m \geq 1$ are obtained through the recursive formula (63).

3.5 Numerical method of solution

To obtain the numerical solution of the governing system we apply the Chebyshev pseudo-spectral collocation method to equations (7) and approximate the unknown function $u(y)$ by a sum of $N+1$ basis functions, $T_n(y)$, that is:

$$u(y) \approx u_N(y) = \sum_{n=0}^{N} a_n T_n(y) \tag{64}$$

where $T_n(y)$ is the Chebyshev polynomial which is defined in the interval $-1 \leq y \leq 1$ as:

$$T_N(y) = \cos(N \cos^{-1} y). \tag{65}$$

We use the Gauss-Lobatto collocation points to define the Chebyshev nodes in $[-1, 1]$. This approach yields a set of N algebraic equations that are solved using Newton's iteration method to find the unknown coefficients a_n. For the SHAM and the full numerical computations we used $N = 60$.

4. Convergence of the series solutions

In this study Maple was used to solve the system of linear higher order deformation equations (32), subject to boundary conditions (equation (33)), to successively obtain:

$$u_1(y) = \hbar\left(\alpha - \frac{1}{2}B\right)(1 - y^2) + 4\hbar\beta\alpha^3(1 - y^4), \tag{66}$$

$$u_2(y) = (1 + \hbar)\left(\alpha - \frac{1}{2}B\right)(1 - y^2) + 2\hbar\beta\alpha^2(8\hbar\alpha + 2\alpha - 3\hbar B)(1 - y^4) + 64\hbar^2\beta^2\alpha^5(1 - y^6), \tag{67}$$

$$\vdots$$

Consequently, from equation (31), the series solution can be written as:

$$u(y) = u_0(y) + u_1(y) + u_2(y) + \cdots + u_m(y), \tag{68}$$

where m is the order of the series. We note that when $\alpha = B/2$, solutions (66) and (67) reduce to the results of Siddiqui *et al.* (2008) who solved the same problem using the HPM and Roohi *et al.* (2009) who used the HAM with $\hbar = -1$ to solve the problem. It is also worth noting that the entire analysis in the latter study is restricted to the case $\alpha = B/2$ and $\hbar = -1$.

The solutions $u_1(y)$, $u_2(y)$, etc. contain the auxiliary parameter $\hbar$ that controls the convergence of the HAM series solution (68). The standard way of choosing admissible values of $\hbar$ is to select a value of $\hbar$ on the horizontal segment of the $\hbar$-curve.

Figure 1(a) shows the $\hbar$-curve at different orders of the HAM and SHAM approximations when $\alpha = B/3$. We note that with the same initial approximation and auxiliary functions, the HAM and SHAM $\hbar$-curves match exactly. At the tenth order of the approximations the admissible values of $\hbar$ lie in $[-0.3, -0.2]$ for $B = 1$ and $\beta = 1$. The $\hbar$-value corresponding to the maximum of the second-order approximations lies

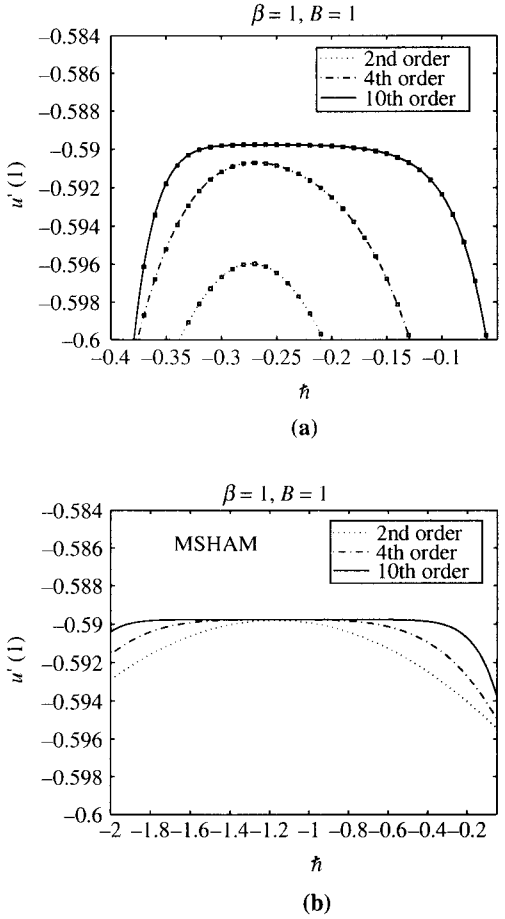

Figure 1.
The $\hbar$-curve at different orders of (a) HAM (squares) and SHAM approximations, and (b) the MSHAM approximation

inside the interval $-0.3 \leq \hbar \leq -0.2$. We propose that, instead of choosing a "random" $\hbar$-value from the horizontal segment of the $\hbar$-curve, we select the critical value of $\hbar$ at which the maximum of the second-order approximation occurs as the value of $\hbar$ to use in generating the approximate solutions. This approach leads to very rapid convergence of the series solution.

Using the second-order HAM approximate solution:

$$u(y) \approx u_0(y) + u_1(y) + u_2(y),$$

we found the critical value of $\hbar$ at which the maximum of the second-order $\hbar$-curve occurs to be:

$$\hbar = \frac{-1}{1 + 24\alpha^2\beta}, \tag{69}$$

where $\alpha = B/3$. The HAM and SHAM results presented in the next section were obtained using this critical value of $\hbar$.

Figure 1(b) shows the $\hbar$-curve at different orders of the MSHAM approximation series. Comparing the two, it is evident that the horizontal segments of the $\hbar$-curves are

much wider in the MSHAM than in the HAM/SHAM. For example, at the tenth order of the MSHAM approximation, the admissible values of $\hbar$ lie in $[-1.7, -0.5]$ compared to the much narrower range $[-0.3, -0.2]$ in the case of the HAM/SHAM. This has implications for the accuracy and the rate of convergence of the solution series, since, as was noted in Motsa *et al.* (2010a, b), a larger range of admissible values of $\hbar$ is associated with fast convergence and improved accuracy of the approximate method. Thus, it can be expected that the MSHAM will give more accurate and fast converging results compared to either the HAM or the SHAM.

Figure 2 shows the tenth-order $\hbar$-curves for different values of B for the HAM and MSHAM solution series, respectively. It is self-evident that the horizontal segment of the HAM $\hbar$-curve shrinks significantly when B is large. The implication is that when B is large the convergence of the HAM becomes much slower and the results less accurate. On the other hand, the horizontal segment of the MSHAM $\hbar$-curve remains very wide even at large values of B. Thus, the convergence of the MSHAM can be expected to remain robust and the results accurate for large values of B.

Figure 3 shows the HAM and MSHAM tenth-order $\hbar$-curves, respectively, for different values of β when $B = 1$. Again the horizontal segment of the HAM $\hbar$-curve

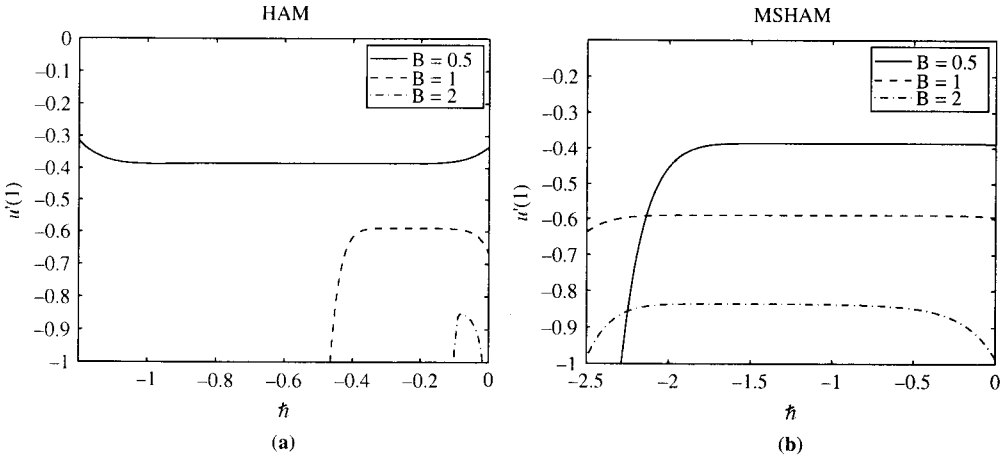

Figure 2.
The $\hbar$-curves at tenth order (a) HAM, and (b) MSHAM approximations for different values of B when $\beta = 1$

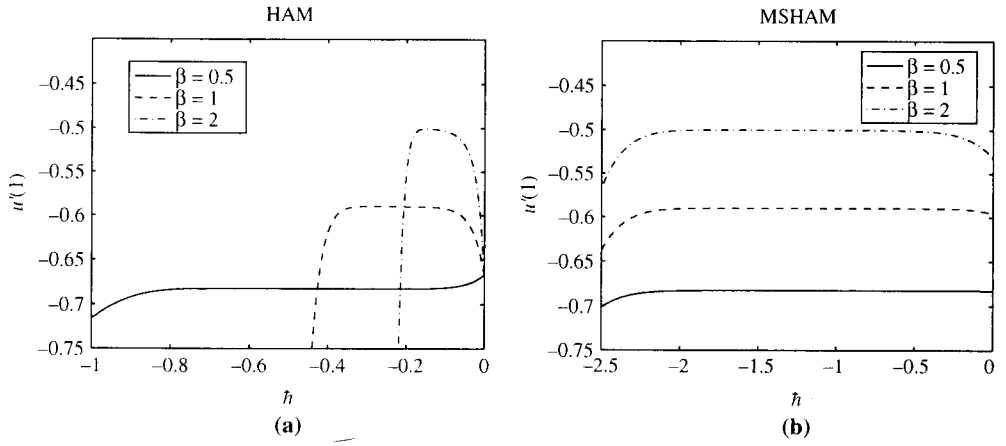

Figure 3.
The $\hbar$-curve at tenth order (a) HAM and, (b) MSHAM approximations for different values of β when $B = 1$

shrinks as β increases whereas that of the MSHAM remains fairly constant even for large values of β. Thus, the convergence of the HAM is expected to decrease with an increase in β whilst the MSHAM can be expected to give results that are accurate for large values of β.

5. Results and discussion

In this section we compare the semi-analytical HAM, SHAM and MSHAM results for several values of the governing parameters β, B and λ. The results are further compared against the full numerical results based on the Chebyshev pseudo-spectral method. All the semi-analytical results presented in this work were obtained using $\alpha = B/3$ and the optimal value of $\hbar$ was deduced from equation (69). The MSHAM results were similarly generated using an $\hbar$-value corresponding to the maxima at the second order of the MSHAM $\hbar$-curve. The number of collocation points used is $N = 100$.

Table I gives a comparison of the HAM, SHAM and MSHAM results for the skin friction coefficient $u'(1)$ at different orders of approximation against the exact results when the non-Newtonian parameter β is varied. The comparison of the results at different orders of approximation against the exact results when B is varied is given in Table II. The magnitude of the skin friction coefficient decreases with β but increases with the pressure gradient term. However, more importantly, Tables I and II show that the HAM and SHAM methods give identical results when the same initial approximation is used. However, the MSHAM converges much more rapidly to the exact solution compared to both the HAM and the SHAM. When both β and B are less than 1, the MSHAM approximations match the exact solutions at the fourth order of the solution series.

Figures 4-6 show the effect of the parameters β, B and λ on the velocity and temperature profiles. In the absence of an exact solution, the velocity and temperature profiles are determined numerically using the Chebyshev spectral collocation method.

β	Second order	Fourth order	Eighth order	Tenth order	Exact
HAM solution for $u'(1)$ for $B = 1$					
0.2	−0.80676	−0.79581	−0.79722	−0.79729	−0.79728
0.4	−0.71326	−0.71154	−0.71166	−0.71166	−0.71166
0.6	−0.65812	−0.65805	−0.65805	−0.65805	−0.65805
0.8	−0.62175	−0.61974	−0.61954	−0.61953	−0.61953
1.0	−0.59596	−0.59070	−0.58979	−0.58976	−0.58975
SHAM solution for $u'(1)$ for $B = 1$					
0.2	−0.80676	−0.79581	−0.79722	−0.79729	−0.79728
0.4	−0.71326	−0.71154	−0.71166	−0.71166	−0.71166
0.6	−0.65812	−0.65805	−0.65805	−0.65805	−0.65805
0.8	−0.62175	−0.61974	−0.61954	−0.61953	−0.61953
1.0	−0.59596	−0.59070	−0.58979	−0.58976	−0.58975
MSHAM solution for $u'(1)$ for $B = 1$					
0.2	−0.79733	−0.79728	−0.79728	−0.79728	−0.79728
0.4	−0.71166	−0.71166	−0.71166	−0.71166	−0.71166
0.6	−0.65805	−0.65805	−0.65805	−0.65805	−0.65805
0.8	−0.61954	−0.61953	−0.61953	−0.61953	−0.61953
1.0	−0.58980	−0.58976	−0.58975	−0.58975	−0.58975

Table I.
Comparison of the values of the HAM and SHAM approximate solutions for $u'(1)$ with the numerical solution for various values of β when $B = 1$

B	Second order	Fourth order	Eighth order	Tenth order	Exact
HAM solution for $u'(1)$ for $\beta = 1$					
0.2	−0.18929	−0.18671	−0.18693	−0.18694	−0.18694
0.4	−0.33354	−0.32810	−0.32883	−0.32887	−0.32887
0.5	−0.38889	−0.38498	−0.38544	−0.38546	−0.38546
0.8	−0.51976	−0.51955	−0.51954	−0.51954	−0.51954
1.0	−0.59596	−0.59070	−0.58979	−0.58976	−0.58975
SHAM solution for $u'(1)$ for $\beta = 1$					
0.2	−0.18929	−0.18671	−0.18693	−0.18694	−0.18694
0.4	−0.33354	−0.32811	−0.32883	−0.32887	−0.32887
0.5	−0.38889	−0.38498	−0.38544	−0.38546	−0.38546
0.8	−0.51976	−0.51954	−0.51954	−0.51954	−0.51954
1.0	−0.59596	−0.59070	−0.58979	−0.58976	−0.58975
MSHAM solution for $u'(1)$ for $\beta = 1$					
0.2	−0.18694	−0.18694	−0.18694	−0.18694	−0.18694
0.4	−0.32889	−0.32887	−0.32887	−0.32887	−0.32887
0.5	−0.38547	−0.38546	−0.38546	−0.38546	−0.38546
0.8	−0.51954	−0.51954	−0.51954	−0.51954	−0.51954
1.0	−0.58980	−0.58976	−0.58975	−0.58975	−0.58975

Table II.
Comparison of the values of the HAM and SHAM approximate solutions for $u'(1)$ with the numerical solution for various values of β when $B = 1$

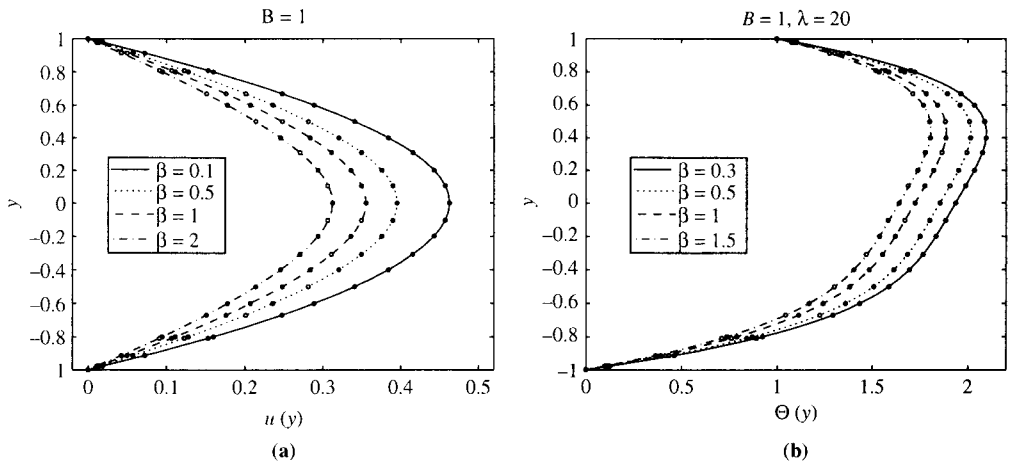

Figure 4.
Comparing the numerical solution with the tenth-order HAM (open circles) and SHAM (filled circles) solutions for (a) the velocity profile $u(y)$, and (b) the temperature profile $\Theta(y)$ when varying β for $B = 1$, $\lambda = 20$

The specific values of the parameters used are taken from Siddiqui *et al.* (2008) and serve to illustrate the efficiency and utility of both the HAM and the SHAM. The purpose of these figures is thus to give a comparison of the convergence rates of the HAM and SHAM approximations to the numerical solutions. We note that the results presented here are more accurate compared to those in Siddiqui *et al.* (2008) and convergence of the HAM is achieved at the tenth order.

Figure 4 shows the effect of the non-Newtonian parameter β on the velocity and temperature profiles for constant pressure gradient B. For fixed Brinkman numbers both the velocity and temperature profiles decrease with increasing material moduli. The HPM results presented in Siddiqui *et al.* (2008) fail to converge to the numerical results. The primary reason for the lack of convergence is that the HPM is equivalent to assuming $\hbar = -1$. However, we have shown above that $\hbar = -1$ lies outside the range

of admissible values of $\hbar$ that would lead to convergence of the HAM series solution. In addition, only a few terms of the HPM solution series were used by Siddiqui *et al.* (2008). It is worth noting also that the results presented in Siddiqui *et al.* (2008) were not validated against any numerical results.

Figure 5 shows the effect of increasing the pressure gradient term for fixed Brinkman numbers λ and material moduli. In this case increasing the pressure gradient has the effect of heating and accelerating the fluid.

Figure 6 shows the effect of Brinkman numbers on the temperature profile. The Brinkman number relates heat conduction from the channel wall to the non-Newtonian viscous fluid and has a role to play in determining the flow regime boundaries from laminar to transition and from transition to turbulent flow (Tso and Mahulikar, 1999). The effect of increasing the Brinkman numbers is to increase the temperature within the channel.

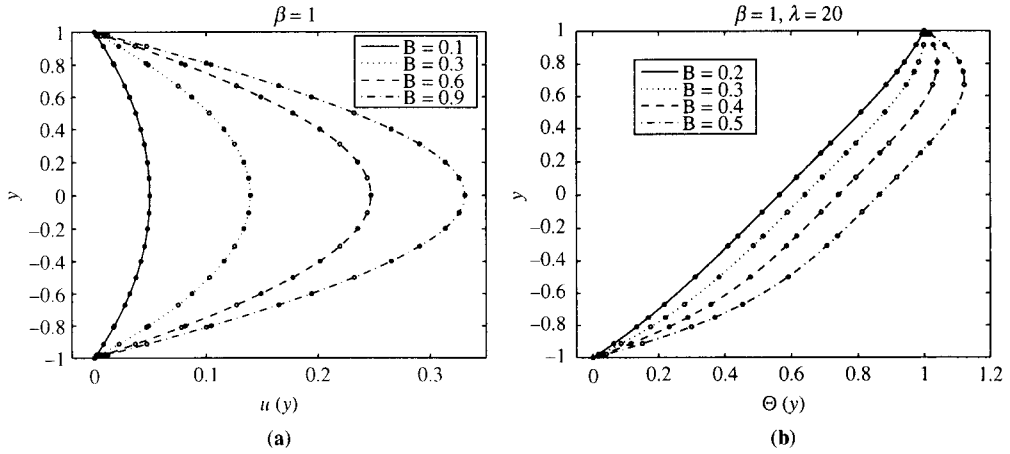

Figure 5.
Comparing the numerical solution with the tenth-order HAM (open circles) and SHAM (filled circles) solutions for (a) the velocity profile $u(y)$, and (b) the temperature profile $\Theta(y)$ when varying B for $\beta = 1$, $\lambda = 20$

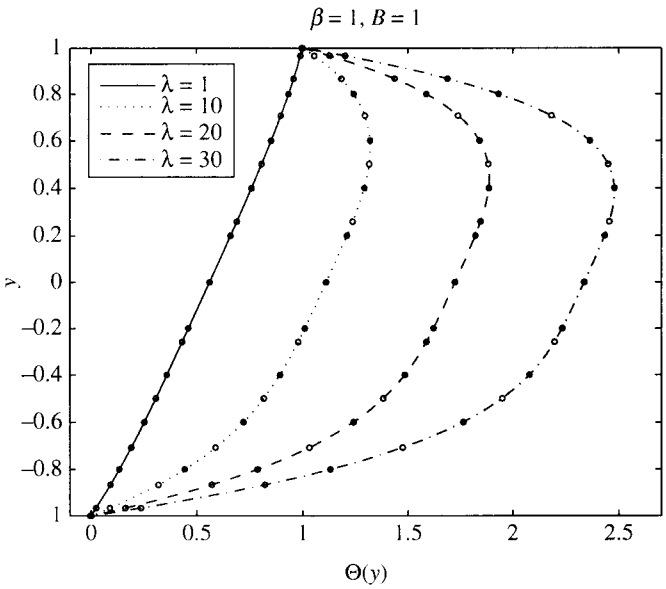

Figure 6.
Comparing the numerical solution with the tenth-order HAM (open circles) and SHAM (filled circles) solution for the temperature profile $\Theta(y)$ when varying λ for $B = 1$, $\beta = 20$

In all cases convergence to the numerical results is achieved at the tenth order of both the HAM and SHAM approximations.

6. Conclusion

In this paper we have examined the steady laminar flow of a third-grade fluid with heat transfer in a horizontal channel. Approximate analytic solutions were constructed using three semi-analytical techniques: the HAM, the SHAM and the MSHAM. The effect of the non-Newtonian parameter, the pressure gradient term and the Brinkman number on the velocity and temperature profiles has been determined. The semi-analytical results compared favourably with the exact solutions in the case of the skin friction and with the full numerical solution of the governing non-linear equations in the case of the velocity and temperature profiles.

An important aspect of this research has been the need to prove the computational efficiency, accuracy and robustness of the SHAM and MSHAM in solving non-linear equations. We have shown that these methods are, in general, more accurate than the HAM. We have further:

- proposed a new approach for calculating the optimal value of $\hbar$ that gives accurate results;
- shown that the HAM and SHAM give identical results when the same initial approximation, auxiliary parameter and linear operator are used;
- shown that both the HAM and the SHAM give more accurate results than the HPM used in Siddiqui *et al.* (2008); and
- shown that the MSHAM is computationally more efficient than both the HAM and the SHAM whose convergence was shown to decrease with an increase in the magnitude of the governing parameters of the problem.

An important feature of the HAM is the presence of the auxiliary parameter $\hbar$ (whose mathematical meaning is explained in Liu (2010)) which gives us freedom to control the convergence rate and region of the solution series. Both the SHAM and MSHAM retain this unique feature of the HAM. However, the advantage of the SHAM/MSHAM over the HAM is that the former do not depend on a conveniently chosen initial approximation and linear operators in order to make the integration of higher order deformation equations possible. The major difference between the SHAM and the MSHAM is that the SHAM algorithm is applied to the original governing equation whereas the MSHAM is applied to a transformed version of the governing equation. In addition, instead of guessing the initial approximation to be used in implementing the higher order deformation equations, the initial approximation is generated in a much more systematic way in the MSHAM by solving the linearized form of the governing equations.

References

Adomian, G. (1991), "A review of the decomposition method and some recent results for nonlinear equations", *Comp. Math. Appl.*, Vol. 21, pp. 101-27.

Akçay, M. and Yukselen, M.A. (1999), "Drag reduction of a non-Newtonian fluid by fluid injection on a moving wall", *Arch. Appl. Mech.*, Vol. 69 No. 3, pp. 215-25.

Ariel, P.D. (2003), "Flow of a third grade fluid through a porous flat channel", *Int. J. Eng. Sci.*, Vol. 41, pp. 1267-85.

Asghar, S., Mohyuddin, M.R., Hayat, T. and Siddiqui, A.M. (2004), "The flow of a non-Newtonian fluid induced due to the oscillations of a porous plate", *Math. Prob. Eng.*, Vol. 2, pp. 133-43, available at: http://dx.doi.org/10.1155/S1024123X04309014

Benharbit, A.M. and Siddiqui, A.M. (1992), "Certain solutions of the equations of the planar motion of a second grade fluid for steady and unsteady cases", *Acta Mech.*, Vol. 94 Nos 1/2, pp. 85-96.

Canuto, C., Hussaini, M.Y., Quarteroni, A. and Zang, T.A. (1988), *Spectral Methods in Fluid Dynamics*, Springer, Berlin.

Dinarvand, S. and Rashidi, M.M. (2010), "A reliable treatment of a homotopy analysis method for two-dimensional viscous flow in arectangular domain bounded by two moving porous walls", *Nonlin. Anal. Real World Appl.*, No. 3, pp. 1502-12.

Don, W.S. and Solomonoff, A. (1995), "Accuracy and speed in computing the Chebyshev collocation derivative", *SIAM. J. Sci. Comput.*, Vol. 16 No. 6, pp. 1253-68.

Dunn, J.E. and Rajagopal, K.R. (1995), "Fluids of differential type: critical review and thermodynamic analysis", *Int. J. Eng. Sci.*, Vol. 33 No. 5, pp. 689-729.

Ellahi, R. and Afzal, S. (2009), "Effects of variable viscosity in a third grade fluid with porous medium: an analytic solution", *Commun. Nonlin. Sci. Numer. Simul.*, Vol. 14 No. 5, pp. 2056-72.

Fakhar, K., Xu, Z. and Yi, C. (2008), "Exact solutions of a third grade fluid flow on a porous plate", *Appl. Math. Comput.*, Vol. 202, pp. 376-82.

Fosdick, R.L. and Rajagopal, K.R. (1980), "Thermodynamics and stability of fluids of third grade", *Proc. R. Soc. Lond. A*, Vol. 369, pp. 351-77.

Guttamann, A.J. (1989), "Asymptotic analysis of power series expansions", in Domb, C. and Lebowitz, J.K. (Eds), *Phase Transitions and Critical Phenomena*, Academic Press, New York, NY, pp. 1-234.

Hayat, T., Ahmed, N. and Sajid, M. (2008a), "Analytic solution for MHD flow of a third order fluid in a porous channel", *J. Comput. Appl. Math.*, Vol. 214, pp. 572-82.

Hayat, T., Asghar, S. and Siddiqui, A.M. (1998), "Periodic unsteady flows of a non-Newtonian fluid", *Acta Mech.*, Vol. 131 Nos 3/4, pp. 169-75.

Hayat, T., Ellahi, R. and Mahomed, F.M. (2008b), "Exact solutions for thin film flow of a third grade fluid down an inclined plane", *Chaos Solit. Fract.*, Vol. 38 No. 5, pp. 1336-41.

Hayat, T., Ellahi, R., Ariel, P.D. and Asghar, S. (2006), "Homotopy solutions for the channel flow of a third grade fluid", *Nonlin. Dyn.*, Vol. 45, pp. 55-64.

He, J.H. (1999), "Homotopy perturbation technique", *Comput. Methods Appl. Mech. Eng.*, Vol. 178, pp. 257-62.

He, J.H. (2000), "A coupling method of a homotopy technique and a perturbation technique for non-linear problems", *Int. J. Nonlin. Mech.*, Vol. 35, pp. 37-43.

Holmes, G.C. (2002), "The use of hyperbolic cosines in solving cubic polynomials", *The Mathematical Gazette*, Vol. 86, pp. 473-7.

Liao, S.J. (2005), "Comparison between the homotopy analysis method and the homotopy perturbation method", *Appl. Math. Comput.*, Vol. 169, pp. 1186-94.

Liao, S.J. (2009), "Notes on the homotopy analysis method: some definitions and theories", *Commun. Nonlin. Sci. Numer. Simul.*, Vol. 14, pp. 983-97.

Lipscombe, T.C. (2010), "Comment on application of the homotopy method for analytical solution of non-Newtonian channel flows", *Physica Scripta*, Vol. 81 No. 3, p. 037001.

Liu, C.-S. (2010), "The essence of the homotopy analysis method", *Appl. Math. Comput.*, Vol. 216, pp. 1299-303.

Makinde, O.D. (2007), "Hermite-Padé approximation approach to thermal criticality for a reactive third-grade liquid in a channel with isothermal walls", *Int. Comm. Heat Mass Transfer*, Vol. 34, pp. 870-7.

Makinde, O.D. (2009), "On thermal stability of a reactive third-grade fluid in a channel with convective cooling the walls", *Appl. Math. Comp.*, Vol. 213, pp. 170-6.

Motsa, S.S., Sibanda, P. and Shateyi, S. (2010a), "A new spectral-homotopy analysis method for solving a nonlinear second order BVP", *Commun. Nonlin. Sci. Numer. Simul.*, Vol. 15, pp. 2293-302.

Motsa, S.S., Sibanda, P., Awad, F.G. and Shateyi, S. (2010b), "A new spectral-homotopy analysis method for the MHD Jeffery-Hamel problem", *Computers & Fluids*, Vol. 39, pp. 1219-25.

Rajagopal, K.R. (1993), "Mechanics of non-Newtonian fluids", *Recent Developments in Theoretical Fluid Mechanics*, Pitman Res. Notes Math. Ser., Vol. 291, Longman Scientific & Technical, Harlow, pp. 129-62.

Roohi, E., Kharazmi, S. and Farjami, Y. (2009), "Application of the homotopy method for analytical solution of non-Newtonian channel flows", *Phys. Scr.*, Vol. 9, p. 10.

Siddiqui, A.M., Zeb, A., Ghori, Q.K. and Benharbit, A.M. (2008), "Homotopy perturbation method for heat transfer flow of a third grade fluid between parallel plates", *Chaos Solit. Frac.*, Vol. 36, pp. 182-92.

Szeri, A.Z. and Rajagopal, K.R. (1985), "Flow of a non-Newtonian fluid between heated parallel plates", *Int. J. Nonlin. Mech.*, Vol. 20, pp. 91-101.

Tourigny, Y. and Drazin, P.G. (2000), "The asymptotic behaviour of algebraic approximants", *Proc. R. Soc. Lond. A*, Vol. 456, pp. 1117-37.

Tso, C.P. and Mahulikar, S.P. (1999), "The role of the Brinkman number in analysing flow transitions in microchannels", *Int. J. Heat Mass Transfer*, Vol. 42, pp. 1813-33.

van Gorder, R.A. and Vajravelu, K. (2009), "On the selection of auxiliary functions, operators, and convergence control parameters in the application of the homotopy analysis method to nonlinear differential equations: a general approach", *Commun. Nonlin. Sci. Numer. Simul.*, Vol. 14, pp. 4078-89.

Further reading

Liao, S.J. (2003), *Beyond Perturbation: Introduction to Homotopy Analysis Method*, CRC Press, Boca Raton, FL.

Corresponding author

Precious Sibanda can be contacted at: sibandap@ukzn.ac.za

3.3. On new solutions for heat transfer in a visco-elastic fluid between parallel plates [3]

[3]Z. G. Makukula, P. Sibanda and S. S. Motsa (2010). *International Journal of Mathematical Models and Methods in Applied Sciences* 4(4):221–230.

INTERNATIONAL JOURNAL OF MATHEMATICAL MODELS AND METHODS IN APPLIED SCIENCES

On new solutions for heat transfer in a visco-elastic fluid between parallel plates

ZODWA G MAKUKULA and PRECIOUS SIBANDA
University of KwaZulu-Natal
School of Mathematical Sciences
Private Bag X01, Scottsville, 3209, Pietermaritzburg
SOUTH AFRICA
sibandap@ukzn.ac.za

SANDILE S MOTSA
University of Swaziland
Department of Mathematics
Private Bag 4, Kwaluseni
SWAZILAND
sandilemotsa@gmail.com

Abstract: The steady, laminar flow of a third grade fluid with heat transfer through a flat channel is studied. We propose and apply a successive linearisation method (SLM) and an improved spectral-homotopy analysis method (ISHAM), to obtain approximate analytical solutions for the velocity and temperature profiles. The methods are primarily based on blending non-perturbation techniques with Chebyshev spectral methods to produce efficient algorithms for solving highly nonlinear systems. The effects of the Brinkman number, pressure gradient and the non-Newtonian parameter on the velocity, temperature, skin friction and heat transfer coefficients are discussed. Exact solutions are also constructed and compared with the SLM and ISHAM solutions.

Key–Words: Viscoelastic flow, heat transfer flow, linearisation method, improved spectral-homotopy analysis method, nonlinear BVPs

1 Introduction

The study of non-Newtonian fluids offers many interesting and exciting challenges due to their technical relevance in modelling fluids with complex rheological properties (such as polymer melts, synovial fluids, paints, etc). Viscoelastic fluids also present some highly peculiar characteristics and mathematical features such as the non-unidirectional nature of the flow of such fluids and the increase in the order of the differential equations characterizing such flows, [1, 2]. A lot of work on the flow and heat transfer characteristics of non-Newtonian fluids has also been done in order to control the quality of the end product in many manufacturing and processing industries, see for instance, [1, 3] and the references therein.

Various constitutive models currently exist to describe the properties of non-Newtonian fluids. The major problem however is that none of these models can adequately describe all non-Newtonian fluids. Among the several constitutive equations that have been suggested in the literature is a Rivlin-Erikson model, the third grade fluid model that is capable of describing the normal stress effects for steady unidirectional flow and to predict shear thinning/thickening, [4, 5]. This model has been analyzed in great detail in previous studies by Dunn and Rajagopal [6] and Fosdick and Rajagopal [7].

A large number of recent studies have investigated various aspects of the third-grade fluid model, including some that have merely used this model to test the effectiveness of a slew of new solution techniques for nonlinear equations. Makinde [4] studied the thermal stability of a reactive third-grade liquid flowing steadily between two parallel plates with symmetrical convective cooling at the walls while slip effects on the on the peristaltic flow of a third grade fluid have been studied by among others, Ali et al. [8, 9], El-Shehawy et al. [10] and Motsa et al. [21]. Studies by, among others, Aksoy and Pakdemirli [11], Hayat and his co-workers [12, 13, 14, 15, 16, 17], have, to a large extent, mainly been concerned with the development and testing of new perturbation techniques.

The present study deals with the problem of flow and heat transfer characteristics of a third grade fluid flow between two parallel plates. Exact analytical solutions for the steady Poiseuille flow, the skin friction and the heat transfer coefficients are found. We use innovation, the successive linearisation technique (SLM) (see Makukula et al. [18] and Motsa and Sibanda [20]) and the improved-spectral-homotopy analysis method (ISHAM) to solve the governing nonlinear equations. The accuracy of each methods is determined by comparing the solutions with the exact results.

2 Governing equations

The flow of an incompressible third grade fluid placed between two horizontal parallel impermeable plates is investigated.

The constitutive law for the Cauchy stress tensor $\mathbf{T}$ associated with an incompressible homogeneous fluid of third grade is given in [4, 7, 22]. This has the form

$$\begin{aligned}\mathbf{T} &= -p\mathbf{I} + \mu\mathbf{A}_1 + \alpha_1\mathbf{A}_2 + \alpha_2\mathbf{A}_1^2 + \beta_1\mathbf{A}_3 \\ &\quad +\beta_2[\mathbf{A}_1\mathbf{A}_2 + \mathbf{A}_2\mathbf{A}_1] + \beta_3(tr\mathbf{A}_1^2)\mathbf{A}_2, \quad (1)\end{aligned}$$

where

$$\begin{aligned}\mathbf{A}_1 &= \nabla\mathbf{v} + (\nabla\mathbf{v})^T, \\ \mathbf{A}_n &= \frac{d}{dt}(\mathbf{A}_{n-1}) + \mathbf{A}_{n-1}\nabla\mathbf{v} + (\nabla\mathbf{v})^T\mathbf{A}_{n-1}.\end{aligned}$$

In the above equations, p is the pressure, μ denotes the viscosity; $\alpha_1, \alpha_2, \beta_1, \beta_2, \beta_3$ are the material moduli, d/dt is the material derivative, $\mathbf{v}$ denotes the velocity field, while $\mathbf{A}_1$, $\mathbf{A}_2$ and $\mathbf{A}_3$ are the first three Rivlin - Ericksen tensors. The spherical stress $p\,\mathbf{I}$ is due to the constraint of incompressibility. The flow is subject to the restrictions

$$\mu \geq 0, \ \alpha_1 \geq 0, \ |\alpha_1 + \alpha_2| \leq \sqrt{24\mu\beta_3} \quad (2)$$

$$\beta_1 = \beta_2 = 0 \quad \text{and} \quad \beta_3 > 0. \quad (3)$$

If $\beta_3 = 0$ the model collapses to that of a second grade fluid. The equations of motion are given by [22, 23];

$$\nabla \cdot \mathbf{v} = 0, \quad (4)$$

$$\rho\frac{d\mathbf{v}}{dt} = \nabla \cdot \mathbf{T} + \rho\mathbf{b}, \quad (5)$$

$$\rho c_p\frac{d\theta}{dt} = \kappa\nabla^2\theta + \mathbf{T} \cdot \nabla\mathbf{v}, \quad (6)$$

where ρ is the mass density, κ the thermal conductivity, c_p is the specific heat at constant pressure, $\mathbf{b}$ is a body force, and θ is the temperature. The x-axis tangential to the plate surface, the y-axis normal to it. The fluid is confined between parallel plates located at $y = -h$ and $y = h$. We assume unidirectional flow so that

$$\mathbf{v} = u(y)\mathbf{i} \quad \text{and} \quad \theta = \theta(y).$$

The temperature of the upper plate is maintained at θ_1 and that of lower plate at θ_0 to give a temperature difference $\Delta\theta = \theta_1 - \theta_0$. The fluid motion is driven either by a constant pressure gradient or by the boundary conditions. Equations (4) - (6) reduce to (see, [4, 22, 21]);

$$\frac{d^2u}{dy^2}\left[1 + 6\beta\left(\frac{du}{dy}\right)^2\right] = -B, \quad (7)$$

$$\frac{d^2\theta}{dy^2} + \lambda\left(\frac{du}{dy}\right)^2\left[1 + 2\beta\left(\frac{du}{dy}\right)^2\right] = 0, \quad (8)$$

where

$$\begin{aligned}\beta &= \frac{\beta^* U^2}{\mu\, h^2}, \ \lambda = \frac{\mu U^2}{\kappa\Delta\theta}, \\ B &= -\frac{h^2}{\mu U}\frac{dp}{dx}, \quad \beta^* = \beta_2 + \beta_3.\end{aligned}$$

The parameters are the characteristic velocity U and the Brinkman number λ which determines the relative importance between the viscous dissipation and fluid conduction.

The appropriate boundary conditions are

$$u(-1) = 0, \quad u(1) = 0 \quad (9)$$

$$\theta(-1) = 0, \quad \theta(1) = 1. \quad (10)$$

In a recent study Motsa et al. [21] showed that the exact solution for the skin friction is

$$u'(y) = \frac{1}{6\beta}[F(y)]^{1/3} - [F(y)]^{-1/3}, \quad (11)$$

where

$$F(y) = 6\beta^2\left[-9By + \sqrt{\frac{6 + 81\beta By^2}{\beta}}\right]. \quad (12)$$

It is evident that this result is only valid when

$$\beta \geq -\frac{2}{27B^2}.$$

The temperature equation now simplifies to

$$\theta'' = \lambda By\, u'(y). \quad (13)$$

Equation (13) can easily be solved using any numerical method.

3 The linearisation method

In this section we apply the successive linearisation method (SLM) to solve equations (7) - (10). Since equation (7) is decoupled from the temperature equation (8) we only need apply the SLM to equation (7). The SLM is based on the assumptions that

- the unknown function $u(y)$ can be expanded as

$$u(y) = U_i(y) + \sum_{n=0}^{i-1} u_n(y), \ i = 1, 2, 3, \ldots \quad (14)$$

where U_i are unknown functions and u_n are approximations which are obtained by recursively solving the linear part of the equation that results from substituting (14) in equation (7), and that

- U_i becomes increasingly smaller as i becomes large, that is

$$\lim_{i\to\infty} U_i = 0. \tag{15}$$

Substituting (14) in equation (7) and neglecting nonlinear terms in U_i, U_i', U_i'' and using $U_i \approx u_i$ gives

$$\begin{aligned}&\left[1+6\beta\left(\sum_{n=0}^{i-1}u_n'\right)^2\right]u_i''\\&+\left[12\beta\sum_{n=0}^{i-1}u_n'\sum_{n=0}^{i-1}u_n''\right]u_i' = -B+\sum_{n=0}^{i-1}u_n''\\&+6\beta\left(\sum_{n=0}^{i-1}u_n'\right)^2\sum_{n=0}^{i-1}u_n'',\end{aligned} \tag{16}$$

which may be written in a more compact form as,

$$a_{i-1}u_i'' + b_{i-1}u_i' = r_{i-1}, \tag{17}$$

subject to the boundary conditions

$$u_i(-1) = u_i(1) = 0, \tag{18}$$

where,

$$\begin{aligned}a_{i-1} &= 1+6\beta\left(\sum_{n=0}^{i-1}u_n'\right)^2,\\b_{i-1} &= 12\beta\sum_{n=0}^{i-1}u_n'\sum_{n=0}^{i-1}u_n'',\\r_{i-1} &= -\left[B+\sum_{n=0}^{i-1}u_n''+6\beta\left(\sum_{n=0}^{i-1}u_n'\right)^2\sum_{n=0}^{i-1}u_n''\right].\end{aligned}$$

Once each solution u_i $(i \geq 1)$ has been found by iteratively solving equations (16), starting from an initial approximation $u_0(y)$, the approximate solutions for $u(y)$ are obtained as

$$u(y) \approx \sum_{n=0}^{M} u_n(y) \tag{19}$$

where M is the order of the SLM approximation. The initial approximation $u_0(y)$ is chosen in such a way that it satisfies the boundary conditions (9). In this study, a suitable initial approximation was chosen to be

$$u_0(y) = 0. \tag{20}$$

We observe that, by making use of the symmetry condition $u_i'(0) = 0$, equation (16) has an integrating factor (IF) given by

$$IF = 1+6\beta\left(\sum_{n=0}^{i-1}u_n'\right)^2. \tag{21}$$

Integrating (16) gives

$$u_i' = -\frac{1}{IF^2}\left[By+\sum_{n=0}^{i-1}u_n'+2\beta\left(\sum_{n=0}^{i-1}u_n'\right)^3\right]. \tag{22}$$

Thus starting from an initial guess $u_0(y) = 0$, the solutions for u_i $(i \geq 1)$ can be obtained iteratively from equation (16). The first three solutions for $i = 1, 2, 3, \ldots$, are given as

$$u_1'(y) = -By, \tag{23}$$

$$u_2'(y) = \frac{2\beta B^3 y^3}{1+6\beta B^2 y^2}, \tag{24}$$

$$u_3'(y) = -\frac{-8\beta^3 B^7 y^7(3+16\beta B^2 y^2)}{k_1(1+6k_2\beta B^2 y^2)}, \tag{25}$$

where

$$\begin{aligned}k_1 &= 1+6\beta B^2 y^2,\\k_2 &= 3+14\beta B^2 y^2+16\beta^2 B^4 y^4.\end{aligned}$$

The explicit solutions for $u_4', u_5', u_6', \ldots$ can be obtained in the same manner.

The analytic solution for the skin friction coefficient C_f is obtained as

$$u'(1) \approx u_0'(1)+u_1'(1)+u_2'(1)+u_3'(1)+\ldots \tag{26}$$

Since the coefficient parameters and the right hand side of equation (16), for $i = 1, 2, 3, \ldots$, are known (from previous iterations), equation (16) can easily be solved using analytical means or numerical methods. Solving equation (16) analytically for u_i was only possible for the first two iterations. For higher order iterations $(i > 3)$ numerical integration was employed. In this work, equations (16) was integrated using the Chebyshev spectral collocation method. This method is based on approximating the unknown functions by the Chebyshev interpolating polynomials in such a way that they are collocated at the Gauss-Lobatto points defined as

$$y_j = \cos\frac{\pi j}{N}, \quad j = 0, 1, \ldots, N. \tag{27}$$

where N is the number of collocation points used. The second derivative of u_i at the collocation points are represented as

$$\frac{d^2u_i}{dy^2} = \sum_{k=0}^{N}\mathbf{D}_{kj}^2 u_i(y_k), \quad j = 0, 1, \ldots, N \tag{28}$$

where $\mathbf{D}$ is the Chebyshev spectral differentiation matrix. Substituting equations (27) - (28) in (17) results in the matrix equation

$$\mathbf{A}_{i-1}\mathbf{U}_i = \mathbf{R}_{i-1}, \tag{29}$$

with boundary conditions

$$u_i(y_0) = u_i(y_N) = 0, \tag{30}$$

in which $\mathbf{A}_{i-1}$ is a $(N+1)\times(N+1)$ square matrix and $\mathbf{U}_i$ and $\mathbf{R}_{i-1}$ are $(N+1)\times 1$ column vectors defined by

$$\begin{aligned}\mathbf{U}_i &= [u_i(y_0),\ldots,u_i(y_{N-1}),u_i(y_N)]^T,\\ \mathbf{R}_{i-1} &= [r_{i-1}(y_0),\ldots,r_{i-1}(y_{N-1}),r_{i-1}(y_N)]^T,\\ \mathbf{A}_{i-1} &= \mathbf{a}_{i-1}\mathbf{D}^2+\mathbf{b}_{i-1}\mathbf{D},\end{aligned}$$

where $\mathbf{b}_{i-1}$ is a diagonal matrix of size $(N+1)\times(N+1)$. After modifying the matrix system (29) to incorporate boundary conditions (30), the solution is obtained as

$$\mathbf{U}_i = \mathbf{A}_{i-1}^{-1}\mathbf{\Phi}_{i-1}. \tag{31}$$

The solution for $\theta(y)$ is obtained by applying the Chebyshev spectral collocation method to (13).

4 The improved spectral homotopy analysis method (ISHAM)

In this section we describe and apply the ISHAM to solve the governing equation (7) with boundary conditions (10). The ISHAM algorithm seeks to improve the initial approximation that is then used in the original SHAM [19] algorithm to solve the governing nonlinear equation. The basic assumption is that the solution $u(y)$ can be expanded as

$$u(y) = U_i(y) + \sum_{n=0}^{i-1} u_n(y), \quad i = 1,2,3,\ldots, \tag{32}$$

where U_i are unknown functions whose solutions are obtained using the SHAM algorithm at the ith iteration and $u_n(y)$, $(n \geq 1)$ are known from previous iterations. The algorithm begins with an initial approximation

$$u_0(y) = \alpha B(1-y^2), \tag{33}$$

which is chosen to satisfy the boundary conditions (10) and α is a scaling parameter. Substituting equation (32) and using $U_i \approx u_i$ in the governing equation (7) gives

$$a_{1,i-1}u_i'' + a_{2,i-1}u_i' + 6\beta u_i''(u_i')^2 = r_{i-1}, \tag{34}$$

subject to the boundary conditions

$$u_i(-1) = u_i(1) = 0, \tag{35}$$

where the coefficient parameters $a_{k,i-1}$ $(k = 1,2)$, r_{i-1} are defined as

$$\begin{aligned}a_{1,i-1} &= 1+6\beta\left(\sum_{n=0}^{i-1}u_n'\right)^2,\\ a_{2,i-1} &= 12\beta\sum_{n=0}^{i-1}u_n'\sum_{n=0}^{i-1}u_n'',\\ r_{i-1} &= -\left[B+\sum_{n=0}^{i-1}u_n''+6\beta\left(\sum_{n=0}^{i-1}u_n'\right)^2\sum_{n=0}^{i-1}u_n''\right].\end{aligned}$$

Starting from the initial approximation (33) the subsequent solutions u_i, $(i \geq 1)$ are obtained by recursively solving equation (34) using the SHAM approach. To find the SHAM solutions of (34) we begin by defining the following linear operator

$$\mathcal{L}[\mathcal{U}_i(y;q)] = a_{1,i-1}\frac{\partial^2\mathcal{U}_i}{\partial y^2} + a_{2,i-1}\frac{\partial\mathcal{U}_i}{\partial y}, \tag{36}$$

where $q \in [0,1]$ is the embedding parameter, and $\mathcal{U}_i(y;q)$ are unknown functions. The zeroth order deformation equation is given by

$$(1-q)\mathcal{L}[\mathcal{U}_i(y;q) - u_{i,0}(y)] = q\hbar\mathcal{N}[\mathcal{U}_i(y;q)] - r_{i-1}, \tag{37}$$

where $\hbar$ is the non-zero convergence controlling auxiliary parameter and $\mathcal{N}$ is a nonlinear operator given by

$$\mathcal{N}[\mathcal{U}_i(y;q)] = a_{1,i-1}\frac{\partial^2\mathcal{U}_i}{\partial y^2} + a_{2,i-1}\frac{\partial\mathcal{U}_i}{\partial y} + 6\beta\frac{\partial^2\mathcal{U}_i}{\partial y^2}\left(\frac{\partial\mathcal{U}_i}{\partial y}\right)^2. \tag{38}$$

Differentiating (37) m times with respect to q and then setting $q = 0$ and finally dividing the resulting equations by $m!$ yields the mth order deformation equations

$$\begin{aligned}&\mathcal{L}[u_{i,m}(y) - \chi_m u_{i,m-1}(y)] = \\ &\hbar\left(a_{1,i-1}u_{i,m-1}'' + a_{2,i-1}u_{i,m-1}'\right.\\ &\left.+6\beta\sum_{j=0}^{m-1}u_{i,m-1-j}''\sum_{n=0}^{j}u_{i,j-n}'u_{i,n}' - (1-\chi_m)r_{i-1}\right),\end{aligned} \tag{39}$$

subject to the boundary conditions

$$u_{i,m}(-1) = u_{i,m}(1) = 0, \tag{40}$$

where

$$\chi_m = \begin{cases}0, & m \leq 1\\ 1, & m > 1\end{cases}. \tag{41}$$

The initial approximation $u_{i,0}$ that is used in the higher order equation (39) is obtained by solving the linear part of equation (34) given by

$$a_{1,i-1}u''_{i,0} + a_{2,i-1}u'_{i,0} = r_{i-1}, \tag{42}$$

with the boundary conditions

$$u_{i,0}(-1) = u_{i,0}(1) = 0. \tag{43}$$

Applying the Chebyshev spectral method, described in the SLM section, to solve equation (42) yields the matrix form

$$\mathbf{A}_{i-1}\mathbf{U}_{i,0} = \mathbf{Q}_{i-1}, \tag{44}$$

subject to the boundary conditions

$$u_{i,0}(y_0) = \quad u_{i,0}(y_N) = 0. \tag{45}$$

where

$$\begin{aligned} \mathbf{A}_{i-1} &= \mathbf{a}_{1,i-1}\mathbf{D}^2 + \mathbf{a}_{2,i-1}\mathbf{D}, \\ \mathbf{U}_{i,0} &= [u_{i,0}(y_0), u_{i,0}(y_1), \ldots, u_{i,0}(y_N)]^T, \\ \mathbf{Q}_{i-1} &= [r_{i-1}(y_0), r_{i-1}(y_1), \ldots, r_{i-1}(y_N)]^T. \end{aligned} \tag{46}$$

After modifying the matrix system (44) to incorporate the boundary conditions (45), the solution is obtained as

$$\mathbf{U}_{i,0} = \mathbf{A}_{i-1}^{-1}\mathbf{Q}_{i-1}. \tag{47}$$

Similarly, applying the Chebyshev spectral transformation on the higher order deformation equation (39) gives

$$\begin{aligned} \mathbf{A}_{i-1}\mathbf{U}_{i,m} &= (\chi_m + \hbar)\mathbf{A}_{i-1}\mathbf{U}_{i,m-1} \\ &- \hbar(1-\chi_m)\mathbf{Q}_{i-1} + \hbar\mathbf{P}_{i,m-1}, \end{aligned} \tag{48}$$

where $\mathbf{A}_{i-1}$ and $\mathbf{Q}_{i-1}$, are as defined in (46) and

$$\begin{aligned} \mathbf{U}_{i,m} &= [u_{i,m}(y_0), u_{i,m}(y_1), \ldots, u_{i,m}(y_N)]^T, \\ \mathbf{P}_{i,m-1} &= 6\beta \sum_{j=0}^{m-1} \mathbf{D}^2 u_{i,m-1-j} \sum_{n=0}^{j} \mathbf{D}u_{i,j-n}\mathbf{D}u_{i,n}. \end{aligned}$$

To implement the boundary conditions on the right hand side of equation (48), we set the first and last rows and columns of $\mathbf{A}_{i-1}$ to be zero and similarly the first and last columns of $\mathbf{Q}_{i-1}$ and $\mathbf{P}_{m-1}$ to be zero. This results in the following recursive formula for $m \geq 1$

$$\begin{aligned} \mathbf{U}_{i,m} &= (\chi_m + \hbar)\mathbf{A}_{i-1}^{-1}\tilde{\mathbf{A}}_{i-1}\mathbf{U}_{i,m-1} \\ &+ \hbar\mathbf{A}_{i-1}^{-1}[\mathbf{P}_{i,m-1} - (1-\chi_m)\mathbf{Q}_{i-1}], \end{aligned} \tag{49}$$

where $\tilde{\mathbf{A}}_{i-1}$ is the modified matrix $\mathbf{A}_{i-1}$ on the right hand side of (48) after incorporating the boundary conditions. Thus starting from the initial approximation, which is obtained from (47), higher order approximations $u_{i,m}(y)$ for $m \geq 1$, can be obtained through the recursive formula (49). The solutions for u_i are then generated using the solutions for $u_{i,m}$ as follows

$$u_i = u_{i,0} + u_{i,1} + u_{i,2} + u_{i,3} + \ldots + u_{i,m}. \tag{50}$$

The $[i,m]$ approximate solution for $u(y)$ is then obtained by substituting u_i obtained from (50) into equation (32).

5 Results and Discussion

In this section we present a comparison of the successive linearisation method (SLM), improved spectral-homotopy analysis method (ISHAM) and the exact analytical results. All the SLM and ISHAM results were generated using $N = 100$ collocation points. To show the accuracy and effectiveness of the methods, a limited parametric study is undertaken.

Table 1 shows a comparison of the convergence rate of the SLM, ISHAM and the exact solution when $B = 1$ and for increasing values of the non-Newtonian parameter β. A match between the SLM results and the exact results, accurate to 10 decimal places is achieved at the sixth order of the SLM series solution for all the selected values of β while the ISHAM converges to the exact solution at order [4,4]. The difference in convergence rates of the two methods is clearly shown in Table 2 where a comparison of the absolute errors in the SLM and ISHAM approximate solutions for $u'(1)$ is given for various values of β when $B = 1$.

In Table 3 the non-Newtonian parameter is fixed at $\beta = 1$ while the pressure gradient term increases monotonically from $\beta = 0.2$. For $B \leq 1$, full convergence of the SLM approximations to the exact solution is achieved at the fourth-order of the SLM series solution while the ISHAM converges at order [3,3]. The precision of the SLM however deteriorates faster than that of the ISHAM with increasing B with more terms needed in the SLM series to match the exact results. Full convergence to the exact results (to ten decimal places) is achieved at the 4th order of the SLM series for $B \leq 1$ and at order [3,3] for ISHAM solutions. For $B > 1$ The SLM converges fully at the sixth order of approximation while the ISHAM approximate solutions converge at order [4,4]. These is clearly indicated in Table 4 where a comparison of the absolute errors between the SLM and ISHAM approximate solutions for $u'(1)$ are given for various values of B when $\beta = 1$.

Table 1: Comparison of the approximate values of $u'(1)$ using the SLM and ISHAM with the exact solution for various values of β when $B = 1$.

			SLM solution		
β	3rd order	4th order	5th order	6th order	Exact
0.2	-0.7972810885	-0.7972810583	-0.7972810583	-0.7972810583	-0.7972810583
0.5	-0.6823395826	-0.6823278039	-0.6823278038	-0.6823278038	-0.6823278038
1.0	-0.5900220423	-0.5897545943	-0.5897545123	-0.5897545123	-0.5897545123
2.0	-0.5023901750	-0.5000085354	-0.5000000001	-0.5000000000	-0.5000000000
			ISHAM solution		
	[2,2]	[3,3]	[4,4]	[5,5]	Exact
0.2	-0.7972810449	-0.7972810583	-0.7972810583	-0.7972810583	-0.7972810583
0.5	-0.6823218302	-0.6823278038	-0.6823278038	-0.6823278038	-0.6823278038
1.0	-0.5896283020	-0.5897545122	-0.5897545123	-0.5897545123	-0.5897545123
2.0	-0.4991584068	-0.4999999475	-0.5000000000	-0.5000000000	-0.5000000000

Table 2: Comparison of the absolute errors between the SLM and ISHAM approximate solutions for $u'(1)$ and the exact solution for various values of β when $B = 1$.

		SLM solution		
β	3rd order	4th order	5th order	6th order
0.2	0.0000000302	0.0000000000	0.0000000000	0.0000000000
0.5	0.0000117788	0.0000000001	0.0000000000	0.0000000000
1.0	0.0002675300	0.0000000820	0.0000000000	0.0000000000
2.0	0.0023901750	0.0000085354	0.0000000001	0.0000000000
		ISHAM solution		
	[2,2]	[3,3]	[4,4]	[5,5]
0.2	0.0000000134	0.0000000000	0.0000000000	0.0000000000
0.5	0.0000059736	0.0000000000	0.0000000000	0.0000000000
1.0	0.0001262103	0.0000000001	0.0000000000	0.0000000000
2.0	0.0008415932	0.0000000525	0.0000000000	0.0000000000

Table 3: Comparison of the approximate values of $u'(1)$ using the SLM and ISHAM with the exact solution for various values of B when $\beta = 1$.

			SLM solution		
B	3rd order	4th order	5th order	6th order	Exact
0.2	-0.1869351878	-0.1869351878	-0.1869351878	-0.1869351878	-0.1869351878
0.5	-0.3854585785	-0.3854584985	-0.3854584985	-0.3854584985	-0.3854584985
1.0	-0.5900220423	-0.5897545943	-0.5897545123	-0.5897545123	-0.5897545123
2.0	-0.8564235361	-0.8355504792	-0.8351225255	-0.8351223485	-0.8351223485
			ISHAM solution		
	[2,2]	[3,3]	[4,4]	[5,5]	Exact
0.2	-0.1869351878	-0.1869351878	-0.1869351878	-0.1869351878	-0.1869351878
0.5	-0.3854584608	-0.3854584985	-0.3854584985	-0.3854584985	-0.3854584985
1.0	-0.5896283020	-0.5897545122	-0.5897545123	-0.5897545123	-0.5897545123
2.0	-0.8318383437	-0.8351152280	-0.8351223485	-0.8351223485	-0.8351223485

Table 4: Comparison of the absolute errors between the SLM and ISHAM approximate solutions for $\dot{u}(1)$ and the exact solution for various values of B when $\beta = 1$.

	SLM solution			
B	3rd order	4th order	5th order	6th order
0.2	0.0000000000	0.0000000000	0.0000000000	0.0000000000
0.5	0.0000000800	0.0000000000	0.0000000000	0.0000000000
1.0	0.0002675300	0.0000000820	0.0000000000	0.0000000000
2.0	0.0213011876	0.0004281307	0.0000001770	0.0000000000
	ISHAM solution			
	[2,2]	[3,3]	[4,4]	[5,5]
0.2	0.0000000000	0.0000000000	0.0000000000	0.0000000000
0.5	0.0000000377	0.0000000000	0.0000000000	0.0000000000
1.0	0.0001262103	0.0000000001	0.0000000000	0.0000000000
2.0	0.0032840048	0.0000071205	0.0000000000	0.0000000000

Figure 1 shows the velocity distribution for the Poiseuille flow with β as calculated using the successive linearisation method. The velocity profiles decrease with β. These results are accurate and qualitatively similar to those obtained by Roohi et al. [25] using the HAM, Motsa et al. [21] using the spectral homotopy analysis method and Siddique et al. [22] using the homotopy perturbation method.

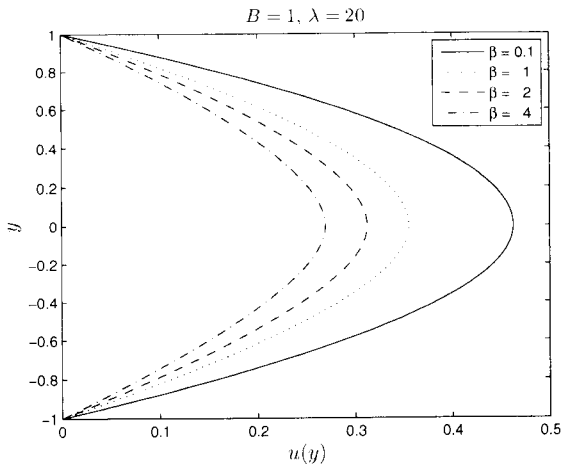

Figure 1: Velocity $u(y)$ profiles for different values of β

Figure 2 shows the effect of the pressure gradient on the temperature profiles for fixed $\beta = 1$ and $\lambda = 20$. Figure 3 shows the effect of the Brinkman number which determines the relative importance between viscous dissipation effects and fluid conduction on the temperature profiles for fixed B and β. Simulations show that as the Brinkman number increases, more heat is generated by the viscous dissipation effect and the temperature rapidly increases with λ, (see also Saouli et al. [26]).

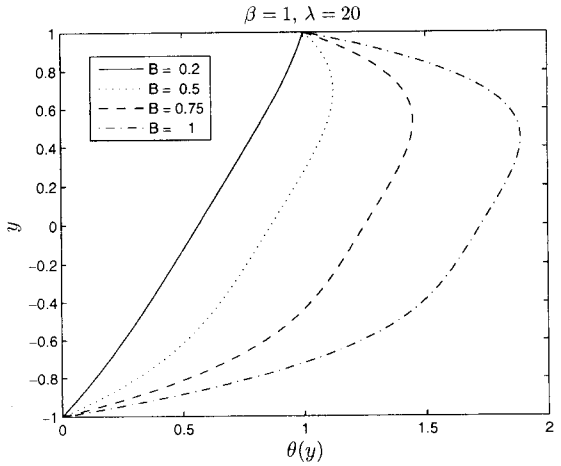

Figure 2: Temperature $\theta(y)$ profiles for different values of B

Figure 4 shows the variation of the skin-friction with B and β for fixed λ. The skin friction increases with β for increasing pressure gradient.

Figure 5 shows the growth of the wall heat transfer rate for various values of the parameter B. Increasing B increases the heat transfer rate.

6 Conclusion

In the present paper we considered the steady laminar flow of a third grade fluid with heat transfer through a flat channel. Two algorithms, namely the successive linearisation method (SLM) and the improved spectral-homotopy analysis method (ISHAM) were

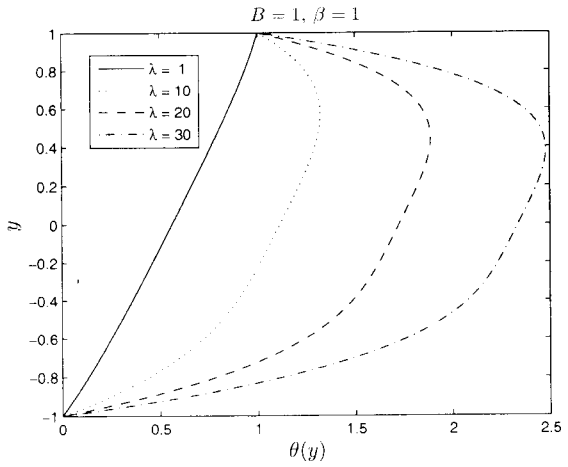

Figure 3: Temperature $\theta(y)$ profiles for different values of λ

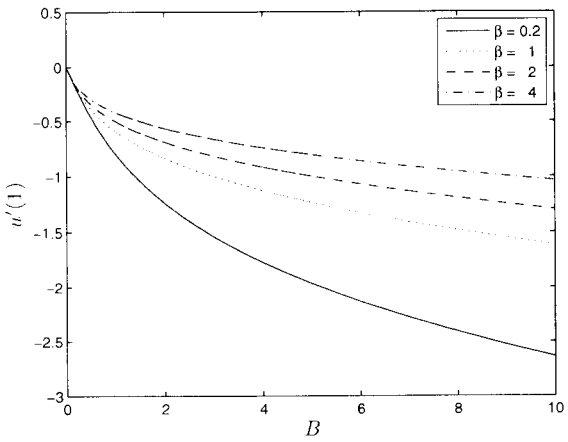

Figure 4: Skin friction $u'(1)$ for different values of B

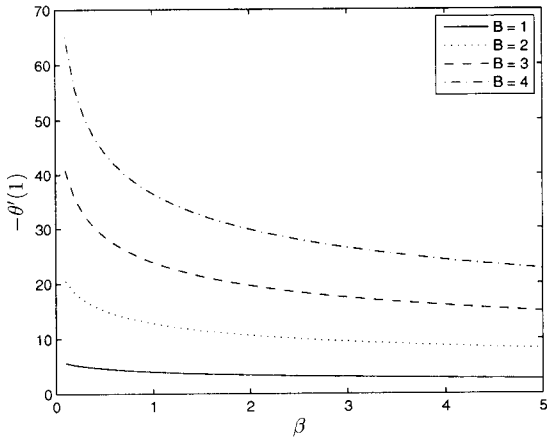

Figure 5: Wall heat transfer rate $-\theta'(1)$ for different values of β when $\lambda = 20$

presented to compute the analytical results for the skin friction coefficient and rate of heat transfer. New analytical results for the skin friction at the channel walls have been found. A comparison of the rate of convergence of the SLM and ISHAM approximations to the exact result shows that while both methods converge rapidly, the ISHAM however converges much more rapidly than the SLM. Both methods converge for all parameter values with the ISHAM showing better convergence for larger parameter values. The SLM and ISHAM were both applied successfully to compute the analytical results for the steady laminar flow of a third grade fluid with heat transfer through a flat channel. The success together with consistency of our results with earlier findings shows that the two methods can be efficiently used to solve nonlinear problems in science and engineering.

References

[1] P. D. Ariel, Flow of a third grade fluid through a porous flat channel, *International Journal of Engineering Science*, Vol. 41, 2003, pp. 1267 – 1285.

[2] K. Fakhar, Exact solutions for nonlinear partial differential equation arising in third grade fluid flows, *Southeast Asian Bulletin of Mathematics*, Vol. 32, 2008, pp. 65 – 70.

[3] T. Altan, H. Gegel, *Metal forming fundamentals and applications*, American Society of Metals, Metals Park, OH, 1979.

[4] O. D. Makinde, On thermal stability of a reactive third-grade fluid in a channel with convective cooling the walls, *Appl. Math. Comp.*, Vol. 213, 2009, pp. 170 – 176.

[5] M. Yurusoy, M. Pakdemirli, Approximate analytical solutions for the flow of a third grade fluid in a pipe, *Int. J. Non-Linear Mech.*, Vol. 37, 2002, pp. 187-195.

[6] J. E. Dunn and K. R. Rajagopal, Fluids of differential type: critical review and thermodynamic analysis, *Int. J. Engrg. Sci.*, Vol. 33 no. 5, 1995, pp. 689-729.

[7] R. L. Fosdick, K. R. Rajagopal, Thermodynamics and stability of fluids of third grade, *Proc. Roy. Soc. London A*, Vol. 369, 1980, pp. 351 – 377.

[8] N. Ali, Y. Wang, T. Hayat, M. Oberlack, Slip Effects on the Peristaltic Flow of a Third Grade Fluid in a Circular Cylindrical Tube *J. Appl. Mech.*, Vol.76, 2009, 011006 (10 pages) doi:10.1115/1.2998761

[9] N. Ali, T. Hayat, Y. Wang, MHD peristaltic flow of a third order fluid in an asymmetric channel, *International Journal for Numerical Methods in Fluids*, 2009 DOI: 10.1002/fld.2184.

[10] E. F. El-Shehawy, N. T. El-Dabe, I. M. El-Desoky, Slip Effects on the Peristaltic Flow of a Non-Newtonian Maxwellian Fluid, *Acta Mech.*, Vol. 186, 2006, pp. 141-159.

[11] Y. Aksoy, M. Pakdemirli, Approximate Analytical Solutions for Flow of a Third-Grade Fluid Through a Parallel-Plate Channel Filled with a Porous Medium, *Journal Transport in Porous Media*, 2009; doi:10.1007/s11242-009-9447-5

[12] T. Hayat, N. Ahmed, M. Sajid, Analytic solution for MHD flow of a third order fluid in a porous channel, *J. Comp. Appl. Math.*, Vol. 214, 2008, pp. 572–582.

[13] T. Hayat, R. Ellahi, F.M. Mahomed, Exact solutions for thin film flow of a third grade fluid down an inclined plane, *Chaos Solit. Fract.*, Vol. 38(5), 2008, pp. 1336–1341.

[14] T. Hayat, M. Khan, M. Ayub, On the explicit analytic solutions of an Oldroyd 6-constant fluid, *Int. J. Eng. Sci.*, Vol. 42, 2004, pp. 123–135.

[15] T. Hayat, S. Asghar, and A. M. Siddiqui, Periodic unsteady flows of a non-Newtonian fluid, *Acta Mech. Vol.*, 131 no. 3-4, 1998, pp. 169-175.

[16] T. Hayat, R. Naz, M. Sajid, On the homotopy solution for Poiseulle flow of a fourth grade fluid, *Commun. Nonlinear Sci. Numer. Simul.*, 2009, doi:10.1016/j.cnsns.2009.04.024.

[17] T. Hayat, R. Ellahi, P.D. Ariel, and S. Asghar, Homotopy solutions for the channel flow of a third grade fluid, *Nonlin. Dyn.* Vol. 45, 2006, pp. 55–64.

[18] Z. Makukula, S. S. Motsa and P. Sibanda, "On a new solution for the viscoelastic squeezing flow between two parallel plates, *Journal of Advanced Research in Applied Mathematics*, vol. 2, no. 4, 2010, pp. 31 - 38.

[19] S.S. Motsa, P. Sibanda, S. Shateyi, A new spectral-homotopy analysis method for solving a nonlinear second order BVP, Commun. Nonlinear Sci. Numer. Simul., 15 (2010) 2293 – 2302.

[20] S. S. Motsa and P. Sibanda, *A new algorithm for solving singular IVPs of Lane-Emden type*, Proceedings of the 4th International Conference on Applied Mathematics, Simulation, Modelling, pp. 176 - 180, NAUN International Conferences, Corfu Island, Greece, July 22-25, 2010.

[21] S. S. Motsa, Z. G. Makukula and P. Sibanda, A spectral-homotopy analysis method for heat transfer flow of a third grade fluid between parallel plates, *International Journal of Numerical Methods for Heat and Fluid Flow*, 2010, in press.

[22] A.M. Siddiqui, A.Zeb, Q.K. Ghori, A.M. Benharbit, Homotopy perturbation method for heat transfer flow of a third grade fluid between parallel plates, *Chaos Solit. Frac.*, Vol. 36, 2008, pp. 182–192.

[23] S. Asghar, M. R. Mohyuddin, T. Hayat, A. M. Siddiqui, The flow of a non-Newtonian fluid induced Due to the oscillations of a porous plate. *Mathematical Problems in Engineering* Vol. 2004: 2, 2004, pp. 133143, URL: http://dx.doi.org/10.1155/S1024123X04309014.

[24] S.J. Liao, Beyond perturbation: *Introduction to homotopy analysis method.* Chapman & Hall/CRC Press, 2003.

[25] E. Roohi, S. Kharazmi, Y. Farjami, Application of the homotopy method for analytical solution of non-Newtonian channel flows, *Phys. Scr.*, 2009, doi:10.1088/0031-8949/79/06/065009.

[26] S. Saouli, S. Aiboud-Saouli, Second-law analysis of laminar nonnewtonian gravity-driven liquid film along an inclined heated plate with viscous dissipation effect, *Braz. J. Chem. Eng.*, Vol. 26, 2009, doi: 10.1590/S0104-66322009000200019.

3.4. Summary

This chapter comprises of three sections where the SLM, SHAM, and ISHAM are used to solve problems involving flow between parallel plates. In Section 3.1 the successive linearisation method was used to find solutions of a squeezing flow problem between two parallel plates. The problem was solved successfully and the numerical results demonstrated the ability of the method to generate convergent results at low orders of approximation. In Section 3.2, the spectral homotopy analysis method was used to solve a heat transfer flow problem of a third grade fluid between parallel plates, while in Section 3.3 the successive linearisation and improved spectral homotopy analysis methods were used to solve the same problem. The robustness and efficiency of the successive linearisation method, spectral homotopy analysis method and the improved spectral homotopy analysis method has been demonstrated. These methods are very useful tools for solving highly nonlinear problems in science and engineering.

4

On heat transfer in rotating disks flows

The theoretical study of swirling flows due to a rotating body was pioneered by von Kármán in 1929 when he gave a mathematical formulation of the problem of fluid flow due to an infinite rotating disk. He introduced transformations that reduced the partial differential equations governing the flow to ordinary differential equations. Cochran (1934) extended the analysis and obtained asymptotic solutions for the von Kármán equations. This solution was later further improved by Benton (1966) who solved the unsteady state equations.

Disk flow problems are important in nature and in industry. They have applications in rotating machinery, heat and mass exchangers, biomechanics and oceanography (Sahoo, 2009; Devi and Devi, 2011), computer disk drives, film condensation (Maleque, 2009), viscometry and spin-coating (Frusteri and Osalusi, 2007). Swirling flows are not only important in fluid dynamics, but also occur frequently in nature. Large rotating flows are also found in the atmosphere and in the oceans (Zandbergen and Dijkstra, 1987). They also enhance combustion and flame propagation (Urzay et al., 2011). Many aspects of rotating disk flows have since been studied. To this regard, we solved in this Chapter the von Kármán equations with and without heat transfer using the successive linearisation method, the spectral homotopy analysis method

and the improved homotopy analysis method.

The improved spectral homotopy analysis method was used to study solutions of the steady flow problem of a Reiner-Rivlin fluid with Joule heating and viscous dissipation in Section 4.1. The solutions obtained by the method were compared with those obtained using the spectral homotopy analysis method and results in the literature. Convergence to the numerical solutions was achieved at the second orders while the SHAM converged at the eighth order for some of the flow parameters.

The spectral homotopy analysis method together with the successive linearisation method was used to find numerical solutions of the von Kármán nonlinear equations for swirling flow with and without suction/injection across the disk walls and an applied magnetic field in Section 4.2. The results were compared with numerical results and against the homotopy analysis method and homotopy-Padé results in the literature. In the study both the spectral homotopy analysis method and the successive linearisation method gave accurate and convergent results after a few iterations compared with the homotopy analysis and the homotopy-Padé methods. However, the successive linearisation method proved to be efficient in that it rapidly converged to the numerical results.

In Section 4.3, the laminar heat transfer problem in a rotating disk was solved using the successive linearisation method. The study revealed that the SLM is accurate and converges at very low orders of the iteration scheme.

4.1. On a linearisation method for Reiner-Rivlin swirling flow [1]

Errata

In this article, we like to add the geometry of the problem below

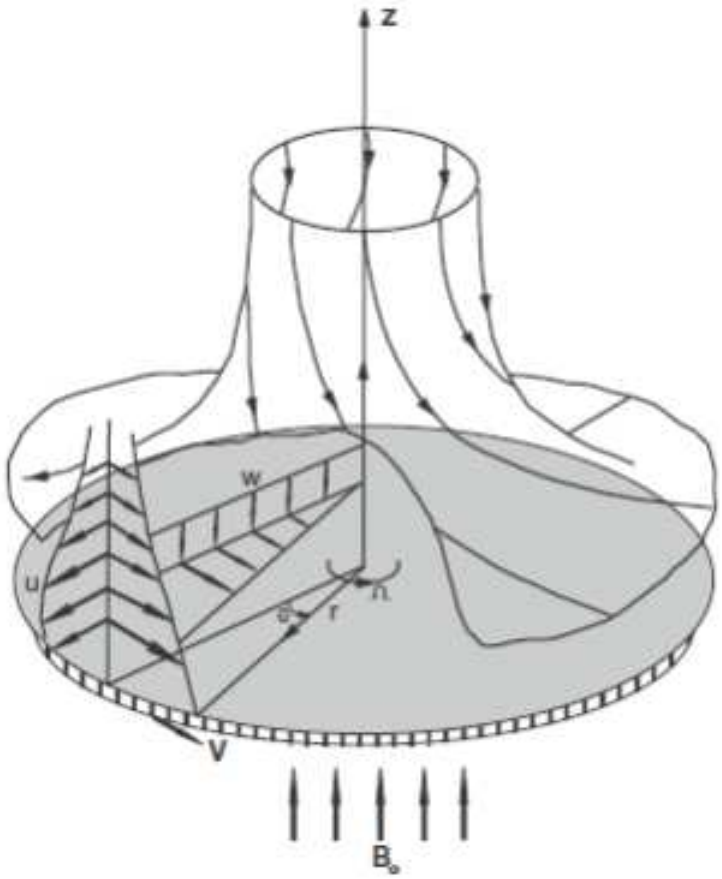

Figure 4.1: *Schematic representation of the flow domain (Sahoo, 2009).*

[1]Accepted; S. S. Motsa, Z. G. Makukula and P. Sibanda. *Journal of Computational and Applied Mathematics*, http://www.journals.elsevier.com/journal-of-computational-and-applied-mathematics/ (Impact factor; 1.029).

ON A LINEARISATION METHOD FOR REINER-RIVLIN SWIRLING FLOW

SANDILE S. MOTSA[2*], PRECIOUS SIBANDA[2] AND ZODWA G. MAKUKULA[2]

[2]School of Mathematical Sciences, University of KwaZulu-Natal, Private Bag X01, Scottsville 3209, Pietermaritzburg, South Africa

E-mails: sandilemotsa@gmail.com / sibandap@ukzn.ac.za /zmzmakukula@gmail.com

ABSTRACT. The steady flow of a Reiner-Rivlin fluid with Joule heating and viscous dissipation is studied. We present a novel technique for accelerating the convergence of the spectral-homotopy analysis method. Solutions of the nonlinear momentum and energy equations are obtained using the improved spectral homotopy analysis method. Solutions were also generated using the spectral-homotopy analysis method and benchmarked against results in the literature.

Key words: Reiner-Rivlin fluid, Chebyshev spectral method, Spectral-homotopy analysis method, Improved spectral-homotopy analysis method

1. INTRODUCTION

The boundary layer induced by a rotating disk arises in many engineering applications, for example, in computer storage devices, viscometry, turbo-machinery and in crystal growth processes (Attia [4]). Since the pioneering study by von Kármán [39], research on swirling flows has been carried out by, among others, Cochran [15] who proposed an improved solution to the von Kármán formulation based on a mixture of analytical and numerical techniques. Benton [12] studied the impulsive rotation from rest of a disk in an infinite viscous fluid. He improved Cochran's solutions by first expanding the variables in a power series and solving for the first two orders analytically, and then numerically computing the next two orders.

The shooting method was used to solve the von Kármán equations and to investigate heat transfer in porous medium in [19, 29, 30, 33, 35]. Numerical schemes involving Runge-Kutta methods, finite element and finite difference approximations were used in [14, 18, 24] to study the effects of a rough disk surface on the flow. The Crank-Nicholson implicit scheme was used in studies involving non-Newtonian characteristic of the fluid [4, 5, 6, 8, 10, 33] and in Newtonian fluids [7, 9, 11]. Perturbation techniques including the differential transform method and Padé approximations (DTM-Padé), the variational iteration method (VIM) and the homotopy perturbation method (HPM) were used in [1, 2, 31, 32, 34].

Analytical methods such as the DTM and the homotopy analysis method (HAM) were applied in, among other studies, [3, 17, 40, 37, 38]. These methods may result in secular terms in the solutions, and may converge very slowly or may even fail to converge for problems with strong non-linearity and/or with very large parameter values. Some approaches may not be applicable at all for certain problems, for example, the DTM for unbounded domain problems. Motsa et al. [22, 23, 25, 26, 27] proposed and applied a modification of the homotopy analysis method that improves the performance of this method and removes some restrictions associated with it. In general, the convergence of many numerical methods depends on how good the initial approximation is to the true solution. In this paper we present an algorithm that first seeks to improve the initial "guess" and then uses the spectral-homotopy analysis method to find solutions to systems of nonlinear equations that govern the Reiner-Rivlin swirling flow. This procedure considerably accelerates the convergence rate of the spectral homotopy analysis method. Here we apply the improved spectral-homotopy analysis method (ISHAM) to solve the nonlinear equations that govern the flow of an electrically conducting Reiner-Rivlin fluid in the presence of Joule heating and viscous dissipation. The governing equations were solved earlier by Sahoo [33] using a numerical scheme that blends the finite difference scheme and the shooting method. Solutions obtained are compared with those of Sahoo [33] and against the 'standard' spectral homotopy analysis method.

2. Equations

We consider an infinite rotating disk coinciding with the plane $z = 0$ with the space $z > 0$ occupied by a viscous, incompressible Reiner-Rivlin fluid. The fluid motion and heat transfer are governed by the equations (see [4, 5, 33]);

$$\frac{\partial u}{\partial r} + \frac{u}{r} + \frac{\partial w}{\partial z} = 0, \tag{2.1}$$

$$\rho\left(u\frac{\partial u}{\partial r} + w\frac{\partial u}{\partial z} - \frac{v^2}{r}\right) + \sigma B_0^2 u = \frac{\partial \tau_r^r}{\partial r} + \frac{\partial \tau_r^z}{\partial z} + \frac{\tau_r^r - \tau_\phi^\phi}{r}, \tag{2.2}$$

$$\rho\left(u\frac{\partial v}{\partial r} + w\frac{\partial v}{\partial z} + \frac{uv}{r}\right) + \sigma B_0^2 v = \frac{\partial \tau_\phi^r}{\partial r} + \frac{\partial \tau_\phi^z}{\partial z} + \frac{2\tau_\phi^r}{r}, \tag{2.3}$$

$$\rho\left(u\frac{\partial w}{\partial r} + w\frac{\partial w}{\partial z}\right) = \frac{\partial \tau_z^r}{\partial r} + \frac{\partial \tau_z^z}{\partial z} + \frac{\tau_z^r}{r}, \tag{2.4}$$

$$\rho c_p\left(u\frac{\partial T}{\partial r} + w\frac{\partial T}{\partial z}\right) = \kappa\left\{\frac{1}{r}\frac{\partial}{\partial r}\left(r\frac{\partial T}{\partial r}\right) + \frac{\partial^2 T}{\partial z^2}\right\} + \mu\left\{\left(\frac{\partial u}{\partial z}\right)^2 + \left(\frac{\partial v}{\partial z}\right)^2\right\} + \sigma B_0^2(u^2 + v^2), \tag{2.5}$$

with the following no-slip boundary conditions

$$u = 0, \quad v = r\Omega, \quad w = 0, \quad T = T_w \quad \text{at} \quad z = 0 \tag{2.6}$$

$$u \to 0, \quad v \to 0, \quad p \to p_\infty, \quad T \to T_\infty \quad \text{as} \quad z \to \infty, \tag{2.7}$$

where the disk is rotating with a constant angular velocity Ω about the line $r = 0$ and an external uniform magnetic field is applied perpendicular to the plane of the disk with a constant magnetic flux density B_0. The velocity components in the directions of increasing r, ϕ, z are u, v, w respectively. ρ is the density of the fluid, σ is the electrical conductivity of the fluid , μ is the coefficient of viscosity, κ is the thermal conductivity, c_p is the specific heat at constant pressure of the fluid. The temperature of the fluid T, equals T_w at the surface of the disk. At large distances from the disk, T tends to T_∞ where T_∞ is the temperature of the ambient fluid. The second term on the right hand side of equation (2.5) represents the viscous dissipation while the last term represents the Joule heating. The constitutive equation for the Reiner-Rivlin fluid is given by

$$\tau^i_j = 2\mu e^i_j + 2\mu_c e^i_k e^k_j - p\delta^i_j, \quad e^j_j = 0, \tag{2.8}$$

where p represents the pressure, τ^i_j is the stress tensor, e^i_j is the rate of strain tensor and μ_c is the coefficient of cross viscosity. The Reiner-Rivlin model is a simple model which can provide some insight into predicting the flow characteristics and heat transfer performance for viscoelastic fluid above a rotating disk [6]. The first term on the right hand side of (2.8) represents the viscous property of the fluid and the third term, the elastic property of the fluid. We introduce the non-dimensional distance $\eta = z\sqrt{\Omega/\nu}$ measured along the axis of rotation and the von Kármán transformations [39]:

$$u = r\Omega F, \quad v = r\Omega G, \quad w = \sqrt{\nu\Omega}H, \quad p - p_\infty = -\rho\nu\Omega P, \quad \Theta = \frac{T - T_\infty}{T_w - T_\infty}, \tag{2.9}$$

where F, G, H, P and Θ are non-dimensional functions of η, $\nu = \mu/\rho$ is the kinematic viscosity. With these transformations equations (2.1) - (2.5) take the form

$$H' + 2F = 0, \tag{2.10}$$

$$F'' - F^2 + G^2 - F'H - MF - \frac{K}{2}(F'^2 - 3G'^2 - 2FF'') = 0, \tag{2.11}$$

$$G'' - G'H - 2FG - MG + K(F'G' + FG'') = 0, \tag{2.12}$$

$$HH' + \frac{7}{2}KH'H'' - P' - H'' = 0, \tag{2.13}$$

$$\frac{1}{Pr}\Theta'' - H\Theta' + Ec(F'^2 + G'^2) + MEc(F^2 + G^2) = 0, \tag{2.14}$$

with

$$F(0) = F(\infty) = 0, \quad G(0) = 1, \quad G(\infty) = 0, \quad H(0) = 0, \tag{2.15}$$

$$P(\infty) = 0, \quad \Theta(0) = 1, \quad \Theta(\infty) = 0, \tag{2.16}$$

where $K = \mu_c\Omega/\mu$ is the parameter that describes the non-Newtonian characteristic of the fluid, $M = \sigma B_0^2/\rho\Omega$ is the magnetic interaction number, Pr is the Prandtl number and Ec is the Eckert number. The system (2.10) - (2.12) with the prescribed boundary conditions (2.15) are sufficient to solve for the three velocity components. Equation (2.13) can be used to find the pressure distribution at any point if required. Simplifying the equation system by substituting equation (2.10) into (2.11), (2.12) and (2.14) yields

$$H''' - H''H + \frac{1}{2}H'H' - 2G^2 - MH' + \frac{K}{2}(\frac{1}{2}H''^2 - 3G'^2 - H'H''') = 0, \tag{2.17}$$

$$G'' - HG' + H'G - MG + \frac{K}{2}(H'G'' - H''G') = 0, \tag{2.18}$$

$$\frac{1}{Pr}\Theta'' - H\Theta' + Ec(\frac{1}{4}H''^2 + G'^2) + MEc(\frac{1}{4}H'^2 + G^2) = 0, \tag{2.19}$$

subject to the boundary conditions

$$H(0) = H'(0) = H'(\infty) = 0, \quad G(0) = \Theta(0) = 1, \; G(\infty) = \Theta(\infty) = 0. \tag{2.20}$$

In the following section we solve the nonlinear coupled system (2.17) - (2.19) with boundary conditions (2.20) by the ISHAM.

3. Method of solution

The main thrust of the method of solution [21, 28], is the improvement of the initial approximation used in the higher order deformation equations of the spectral homotopy analysis method. A systematic approach is used to find optimal initial "guesses" which are then used in the SHAM algorithm to accelerate convergence. In the first instance we assume that solutions for $H(\eta)$, $G(\eta)$ and $\Theta(\eta)$ in equations (2.17) - (2.19) can be found in the form

$$H(\eta) = h_i(\eta) + \sum_{m=0}^{i-1} h_m(\eta), \quad G(\eta) = g_i(\eta) + \sum_{m=0}^{i-1} g_m(\eta), \tag{3.21}$$

$$\Theta(\eta) = \theta_i(\eta) + \sum_{m=0}^{i-1} \theta_m(\eta), \quad i = 1, 2, 3, \ldots,$$

where h_i, g_i and θ_i are unknown functions whose solutions are obtained using the SHAM approach at the ith iteration and h_m , g_m and θ_m $(m \geq 1)$ are

known from previous iterations. For $m = 0$, suitable initial guesses satisfying the boundary conditions (2.20) are

$$h_0(\eta) = -1 + e^{-\eta} + \eta e^{-\eta}, \quad g_0(\eta) = e^{-\eta}, \quad \theta_0(\eta) = e^{-\eta}. \tag{3.22}$$

The initial guesses (3.22) are improved upon as follows. Substituting (3.21) into the governing equations (2.17) - (2.19) gives

$$\begin{aligned} &a_{0,i-1}h_i''' + a_{1,i-1}h_i'' + a_{2,i-1}h_i' + a_{3,i-1}h_i + a_{4,i-1}g_i' + a_{5,i-1}g_i - h_i''h_i \\ &\quad + \frac{1}{2}h_i'h_i' - 2g_i^2 + K(\frac{1}{4}h_i''^2 - 3g_i'^2 - \frac{1}{2}h_i'h_i''') = r_{1,i-1}, \end{aligned} \tag{3.23}$$

$$\begin{aligned} &b_{0,i-1}g_i'' + b_{1,i-1}g_i' + b_{2,i-1}g_i + b_{3,i-1}h_i'' + b_{4,i-1}h_i' + b_{5,i-1}h_i - h_ig_i' \\ &\quad + h_i'g_i - \frac{K}{2}(h_i'g_i'' + h_i''g_i') = r_{2,i-1}, \end{aligned} \tag{3.24}$$

$$\begin{aligned} &c_{0,i-1}\theta_i'' + c_{1,i-1}\theta_i' + c_{2,i-1}h_i'' + c_{3,i-1}h_i' + c_{4,i-1}h_i + c_{5,i-1}g_i' + c_{6,i-1}g_i \\ &-Prh_i\theta_i' + EcPr(\frac{1}{4}h_i''^2 + g_i'^2) + MEcPr(\frac{1}{4}h_i'^2 + g_i^2) = r_{3,i-1}, \end{aligned} \tag{3.25}$$

subject to the boundary conditions

$$h_i(0) = g_i(0) = \theta_i(0) = 0, \quad h_i'(0) = h_i'(\infty) = 0, \quad g_i(\infty) = \theta_i(\infty) = 0. \tag{3.26}$$

The coefficient parameters $a_{k,i-1}$, $b_{k,i-1}$, $c_{k,i-1}$ $(k = 0, \ldots, 6)$, $r_{1,i-1}$, $r_{2,i-1}$ and $r_{3,i-1}$ are defined as

$$a_{0,i-1} = 1 - \frac{K}{2}\sum_{m=0}^{i-1} h_m', \quad a_{1,i-1} = \frac{K}{2}\sum_{m=0}^{i-1} h_m'' - \sum_{m=0}^{i-1} h_m, \tag{3.27}$$

$$a_{2,i-1} = \sum_{m=0}^{i-1} h_m' - M - \frac{K}{2}\sum_{m=0}^{i-1} h_m''' \quad a_{3,i-1} = -\sum_{m=0}^{i-1} h_m'', \tag{3.28}$$

$$a_{4,i-1} = -6K\sum_{m=0}^{i-1} g_m' \quad a_{5,i-1} = -4\sum_{m=0}^{i-1} g_m, \tag{3.29}$$

$$b_{0,i-1} = 1 - \frac{K}{2}\sum_{m=0}^{i-1} h_m', \tag{3.30}$$

$$b_{1,i-1} = -\sum_{m=0}^{i-1} h_m - \frac{K}{2}\sum_{m=0}^{i-1} h_m'', b_{2,i-1} = \sum_{m=0}^{i-1} h_m' - M, \tag{3.31}$$

$$b_{3,i-1} = -\frac{K}{2}\sum_{m=0}^{i-1} g'_m,\ b_{4,i-1} = \sum_{m=0}^{i-1} g_m - \frac{K}{2}\sum_{m=0}^{i-1} g''_m, \tag{3.32}$$

$$b_{5,i-1} = -\sum_{m=0}^{i-1} g'_m, \tag{3.33}$$

$$c_{0,i-1} = 1,\quad c_{1,i-1} = -Pr\sum_{m=0}^{i-1} h_m,\quad c_{2,i-1} = \frac{1}{2}EcPr\sum_{m=0}^{i-1} h''_m, \tag{3.34}$$

$$c_{3,i-1} = \frac{1}{2}PrEcM\sum_{m=0}^{i-1} h'_m,\quad c_{4,i-1} = -Pr\sum_{m=0}^{i-1}\theta'_m, \tag{3.35}$$

$$c_{5,i-1} = 2EcPr\sum_{m=0}^{i-1} g'_m,\quad c_{6,i-1} = 2PrMEc\sum_{m=0}^{i-1} g_m, \tag{3.36}$$

$$\begin{aligned} r_{1,i-1} = -\Bigg[&\sum_{m=0}^{i-1} h'''_m - \sum_{m=0}^{i-1} h''_m\sum_{m=0}^{i-1} h_m + \frac{1}{2}\sum_{m=0}^{i-1} h'_m\sum_{m=0}^{i-1} h'_m \\ &- 2\sum_{m=0}^{i-1} g_m\sum_{m=0}^{i-1} g_m \\ &+K\left(\frac{1}{4}\sum_{m=0}^{i-1} h''_m\sum_{m=0}^{i-1} h''_m - 3\sum_{m=0}^{i-1} g'_m\sum_{m=0}^{i-1} g'_m - \frac{1}{2}\sum_{m=0}^{i-1} h'_m\sum_{m=0}^{i-1} h'''_m\right)\Bigg], \end{aligned} \tag{3.37}$$

$$\begin{aligned} r_{2,i-1} = -\Bigg[&\sum_{m=0}^{i-1} g''_m - \sum_{m=0}^{i-1} h_m\sum_{m=0}^{i-1} g'_m + \sum_{m=0}^{i-1} h'_m\sum_{m=0}^{i-1} g_m \\ &+\frac{K}{2}\left(\sum_{m=0}^{i-1} h'_m\sum_{m=0}^{i-1} g''_m - \sum_{m=0}^{i-1} h''_m\sum_{m=0}^{i-1} g'_m\right)\Bigg], \end{aligned} \tag{3.38}$$

$$\begin{aligned} r_{3,i-1} = -\Bigg[&\sum_{m=0}^{i-1}\theta''_m - Pr\sum_{m=0}^{i-1} h_m\sum_{m=0}^{i-1}\theta'_m + PrEc\left\{\left(\sum_{m=0}^{i-1} h''_m\right)^2\right. \\ &\left.+\left(\sum_{m=0}^{i-1} g'_m\right)^2\right\} + PrMEc\left\{\left(\sum_{m=0}^{i-1} h'_m\right)^2 + \left(\sum_{m=0}^{i-1} g_m\right)^2\right\}\Bigg]. \end{aligned} \tag{3.39}$$

Starting from the initial guesses (3.22), the subsequent solutions h_i, g_i and θ_i ($i \geq 1$) are obtained by recursively solving equations (3.23) - (3.25). To solve equations (3.23) - (3.25), we start by defining the following linear operators

$$\mathcal{L}_h[\mathcal{H}_i(\eta;q),\mathcal{G}_i(\eta;q)] = a_{0,i-1}\frac{\partial^3\mathcal{H}_i}{\partial\eta^3} + a_{1,i-1}\frac{\partial^2\mathcal{H}_i}{\partial\eta^2} + a_{2,i-1}\frac{\partial\mathcal{H}_i}{\partial\eta} + a_{3,i-1}\mathcal{H}_i$$

$$+a_{4,i-1}\frac{\partial \mathcal{G}_i}{\partial \eta}+a_{5,i-1}\mathcal{G}_i, \tag{3.40}$$

$$\mathcal{L}_g[\mathcal{H}_i(\eta;q),\mathcal{G}_i(\eta;q)]=b_{0,i-1}\frac{\partial^2\mathcal{G}_i}{\partial\eta^2}+b_{1,i-1}\frac{\partial\mathcal{G}_i}{\partial\eta}+b_{2,i-1}\mathcal{G}_i+b_{3,i-1}\frac{\partial^2\mathcal{H}_i}{\partial\eta^2}$$
$$+b_{4,i-1}\frac{\partial\mathcal{H}_i}{\partial\eta}+b_{5,i-1}\mathcal{H}_i, \tag{3.41}$$

$$\mathcal{L}_\theta[\mathcal{H}_i(\eta;q),\mathcal{G}_i(\eta;q),\Theta_i(\eta;q)]=c_{0,i-1}\frac{\partial^2\Theta_i}{\partial\eta^2}+c_{1,i-1}\frac{\partial\Theta}{\partial\eta}+c_{2,i-1}\frac{\partial^2\mathcal{H}_i}{\partial\eta^2}$$
$$+c_{3,i-1}\frac{\partial\mathcal{H}_i}{\partial\eta}+c_{4,i-1}\mathcal{H}_i+c_{5,i-1}\frac{\partial\mathcal{G}_i}{\partial\eta}+c_{6,i-1}\mathcal{G}_i, \tag{3.42}$$

where $q\in[0,1]$ is the embedding parameter, and $\mathcal{H}_i(\eta;q)$, $\mathcal{G}_i(\eta;q)$ and $\Theta_i(\eta;q)$ are unknown functions. The zeroth order deformation equations are given by

$$(1-q)\mathcal{L}_h[\mathcal{H}_i(\eta;q)-h_{i,0}(\eta)]=q\hbar\left\{\mathcal{N}_h[\mathcal{H}_i(\eta;q),\mathcal{G}_i(\eta;q)]-r_{1,i-1}\right\},$$
$$(1-q)\mathcal{L}_g[\mathcal{G}_i(\eta;q)-g_{i,0}(\eta)]=q\hbar\left\{\mathcal{N}_g[\mathcal{H}_i(\eta;q),\mathcal{G}_i(\eta;q)]-r_{2,i-1}\right\},$$
$$(1-q)\mathcal{L}_\theta[\Theta_i(\eta;q)-\theta_{i,0}(\eta)]=q\hbar\left\{\mathcal{N}_\theta[\mathcal{H}_i(\eta;q),\mathcal{G}_i(\eta;q),\Theta_i(\eta;q)]-r_{3,i-1}\right\},$$

where $\hbar$ is the non-zero convergence controlling auxiliary parameter and $\mathcal{N}_h$, $\mathcal{N}_g$ and $\mathcal{N}_\theta$ are nonlinear operators given by

$$\mathcal{N}_h[\mathcal{H}_i(\eta;q),\mathcal{G}_i(\eta;q)]=\mathcal{L}_h[\mathcal{H}_i(\eta;q),\mathcal{G}_i(\eta;q)]-\mathcal{H}_i\frac{\partial^2\mathcal{H}_i}{\partial\eta^2}+\frac{1}{2}\left(\frac{\partial\mathcal{H}_i}{\partial\eta}\right)^2$$
$$-2\mathcal{G}_i^2-M\frac{\partial\mathcal{H}_i}{\partial\eta}+K\left\{\frac{1}{4}\left(\frac{\partial^2\mathcal{H}_i}{\partial\eta^2}\right)^2-3\left(\frac{\partial\mathcal{G}_i}{\partial\eta}\right)^2-\frac{1}{2}\frac{\partial\mathcal{H}_i}{\partial\eta}\frac{\partial^3\mathcal{H}_i}{\partial\eta^3}\right\}, \tag{3.43}$$

$$\mathcal{N}_g[\mathcal{H}_i(\eta;q),\mathcal{G}_i(\eta;q)]=\mathcal{L}_\theta[\mathcal{H}_i(\eta;q),\mathcal{G}_i(\eta;q)]-\mathcal{H}_i\frac{\partial\mathcal{G}_i}{\partial\eta}+\mathcal{G}_i\frac{\partial\mathcal{H}_i}{\partial\eta}-M\mathcal{G}_i$$
$$-\frac{K}{2}\left\{\frac{\partial\mathcal{H}_i}{\partial\eta}\frac{\partial^2\mathcal{G}_i}{\partial\eta^2}+\frac{\partial\mathcal{G}_i}{\partial\eta}\frac{\partial^2\mathcal{H}_i}{\partial\eta^2}\right\}, \tag{3.44}$$

$$\mathcal{N}_\theta[\mathcal{H}_i(\eta;q),\mathcal{G}_i(\eta;q),\Theta_i(\eta;q)]=\mathcal{L}_\theta[\mathcal{H}_i(\eta;q),\mathcal{G}_i(\eta;q),\Theta_i(\eta;q)]-Pr\frac{\partial\Theta_i}{\partial\eta}\mathcal{H}_i$$
$$+PrEc\left\{\frac{1}{4}\left(\frac{\partial^2\mathcal{H}_i}{\partial\eta^2}\right)^2+\left(\frac{\partial\mathcal{G}_i}{\partial\eta}\right)^2\right\}+PrMEc\left\{\frac{1}{4}\left(\frac{\partial\mathcal{H}_i}{\partial\eta}\right)^2+\mathcal{G}_i^2\right\}. \tag{3.45}$$

Differentiating (3.43) - (3.45) m times with respect to q and then setting $q=0$ and finally dividing the resulting equations by $m!$ yields the mth order deformation equations

$$\mathcal{L}_h[h_{i,m}(\eta)-\chi_m h_{i,m-1}(\eta)] = \hbar R^h_{i,m}, \tag{3.46}$$
$$\mathcal{L}_g[g_{i,m}(\eta)-\chi_m g_{i,m-1}(\eta)] = \hbar R^g_{i,m}, \tag{3.47}$$
$$\mathcal{L}_\theta[\theta_{i,m}(\eta)-\chi_m \theta_{i,m-1}(\eta)] = \hbar R^\theta_{i,m}, \tag{3.48}$$

subject to the boundary conditions

$$h_{i,m}(0) = h'_{i.m}(0) = h'_{i,m}(\infty) = g_{i,m}(0) = g_{i,m}(\infty) = \theta_{i,m}(0) = \theta_{i,m}(\infty) = 0, \tag{3.49}$$

where

$$\begin{aligned} R^h_{i,m}(\eta) &= a_{0,i-1}h'''_{i,m-1} + a_{1,i-1}h''_{i,m-1} + a_{2,i-1}h'_{i,m-1} + a_{3,i-1}h_{i,m-1} \\ &\quad + a_{4,i-1}g'_{i,m-1} + a_{5,i-1}g_{i,m-1} - Mh'_{i,m-1} - r_{1,i-1}(\eta)(1-\chi_m) \\ &\quad + \sum_{n=0}^{m-1}(-h_{i,n}h''_{i,m-1-n} + \frac{1}{2}h'_{i,n}h'_{i,m-1-n} - 2g_{i,n}g_{i,m-1-n}) \\ &\quad + K\sum_{n=0}^{m-1}(\frac{1}{4}h'_{i,n}h''_{i,m-1-n} - 3g'_n g'_{m-1-n} - \frac{1}{2}h'_n h_{m-1-n}), \end{aligned} \tag{3.50}$$

$$\begin{aligned} R^g_{i,m}(\eta) &= b_{0,i-1}g''_{i,m-1} + b_{1,i-1}g'_{i,m-1} + b_{2,i-1}g_{i,m-1} + b_{3,i-1}h''_{i,m-1} \\ &\quad + b_{4,i-1}h'_{i,m-1} + b_{5,i-1}h_{i,m-1} - Mg_{i,m-1} - r_{2,i-1}(\eta)(1-\chi_m) \\ &\quad + \sum_{n=0}^{m-1}(h'_{i,n}g_{i,m-1-n} - g'_{i,n}h_{i.m-1-n}) \\ &\quad - \frac{K}{2}\sum_{n=0}^{m-1}(h'_{i,n}g''_{i,m-1-n} + 3g'_n h''_{m-1-n}), \end{aligned} \tag{3.51}$$

$$\begin{aligned} R^\theta_{i,m}(\eta) &= c_{0,i-1}\theta''_{i,m-1} + c_{1,i-1}\theta'_{i,m-1} + c_{2,i-1}h''_{i,m-1} + +c_{3,i-1}h'_{i,m-1} \\ &\quad + c_{4,i-1}h_{i,m-1} + c_{5,i-1}g'_{i,m-1} + c_{6,i-1}g_{i,m-1} \\ &\quad - Pr\sum_{n=0}^{m-1}\theta'_n h_{m-1-n} - r_{3,i-1}(\eta)(1-\chi_m) \\ &\quad + MEcPr\sum_{n=0}^{m-1}\left(4^{-1}h'_n h'_{m-1-n} + g_{i,n}g_{i,m-1-n}\right) \\ &\quad + EcPr\sum_{n=0}^{m-1}\left(4^{-1}h''_n h''_{m-1-n} + g'_{i,n}g'_{i,m-1-n}\right), \end{aligned} \tag{3.52}$$

and

$$\chi_m = \begin{cases} 0, & m \le 1 \\ 1, & m > 1 \end{cases}. \tag{3.53}$$

The initial approximations $h_{i,0}$, $g_{i,0}$ and $\theta_{i,0}$ that are used in the higher order equations (3.46) - (3.48) are obtained by solving the linear part of equations (3.23) - (3.25) given by

$$\begin{aligned} &a_{0,i-1}h'''_{i,0} + a_{1,i-1}h''_{i,0} + a_{2,i-1}h'_{i,0} + a_{3,i-1}h_{i,0} + a_{4,i-1}g'_{i,0} \\ &\quad + a_{5,i-1}g_{i,0} = r_{1,i-1}, \end{aligned} \tag{3.54}$$

$$\begin{aligned} &b_{0,i-1}g''_{i,0} + b_{1,i-1}g'_{i,0} + b_{2,i-1}g_{i,0} + b_{3,i-1}h''_{i,0} + b_{4,i-1}h'_{i,0} \\ &\quad + b_{5,i-1}h_{i,0} = r_{2,i-1}, \end{aligned} \tag{3.55}$$

$$c_{0,i-1}\theta''_{i,0} + c_{1,i-1}\theta'_{i,0} + c_{2,i-1}h''_{i,0} + c_{3,i-1}h'_{i,0} + c_{4,i-1}h_{i,0}$$

$$+c_{5,i-1}g'_{i,0} + c_{6,i-1}g_{i,0} = r_{3,i-1} \tag{3.56}$$

with the boundary conditions

$$h_{i,0}(0) = h'_{i,0}(0) = h'_{i,0}(\infty) = g_{i,0}(0) = g_{i,0}(\infty) = \theta_{i,0}(0) = \theta_{i,0}(\infty) = 0. \tag{3.57}$$

It is worthwhile to note at this stage that the initial approximate solutions are no longer just h_0, g_0 and θ_0 but $h_{i,0}, g_{i,0}$ and $\theta_{i,0}$ at the ith iteration. Essentially, this procedure allows for the improvement of the initial guesses at each iteration. Since the right hand side of equations (3.54) - (3.56) for $i = 1, 2, 3, ...$, are known from previous iterations, the equations may be solved using any numerical method. In this work, we apply the Chebyshev spectral collocation method to integrate equations (3.54) - (3.56). The method is based on the Chebyshev polynomials defined on the interval $[-1, 1]$ by

$$T_k(\xi) = \cos[k \cos^{-1}(\xi)]. \tag{3.58}$$

We first transform the physical region $[0, \infty)$ into the region $[-1, 1]$ using the domain truncation technique. The problem is solved in the interval $[0, L]$ instead of $[0, \infty)$. This leads to the following algebraic mapping

$$\xi = \frac{2\eta}{L} - 1, \quad \xi \in [-1, 1], \tag{3.59}$$

where L is the scaling parameter used to invoke the boundary condition at infinity. The Chebyshev nodes in $[-1, 1]$ are defined by the Gauss-Lobatto collocation points [13, 36] given by

$$\xi_j = \cos \frac{\pi j}{N}, \quad \xi \in [-1, 1] \quad j = 0, 1, \ldots, N, \tag{3.60}$$

where N is the number of collocation points. The variables $h_{i,0}(\eta)$, $g_{i,0}(\eta)$ and $\theta_{i,0}(\eta)$ are approximated as truncated series of Chebyshev polynomials of the form

$$h_{i,0}(\xi) \approx h^N_{i,0}(\xi_j) = \sum_{k=0}^{N} h_{i,0}(\xi_k) T_{1,k}(\xi_j), \quad j = 0, 1, \ldots, N, \tag{3.61}$$

$$g_{i,0}(\xi) \approx g^N_{i,0}(\xi_j) = \sum_{k=0}^{N} g_{i,0}(\xi_k) T_{2,k}(\xi_j), \quad j = 0, 1, \ldots, N, \tag{3.62}$$

$$\theta_{i,0}(\xi) \approx \theta^N_{i,0}(\xi_j) = \sum_{k=0}^{N} \theta_{i,0}(\xi_k) T_{3,k}(\xi_j), \quad j = 0, 1, \ldots, N, \tag{3.63}$$

where $T_{1,k}$, $T_{2,k}$ and $T_{3,k}$ are the k^{th} Chebyshev polynomials. Derivatives of the variables at the collocation points are represented as

$$\frac{d^r h_{i,0}}{d\xi^r} = \sum_{k=0}^{N} \mathbf{D}_{kj}^r h_{i,0}(\xi_j), \frac{d^r g_{i,0}}{d\xi^r} = \sum_{k=0}^{N} \mathbf{D}_{kj}^r g_{i,0}(\xi_j), \frac{d^r \theta_{i,0}}{d\xi^r} = \sum_{k=0}^{N} \mathbf{D}_{kj}^r \theta_{i,0}(\xi_j), \tag{3.64}$$

where r is the order of differentiation, $\mathbf{D} = \frac{2}{L}\mathcal{D}$ and $\mathcal{D}$ is the Chebyshev spectral differentiation matrix. Substituting equations (3.61) - (3.64) in (3.53) - (3.56) yields

$$\mathbf{B}_{i-1}\mathbf{X}_{i,0} = \mathbf{Q}_{i-1}, \tag{3.65}$$

subject to the boundary conditions

$$\sum_{k=0}^{N} \mathbf{D}_{0k} h_{i,0}(\xi_k) = 0, \quad \sum_{k=0}^{N} \mathbf{D}_{Nk} h_{i,0}(\xi_k) = 0, \quad h_{i,0}(\xi_N) = 0, \tag{3.66}$$

$$g_{i,0}(\xi_0) = 0, \quad g_{i,0}(\xi_N) = 0, \tag{3.67}$$

$$\theta_{i,0}(\xi_0) = 0, \quad \theta_{i,0}(\xi_N) = 0, \tag{3.68}$$

where

$$\mathbf{B}_{i-1} = \begin{pmatrix} B_{11} & B_{12} & B_{13} \\ B_{21} & B_{22} & B_{23} \\ B_{31} & B_{32} & B_{33} \end{pmatrix},$$

$$\begin{aligned}
&B_{11} = \mathbf{a}_{0,i-1}\mathbf{D}^3 + \mathbf{a}_{1,i-1}\mathbf{D}^2 + \mathbf{a}_{2,i-1}\mathbf{D} + \mathbf{a}_{3,i-1}\mathbf{I}, \\
&B_{12} = \mathbf{a}_{4,i-1}\mathbf{D} + \mathbf{a}_{5,i-1}\mathbf{I}, \\
&B_{13} = 0\mathbf{I}, \quad B_{21} = \mathbf{b}_{3,i-1}\mathbf{D}^2 + \mathbf{b}_{4,i-1}\mathbf{D} + \mathbf{b}_{5,i-1}\mathbf{I}, \\
&B_{22} = \mathbf{b}_{0,i-1}\mathbf{D}^2 + \mathbf{b}_{1,i-1}\mathbf{D} + \mathbf{b}_{2,i-1}\mathbf{I}, \; B_{23} = 0\mathbf{I}, \\
&B_{31} = \mathbf{c}_{2,i-1}\mathbf{D}^2 + \mathbf{c}_{3,i-1}\mathbf{D} + \mathbf{c}_{4,i-1}\mathbf{I}, \; B_{32} = \mathbf{c}_{5,i-1}\mathbf{D} + \mathbf{c}_{6,i-1}\mathbf{I}, \\
&B_{33} = \mathbf{c}_{0,i-1}\mathbf{D}^2 + \mathbf{c}_{1,i-1}\mathbf{D}, \\
&\mathbf{X}_{i,0} = [h_{i,0}(\xi_0), h_{i,0}(\xi_1), \ldots, h_{i,0}(\xi_N), g_{i,0}(\xi_0), g_{i,0}(\xi_1), \ldots, g_{i,0}(\xi_N), \\
&\theta_{i,0}(\xi_0), \theta_{i,0}(\xi_1), \ldots, \theta_{i,0}(\xi_N)]^T, \\
&\mathbf{Q}_{i,0} = [r_{1,i-1}(\eta_0), r_{1,i-1}(\eta_1), \ldots, r_{1,i-1}(\eta_N), r_{2,i-1}(\eta_0), \\
&r_{2,i-1}(\eta_1), \ldots, r_{2,i-1}(\eta_N), \\
&r_{3,i-1}(\eta_0), r_{3,i-1}(\eta_1), \ldots, r_{3,i-1}(\eta_N)]^T.
\end{aligned} \tag{3.69}$$

In the above definitions T stands for transpose, I is an $(N+1)\times(N+1)$ identity matrix and $\mathbf{a}_{k,i-1}$, $\mathbf{b}_{k,i-1}$ and $\mathbf{c}_{s,i-1}$ $(k = 0, \ldots, 5, \quad s = 0, \ldots, 6)$ are diagonal matrices of size $(N+1)\times(N+1)$. After modifying the matrix system (3.65) to incorporate the boundary conditions, the solution is obtained as

$$\mathbf{X}_{i,0} = \mathbf{B}_{i-1}^{-1}\mathbf{Q}_{i-1}. \tag{3.70}$$

Similarly, applying the Chebyshev spectral transformation on the higher order deformation equations (3.46) - (3.48) gives

$$\mathbf{B}_{i-1}\mathbf{X}_{i,m} = (\chi_m + \hbar)\mathbf{B}_{i-1}\mathbf{X}_{i,m-1} - \hbar(1-\chi_m)\mathbf{Q}_{i-1} + \hbar\mathbf{P}_{i,m-1}, \quad (3.71)$$

subject to the boundary conditions

$$\sum_{k=0}^{N}\mathbf{D}_{0k}h_{i,m}(\xi_k) = 0, \quad \sum_{k=0}^{N}\mathbf{D}_{Nk}h_{i,m}(\xi_k) = 0, \quad h_{i,m}(\xi_N) = 0, \quad (3.72)$$

$$g_{i,m}(\xi_0) = 0, \quad g_{i,m}(\xi_N) = 0, \quad (3.73)$$

$$\theta_{i,m}(\xi_0) = 0, \quad \theta_{i,m}(\xi_N) = 0, \quad (3.74)$$

where $\mathbf{B}_{i-1}$ and $\mathbf{Q}_{i-1}$, are as defined in (3.69) and

$$\mathbf{X}_{i,m} = [h_{i,m}(\xi_0), h_{i,m}(\xi_1), \ldots, h_{i,m}(\xi_N), g_{i,m}(\xi_0), g_{i,m}(\xi_1), \ldots, g_{i,m}(\xi_N), \theta_{i,m}(\xi_0), \theta_{i,m}(\xi_1), \ldots, \theta_{i,m}(\xi_N)]^T, \quad (3.75)$$

$$\mathbf{P}_{i,m-1} = [P^{(1)}_{i,m-1}, P^{(2)}_{i,m-1}, P^{(3)}_{i,m-1}]^T, \quad (3.76)$$

$$P^{(1)}_{i,m-1} = \sum_{n=0}^{m-1}\left[\frac{1}{2}\mathbf{D}h_{i,n}\mathbf{D}h_{i,m-1-n} - h_{i,n}\mathbf{D}^2h_{i,m-1-n} - 2g_{i,n}g_{i,m-1-n}\right] + K\sum_{n=0}^{m-1}\left[\frac{1}{4}\mathbf{D}^2h_{i,n}\mathbf{D}^2h_{i,m-1-n} - 3\mathbf{D}g_{i,n}\mathbf{D}g_{i,m-1-n}\right] - K\sum_{n=0}^{m-1}\left[\frac{1}{2}\mathbf{D}h_{i,n}\mathbf{D}^3h_{i,m-1-n}\right],$$

$$P^{(2)}_{i,m-1} = \sum_{n=0}^{m-1}[\mathbf{D}h_{i,n}g_{i,m-1-n} - \mathbf{D}g_{i,n}h_{i,m-1-n}] - \sum_{n=0}^{m-1}\left[\frac{K}{2}\left(\mathbf{D}h_{i,n}\mathbf{D}^2g_{i,m-1-n} + \mathbf{D}^2h_{i,n}\mathbf{D}g_{i,m-1-n}\right)\right],$$

$$P^{(3)}_{i,m-1} = PrEc\sum_{n=0}^{m-1}\left[\frac{1}{4}\mathbf{D}^2h_{i,n}\mathbf{D}^2h_{i,m-1-n} + \mathbf{D}g_{i,n}\mathbf{D}g_{i,m-1-n}\right] + Pr\sum_{n=0}^{m-1}\left[MEc\left(\frac{1}{4}\mathbf{D}h_{i,n}\mathbf{D}h_{i,m-1-n} + g_{i,n}g_{i,m-1-n}\right)\right] - Pr\sum_{n=0}^{m-1}[\mathbf{D}\theta_{i,n}h_{i,m-1-n}].$$

The boundary conditions (3.72) - (3.74) are implemented in matrix $\mathbf{B}_{i-1}$ on the left hand side of equation (3.71) in rows 1, N, $N+1$, $N+2$, $2(N+1)$ $2N+3$ and $3(N+1)$ respectively as before with the initial solution above. The corresponding rows, all columns, of $\mathbf{B}_{i-1}$ on the right hand side of (3.71), $\mathbf{Q}_{i-1}$ and $\mathbf{P}_{m-1}$ are all set to be zero. This results in the following recursive formula

for $m \geq 1$.

$$\mathbf{X}_{i,m} = (\chi_m + \hbar)\mathbf{B}_{i-1}^{-1}\tilde{\mathbf{B}}_{i-1}\mathbf{X}_{i,m-1} + \hbar\mathbf{B}_{i-1}^{-1}[\mathbf{P}_{i,m-1} - (1-\chi_m)\mathbf{Q}_{i-1}], \tag{3.77}$$

where $\tilde{\mathbf{B}}_{i-1}$ is the modified matrix $\mathbf{B}_{i-1}$ on the right hand side of (3.71) after incorporating the boundary conditions (3.72) - (3.74). Thus starting from the initial approximation, which is obtained from (3.70), higher order approximations $X_{i,m}(\xi)$ for $m \geq 1$, can be obtained through the recursive formula (3.77). The solutions for h_i , g_i and θ_i are then generated using the solutions for $h_{i,m}$, $g_{i,m}$ and $\theta_{i,m}$ as follows

$$h_i = h_{i,0} + h_{i,1} + h_{i,2} + h_{i,3} + \cdots + h_{i,m}, \tag{3.78}$$

$$g_i = g_{i,0} + g_{i,1} + g_{i,2} + g_{i,3} + \cdots + g_{i,m}, \tag{3.79}$$

$$\theta_i = \theta_{i,0} + \theta_{i,1} + \theta_{i,2} + g_{i,3} + \cdots + \theta_{i,m}. \tag{3.80}$$

The $[i,m]$ approximate solutions for $h(\eta)$, $g(\eta)$ and $\theta(\eta)$ are then obtained by substituting h_i , g_i and θ_i which are obtained from (3.78), (3.79) and (3.80) into equation (3.21), where i represents the ith iteration of the initial approximation and m represents the mth iteration of the spectral homotopy analysis method.

4. Convergence theorem

The approximate solutions of the nonlinear equations are generated using the higher order deformation equations (3.46) - (3.48). The right hand sides of these equations are governed by the unknown functions $\mathcal{H}_i(\eta;q), \mathcal{G}_i(\eta;q)$ and $\Theta(\eta;q)$. As the embedding parameter q gradually increases from 0 to 1, the solutions vary from the initial approximations to the exact solutions, i.e.

$$\mathcal{H}_i(\eta;0) = h_{i,0}(\eta), \quad \text{and} \quad \mathcal{H}_i(\eta;1) = h_i(\eta), \tag{4.81}$$

$$\mathcal{G}_i(\eta;0) = g_{i,0}(\eta), \quad \text{and} \quad \mathcal{G}_i(\eta;1) = g_i(\eta), \tag{4.82}$$

$$\Theta_i(\eta;0) = \theta_{i,0}(\eta), \quad \text{and} \quad \Theta_i(\eta;1) = \theta_i(\eta). \tag{4.83}$$

Expanding $\mathcal{H}_i(\eta;q), \mathcal{G}_i(\eta;q)$ and $\Theta_i(\eta;q)$ using the Taylor series expansion about q yields

$$\mathcal{H}_i(\eta;q) = h_{i,0}(\eta) + \sum_{m=1}^{\infty} h_{i,m}(\eta)q^m, \; h_{i,m},(\eta) = \frac{1}{m!}\frac{\partial^m \mathcal{H}_i(\eta;q)}{\partial q^m}\bigg|_{q=0} \tag{4.84}$$

$$\mathcal{G}_i(\eta;q) = g_{i,0}(\eta) + \sum_{m=1}^{\infty} g_{i,m}(\eta)q^m, \; g_{i,m},(\eta) = \frac{1}{m!}\frac{\partial^m \mathcal{G}_i(\eta;q)}{\partial q^m}\bigg|_{q=0}, \tag{4.85}$$

$$\Theta_i(\eta;q) = \theta_{i,0}(\eta) + \sum_{m=1}^{\infty} \theta_{i,m}(\eta)q^m, \; \theta_{i,m},(\eta) = \frac{1}{m!}\frac{\partial^m \Theta_i(\eta;q)}{\partial q^m}\bigg|_{q=0} \tag{4.86}$$

We note that at $q = 1$ the series becomes the exact solutions

$$\mathcal{H}_i(\eta; 1) = h_i(\eta) = h_{i,0}(\eta) + \sum_{m=1}^{\infty} h_{i,m}(\eta), \tag{4.87}$$

$$\mathcal{G}_i(\eta; 1) = g_i(\eta) = g_{i,0}(\eta) + \sum_{m=1}^{\infty} g_{i,m}(\eta), \tag{4.88}$$

$$\Theta_i(\eta; 1) = \theta_i(\eta) = \theta_{i,0}(\eta) + \sum_{m=1}^{\infty} \theta_{i,m}(\eta) q^m. \tag{4.89}$$

For validity of the solutions generated by these equations, it is important to show that these series converge at $q = 1$. As stated earlier, the SHAM is a hybrid method founded on the HAM. We kindly refer readers to Liao's proof [20, ch.3] since the higher order deformation equations are similar in the two methods.

5. Results and Discussion

In this section we present and discuss results computed using the improved spectral homotopy analysis method, the original spectral homotopy analysis method and the numerical bvp4c routine which is based on Runge-Kutta schemes. Comparison is also made between the current results and those in the literature. For our simulations we used $\hbar = -1$, $L = 30$ and $N = 150$. The CPU run times (RT) in seconds are shown for the ISHAM and SHAM for comparison of computational efficiency.

Table 1. Benchmark results for the approximate radial shear stress $F'(0)$ at different orders $[i, m]$ of the ISHAM with the bvp4c and Sahoo [33] for different values of M when $Pr = 0.71$, $K = 0$.

M	[1,1]	RT	[2,2]	RT	Numerical	Ref [33]
0	0.51083620	0.1286	0.51023262	0.1143	0.51023262	0.510214
0.4	0.40501875	0.1149	0.40557564	0.1140	0.40557565	0.405575
0.8	0.33564882	0.1164	0.33508970	0.1155	0.33508970	0.335090
1.0	0.31004423	0.1153	0.30925799	0.1146	0.30925799	0.309259
10	0.10384518	0.1201	0.10531004	0.1126	0.10531004	0.105310
16	0.08235395	0.1172	0.08330263	0.1119	0.08330263	0.083303
18	0.07771253	0.1188	0.07854454	0.1117	0.07854454	0.078545
20	0.07378272	0.1170	0.07451802	0.1119	0.07451802	0.074518
50	0.04693143	0.1133	0.04713867	0.1108	0.04713867	0.047139
100	0.03326500	0.1135	0.03333302	0.1130	0.03333302	0.033334

Tables 1 and 2 present approximate solutions of the shear stresses in the radial $F'(0)$ and tangential $-G'(0)$ directions respectively. The results are computed

for a Newtonian fluid ($K = 0$) and for different values of the magnetic parameter M. We note that the ISHAM approximate solutions for both $F'(0)$ and $-G'(0)$ converge to the numerical solutions at 2nd order approximations for up to 8 decimal places. Comparison with Sahoo [33] shows a good agreement. The effect of the magnetic parameter on the Newtonian fluid shows that $F'(0)$ decreases while $-G'(0)$ increases as M is increased.

TABLE 2. Tangential shear stress $-G'(0)$ at different orders $[i, m]$ of the ISHAM, bvp4c and Sahoo [33] for different values of M when $Pr = 0.71$, $K = 0$.

M	[1,1]	RT	[2,2]	RT	Numerical	Ref [33]
0	0.61499561	0.1209	0.61592201	0.1132	0.61592201	0.615909
0.4	0.80314224	0.1257	0.80237637	0.1136	0.80237636	0.802376
0.8	0.98432782	0.1151	0.98360710	0.1143	0.98360710	0.983607
1.0	1.06924679	0.1207	1.06905336	0.1158	1.06905336	1.069053
10	3.16526084	0.1225	3.16490669	0.1124	3.16490669	3.164907
16	4.00186131	0.1251	4.00130088	0.1126	4.00130088	4.001301
18	4.24429674	0.1235	4.24373111	0.1146	4.24373111	4.243731
20	4.47362668	0.1358	4.47306710	0.1119	4.47306710	4.473067
50	7.07163149	0.1199	7.07130349	0.1139	7.07130349	7.071303
100	10.00024893	0.1227	10.00008333	0.1111	10.00008333	10.000083

The radial shear stress when $M = 2$ and for different values of K is presented in Table 3. For validation of the current method, and to determine the effect of improving the initial guesses, we compare the results against the numerical solution. For convergence of the method the results are compared with the 'standard' spectral homotopy analysis method for the same values of N, L and $\hbar$. For $0 \leq K \leq 2$ the ISHAM converges at 2nd order while the SHAM would not have converged even at the 8th order for some values of K. Comparatively therefore the ISHAM converges much faster than the SHAM. This is clearly seen in Table 4 where the absolute errors in the solution are given.

In Table 5, the tangential stress results obtained using the ISHAM and the SHAM are compared with the numerical results when $M = 2$ and for different values of K. Convergence of the ISHAM to the numerical solutions was achieved at the 2nd order of approximation. When using the SHAM convergence to the numerical solution was achieved at the 8th order for values of K up to 2. It is also clear that the ISHAM is computationally much more efficient compared to the SHAM. A comparison of the absolute errors is made in Table 6 where the fast convergence of the ISHAM when compared with the SHAM is confirmed. It is worth noting that the SHAM converges faster for $-G'(0)$ compared to $F'(0)$.

TABLE 3. Radial shear stress $F'(0)$: A comparison of the convergence rate of the ISHAM and SHAM to the numerical solutions for different values of K when $M = 2$, $Pr = 1$, $Ec = 0.3$.

	ISHAM			SHAM	
K	[1,1]	[2,2]	Numerical	2	8
0.0	0.23039754	0.23055912	0.23055912	0.23051941	0.23055926
0.4	0.51021898	0.51277769	0.51277769	0.51271021	0.51277764
0.8	0.77142224	0.77299784	0.77299784	0.77296707	0.77299784
1.2	0.99900210	0.99668062	0.99668062	0.99662531	0.99668062
1.6	1.18783561	1.18425675	1.18425675	1.18437955	1.18425667
2.0	1.33945767	1.34211178	1.34211178	1.34210513	1.34211213

TABLE 4. Comparison of the absolute errors in the ISHAM and SHAM solutions for different values of K when $M = 2$, $Pr = 1$, $Ec = 0.3$.

	ISHAM		SHAM	
K	[1,1]	[2,2]	2	8
0.0	0.00016158	0.00000000	0.00003971	0.00000014
0.4	0.00255871	0.00000000	0.00006748	0.0000005
0.8	0.0015756	0.00000000	0.00003077	0.00000000
1.2	0.00232148	0.00000000	0.00005531	0.00000000
1.6	0.00357886	0.00000000	0.00012280	0.00000008
2.0	0.00265411	0.00000000	0.00000665	0.00000035

This is due to the differences in the level of nonlinearity of the equations of $F(\eta)$ and $G(\eta)$. For the ISHAM however, convergence has not been affected by this difference in the nonlinearity of functions. This there appears to be an added advantage of the ISHAM over the SHAM.

Table 7 gives a comparison of the convergence rate of the ISHAM and the SHAM versus the numerical solutions for $F'(0)$ for different values M when $K = 1$. Convergence to the numerical solution is achieved at 2nd order of the ISHAM and at the 8th order of the SHAM. The absolute errors are shown in Table 8. In Table 9 the ISHAM and the SHAM solutions are compared with the numerical solutions for different values M when $K = 1$. An increase in the tangential shear stress is observed with an increase in M. The absolute errors are shown in Table 10. The nonlinearity of the equations has no effect on the convergence of the ISHAM.

TABLE 5. Comparison of the approximate solutions of $-G'(0)$ at different ISHAM and SHAM orders against the numerical solutions for different values of K when $M = 2, Pr = 1, Ec = 0.3$.

	ISHAM			SHAM	
K	[1,1]	[2,2]	Numerical	2	8
0.0	1.44053856	1.44209401	1.44209401	1.44206605	1.44209401
RT	0.1225	0.1125		0.2423	0.6168
0.4	1.49006904	1.49157841	1.49157841	1.49155902	1.49157841
RT	0.1214	0.1231		0.2589	0.6843
0.8	1.55193969	1.55323222	1.55323222	1.55322026	1.55323222
RT	0.1233	0.1121		0.2378	0.6819
1.2	1.62016082	1.62071752	1.62071752	1.62069708	1.62071752
RT	0.1199	0.1129		0.2626	0.6563
1.6	1.68975142	1.68973507	1.68973507	1.68973529	1.68973507
RT	0.1249	0.1192		0.2415	0.6850
2.0	1.75748201	1.75808304	1.75808304	1.75808336	1.75808306
RT	0.1264	0.1150		0.2484	0.6638

TABLE 6. Comparison of the absolute errors in the ISHAM and SHAM solutions compared to the numerical solution for different values of K when $M = 2,\ Pr = 1,\ Ec = 0.3$.

	ISHAM		SHAM	
K	[1,1]	[2,2]	2	8
0.0	0.00155545	0.00000000	0.00002796	0.00000000
0.4	0.00150937	0.00000000	0.00001939	0.00000000
0.8	0.00129253	0.00000000	0.00001196	0.00000000
1.2	0.00055670	0.00000000	0.00002044	0.00000000
1.6	0.00001635	0.00000000	0.00000022	0.00000000
2.0	0.00060103	0.00000000	0.00000032	0.00000002

Table 11 shows the heat transfer coefficient $-\Theta'(0)$ at different orders of the ISHAM compared against numerical results for different values of M, Pr, and Ec when K is fixed. For all cases convergence of the ISHAM approximate solutions to the numerical solution is achieved at 2nd orders of approximations. For a fixed value of K, increasing M, Pr, and Ec decreases $-\Theta'(0)$. For all results with CPU run times, the ISHAM has shown great computer efficiency as well. In all simulations the run times are significantly lower with the ISHAM than with the SHAM.

TABLE 7. Comparison of the approximate solutions of $F'(0)$ at different $[i, m]$ orders of the ISHAM, SHAM orders and against the numerical solutions for different values of M when $K = 1$, $Pr = 1$, $Ec = 0.3$.

	ISHAM			SHAM		
M	[1,1]	[2,2]	Numerical	2	4	8
0.0	0.74463163	0.74587441	0.74587441	0.74622472	0.74622472	0.74587397
0.5	0.76094065	0.75531485	0.75531485	0.75531092	0.75531501	0.75531485
1.0	0.79380816	0.79227536	0.79227536	0.79227047	0.79227489	0.79227536
1.5	0.83043422	0.83953516	0.83953516	0.83950410	0.83953434	0.83953516
2.0	0.86716576	0.88962012	0.88962012	0.88957427	0.88962074	0.88962012

TABLE 8. Comparison of the absolute errors for the approximate solutions of $F'(0)$ at different $[i, m]$ orders of the ISHAM, SHAM orders and against the numerical solutions for different values of M when $K = 1$, $Pr = 1$, $Ec = 0.3$.

	ISHAM		SHAM		
M	[1,1]	[2,2]	2	4	8
0.0	0.00124279	0.00000000	0.00035031	0.00003159	0.00000044
0.5	0.00562580	0.00000000	0.00000393	0.00000016	0.0000000
1.0	0.00153280	0.00000000	0.00000489	0.00000047	0.00000000
1.5	0.00910094	0.00000000	0.00003106	0.00000082	0.00000000
2.0	0.02245436	0.00000000	0.00004585	0.00000062	0.00000000

TABLE 9. Comparison of the approximate solutions of $-G'(0)$ at different ISHAM and SHAM orders and against the numerical solutions for different values of M when $K = 1$, $Pr = 1$, $Ec = 0.3$.

	ISHAM			SHAM		
M	[1,1]	[2,2]	Numerical	2	4	8
0.0	0.77672002	0.77834765	0.77834765	0.77854199	0.77836167	0.77834730
0.5	1.01294536	1.01069483	1.01069483	1.01070160	1.01069527	1.01069483
1.0	1.22319102	1.22367051	1.22367051	1.22366267	1.22367003	1.22367051
1.5	1.40999393	1.41449208	1.41449208	1.41447134	1.41449166	1.41449208
2.0	1.57840020	1.58657262	1.58657262	1.58655736	1.58657305	1.58657262

TABLE 10. Comparison of the absolute errors for the approximate solutions of $-G'(0)$ at different ISHAM and SHAM orders and against the numerical solution for different values of M when $K = 1$, $Pr = 1$, $Ec = 0.3$.

	ISHAM		SHAM		
M	[1,1]	[2,2]	2	4	8
0.0	0.00162763	0.00000000	0.00019434	0.00001402	0.00000035
0.5	0.00225053	0.00000000	0.00000677	0.00000044	0.0000000
1.0	0.00047949	0.00000000	0.00000784	0.00000048	0.00000000
1.5	0.00449815	0.00000000	0.00002074	0.00000042	0.00000000
2.0	0.00817242	0.00000000	0.00001526	0.00000043	0.00000000

TABLE 11. Heat transfer coefficient $-\Theta'(0)$ at different $[i, m]$ orders of the ISHAM compared with the numerical solutions for different values of M, Pr and Ec when $K = 1$.

M	Pr	Ec	[1,1]	[2,2]	[3,3]	[4,4]	Numerical
0			0.33894036	0.33798332	0.33798332	0.33798332	0.33798332
0.5	1	0.3	0.18638822	0.18165630	0.18165630	0.18165630	0.18165630
1.0			0.07138752	0.05317238	0.05317238	0.05317238	0.05317238
1.5			-0.01803593	-0.05185078	-0.05185078	-0.05185078	-0.05185078
	3		0.13954354	0.13959137	0.13959137	0.13959137	0.13959137
0.5	5	0.3	0.00576310	0.00730445	0.00730445	0.00730445	0.00730445
	7		-0.15265228	-0.15060972	-0.15060972	-0.15060972	-0.15060972
	10		-0.40767193	-0.40565482	-0.40565482	-0.40565482	-0.40565482
		1	-0.32997005	-0.33670269	-0.33670269	-0.33670269	-0.33670269
0.5	1	3	-1.80527938	-1.81772838	-1.81772838	-1.81772838	-1.81772838
		6	-4.01824339	-4.03926691	-4.03926691	-4.03926691	-4.03926691
		9	-6.23120739	-6.26080545	-6.26080545	-6.26080545	-6.26080545

Figures 1 - 2 show the effect of M and K on the radial and axial velocity profiles respectively. Increasing M reduces the radial component of the velocity while increasing K enhances F. The axial velocity $H(\eta)$ increases with the magnetic parameter but decreases when K is increased. There is excellent agreement between the second order ISHAM solutions for $F(\eta)$ and $H(\eta)$ and the numerical result.

The tangential velocity component and the temperature profiles are show in Figures 3 - 4 for different values of M and K respectively. An increase in M reduces $G(\eta)$ while enhancing the $\Theta(\eta)$. When K values are increased both $G(\eta)$ and $\Theta(\eta)$ decrease.

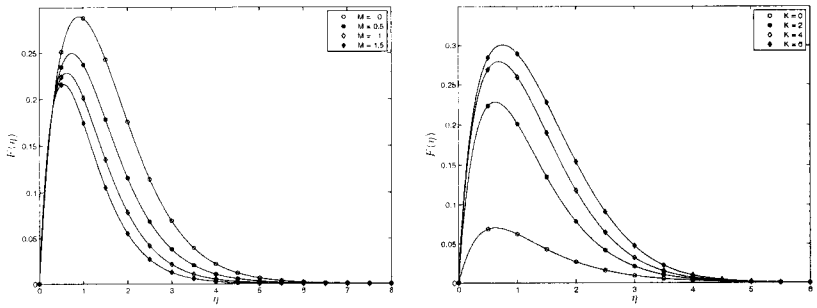

FIGURE 1. On the comparison between the 2nd order ISHAM solution and the numerical solution (solid line) for $F(\eta)$ at different values of M ($K = 2$) and K ($M = 1$) when $Pr = 1$, $Ec = 0.3$.

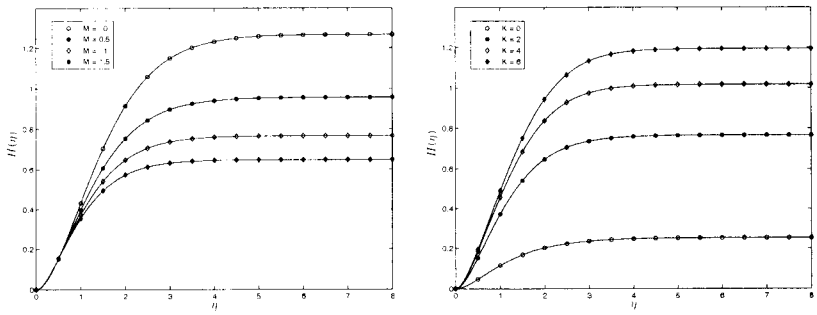

FIGURE 2. On the comparison between the 2nd order ISHAM solution and the numerical solution (solid line) for $-H(\eta)$ at different values of M ($K = 2$) and K ($M = 1$) when $Pr = 1$, $Ec = 0.3$.

In Figure 5 temperature profiles are presented for varying values of Pr and Ec. The temperature decreases with increasing Prandtl numbers while an increase in the Eckert number enhances the temperature.

6. CONCLUSION

A novel approach for accelerating the convergence of the spectral homotopy analysis method that is used to solve nonlinear equations in science and engineering has been proposed and applied successfully to the nonlinear system of equations governing the Reiner-Rivlin fluid in with Joule heating and viscous dissipation. The primary objective of the algorithm is to improve the initial approximate

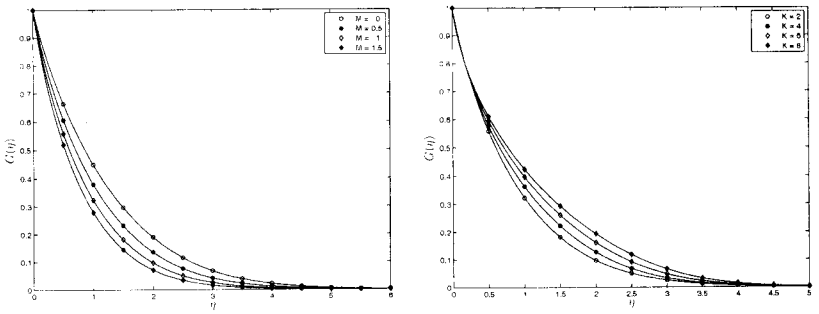

FIGURE 3. On the comparison between the 2nd order ISHAM solution (figures) and the bvp4c numerical solution (solid line) for $G(\eta)$ at different values of M ($K = 2$) and K ($M = 1$) when $Pr = 1$, $Ec = 0.3$.

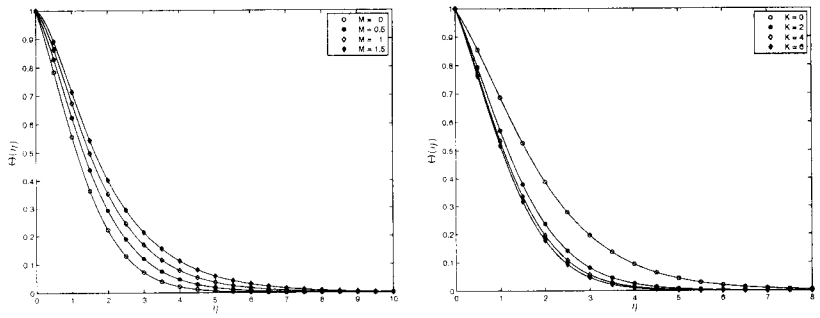

FIGURE 4. On the comparison between the 2nd order ISHAM solution (figures) and the bvp4c numerical solution (solid line) for $\Theta(\eta)$ at different values of M ($K = 2$) and K ($M = 0.1$) when $Pr = 1$, $Ec = 0.3$.

solution. The improved approximations are then used in the algorithm of the spectral-homotopy analysis method to reduce the number of iterations required to achieve convergence and better accuracy. The shear stresses in the radial and azimuthal directions were computed and the corresponding absolute errors determined. Convergence to the numerical solutions of the ISHAM approximate solutions was achieved at the 2nd orders for all flow parameters while the SHAM converged at the 8th order for some of the flow parameters.

The effects of flow parameters was also investigated for the radial and tangential shear stresses for both the Newtonian ($K = 0$) and non-Newtonian ($K \neq 0$)

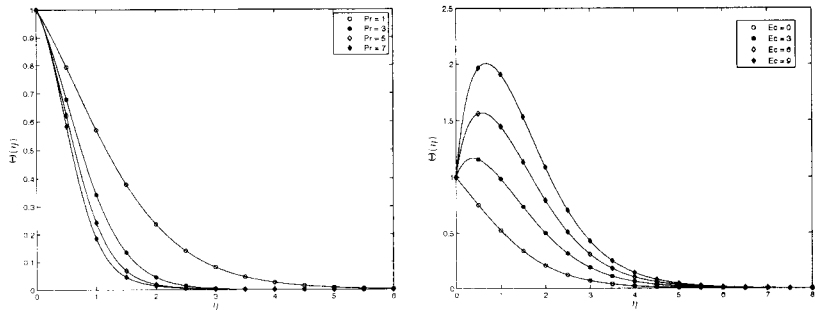

FIGURE 5. On the comparison between the 2nd order ISHAM solution (figures) and the bvp4c numerical solution (solid line) for $\Theta(\eta)$ at different values of Pr ($Ec = 0.3$) and Ec ($Pr = 1$) when $M = 0.1$, $K = 1$, $L = 30$, $N = 150$.

cases. For the Newtonian case, increasing M reduces $F'(0)$ and enhances $-G'(0)$ while in the non-Newtonian case increasing M enhances both $F'(0)$ and $-G'(0)$. The effect of K and M was determined and it was observed that an increase in K results in an increase in $F(\eta)$, and a decrease in $H(\eta)$, $G(\eta)$ and $\Theta(\eta)$ while increasing M increases $H(\eta)$ and $\Theta(\eta)$ while both $F(\eta)$ and $G(\eta)$ decreases. $\Theta(\eta)$ decreased with an increase in the Ec and decreased with an increase in Pr. The success of the ISHAM in solving the non-linear equations governing the von Kármán flow of an electrically conducting non-Newtonian Reiner-Rivlin fluid in the presence of viscous dissipation, Joule heating and heat transfer proves that the ISHAM fits as a newly improved method of solution that can be used to solve non-linear problems arising in science and engineering.

Acknowledgements. The authors wish to acknowledge financial support from the University of KwaZulu-Natal and the National Research Foundation (NRF).

REFERENCES

[1] M. A. Abdou, *New Analytical Solution of Von Karman swirling viscous flow.* Acta. Appl. Math., **111** (2010), 7 – 13.

[2] P. D. Ariel, *The homotopy perturbation method and analytical solution of the problem of flow past a rotating disk.* Computers and Mathematics with Applications, **58** (2009), 2504 - 2513.

[3] A. Arikoglu, I. Ozkol, G. Komurgoz, *Effect of slip on entropy generation in a single rotating disk in MHD flow.* Applied Energy, **85** (2008), 1225 – 1236.

[4] H. A. Attia, *The effect of ion slip on the flow of Reiner-Rivlin fluid due to a rotating disk with heat transfer.* J. of Mechanical Science and Technology, **21** (2007), 174 – 183.

[5] H. A. Attia, *Rotating disk flow and heat transfer through a porous medium of a non-Newtonian fluid with suction and injection.* Communications in Nonlinear Science and Numerical Simulation, **13** (2008), 1571 – 1580.

[6] H. A. Attia, M. E. S. Ahmed, *Non-Newtonian conducting fluid flow and heat transfer due to a ratating disk.* ANZIAM Journal, **46** (2004), 237 - 248.

[7] H. A. Attia, *Ion-slip effect on the flow due to a rotating disk.* The Arabian J. for Sc. and Eng., **29** (2004), 165 – 172.

[8] H. A. Attia, *Rotating Disk Flow and Heat Transfer of a Conducting Non-Newtonian Fluid with Suction-Injection and Ohmic Heating.* J. of the Braz. Soc. of Mech. Sci. & Eng., (**XXIX**) (2007), .

[9] H. A. Attia, *Steady Flow over a Rotating Disk in Porous Medium with Heat Transfer.* Nonlinear Analysis: Modelling and Control, **14** (2009) 21 – 26.

[10] H. A. Attia, *Rotating disk flow with heat transfer of a non-Newtonian fluid in porous medium.* Turk. J. Phys., **30** (2006), 103 – 108.

[11] H. A. Attia, *On the effectiveness of uniform suction and injection on steady rotating disk flow in porous medium with heat transfer.* Turkish J. Eng. Env. Sci., **30** (2006), 231 – 236.

[12] E. R. Benton, *On the flow due to a rotating disk.* J. Fluid Mech. **24** (1966), 781 – 800.

[13] C. Canuto, M. Y. Hussaini, A. Quarteroni, and T. A. Zang, *Spectral Methods in Fluid Dynamics*, Springer-Verlag, Berlin (1988).

[14] C. S. Chien, Y. T. Shih, *A cubic Hermite finite element-continuation method for numerical solutions of the von Kármán equations.* Appl. Math. and Comp., **209** (2009), 356 – 368.

[15] W. G. Cochran, *The flow due to a rotating disk.* Math. Proc. Cambridge Philos. Soc., **30** (1934), 365 – 375.

[16] W. S. Don, A. Solomonoff, *Accuracy and speed in computing the Chebyshev Collocation Derivative.* SIAM J. Sci. Comput., **16** (1995) 1253 - 1268.

[17] A. El-Nahhas, *Analytic approximations for von Kármán swirling flow.* Proc. Pakistan Acad. Sci., 44(3) (2007), 181 - 187.

[18] P. Hatzikonstantinou, *Magnetic and viscous effects on a liquid metal flow due to a rotating disk.* Astrophysics and Space Science, **161** (1989), 17 - 25.

[19] N. Kelson, A. Desseaux, *Note on porous rotating disk flow.* ANZIAM Journal, **42**(E)(2000), C837 - C855.

[20] S. J. Liao, Beyond perturbation: *Introduction to homotopy analysis method.* Chapman & Hall/CRC Press, 2003.

[21] Z. G Makukula, P. Sibanda, S. S. Motsa, *On new solutions for heat transfer in a viscoelastic fluid between parallel plates*, International journal of mathematical models and methods in applied sciences, **4**(4) (2010) 221 - 230.

[22] Z. G Makukula, P. Sibanda, S. S. Motsa, *A Novel Numerical Technique for Two-Dimensional Laminar Flow between Two Moving Porous Walls*, Mathematical Problems in Engineering, **2010** (2010), Article ID 528956, 15 pages doi:10.1155/2010/528956.

[23] Z. G Makukula, P. Sibanda, S. S. Motsa, *A Note on the Solution of the Von Kármán Equations Using Series and Chebyshev Spectral Methods*, Boundary Value Problems, **2010** (2010), Article ID 471793, 17 pages doi:10.1155/2010/471793.

[24] M. Miklavčič, C. Y. Wang, *The flow due to a rough rotating disk.* Z. Angew. Math. Phys. 54 (2004) 1 - 12.

[25] S. S. Motsa, P. Sibanda, S. Shateyi, *A new spectral-homotopy analysis method for solving a nonlinear second order BVP*, Communications in Nonlinear Science and Numerical Simulation, **15** (2010) 2293 - 2302.

[26] S. S. Motsa, P. Sibanda, F. G. Awad, S. Shateyi, *A new spectral-homotopy analysis method for the MHD Jeffery-Hamel problem.* Computers & Fluids, **39** (2010), 1219 – 1225.

[27] S. S. Motsa, P. Sibanda *On the solution of MHD flow over a nonlinear stretching sheet by an efficient semi-analytical technique.* Int. J. Numer. Meth. Fluids, (2011), DOI: 10.1002/fld.

[28] S. S. Motsa, G. T. Marewo, P. Sibanda, S. Shateyi, *An improved spectral homotopy analysis method for solving boundary layer problems.* Boundary Value Problems, **3** (2011), doi:10.1186/1687-2770-2011-3, 11 pages.

[29] E. Osalusi, *Effects of thermal radiation on MHD and slip flow over a porous rotating disk with variable properties.* Romanian Journal Physics, **52** (2007) 217 - 229.

[30] E. Osalusi, P. Sibanda, *On variable laminar convective flow properties due to a porous rotating disk in a magnetic field.* Romanian Journal Physics, **51** (2006), 937 - 950.

[31] M. M. Rashidi, S. A. M. Pour, *A novel analytical solution of steady flow over a rotating disk in porous medium with heat transfer by DTM-padé.* African J. of Math. and Comp. Sc. Research, **3** (2010), 93 - 100.

[32] M. M. Rashidi, H. Shahmohamadi, *Analytical solution of three-dimensional NavierStokes equations for the flow near an infinite rotating disk.* Communications in Nonlinear Science and Numerical Simulation, **14** (2009), 2999 - 3006.

[33] B. Sahoo, *Effects of partial slip, viscous dissipation and Joule heating on von Kármán flow and heat transfer of an electrically conducting non-Newtonian fluid.* Communications in Nonlinear Science and Numerical Simulation, **14** (2009) 2982 - 2998.

[34] B. K. Sharma, A. K. Jha, R. C. Chaudhary, *MHD forced flow of a conducting viscous fluid through a porous medium induced by an impervious rotating disk.* Rom. Journ. Phys., **52** (2007), 73 - 84.

[35] P. Sibanda, O.D. Makinde, *On steady MHD flow and heat transfer past a rotating disk in a porous medium with ohmic heating and viscous dissipation.* Int. J. of Num. Methods for Heat & Fluid Flow, **20** (2010), 269 - 285.

[36] L. N. Trefethen, *Spectral Methods in MATLAB.* SIAM (2000).

[37] M. Turkyilmazoglu, *Purely analytic solutions of magnetohydrodynamic swirling boundary layer flow over a porous rotating disk.* Computers & Fluids, **39** (2010), 793 – 799.

[38] M. Turkyilmazoglu, *Purely analytic solutions of the compressible boundary layer flow due to a porous rotating disk with heat transfer.* Physics of fluids, **21** (2009), 106104 – 12.

[39] T. von Kármán, *Uberlaminare und turbulence reibung.* ZAMM **1** (1921), 233 – 52.

[40] C. Yang, S. J. Liao, *On the explicit, purely analytic solution of von Kármán swirling viscous flow.* Comm. in Nonlinear Science and Num. Simulation, **11** (2006), 83 – 93.

4.2. A note on the solution of the von Kármán equations using series and Chebyshev spectral methods [2]

Corrigenda

The following corrections and further explanations have been added in this section;

(i) Below we is the geometry of the problem;

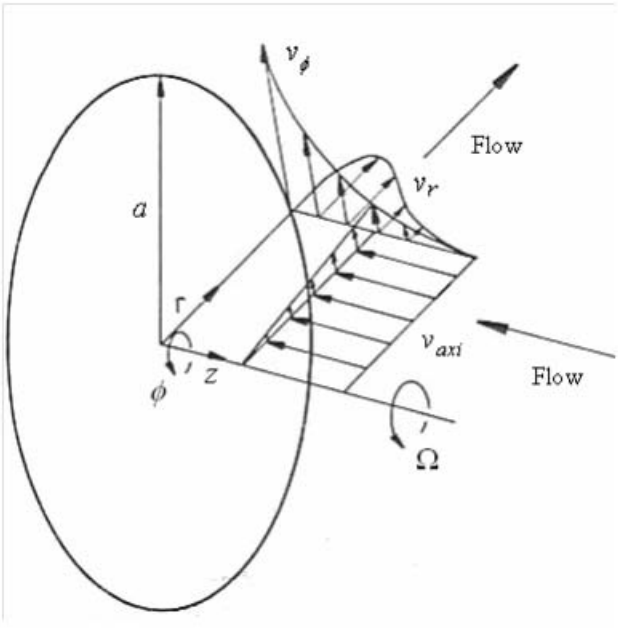

Figure 4.2: *Flow configuration of the von Kàmàrn swirling flow (Shanbghazani et al., 2009).*

(ii) On page 11 a different dimensionless variable m_1 in equations (5.1) and (5.2) should have been used.

[2] Z. G. Makukula, P. Sibanda and S. S. Motsa (2010). *Boundary Value Problems* Volume 2010, Article ID 471793, 17 pages doi:10.1155/2010/471793 (Impact factor; 1.047)

Further explanation

On pages 14 and 15, Tables 5 and 6, the collocation points used were $N = 120$ compared to $N = 60$ in the previous Tables. This necessary since increasing the parameter values s and m increased the nonlinearity of the equations.

Hindawi Publishing Corporation
Boundary Value Problems
Volume 2010, Article ID 471793, 17 pages
doi:10.1155/2010/471793

Research Article

A Note on the Solution of the Von Kármán Equations Using Series and Chebyshev Spectral Methods

Zodwa G. Makukula,[1] Precious Sibanda,[1] and Sandile Sydney Motsa[2]

[1] *School of Mathematical Sciences, University of KwaZulu-Natal, Private Bag X01 Scottsville, Pietermaritzburg 3209, South Africa*
[2] *Department of Mathematics, University of Swaziland, Private Bag 4, Kwaluseni M201, Swaziland*

Correspondence should be addressed to Precious Sibanda, sibandap@ukzn.ac.za

Received 23 March 2010; Revised 2 August 2010; Accepted 2 October 2010

Academic Editor: Sandro Salsa

The classical von Kármán equations governing the boundary layer flow induced by a rotating disk are solved using the spectral homotopy analysis method and a novel successive linearisation method. The methods combine nonperturbation techniques with the Chebyshev spectral collocation method, and this study seeks to show the accuracy and reliability of the two methods in finding solutions of nonlinear systems of equations. The rapid convergence of the methods is determined by comparing the current results with numerical results and previous results in the literature.

1. Introduction

Most natural phenomena can be described by nonlinear equations that, in general, are not easy to solve in closed form. The search for computationally efficient, robust, and easy to use numerical and analytical techniques for solving nonlinear equations is therefore of great interest to researchers in engineering and science. The study of the steady, laminar, and axially symmetric viscous flow induced by an infinite disk rotating steadily with constant angular velocity was pioneered by von Kármán [1]. He showed that the Navier-Stokes equations could be reduced to a set of ordinary differential equations and solved using an approximate integral method. His solution, however, contained errors that were later corrected by Cochran [2] by patching together two series expansions.

Numerical and semianalytical methods including the cubic Hermite finite element, pseudospectral, Galerkin-B-Spline, and Chebyshev-collocation methods have been used previously to find solutions of the von Kármán equations [3–6]. These methods have

their shortcomings, including instability, and hence the last few decades have seen the popularization of a number of new perturbation or nonperturbation techniques such as the Adomian decomposition method [7], the Lyapunov artificial small parameter method [8], the homotopy perturbation method [9, 10], and the homotopy analysis method [11].

The homotopy analysis method (HAM) was used recently by Yang and Liao [12] to find explicit, purely analytic solutions of the swirling von Kármán equations. Turkyilmazoglu [13] used the homotopy analysis method to solve the equations governing the flow of a steady, laminar, incompressible, viscous, and electrically conducting fluid due to a rotating disk subjected to a uniform suction and injection through the walls in the presence of a uniform transverse magnetic field. For this extended form of the von Kármám problem, the homotopy analysis method, however, produced secular terms in the series solution. Turkyilmazoglu [13] overcame this weakness by using initial guesses based on Ackroyd's (see the work of Ackroyd [14]) exponentially decaying functions, and a new linear operator which resulted in a method capable of tracking the shape of the exact solution. An alternative approach that serves to address these and other limitations of the HAM is the spectral homotopy analysis method; see the work of Motsa et al. [15, 16]. It is an efficient hybrid method that blends the HAM algorithm with Chebyshev spectral methods. The method retains the proven qualities of the HAM while effectively using Chebyshev polynomials as basis functions to ensure rapid convergence of the solution series. A novel quasilinearisation method—the successive linearisation method (see the work of Makukula et al. [17] and Motsa and Sibanda [18])—promises further improvement in accuracy and convergence rates compared to both the HAM and the SHAM.

In this study we apply the spectral homotopy analysis method (SHAM) and the successive linearisation method (SLM) to solve the von Kármán equations. The results are compared with those in the literature [11, 12] and against numerical approximations. Comparison of current results is further made with the recent results of Turkyilmazoglu [13] that include suction/injection and an applied magnetic field. We show, *inter alia*, that notwithstanding the fact that these two methods may involve more computations per step than the HAM, both the SHAM and SLM are efficient, robust, and converge much more rapidly compared to the standard homotopy analysis method.

2. Governing Equations

Our focus in this section is on the original von Kármán equation for the steady, laminar, axially symmetric viscous flow induced by an infinite disk rotating steadily with angular velocity Ω about the z-axis with the fluid confined to the half-space $z > 0$ above the disk. In cylindrical coordinates (r, θ, z) the equations of motion are given by

$$\frac{1}{r}\frac{\partial(rV_r)}{\partial r} + \frac{1}{r}\frac{\partial V_\theta}{\partial \theta} + \frac{\partial V_z}{\partial z} = 0,$$

$$V_r\frac{\partial V_r}{\partial r} + V_z\frac{\partial V_r}{\partial z} - \frac{V_\theta^2}{r} = \nu\left[\frac{\partial^2 V_r}{\partial r^2} + \frac{1}{r}\frac{\partial V_r}{\partial r} + \frac{\partial^2 V_r}{\partial z^2} - \frac{V_r}{r^2}\right] - \frac{1}{\rho}\frac{\partial \tilde{P}}{\partial r},$$

$$V_r\frac{\partial V_\theta}{\partial r} + V_z\frac{\partial V_\theta}{\partial z} + \frac{V_r V_\theta}{r} = \nu\left[\frac{\partial^2 V_\theta}{\partial r^2} + \frac{1}{r}\frac{\partial V_\theta}{\partial r} + \frac{\partial^2 V_\theta}{\partial z^2} - \frac{V_\theta}{r^2}\right],$$

$$V_r \frac{\partial V_z}{\partial r} + V_z \frac{\partial V_z}{\partial z} = \nu \left[\frac{\partial^2 V_z}{\partial r^2} + \frac{1}{r} \frac{\partial V_z}{\partial r} + \frac{\partial^2 V_z}{\partial z^2} \right] - \frac{1}{\rho} \frac{\partial \tilde{P}}{\partial z}, \tag{2.1}$$

subject to the nonslip boundary conditions on the disk and boundary conditions at infinity

$$\begin{aligned} V_\theta = r\Omega, \qquad V_r = V_z = 0, \quad z = 0, \\ V_r = V_z = 0, \quad z = +\infty, \end{aligned} \tag{2.2}$$

where ρ is the fluid density, ν is the kinematic viscosity coefficient, $\tilde{P}$ is the pressure, V_r, V_θ, and V_z are the velocity components in the radial, azimuthal, and axial directions, respectively, and Ω is the constant angular velocity. Using von Kármán's similarity transformations [1]

$$\begin{aligned} V_r = r\Omega F(\eta), \qquad V_\theta = r\Omega G(\eta), \\ V_z = \sqrt{\nu\Omega} H(\eta), \qquad \tilde{P} = -\rho\nu\Omega P(\eta), \end{aligned} \tag{2.3}$$

where $\eta = z\sqrt{\Omega/\nu}$ is a nondimensional distance measured along the axis of rotation, the governing partial differential equations (2) reduce to a set of ordinary differential equations:

$$F'' - F'H - F^2 + G^2 = 0, \tag{2.4}$$

$$G'' - G'H - 2FG = 0, \tag{2.5}$$

$$H'' - HH' + P' = 0, \tag{2.6}$$

$$2F + H' = 0, \tag{2.7}$$

subject to the boundary conditions

$$F(0) = F(\infty) = 0, \qquad G(0) = 1, \qquad G(\infty) = 0, \qquad H(0) = 0. \tag{2.8}$$

Substituting (2.7) into (2.4) and (2.5) yields

$$\begin{aligned} H''' - H''H + \frac{1}{2} H'H' - 2G^2 = 0, \\ G'' - HG' + H'G = 0, \end{aligned} \tag{2.9}$$

subject to the boundary conditions

$$H(0) = H'(0) = H'(\infty) = 0, \qquad G(0) = 1, \qquad G(\infty) = 0. \tag{2.10}$$

Equations (2.9) with the prescribed boundary conditions (2.10) are sufficient to give the three components of the flow velocity. The pressure distribution, if required, can be obtained from (2.6). This fully coupled and highly nonlinear system was solved using the spectral homotopy analysis method and the successive linearisation method. The results were validated using the Matlab bvp4c numerical routine and against results in the literature.

3. The Spectral Homotopy Analysis Method

Following Boyd [19], we begin by transforming the domain of the problem from $[0,\infty)$ to $[-1,1]$ using the domain truncation method. This approximates $[0,\infty)$ by the computational domain $[0,L]$ where L is a fixed length that is taken to be larger than the thickness of the boundary layer. The interval $[0,L]$ is then transformed to the domain $[-1,1]$ using the algebraic mapping

$$\xi = \frac{2\eta}{L} - 1, \quad \xi \in [-1,1]. \tag{3.1}$$

For convenience we make the boundary conditions homogeneous by applying the transformations

$$\begin{aligned} H(\eta) &= h(\xi) + H_0(\eta), \\ G(\eta) &= g(\xi) + G_0(\eta), \end{aligned} \tag{3.2}$$

where $H_0(\eta)$ and $G_0(\eta)$ are chosen so as to satisfy boundary conditions (2.10). The chain rule gives

$$\begin{gathered} H'(\eta) = \frac{2}{L}h'(\xi) + H_0'(\eta), \qquad H''(\eta) = \frac{4}{L^2}h''(\xi) + H_0''(\eta), \\ H'''(\eta) = \frac{8}{L^3}h'''(\xi) + H_0'''(\eta), \end{gathered} \tag{3.3}$$

$$G'(\eta) = \frac{2}{L}g'(\xi) + G_0'(\eta), \qquad G''(\eta) = \frac{4}{L^2}g''(\xi) + G_0''(\eta). \tag{3.4}$$

Substituting (3.2) and (3.3)-(3.4) in the governing equations gives

$$\begin{aligned} a_0h''' + a_1h'' + a_2h' + a_3g + a_4h - \frac{4}{L^2}h''h + \frac{2}{L^2}h'h' - 2g^2 &= \phi_1(\eta), \\ b_0g'' + b_1h' + b_2g' + b_3h + b_4g - \frac{2}{L}hg' + \frac{2}{L}h'g &= \phi_2(\eta), \end{aligned} \tag{3.5}$$

where prime denotes derivative with respect to ξ and

$$a_0 = \frac{8}{L^3}, \quad a_1 = -\frac{4}{L^2}H_0, \quad a_2 = \frac{2}{L}H_0', \quad a_3 = -4G_0, \quad a_4 = -H_0'',$$
$$\phi_1(\eta) = -H_0''' + H_0H_0'' - \frac{1}{2}H_0'H_0' + 2G_0^2,$$
$$b_0 = \frac{4}{L^2}, \quad b_1 = \frac{2}{L}G_0, \quad b_2 = -\frac{2}{L}H_0, \quad b_3 = -G_0', \quad b_4 = H_0', \tag{3.6}$$
$$\phi_2(\eta) = -G_0'' + H_0G_0' - H_0'G_0.$$

As initial guesses we employ the exponentially decaying functions used by Yang and Liao [12], namely,

$$H_0(\eta) = e^{-\eta} + \eta e^{-\eta} - 1,$$
$$G_0(\eta) = e^{-\eta}. \tag{3.7}$$

The initial solution is obtained by solving the linear parts of (3.5), namely,

$$a_0h_0''' + a_1h_0'' + a_2h_0' + a_3g_0 + a_4h_0 = \phi_1(\eta),$$
$$b_0g_0'' + b_1h_0' + b_2g_0' + b_3h_0 + b_4g_0 = \phi_2(\eta), \tag{3.8}$$

subject to

$$h_0(-1) = \frac{2}{L}h_0'(-1) = \frac{2}{L}h_0'(1) = 0, \quad g_0(-1) = 0, \quad g_0(1) = 0. \tag{3.9}$$

The system (3.8)-(3.9) is solved using the Chebyshev pseudospectral method where the unknown functions $h_0(\xi)$ and $g_0(\xi)$ are approximated as truncated series of Chebyshev polynomials of the form

$$h_0(\xi) \approx h_0^N(\xi_j) = \sum_{k=0}^{N} \widehat{h}_k T_{1,k}(\xi_j), \quad j = 0, 1, \ldots, N,$$
$$g_0(\xi) \approx g_0^N(\xi_j) = \sum_{k=0}^{N} \widehat{g}_k T_{2,k}(\xi_j), \quad j = 0, 1, \ldots, N, \tag{3.10}$$

where $T_{1,k}$ and $T_{2,k}$ are the kth Chebyshev polynomials with coefficients $\widehat{h}_k$ and $\widehat{g}_k$, respectively, $\xi_0, \xi_1, \ldots, \xi_N$ are Gauss-Lobatto collocation points defined by

$$\xi_j = \cos\frac{\pi j}{N}, \quad j = 0, 1, \ldots, N, \tag{3.11}$$

and $N+1$ is the number of collocation points. Derivatives of the functions $h_0(\xi)$ and $g_0(\xi)$ at the collocation points are represented as

$$\frac{d^r h_0}{d\xi^r} = \sum_{k=0}^{N} \mathfrak{D}_{kj}^r h_0(\xi_j), \qquad \frac{d^r g_0}{d\xi^r} = \sum_{k=0}^{N} \mathfrak{D}_{kj}^r g_0(\xi_j), \tag{3.12}$$

where r is the order of differentiation and $\mathfrak{D}$ is the Chebyshev spectral differentiation matrix (see, e.g., [20, 21]). Substituting (3.10)–(3.12) in (3.8)-(3.9) yields

$$\mathbf{A}\mathbf{F}_0 = \mathbf{\Phi}, \tag{3.13}$$

subject to the boundary conditions

$$\frac{2}{L}\sum_{k=0}^{N} \mathfrak{D}_{0k} h_0(\xi_k) = 0, \qquad \frac{2}{L}\sum_{k=0}^{N} \mathfrak{D}_{Nk} h_0(\xi_k) = 0, \qquad h_0(\xi_N) = 0, \tag{3.14}$$

$$g_0(\xi_0) = 0, \qquad g_0(\xi_N) = 0, \tag{3.15}$$

where

$$\begin{gathered}
\mathbf{A} = \begin{pmatrix} \mathbf{a}_0\mathfrak{D}^3 + \mathbf{a}_1\mathfrak{D}^2 + \mathbf{a}_2\mathfrak{D} + \mathbf{a}_4\mathbf{I} & \mathbf{a}_3\mathbf{I} \\ \mathbf{b}_1\mathfrak{D} + \mathbf{b}_3\mathbf{I} & \mathbf{b}_0\mathfrak{D}^2 + \mathbf{b}_2\mathfrak{D} + \mathbf{b}_4\mathbf{I} \end{pmatrix}, \\
\mathbf{F}_0 = \left[h_0(\xi_0), h_0(\xi_1), \ldots, h_0(\xi_N), g_0(\xi_0), g_0(\xi_1), \ldots, g_0(\xi_N)\right]^T, \\
\mathbf{\Phi} = \left[\phi_1(\eta_0), \phi_1(\eta_1), \ldots, \phi_1(\eta_N), \phi_2(\eta_0), \phi_2(\eta_1), \ldots, \phi_2(\eta_N)\right]^T, \\
\mathbf{a}_i = \mathrm{diag}(\left[a_i(\eta_0), a_i(\eta_1), \ldots, a_i(\eta_{N-1}), a_i(\eta_N)\right]), \\
\mathbf{b}_i = \mathrm{diag}(\left[b_i(\eta_0), b_i(\eta_1), \ldots, b_i(\eta_{N-1}), b_i(\eta_N)\right]), \quad i = 0, 1, 2, 3, 4.
\end{gathered} \tag{3.16}$$

The superscript T denotes the transpose, diag is a diagonal matrix, and $\mathbf{I}$ is an identity matrix of size $(N+1) \times (N+1)$. We implement boundary conditions (3.14) in rows 1, N, and $N+1$ of $\mathbf{A}$ in columns 1 through to $N+1$ by setting all entries in the remaining columns to be zero. The second set (3.15) is implemented in rows $N+2$ and $2(N+1)$, respectively, by setting $A(N+2, N+2) = 1$, $A(2(N+1), 2(N+1)) = 1$ and setting all other columns to be zero. We further set entries of $\mathbf{\Phi}$ in rows 1, N, $N+1$, $N+2$, and $2(N+1)$ to zero.

The values of $[F_0(\xi_1), F_0(\xi_2), \ldots, F_0(\xi_{N-1})]$ are determined from the equation

$$\mathbf{F}_0 = \mathbf{A}^{-1}\mathbf{\Phi}, \tag{3.17}$$

which provides the initial approximation for the solution of (3.5).

We now seek the approximate solutions of (3.5) by first defining the following linear operators:

$$\begin{aligned}\mathcal{L}_h\left[\tilde{h}(\xi;q),\tilde{g}(\xi;q)\right] &= a_0\frac{\partial^3\tilde{h}}{\partial\xi^3}+a_1\frac{\partial^2\tilde{h}}{\partial\xi^2}+a_2\frac{\partial\tilde{h}}{\partial\xi}+a_3\tilde{g}+a_4\tilde{h},\\ \mathcal{L}_g\left[\tilde{h}(\xi;q),\tilde{g}(\xi;q)\right] &= b_0\frac{\partial^2\tilde{g}}{\partial\xi^2}+b_1\frac{\partial\tilde{h}}{\partial\xi}+b_2\frac{\partial\tilde{g}}{\partial\xi}+b_3\tilde{h}+b_4\tilde{g},\end{aligned} \tag{3.18}$$

where $q \in [0,1]$ is the embedding parameter and $\tilde{h}(\xi;q)$ and $\tilde{g}(\xi;q)$ are unknown functions. The *zero*th-order deformation equations are given by

$$\begin{aligned}(1-q)\mathcal{L}_h\left[\tilde{h}(\xi;q)-h_0(\xi)\right] &= q\hbar\left\{\mathcal{N}_h\left[\tilde{h}(\xi;q),\tilde{g}(\xi;q)\right]-\phi_1\right\},\\ (1-q)\mathcal{L}_g\left[\tilde{g}(\xi;q)-g_0(\xi)\right] &= q\hbar\left\{\mathcal{N}_g\left[\tilde{h}(\xi;q),\tilde{g}(\xi;q)\right]-\phi_2\right\},\end{aligned} \tag{3.19}$$

where $\hbar$ is the nonzero convergence controlling auxiliary parameter and $\mathcal{N}_h$ and $\mathcal{N}_g$ are nonlinear operators given by

$$\begin{aligned}\mathcal{N}_h\left[\tilde{h}(\xi;q),\tilde{g}(\xi;q)\right] &= a_0\frac{\partial^3\tilde{h}}{\partial\xi^3}+a_1\frac{\partial^2\tilde{h}}{\partial\xi^2}+a_2\frac{\partial\tilde{h}}{\partial\xi}+a_3\tilde{g}+a_4\tilde{h}-\frac{4}{L^2}\tilde{h}\frac{\partial^2\tilde{h}}{\partial\xi^2}+\frac{2}{L^2}\frac{\partial\tilde{h}}{\partial\xi}\frac{\partial\tilde{h}}{\partial\xi}-2\tilde{g}^2,\\ \mathcal{N}_g\left[\tilde{h}(\xi;q),\tilde{g}(\xi;q)\right] &= b_0\frac{\partial^2\tilde{g}}{\partial\xi^2}+b_1\frac{\partial\tilde{h}}{\partial\xi}+b_2\frac{\partial\tilde{g}}{\partial\xi}+b_3\tilde{h}+b_4\tilde{g}+\frac{2}{L}\left(\tilde{g}\frac{\partial\tilde{h}}{\partial\xi}-\tilde{h}\frac{\partial\tilde{g}}{\partial\xi}\right).\end{aligned} \tag{3.20}$$

The mth-order deformation equations are given by

$$\begin{aligned}\mathcal{L}_h\left[h_m(\xi)-\chi_m h_{m-1}(\xi)\right] &= \hbar R_m^h,\\ \mathcal{L}_g\left[g_m(\xi)-\chi_m g_{m-1}(\xi)\right] &= \hbar R_m^g,\end{aligned} \tag{3.21}$$

subject to the boundary conditions

$$h_m(-1)=h_m'(-1)=h_m'(1)=0, \qquad g_m(-1)=g_m(1)=0, \tag{3.22}$$

where

$$\begin{aligned} R_m^h(\xi) &= a_0 h_{m-1}''' + a_1 h_{m-1}'' + a_2 h_{m-1}' + a_3 g_{m-1} + a_4 h_{m-1} \\ &\quad + \sum_{n=0}^{m-1}\left(\frac{2}{L^2} h_n' h_{m-1-n}' - \frac{4}{L^2} h_n h_{m-1-n}'' - 2 g_n g_{m-1-n}\right) - \phi_1(\eta)(1-\chi_m), \\ R_m^g(\xi) &= b_0 g_{m-1}'' + b_1 h_{m-1}' + b_2 g_{m-1}' + b_3 h_{m-1} + b_4 g_{m-1} \\ &\quad + \frac{2}{L}\sum_{n=0}^{m-1}(h_n g_{m-1-n}' - g_n' h_{m-1-n}) - \phi_2(\eta)(1-\chi_m), \end{aligned} \tag{3.23}$$

$$\chi_m = \begin{cases} 0, & m \le 1, \\ 1, & m > 1. \end{cases} \tag{3.24}$$

Applying the Chebyshev pseudospectral transformation to (3.21)–(3.23) gives

$$\mathbf{A}\mathbf{F}_m = (\chi_m + \hbar)\mathbf{A}\mathbf{F}_{m-1} - \hbar(1-\chi_m)\mathbf{\Phi} + \hbar\mathbf{Q}_{m-1}, \tag{3.25}$$

subject to the boundary conditions

$$\begin{gathered} \sum_{k=0}^{N} \mathfrak{D}_{0k} h_m(\xi_k) = 0, \qquad \sum_{k=0}^{N} \mathfrak{D}_{Nk} h_m(\xi_k) = 0, \qquad h_m(\xi_N) = 0, \\ g_m(\xi_0) = 0, \qquad g_m(\xi_N) = 0, \end{gathered} \tag{3.26}$$

where $\mathbf{A}$ and $\mathbf{\Phi}$ are as defined in (3.16) and

$$\begin{aligned} \mathbf{F}_m &= \left[h_m(\xi_0), h_m(\xi_1), \ldots, h_m(\xi_N), g_m(\xi_0), g_m(\xi_1), \ldots, g_m(\xi_N)\right]^T, \\ \mathbf{Q}_{m-1} &= \begin{pmatrix} \sum_{n=0}^{m-1}\left[\frac{2}{L^2}(\mathfrak{D}h_n)(\mathfrak{D}h_{m-1-n}) - \frac{4}{L^2} h_n(\mathfrak{D}^2 h_{m-1-n}) - 2 g_n g_{m-1-n}\right] \\ \frac{2}{L}\sum_{n=0}^{m-1}\left[(\mathfrak{D}h_n) g_{m-1-n} - (\mathfrak{D}g_n) h_{m-1-n}\right] \end{pmatrix}. \end{aligned} \tag{3.27}$$

Boundary conditions (3.26) are implemented in matrix $\mathbf{A}$ on the left-hand side of (3.25) in rows 1, N, $N+1$, $N+2$, and $2(N+1)$, respectively, as before with the initial solution above. The corresponding rows, all columns, of A on the right-hand side of (3.25), $\mathbf{\Phi}$ and $\mathbf{Q}_{m-1}$ are all set to be zero. This results in the following recursive formula for $m \ge 1$:

$$\mathbf{F}_m = (\chi_m + \hbar)\mathbf{A}^{-1}\tilde{\mathbf{A}}\mathbf{F}_{m-1} + \hbar\mathbf{A}^{-1}\left[\mathbf{Q}_{m-1} - (1-\chi_m)\mathbf{\Phi}\right]. \tag{3.28}$$

The matrix $\tilde{\mathbf{A}}$ is the matrix $\mathbf{A}$ on the right-hand side of (3.25) but with the boundary conditions incorporated by setting the first, N, $N+1$, $N+2$, and $2(N+1)$, rows and columns to zero.

Thus, starting from the initial approximation, which is obtained from (3.17), higher-order approximations $F_m(\xi)$ for $m \geq 1$ can be obtained through recursive formula (3.28).

4. Successive Linearisation Method

The spectral homotopy analysis method, just like the original HAM, depends for its convergence rate on the careful selection of an embedded arbitrary parameter $\hbar$. Turkyilmazoglu [13] showed that the solution of the von Kármán problem by the homotopy analysis method is prone to wild oscillations when suction/injection is present. In this section we apply the successive linearisation method that requires no artificial parameters to control convergence to solve the governing equations (2.9)-(2.10). The method assumes that the unknown functions $H(\eta)$ and $G(\eta)$ can be expanded as

$$H(\eta) = H_i(\eta) + \sum_{n=0}^{i-1} h_n(\eta), \quad G(\eta) = G_i(\eta) + \sum_{n=0}^{i-1} g_n(\eta), \quad i = 1,2,3,\ldots, \tag{4.1}$$

where H_i, G_i are unknown functions and h_n and g_n ($n \geq 1$) are approximations that are obtained by recursively solving the linear part of the equation system that results from substituting (4.1) in the governing equations (2.9)-(2.10). Substituting (4.1) in the governing equations gives

$$\begin{aligned} H_i''' - a_{1,i-1}H_i'' + a_{2,i-1}H_i' - a_{3,i-1}H_i - 4a_{4,i-1}G_i - H_i''H_i + \frac{1}{2}H_i'H_i' - 2G_i^2 &= r_{i-1}, \\ G_i'' - b_{1,i-1}G_i' + b_{2,i-1}G_i + b_{3,i-1}H_i' - b_{4,i-1}H_i - H_iG_i' + H_i'G_i &= s_{i-1}, \end{aligned} \tag{4.2}$$

where the coefficient parameters $a_{k,i-1}$, $b_{k,i-1}$ ($k = 1,\ldots,4$), r_{i-1}, and s_{i-1} are defined as

$$\begin{aligned} a_{1,i-1} &= \sum_{n=0}^{i-1} h_n, \quad a_{2,i-1} = \sum_{n=0}^{i-1} h_n', \quad a_{3,i-1} = \sum_{n=0}^{i-1} h_n'', \quad a_{4,i-1} = \sum_{n=0}^{i-1} g_n, \\ b_{1,i-1} &= \sum_{n=0}^{i-1} h_n, \quad b_{2,i-1} = \sum_{n=0}^{i-1} h_n', \quad b_{3,i-1} = \sum_{n=0}^{i-1} g_n, \quad b_{4,i-1} = \sum_{n=0}^{i-1} g_n', \\ r_{i-1} &= -\left[\sum_{n=0}^{i-1} h_n''' - \sum_{n=0}^{i-1} h_n'' \sum_{n=0}^{i-1} h_n + \frac{1}{2}\sum_{n=0}^{i-1} h_n' \sum_{n=0}^{i-1} h_n' - 2\sum_{n=0}^{i-1} g_n \sum_{n=0}^{i-1} g_n\right], \\ s_{i-1} &= -\left[\sum_{n=0}^{i-1} g_n'' - \sum_{n=0}^{i-1} h_n \sum_{n=0}^{i-1} g_n' + \sum_{n=0}^{i-1} h_n' \sum_{n=0}^{i-1} g_n\right]. \end{aligned} \tag{4.3}$$

To facilitate direct comparison of the methods, we use the same initial approximations as in the case of the spectral homotopy analysis method of Yang and Liao [12]:

$$h_0(\eta) = -1 + e^{-\eta} + \eta e^{-\eta} \qquad g_0(\eta) = e^{-\eta}. \tag{4.4}$$

The solutions for h_n, g_n, $i - 1 \geq n \geq 1$, are obtained by successively solving the linearized form of (4.2), namely,

$$\begin{aligned} h_i''' - a_{1,i-1}h_i'' + a_{2,i-1}h_i' - a_{3,i-1}h_i - 4a_{4,i-1}g_i &= r_{i-1}, \\ g_i'' - b_{1,i-1}g_i' + b_{2,i-1}g_i + b_{3,i-1}h_i' - b_{4,i-1}h_i &= s_{i-1}, \end{aligned} \tag{4.5}$$

subject to the boundary conditions

$$h_i(0) = h_i'(0) = h_i'(\infty) = g_i(0) = g_i(\infty) = 0. \tag{4.6}$$

Once each h_i, g_i $(i \geq 1)$ has been found, the approximate solutions for $H(\eta)$ and $G(\eta)$ are obtained as

$$H(\eta) \approx \sum_{n=0}^{M} h_n(\eta), \qquad G(\eta) \approx \sum_{n=0}^{M} g_n(\eta), \tag{4.7}$$

where M is the order of the SLM approximation. In coming up with (4.7), we have assumed that

$$\lim_{i \to \infty} H_i = \lim_{i \to \infty} G_i = 0. \tag{4.8}$$

Equations (4.5)-(4.6) can be solved using analytical techniques (whenever possible) or any numerical method. In this work the equations were solved using the Chebyshev spectral collocation method in the manner described in the previous section. This leads to the matrix equation

$$\mathbf{A}_{i-1}\mathbf{Y}_i = \mathbf{R}_{i-1}, \tag{4.9}$$

where $\mathbf{A}_{i-1}$ is a $(2N + 2) \times (2N + 2)$ square matrix and $\mathbf{Y}_i$ and $\mathbf{R}_{i-1}$ are $(2N + 2) \times 1$ column vectors defined by

$$\mathbf{A}_{i-1} = \begin{bmatrix} A_{11} & A_{12} \\ A_{21} & A_{22} \end{bmatrix}, \qquad \mathbf{Y}_i = \begin{bmatrix} \mathbf{H}_i \\ \mathbf{G}_i \end{bmatrix}, \qquad \mathbf{R}_{i-1} = \begin{bmatrix} \mathbf{r}_{i-1} \\ \mathbf{s}_{i-1} \end{bmatrix}, \tag{4.10}$$

with

$$\begin{aligned}
\mathbf{H}_i &= [h_i(\xi_0), h_i(\xi_1), \ldots, h_i(\xi_{N-1}), h_i(\xi_N)]^T, \\
\mathbf{G}_i &= [g_i(\xi_0), g_i(\xi_1), \ldots, g_i(\xi_{N-1}), g_i(\xi_N)]^T, \\
\mathbf{r}_{i-1} &= [r_{i-1}(\xi_0), r_{i-1}(\xi_1), \ldots, r_{i-1}(\xi_{N-1}), r_{i-1}(\xi_N)]^T, \\
\mathbf{s}_{i-1} &= [s_{i-1}(\xi_0), s_{i-1}(\xi_1), \ldots, s_{i-1}(\xi_{N-1}), s_{i-1}(\xi_N)]^T, \\
A_{11} &= \mathbf{D}^3 - \mathbf{a}_{1,i-1}\mathbf{D}^2 + \mathbf{a}_{2,i-1}\mathbf{D} - \mathbf{a}_{3,i-1}, \\
A_{12} &= -4\mathbf{a}_{4,i-1}, \\
A_{21} &= \mathbf{b}_{3,i-1}\mathbf{D} - \mathbf{b}_{4,i-1}, \\
A_{22} &= \mathbf{D}^2 - \mathbf{b}_{1,i-1}\mathbf{D} + \mathbf{b}_{2,i-1}.
\end{aligned} \tag{4.11}$$

In the above definitions, $\mathbf{a}_{k,i-1}$, $\mathbf{b}_{k,i-1}$ $(k = 1, \ldots, 4)$ are diagonal matrices of size $(N+1)\times(N+1)$ and $D = (2/L)\mathfrak{D}$ with $\mathfrak{D}$ being the Chebyshev spectral differentiation matrix. After modifying the matrix system (4.9) to incorporate boundary conditions, the solution is obtained as

$$\mathbf{Y}_i = \mathbf{A}_{i-1}^{-1}\mathbf{R}_{i-1}. \tag{4.12}$$

5. MHD Swirling Boundary Layer Flow

The study of the magnetohydrodynamic swirling boundary layer flow over a rotating disk with suction or injection through the porous surface of the disk has recently been undertaken by Turkyilmazoglu [13]. In this case the Navier-Stokes equations reduce to a set of ordinary differential equations

$$F'' - F'H - F^2 + G^2 - mF = 0, \tag{5.1}$$

$$G'' - G'H - 2FG - mG = 0, \tag{5.2}$$

$$H'' - HH' + P' = 0, \tag{5.3}$$

$$2F + H' = 0, \tag{5.4}$$

subject to the boundary conditions

$$F(0) = F(\infty) = 0, \qquad G(0) = 1, \qquad G(\infty) = 0, \qquad H(0) = -s, \tag{5.5}$$

where m is the magnetic interaction parameter due to the externally applied magnetic field and s denotes uniform suction $(s > 0)$ or blowing $(s < 0)$ through the surface of the disk.

Turkyilmazoglu [13] utilized a twin strategy, using Ackroyd's series expansion and the homotopy analysis method to find purely analytic solutions to (5.1)–(5.5). In this study we use the SLM to obtain solutions to this system of equations.

Table 1: Comparison of $H(\infty)$ at different orders of the HAM [12], Homotopy-Padé [11], SHAM, and the SLM approximations when $\hbar = -1$, $L = 20$, and $N = 60$.

Order	HAM [12]	$[m,m]$	Hom-Padé [11]	Order	SHAM	Order	SLM	Numerical
0	−1	[5,5]	−0.885308	2	−0.884944	1	−0.871912	−0.884474
5	−0.9173	[10,10]	−0.884475	4	−0.884449	2	−0.884521	
10	−0.8747	[15,15]	−0.884474	6	−0.884476	3	−0.884474	
15	−0.8833	[20,20]	−0.884474	8	−0.884474	4	−0.884474	
20	−0.8845	[25,25]	−0.884474	10	−0.884474	5	−0.884474	

Eliminating F in (5.1) and (5.2) using (5.4) gives the following system of equations:

$$H''' - H''H + \frac{1}{2}H'H' - 2G^2 - mH' = 0, \tag{5.6}$$

$$G'' - HG' + H'G - mG = 0, \tag{5.7}$$

subject to the boundary conditions

$$H(0) = -s, \qquad H'(0) = H'(\infty) = 0, \qquad G(0) = 1, \qquad G(\infty) = 0. \tag{5.8}$$

The SLM is applied to (5.6) to (5.8) in the manner described in Section 4, and for brevity we omit the finer details. The intrinsic parameters of the SLM are essentially the same as those defined in Section 4 except for the following:

$$\begin{aligned} a_{2,i-1} &= \sum_{n=0}^{i-1} h_n' - m, \qquad b_{2,i-1} = \sum_{n=0}^{i-1} h_n' - m, \\ r_{i-1} &= -\left[\sum_{n=0}^{i-1} h_n''' - \sum_{n=0}^{i-1} h_n'' \sum_{n=0}^{i-1} h_n + \frac{1}{2}\sum_{n=0}^{i-1} h_n' \sum_{n=0}^{i-1} h_n' - 2\sum_{n=0}^{i-1} g_n \sum_{n=0}^{i-1} g_n - m\sum_{n=0}^{i-1} h_n'\right], \\ s_{i-1} &= -\left[\sum_{n=0}^{i-1} g_n'' - \sum_{n=0}^{i-1} h_n \sum_{n=0}^{i-1} g_n' + \sum_{n=0}^{i-1} h_n' \sum_{n=0}^{i-1} g_n - m\sum_{n=0}^{i-1} g_n\right]. \end{aligned} \tag{5.9}$$

An appropriate initial approximation for finding $H(\eta)$ in this case is

$$h_0(\eta) = -s - 1 + e^{-\eta} + \eta e^{-\eta}. \tag{5.10}$$

6. Results and Discussion

In this section we present the results for the velocity distributions $H(\eta)$ and $G(\eta)$. To check the accuracy of the successive linearisation method and the spectral homotopy analysis method, comparison is made with numerical solutions obtained using the Matlab bvp4c routine, which is an adaptive Lobatto quadrature scheme (see [22]). The current results are compared with previously published results by Liao [11], Yang and Liao [12], and Turkyilmazoglu [13].

Table 2: Comparison of $P(\infty) - P(0)$ obtained at different orders for the HAM [12], SHAM, and SLM approximations when $\hbar = -1$, $L = 20$, and $N = 60$.

HAM [12] order	$P(\infty) - P(0)$ order	SHAM order	$P(\infty) - P(0)$	SLM	$P(\infty) - P(0)$	Numerical
0	0.3901	2	0.391563	1	0.380115	0.391147
5	0.3910	4	0.391125	2	0.391189	
10	0.3911	6	0.391149	3	0.391147	
15	0.3911	8	0.391147	4	0.391147	
20	0.3911	10	0.391147	5	0.391147	

Table 3: Comparison of $F'(0)$ at different orders for the SLM approximations when $L = 20$, $N = 60$ against the results of [13] for different s values when $m = 1$.

s	1st order	2nd order	3rd order	4th order	Numerical	Reference [13]
−2.0	0.28399669	0.29148466	0.29148082	0.29148082	0.29148082	0.29148086
−1.0	0.31835562	0.32165707	0.32166220	0.32166220	0.32166220	0.32166220
0.0	0.31619804	0.30929864	0.30925799	0.30925798	0.30925798	0.30925798
1.0	0.26848288	0.25115842	0.25104369	0.25104397	0.25104397	0.25104397
2.0	0.19789006	0.18779923	0.18871806	0.18871902	0.18871902	0.18871903

The results presented in this work were generated using mostly $N = 60$ collocation points and $L = 20$.

Table 1 gives a comparison of the values of $H(\infty)$ obtained at different orders of the SLM and the SHAM approximations against the homotopy analysis method results, the homotopy-Padé results, and the numerical results. Our finding is that the SLM results converge most rapidly to the numerical result of −0.884474. Full convergence is achieved at the very low third order. Comparatively, convergence (to 6 decimal places) was achieved at the twentieth order using the homotopy analysis method and at the fifteenth order in the case of the homotopy-Padé method. When the same $\hbar$ value is used, convergence of the spectral homotopy analysis method is achieved at the eighth order compared to the twentieth order for the homotopy analysis method approximations. This suggests that the SLM is a very useful computational tool that converges much more rapidly than the homotopy analysis method, the homotopy-Padé method, and the spectral homotopy analysis method, although, the SLM may, in fact, require more computations per step than the other methods.

Table 2 gives a comparison of the pressure difference $P(\infty) - P(0)$ at different orders of the homotopy analysis method, SHAM, and SLM against the numerical results. A similar pattern as in Table 1 emerges where the SLM results converge rapidly to the numerical result of 0.391147 with full convergence achieved at the third order. In the case of the HAM, convergence up to four decimal places was achieved at the tenth order. For the same $\hbar$ values, the SHAM converges at the sixth order.

Tables 3–6 give a comparison between the SLM and the results reported by Turkyilmazoglu [13] for several suction/injection velocities and magnetic parameter values. Comparison of the results of Turkyilmazoglu [13] with the SLM seems most appropriate since the former study also partly utilizes a linearizing technique, the Newton-Raphson method to compute elements of the solutions. Turkyilmazoglu [13] showed that for large injection velocities, the number of terms required to attain convergence of the series solution increases dramatically, for instance, for injection velocities $s = -3.2$, up to 2000 terms are required

Table 4: Comparison of $G'(0)$ at different orders for the SLM approximations when $L = 20$, $N = 60$ against the results of [13] for different s values when $m = 1$.

s	1st order	2nd order	3rd order	4th order	Numerical	Reference [13]
−2.0	−0.46621214	−0.46571639	−0.46571471	−0.46571471	−0.46571471	−0.46571471
−1.0	−0.69404148	−0.69065793	−0.69066292	−0.69066292	−0.69066292	−0.69066292
0.0	−1.06924152	−1.06907700	−1.06905336	−1.06905336	−1.06905336	−1.06905336
1.0	−1.61663439	−1.65615591	−1.65707514	−1.65707580	−1.65707580	−1.65707588
2.0	−2.31476548	−2.42896548	−2.43136137	−2.43136154	−2.43136154	−2.43136154

Table 5: Flow parameters $F'(0)$ and $G'(0)$ at different orders for the SLM approximations when $L = 20$, $N = 120$ for different s values when $m = 1$.

s	$F'(0)$			$G'(0)$		
	2nd order	4th order	Numerical	2nd order	4th order	Numerical
−5	0.17788071	0.17788125	0.17788125	−0.20387855	−0.20387920	−0.20387920
−4	0.20924002	0.20924073	0.20924073	−0.25452255	−0.25452370	−0.25452370
−3	0.24839904	0.24839882	0.24839882	−0.33393576	−0.33393640	−0.33393640
3	0.14238972	0.14422157	0.14422157	−3.30816863	−3.31056638	−3.31056638
4	0.11266351	0.11466456	0.11466456	−4.23823915	−4.24002059	−4.24002059
5	0.09266580	0.09447344	0.09447344	−5.19357411	−5.19480492	−5.19480492

to achieve convergence of the series solution method, and hence the study resorts to the Chebyshev collocation method to solve the governing equations. Nonetheless, our findings indicate that with only a few terms of the SLM series good levels of accuracy are achieved for all suction and injection velocities. For the suction and injection velocities in the range $-2 \leq s \leq 2$ and $m = 1$ in Tables 3-4 there is an excellent agreement between the fourth-order SLM, the numerical, and the results reported by Turkyilmazoglu [13].

Table 5 gives a comparison between the numerical and the SLM results for larger values of s, up to $s = \pm 5$ when $m = 1$. Moderate increases in the suction/injection velocities appear to have no effect on the precision of the method with convergence again achieved at the fourth order of the SLM series. In Table 6, $s = 1$ is fixed and the magnetic parameter varied. We compare the convergence rate of the SLM to the numerical computations and show that increasing this parameter has no effect either on the convergence rate of the successive linearisation method.

Figure 1 gives a comparison between the fourth-order SHAM, second-order SLM, and numerical results for the dimensionless velocity distributions $H(\eta)$ and $G(\eta)$, respectively. There is an excellent agreement among the three sets of results. For purposes of comparison, it is worth noting that in case of the HAM in the work of Yang and Liao [12], agreement between the numerical and the HAM results was only observed at the 30th order of approximation for $H(\eta)$ and at the 10th order for $G(\eta)$. As with most iterative methods, it is worth noting that the convergence rate may depend on the initial approximation used. However, since we have used the same initial approximations as Yang and Liao [12], the graphical results suggest that the SLM converges much more rapidly than both the HAM and SHAM. This may, however, be offset by the fact that the SLM may require more computations per step than the other two methods.

Table 6: Flow parameters $F'(0)$ and $G'(0)$ at different orders for the SLM approximations when $L = 20$, $N = 120$ for different m values when $s = 1$.

m	$F'(0)$			$G'(0)$		
	2nd order	4th order	Numerical	2nd order	4th order	Numerical
0	0.39183500	0.38956624	0.38956624	−1.17700614	−1.17522084	−1.17522083
2	0.19726747	0.19756823	0.19756823	−2.01809456	−2.01847353	−2.01847353
4	0.14885275	0.14901611	0.14901611	−2.56931412	−2.56932504	−2.56932504
6	0.12469326	0.12476317	0.12476317	−3.00455809	−3.00452397	−3.00452397
8	0.10953285	0.10956389	0.10956389	−3.37536371	−3.37533046	−3.37533046
10	0.09887642	0.09889037	0.09889037	−3.703823547	−3.70379689	−3.70379689

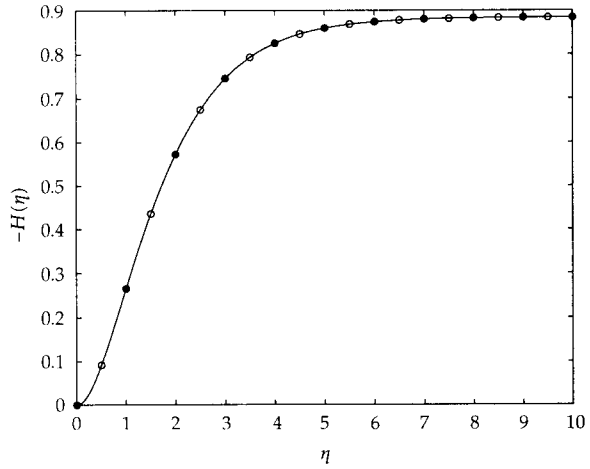

(a)

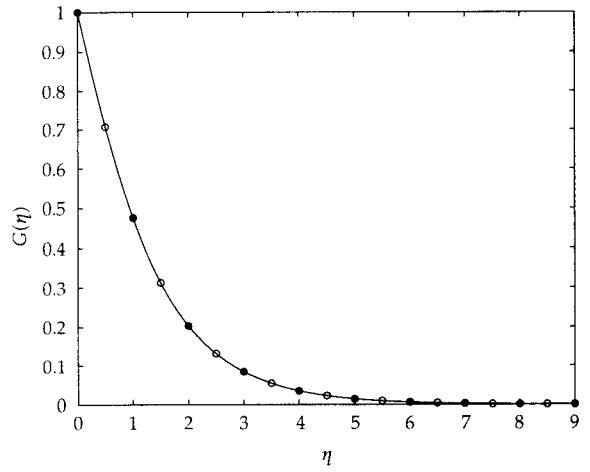

(b)

Figure 1: Comparison between the SHAM, SLM, and numerical solution of $-H(\eta)$ and $G(\eta)$ when $\hbar = -1$, $L = 20$, and $N = 60$. The open circles represent the SHAM 4th-order solution, the filled circles represent the 2nd-order SLM solution, and the solid line represent the numerical solution.

7. Conclusions

In this work two relatively new methods, the spectral homotopy analysis method and the successive linearisation method, have been successfully used to solve the von Kármán nonlinear equations for swirling flow with and without suction/injection across the disk walls and an applied magnetic field. The velocity components were compared with numerical results generated using the built-in Matlab `bvp4c` solver and against the homotopy analysis method and homotopy-Padé results in the literature. The results indicate that both the spectral homotopy analysis method and the successive linearisation method may give accurate and convergent results using only few solution terms compared with the homotopy analysis method and the Homotopy-Padé methods. Comparison has also been made with the recent findings by Turkyilmazoglu [13]. The successive linearisation method gives better accuracy at lower orders than the spectral homotopy analysis method. The tradeoff, however, is that both the spectral homotopy analysis method and the successive linearisation method may involve more computations per step compared to the methods in the literature.

Nonetheless, the sccessive linearisation method has been shown to be very efficient in that it rapidly converges to the numerical results. The study by Turkyilmazoglu [13] shows that whenever suction/blowing through the disk walls is present, the homotopy analysis method is prone to give wildly oscillating solutions. These oscillations have to be controlled by a careful choice of the embedded parameter $\hbar$. The advantage of the successive linearisation method is that such a parameter does not exist and no such oscillations are observed in the solution of the von Kármán equations for swirling flow.

Acknowledgment

The authors wish to acknowledge financial support from the National Research Foundation (NRF).

References

[1] T. von Kármán, "Uberlaminare und turbulence reibung," *Zeitschrift für Angewandte Mathematik und Mechanik*, vol. 52, no. 1, pp. 233–252, 1921.

[2] W. G. Cochran, "The flow due to a rotating disc," *Proceedings of the Cambridge Philisophical Society*, vol. 30, pp. 365–375, 1934.

[3] C.-S. Chien and Y.-T. Shih, "A cubic Hermite finite element-continuation method for numerical solutions of the von Kármán equations," *Applied Mathematics and Computation*, vol. 209, no. 2, pp. 356–368, 2009.

[4] R. M. Kirby and Z. Yosibash, "Solution of von-Kármán dynamic non-linear plate equations using a pseudo-spectral method," *Computer Methods in Applied Mechanics and Engineering*, vol. 193, no. 6–8, pp. 575–599, 2004.

[5] Z. Yosibash, R. M. Kirby, and D. Gottlieb, "Collocation methods for the solution of von-Kármán dynamic non-linear plate systems," *Journal of Computational Physics*, vol. 200, no. 2, pp. 432–461, 2004.

[6] A. Zerarka and B. Nine, "Solutions of the von Kàrmàn equations via the non-variational Galerkin–spline approach," *Communications in Nonlinear Science and Numerical Simulation*, vol. 13, no. 10, pp. 2320–2327, 2008.

[7] G. Adomian, "A review of the decomposition method and some recent results for nonlinear equations," *Computers & Mathematics with Applications*, vol. 21, no. 5, pp. 101–127, 1991.

[8] A. M. Lyapunov, *The General Problem of the Stability of Motion*, Taylor & Francis, London, UK, 1992.

[9] J.-H. He, "Homotopy perturbation method for solving boundary value problems," *Physics Letters A*, vol. 350, no. 1-2, pp. 87–88, 2006.

[10] J.-H. He, "A coupling method of a homotopy technique and a perturbation technique for non-linear problems," *International Journal of Non-Linear Mechanics*, vol. 35, no. 1, pp. 37–43, 2000.

[11] S. Liao, *Beyond Perturbation. Introduction to the Homotopy Analysis Method*, vol. 2 of *CRC Series: Modern Mechanics and Mathematics*, Chapman & Hall/CRC, Boca Raton, Fla, USA, 2004.
[12] C. Yang and S. Liao, "On the explicit, purely analytic solution of von Kármán swirling viscous flow," *Communications in Nonlinear Science and Numerical Simulation*, vol. 11, no. 1, pp. 83–93, 2006.
[13] M. Turkyilmazoglu, "Purely analytic solutions of magnetohydrodynamic swirling boundary layer flow over a porous rotating disk," *Computers and Fluids*, vol. 39, no. 5, pp. 793–799, 2010.
[14] J. A. D. Ackroyd, "On the steady flow produced by a rotating disc with either surface suction or injection," *Journal of Engineering Physics*, vol. 12, pp. 207–220, 1978.
[15] S. S. Motsa, P. Sibanda, and S. Shateyi, "A new spectral-homotopy analysis method for solving a nonlinear second order BVP," *Communications in Nonlinear Science and Numerical Simulation*, vol. 15, no. 9, pp. 2293–2302, 2010.
[16] S. S. Motsa, P. Sibanda, F. G. Awad, and S. Shateyi, "A new spectral-homotopy analysis method for the MHD Jeffery-Hamel problem," *Computers and Fluids*, vol. 39, no. 7, pp. 1219–1225, 2010.
[17] Z. Makukula, S. S. Motsa, and P. Sibanda, "On a new solution for the viscoelastic squeezing flow between two parallel plates," *Journal of Advanced Research in Applied Mathematics*, vol. 2, no. 4, pp. 31–38, 2010.
[18] S. S. Motsa and P. Sibanda, "A new algorithm for solving singular IVPs of Lane-Emden type," in *Proceedings of the 4th International Conference on Applied Mathematics, Simulation, Modelling*, NAUN International Conferences, pp. 176–180, Corfu Island, Greece, July 2010.
[19] J. P. Boyd, *Chebyshev and Fourier Spectral Methods*, Dover, Mineola, NY, USA, 2nd edition, 2001.
[20] C. Canuto, M. Y. Hussaini, A. Quarteroni, and T. A. Zang, *Spectral Methods in Fluid Dynamics*, Springer Series in Computational Physics, Springer, New York, NY, USA, 1988.
[21] W. S. Don and A. Solomonoff, "Accuracy and speed in computing the Chebyshev Collocation Derivative," *SIAM Journal on Scientific Computing*, vol. 16, no. 6, pp. 1253–1268, 1995.
[22] J. Kierzenka and L. F. Shampine, "A BVP solver based on residual control and the MATLAB PSE," *ACM Transactions on Mathematical Software*, vol. 27, no. 3, pp. 299–316, 2001.

4.3. On a quasilinearisation method for the Von Kármán flow problem with heat transfer [3]

Corrigendum

Please note the geometry of the flow studied in this Section;

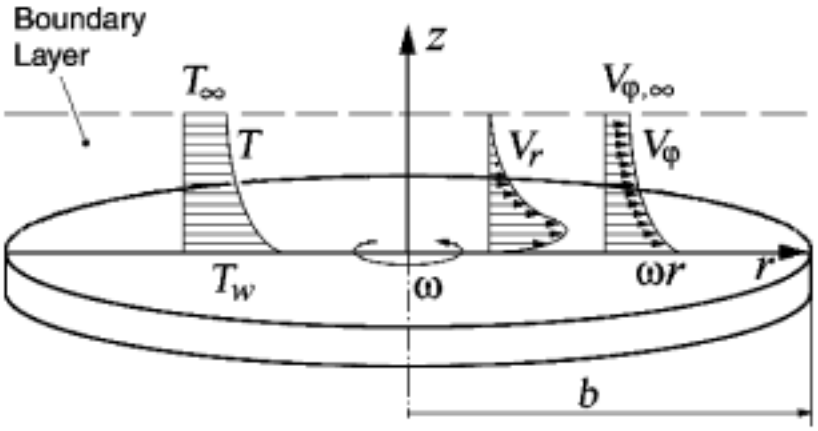

Figure 4.3: *Flow configuration for the von Kàmàrn swirling flow with heat transfer.*

[3]Accepted; Z. G. Makukula, P. Sibanda and S. S. Motsa. *Latin American Applied Research*, http://www.laar.uns.edu.ar/ (Impact factor; 0.16).

ON A QUASILINEARISATION METHOD FOR THE VON KÁRMÁN FLOW PROBLEM WITH HEAT TRANSFER

Z. G. MAKUKULA†, P. SIBANDA† and S. S. MOTSA†

†*School of Mathematical Sciences, University of KwaZulu-Natal, Private Bag X01, Scottsville 3209 Pietermaritzburg, South Africa*
Emails: zmzmakukula@gmail.com / sibandap@ukzn.ac.za / sandilemotsa@gmail.com

***Abstract*— A quasilinearisation method for solving the nonlinear equations is presented. The method works successively in linearizing the nonlinear equations and solving the resulting higher order deformation equations using spectral methods. We illustrate the application of the method by solving the laminar heat transfer problem in a rotating disk. Comparison between the linearisation method and numerical results obtained using the MATLAB in-built bvp4c solver reveals that the linearisation method is accurate and converges at very low orders of the iteration scheme.**

***Keywords*— Heat transfer; linearisation method; rotating disk; spectral methods.**

I. INTRODUCTION

Disk-shaped bodies are encountered in many engineering, geophysical and meteorological applications. The study of fluid flow due to a rotating disk was pioneered by von Kármán (1921) who provided the basis for the mathematical study of the rotating disk problem in an incompressible viscous flow of infinite extent. He introduced transformations that reduced the governing partial differential equations to ordinary differential equations. Since then, solutions of the von Kármán equations describing different aspects of the disk flow problem such as the effect of combined viscous dissipation and joule heating in the presence of Hall and ion-slip currents, the effect of suction on the flow with or without an applied magnetic field and thermal and mass diffusive effects have been of interest to researchers in diverse fields of science.

As with most problems in science and engineering, the equations that describe swirling flow are nonlinear and do not have closed form solutions. In most instances the von Kármán equations have been solved numerically using either the shooting method or the implicit finite difference scheme in combination with a linearisation technique. While numerical methods are effective and give accurate solutions, they often give no insights into the structure of the solution, particularly the effects of multi-parameters embedded in the problem. Numerical methods also often fail to give sufficient resolution to domains with very sharp changes or to problems with multiple solutions. These limitations necessitate the development of computationally improved semi-analytical methods for solving strongly nonlinear problems. Recent semi-analytical methods include, among others, the variational iteration method and the homotopy perturbation method (He, 2000, 2007), the Adomian decomposition method (Adomian, 1976), the homotopy analysis method (Liao, 2003) and the spectral-homotopy analysis methods (Motsa et al., 2010). These methods may converge slowly or fail to converge for problems that are strongly nonlinear or for problems with very large parameters.

In this paper we present a method for solving nonlinear equations that is based on iteratively linearizing the equations to obtain a system of higher order deformation equations that are solved using spectral methods. The application of the method is demonstrated by solving the laminar heat transfer problem in a rotating disk. The problem was studied by Shevchuk and Buschmann (2005) who solved the transformed ordinary differential equations using a numerical method. Other recent studies on various aspects of the rotating disk flow problem include the works of Takhar et al. (2002) who considered electrically conducting fluids in MHD flow and Arikoglu and Ozkol (2006) who considered heat transfer characteristics on MHD flow. The series of studies by Attia (2004, 2006, 2007) considered the effects of (i) ion slip, (ii) temperature dependent viscosity and (iii) ohmic heating on rotating disk flow. Sibanda and Makinde (2010) considered the effects of ohmic and viscous heat dissipation, Hall currents, porosity and an applied magnetic field on a rotating disk flow with constant properties.

II. GOVERNING EQUATIONS

We consider a disk rotating with angular velocity ω in a fluid which rotates in the same direction with a different angular velocity Ω. In cylindrical polar coordinates (r, ϕ, z) the Navier-Stokes equations governing the flow are (Schlichting, 1979);

$$\frac{\partial u}{\partial r} + \frac{u}{r} + \frac{\partial w}{\partial z} = 0. \tag{1}$$

$$u\frac{\partial u}{\partial r}+w\frac{\partial u}{\partial z}-\frac{v^2}{r}=-\frac{1}{\rho}\frac{\partial p}{\partial r} +\nu\left\{\frac{\partial^2 u}{\partial r^2}+\frac{\partial}{\partial r}\left(\frac{u}{r}\right)+\frac{\partial^2 u}{\partial z^2}\right\}, \quad (2)$$

$$u\frac{\partial v}{\partial r}+w\frac{\partial v}{\partial z}+\frac{uv}{r}=\nu\left\{\frac{\partial^2 v}{\partial r^2}+\frac{\partial}{\partial r}\left(\frac{v}{r}\right)+\frac{\partial^2 v}{\partial z^2}\right\}, \quad (3)$$

$$u\frac{\partial w}{\partial r}+w\frac{\partial w}{\partial z}=-\frac{1}{\rho}\frac{\partial p}{\partial z} +\nu\left\{\frac{\partial^2 w}{\partial r^2}+\frac{1}{r}\frac{\partial w}{\partial r}+\frac{\partial^2 w}{\partial z^2}\right\}, \quad (4)$$

$$u\frac{\partial T}{\partial r}+w\frac{\partial T}{\partial z}=-\frac{uT}{r} +\frac{1}{Pr}\left\{\frac{\partial^2 T}{\partial r^2}+\frac{1}{r}\frac{\partial T}{\partial r}+\frac{\partial^2 T}{\partial z^2}\right\}. \quad (5)$$

The boundary conditions are

$$u=0,\ v=r\omega,\ w=0,\ T=T_w \quad \text{at} \quad z=0, \quad (6)$$

$$u=0,\ v=r\Omega,\ T\to T_\infty \quad \text{as} \quad z\to\infty, \quad (7)$$

where u, v, and w are the velocity components in the radial, tangential and axial directions respectively, ν is the kinematic viscosity, ρ is the density, p is the static pressure, T is the temperature and the subscripts w and ∞ refer to the wall and the outer boundary layer edge respectively, and Pr is the Prandtl number. We introduce a dimensionless coordinate $\eta=z\sqrt{\omega/\nu}$ and the von Kármán transformations;

$$u=r\omega F(\eta), \quad v=r\omega G(\eta) \quad w=\sqrt{\omega\nu}H(\eta),$$
$$P(\eta)=-\frac{p}{\rho\nu\omega}, \quad \Theta=\frac{T-T_\infty}{T_w-T_\infty}, \quad (8)$$

where F, G and H are the dimensionless velocity components along the radial, tangential and axial directions respectively and Θ is the dimensionless temperature. The radial pressure gradient can be computed for the frictionless flow at a large distance from the wall using the condition:

$$\frac{1}{\rho}\frac{\partial p}{\partial r}=r\Omega^2. \quad (9)$$

Shevchuk and Buschmann (2005) showed that by using the transformations (8), the Navier-Stokes equations reduce to the following system of nonlinear ordinary differential equations,

$$H' = -2F, \quad (10)$$
$$F'' = F^2-G^2+F'H+\beta^2, \quad (11)$$
$$G'' = 2FG+G'H, \quad (12)$$
$$H' = (P'+H'')H^{-1}, \quad (13)$$
$$\Theta'' = Pr(H\Theta'+\alpha F\theta), \quad (14)$$

with boundary conditions

$$F(0)=H(0)=0,\ G(0)=1, \quad (15)$$
$$\Theta(0)=1,\ F'(\infty)=0,\ \Theta(\infty)=0, \quad (16)$$
$$G(\infty)=\beta. \quad (17)$$

Using (10), equations (11), (12) and (14) can be expressed as

$$H'''=H''H+2G^2-\frac{1}{2}H'^2-2\beta^2, \quad (18)$$
$$G''=G'H-H'G, \quad (19)$$
$$\Theta''=Pr(H\Theta'-\frac{1}{2}\alpha H'\Theta), \quad (20)$$

subject to

$$H(0) = H'(0)=H'(\infty)=\Theta(\infty)=0, \quad (21)$$
$$G(0) = \Theta(0)=1, G(\infty)=\beta, \quad (22)$$

where α is a constant and $\beta=\Omega/\omega$ is the flow swirl parameter. Equation (13) can be used to find the pressure.

III. METHOD OF SOLUTION

The quasilinearisation method (see Makukula et al. 2010a-e, Motsa and Shateyi, 2010, Shateyi and Motsa, 2010) is applied to solve equations (18) - (20). The starting point is to assume that the independent variables $H(\eta)$, $G(\eta)$ and $\Theta(\eta)$ may be expanded as

$$H(\eta)=h_i(\eta)+\sum_{m=0}^{i-1}H_m(\eta), \quad (23)$$
$$G(\eta)=g_i(\eta)+\sum_{m=0}^{i-1}G_m(\eta), \quad (24)$$
$$\Theta(\eta)=\theta_i(\eta)+\sum_{m=0}^{i-1}\Theta_m(\eta), \quad (25)$$

where h_i, g_i and θ_i $(i=1,2,3,\ldots)$ are unknown functions and H_m , G_m and Θ_m $(m\geq 1)$ are approximations that are obtained by recursively solving the linear part of the equation that results from substituting (23) - (25) into equations (18) - (20). This gives the equations

$$h_i'''+a_{1,i-1}h_i''+a_{2,i-1}h_i'+a_{3,i-1}h_i+a_{4,i-1}g_i -h_i''h_i+\frac{1}{2}h_i'h_i'-2g_i^2=r_{i-1}, \quad (26)$$

$$g_i''+b_{1,i-1}g_i'+b_{2,i-1}g_i+b_{3,i-1}h_i' +b_{4,i-1}h_i-h_ig_i'+h_i'g_i=s_{i-1}, \quad (27)$$

$$\theta_i''+c_{1,i-1}\theta_i'+c_{2,i-1}\theta_i+c_{3,i-1}h_i' +c_{4,i-1}h_i-Pr(h_i\theta_i'-\frac{1}{2}\alpha h_i'\theta_i)=t_{i-1}, \quad (28)$$

where the coefficient parameters $a_{k,i-1}$, $b_{k,i-1}$, $c_{k,i-1}$ $(k=1,..,4)$, r_{i-1} , s_{i-1} and t_{i-1} are defined as

$$a_{1,i-1}=-\sum_{m=0}^{i-1}H_m,\ a_{2,i-1}=\sum_{m=0}^{i-1}H_m', \quad (29)$$
$$a_{3,i-1}=-\sum_{m=0}^{i-1}H_m'',\ a_{4,i-1}=-4\sum_{m=0}^{i-1}G_m, \quad (30)$$
$$b_{1,i-1}=-\sum_{m=0}^{i-1}H_m,\ b_{2,i-1}=\sum_{m=0}^{i-1}H_m', \quad (31)$$

$$b_{3,i-1} = \sum_{m=0}^{i-1} G_m, \; b_{4,i-1} = -\sum_{m=0}^{i-1} G'_m, \tag{32}$$

$$c_{1,i-1} = -Pr \sum_{m=0}^{i-1} H_m, \tag{33}$$

$$c_{2,i-1} = \frac{1}{2}\alpha Pr \sum_{m=0}^{i-1} H'_m, \tag{34}$$

$$c_{3,i-1} = \frac{1}{2}\alpha Pr \sum_{m=0}^{i-1} \Theta_m, \tag{35}$$

$$c_{4,i-1} = -Pr \sum_{m=0}^{i-1} \Theta'_m, \tag{36}$$

$$\begin{aligned} r_{i-1} &= -\sum_{m=0}^{i-1} \Big(H'''_m - H''_m H_m \\ &\quad + \frac{1}{2}(H'_m)^2 - 2G_m^2 + 2\beta^2 \Big), \end{aligned} \tag{37}$$

$$s_{i-1} = -\sum_{m=0}^{i-1} \left(G''_m - H_m G'_m + H'_m G_m \right), \tag{38}$$

$$\begin{aligned} t_{i-1} &= -\sum_{m=0}^{i-1} \Big(\Theta''_m - PrH_m \Theta'_m \\ &\quad - \frac{1}{2}\alpha PrH'_m \Theta_m \Big). \end{aligned} \tag{39}$$

Starting from the initial approximations

$$\begin{aligned} H_0(\eta) &= -1 + (1+\eta)e^{-\eta}, & (40)\\ G_0(\eta) &= \beta + (1-\beta)e^{-\eta}, & (41)\\ \Theta_0(\eta) &= e^{-\eta}, & (42) \end{aligned}$$

which are chosen to satisfy the boundary conditions (21) - (22), the subsequent solutions for H_m, G_m, Θ_m, $m \geq 1$ are obtained by successively solving the linearized form of equations (26), (27) and (28) subject to the boundary conditions

$$\begin{aligned} h_i(0) &= h'_i(0) = h'_i(\infty) = 0, \; g_i(0) = g_i(\infty) = 0, \\ \theta_i(0) &= \theta_i(\infty) = 0. \end{aligned} \tag{43}$$

Once each solution h_i, g_i and θ_i $(i \geq 1)$ has been found, the approximate solutions for $H(\eta)$, $G(\eta)$ and $\Theta(\eta)$ are obtained as

$$\begin{aligned} H(\eta) &\approx \sum_{m=0}^{M} h_m(\eta), \; G(\eta) \approx \sum_{m=0}^{M} g_m(\eta), \\ \Theta(\eta) &\approx \sum_{m=0}^{M} \theta_m(\eta). \end{aligned} \tag{44}$$

where M is the order of the approximation.

Equations (26) - (28) are integrated using the Chebyshev spectral collocation method. The unknown functions are defined by the Chebyshev interpolating polynomials with the Gauss-Lobatto points defined as

$$y_j = \cos\frac{\pi j}{N}, \quad j = 0, 1, \ldots, N, \tag{45}$$

where N is the number of collocation points used. The physical region $[0, \infty]$ is transformed into the domain $[-1, 1]$ using the domain truncation technique in which the problem is solved on the interval $[0, L]$ instead of $[0, \infty)$. This leads to the mapping

$$\frac{\eta}{L} = \frac{\xi + 1}{2}, \quad -1 \leq \xi \leq 1, \tag{46}$$

where L is the scaling parameter used to invoke the boundary condition at infinity. The unknown functions h_i, g_i and θ_i are approximated at the collocation points by

$$\begin{aligned} h_i(\xi) &\approx \sum_{k=0}^{N} h_i(\xi_k) T_k(\xi_j), \; g_i(\xi) \approx \sum_{k=0}^{N} g_i(\xi_k) T_k(\xi_j), \\ \theta_i(\xi) &\approx \sum_{k=0}^{N} \theta_i(\xi_k) T_k(\xi_j), \; j = 0, 1, \ldots, N, \end{aligned} \tag{47}$$

where T_k is the kth Chebyshev polynomial defined as

$$T_k(\xi) = \cos[k \cos^{-1}(\xi)]. \tag{48}$$

The derivatives of the variables at the collocation points are represented as

$$\begin{aligned} \frac{d^a h_i}{d\eta^a} &= \sum_{k=0}^{N} \mathbf{D}^a_{kj} h_i(\xi_k), \; \frac{d^a g_i}{d\eta^a} = \sum_{k=0}^{N} \mathbf{D}^a_{kj} g_i(\xi_k), \\ \frac{d^a \theta_i}{d\eta^a} &= \sum_{k=0}^{N} \mathbf{D}^a_{kj} \theta_i(\xi_k), \quad j = 0, 1, \ldots, N, \end{aligned} \tag{49}$$

where a is the order of differentiation and $\mathbf{D} = \frac{2}{L}\mathcal{D}$ with $\mathcal{D}$ being the Chebyshev spectral differentiation matrix (see Canuto et al., 1988 and Trefethen, 2000). This leads to the matrix equation

$$\mathbf{A}_{i-1}\mathbf{X}_i = \mathbf{B}_{i-1}, \tag{50}$$

in which $\mathbf{A}_{i-1}$ is a $(3N+3) \times (3N+3)$ square matrix and $\mathbf{X}_i$ and $\mathbf{B}_{i-1}$ are $(3N+3) \times 1$ column vectors defined by

$$\begin{aligned} \mathbf{A}_{i-1} &= \begin{bmatrix} A_{11} & A_{12} & A_{13} \\ A_{21} & A_{22} & A_{23} \\ A_{31} & A_{32} & A_{33} \end{bmatrix}, \; \mathbf{X}_i = \begin{bmatrix} \mathbf{H}_i \\ \mathbf{G}_i \\ \mathbf{\Theta_i} \end{bmatrix}, \\ \mathbf{B}_{i-1} &= \begin{bmatrix} \mathbf{r}_{i-1} \\ \mathbf{s}_{i-1} \\ \mathbf{t}_{i-1} \end{bmatrix}, \end{aligned} \tag{51}$$

with

$$\begin{aligned} \mathbf{H}_i &= [h_i(\xi_0), h_i(\xi_1), \ldots, h_i(\xi_{N-1}), h_i(\xi_N)]^T, \\ \mathbf{G}_i &= [g_i(\xi_0), g_i(\xi_1), \ldots, g_i(\xi_{N-1}), g_i(\xi_N)]^T, \\ \mathbf{\Theta}_i &= [\theta_i(\xi_0), \theta_i(\xi_1), \ldots, \theta_i(\xi_{N-1}), \theta_i(\xi_N)]^T, \\ \mathbf{r}_{i-1} &= [r_{i-1}(\xi_0), r_{i-1}(\xi_1), \ldots, r_{i-1}(\xi_N)]^T, \\ \mathbf{s}_{i-1} &= [s_{i-1}(\xi_0), s_{i-1}(\xi_1), \ldots, s_{i-1}(\xi_N)]^T, \\ \mathbf{t}_{i-1} &= [t_{i-1}(\xi_0), t_{i-1}(\xi_1), \ldots, t_{i-1}(\xi_N)]^T, \end{aligned}$$

$$A_{11} = \mathbf{D}^3 + \mathbf{a}_{1,i-1}\mathbf{D}^2 + \mathbf{a}_{2,i-1}\mathbf{D} + \mathbf{a}_{3,i-1},$$
$$A_{12} = \mathbf{a}_{4,i-1}, \quad A_{13} = 0\mathbf{I},$$
$$A_{21} = \mathbf{b}_{3,i-1}\mathbf{D} + \mathbf{b}_{4,i-1},$$
$$A_{22} = \mathbf{D}^2 + \mathbf{b}_{1,i-1}\mathbf{D} + \mathbf{b}_{2,i-1}, \quad A_{23} = 0\mathbf{I},$$
$$A_{31} = \mathbf{c}_{3,i-1}\mathbf{D} + \mathbf{c}_{4,i-1}, \quad A_{32} = 0\mathbf{I},$$
$$A_{33} = \mathbf{D}^2 + \mathbf{c}_{1,i-1}\mathbf{D} + \mathbf{c}_{2,i-1}.$$

In the definitions above, $\mathbf{a}_{k,i-1}$, $\mathbf{b}_{k,i-1}$, $\mathbf{c}_{k,i-1}$ $(k = 1,..,4)$ are diagonal matrices of size $(N+1) \times (N+1)$ and $\mathbf{I}$ is the $(N+1) \times (N+1)$ identity matrix. After modifying the matrix system (50) to incorporate boundary conditions, the solution is obtained as

$$\mathbf{X}_i = \mathbf{A}_{i-1}^{-1}\mathbf{B}_{i-1}. \tag{52}$$

IV. RESULTS AND DISCUSSION

A quasilinearisation method (the SLM) has been used to solve the nonlinear equations for the rotating disk problem. The accuracy of the method is determined by benchmarking the results with numerical results obtained using the bvp4c, an in-built MATLAB solver for boundary value problems. This solver is based on the fourth order Runge-Kutta schemes. The results were generated using $N = 150$ and $L = 30$ which was found to give good accuracy. Tables 1 - 4 show the results of the laminar heat transfer problem for a rotating disk in a forced vortex. Table 1 gives a sense of the convergence rate of the linearisation method through a comparison of the values of the axial velocity $H(\infty)$ at different orders of the SLM approximation and for different values of β against the numerical results. Simulations show a decrease in the magnitude of the axial velocities with the swirl parameter β. Convergence up to seven decimal places of the linearized results to the numerical results is achieved at the third order of the SLM approximation.

Table 1: Comparison of the values of the SLM solutions for $H(\infty)$ with the bvp4c solutions when $\alpha = 0.25$ and $Pr = 0.71$.

β	1st order	2nd order	3rd order	numerical
0.0	-0.8719123	-0.8845211	-0.8844741	-0.8844741
0.2	-0.8747141	-0.8617650	-0.8616990	-0.8616990
0.4	-0.7014692	-0.6600254	-0.6599807	-0.6599807
0.6	-0.4301355	-0.4307716	-0.4307715	-0.4307715
0.8	-0.2063600	-0.2080067	-0.2080065	-0.2080065

Tables 2 - 4 serve two purposes, to show the effects of the parameters Pr, α and β respectively on the surface heat transfer rate $-\Theta'(0)$, and to demonstrate the rapid convergence of the linearisation method by comparing the SLM approximations at different orders with the numerical results.

Table 2 shows the effect of increasing Prandtl numbers on the heat transfer rate. The heat transfer rate evidently increases with Prandtl numbers. A similar patten is observed in Table 3 where $-\Theta'(0)$ increases with α.

Table 2: Comparison of the values of the SLM solutions for $-\Theta'(0)$ with the bvp4c solutions when $\alpha = -1$ and $\beta = 0.2$.

Pr	1st order	2nd order	3rd order	numerical
0.50	0.1561211	0.1484358	0.1483821	0.1483821
0.71	0.1960747	0.1890687	0.1890219	0.1890219
1.00	0.2409260	0.2351828	0.2351495	0.2351495
5.00	0.5393097	0.5442660	0.5442912	0.5442912
7.00	0.6239296	0.6318794	0.6319128	0.6319128
10.0	0.7241602	0.7357068	0.7357498	0.7357498

Table 3: Comparison of the values of the SLM solutions for $-\Theta'(0)$ with the bvp4c solutions when $Pr = 0.71$ and $\beta = 0.2$.

α	1st order	2nd order	3rd order	numerical
-0.6	0.2483688	0.2483120	0.2483119	0.2483119
0.0	0.3333432	0.3255588	0.3254945	0.3254945
1.0	0.4384019	0.4315601	0.4314959	0.4314959
2.0	0.5235998	0.5180981	0.5180416	0.5180416
3.0	0.5954972	0.5913154	0.5912690	0.5912690

Table 4: Comparison of the values of the SLM solutions for $-\Theta'(0)$ with the bvp4c solutions when $Pr = 5$ and $\alpha = 4$.

β	1st order	2nd order	3rd order	numerical
0.0	1.4975774	1.4971121	1.4971120	1.4971120
0.2	1.4872255	1.4927180	1.4927405	1.4927405
0.4	1.3771388	1.4152675	1.4157121	1.4157121
0.6	1.2577045	1.2601420	1.2601404	1.2601404
0.8	0.9700408	0.9738696	0.9738516	0.9738516

Increasing the swirl parameter β in Table 4 results in the surface heat transfer rate being reduced. In terms of the accuracy of the linearisation method, it is evident that convergence of the SLM results up to seven decimal place accuracy is achieved at the third order of the SLM approximation. Figures 1 - 4 show the results for the laminar heat transfer problem of a rotating disk in a forced vortex. Figures 1 - 2 show the effect of β on the radial and axial velocity profiles respectively. Here the third order SLM approximations are plotted alongside the numerical solution. We observe an excellent agreement between the SLM and the numerical results and the results show that increasing the swirl parameter β reduces the radial velocity while increasing the axial velocity. It is worth noting here that the radial velocity profiles given in Shevchuk and Buschmann (2005) are not consistent with some previous results in the literature, for example, those of Attia (2008) and Turkyilmazoglu (2010).

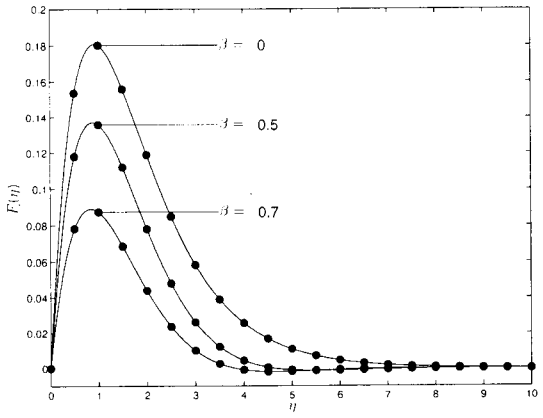

Figure 1: Comparison between the 3rd order (filled circles) and the numerical solutions (solid line) for $F(\eta)$ when $\alpha = 1$ and $Pr = 0.25$.

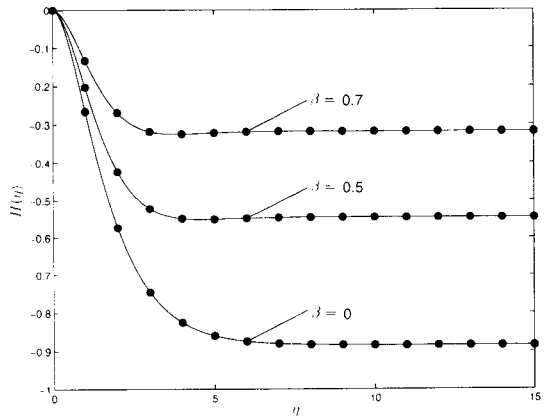

Figure 2: Comparison between the 3rd order (filled circles) and the numerical solutions (solid line) for $H(\eta)$ when $\alpha = 1$ and $Pr = 0.25$.

Figures 3 - 4 show the effect of β on the tangential velocity profile $G(\eta)$ and the temperature $\Theta(\eta)$ for fixed Prandtl numbers. The agreement between the third order SLM approximations and the numerical solutions excellent. An increase in the swirl parameter leads to an increase in both the temperature and the tangential velocity profiles.

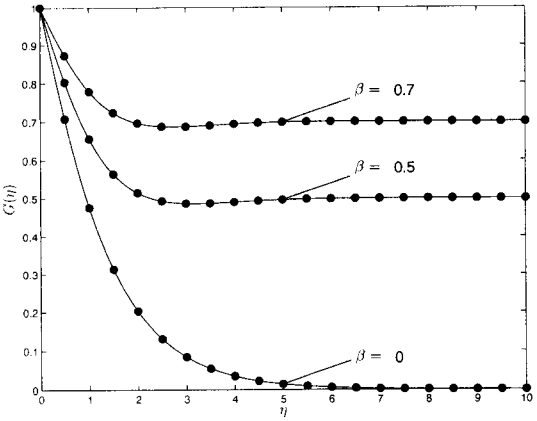

Figure 3: Comparison between the 3rd order solution (filled circles) and the numerical solution (solid line) for $G(\eta)$ when $\alpha = 1$ and $Pr = 0.25$.

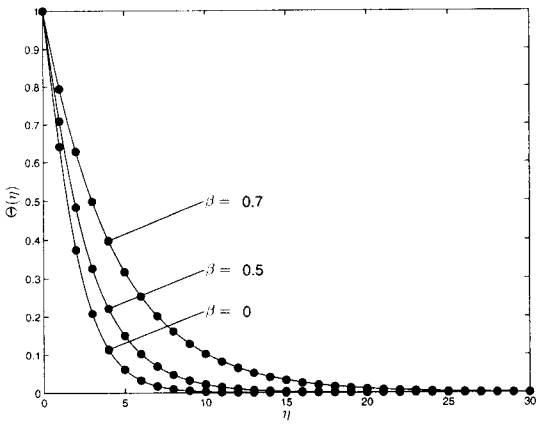

Figure 4: Comparison between the 3rd order solution (filled circles) and the numerical solution (solid line) for $\Theta(\eta)$ when $\alpha = 1$ and $Pr = 0.25$.

V. CONCLUSION

A successive linearisation algorithm to compute the numerical solution for the laminar heat transfer problem of a rotating disk in a forced vortex has been presented. Values of the axial velocity far from the surface of the disk were obtained for various swirl parameter values β. An increase in $H(\infty)$ was observed with increase in β. The heat transfer rate was found

for different Prandtl numbers and β. The heat transfer rate increases with increase in the Prandtl number but decreases with β. The axial and tangential velocity and the temperature profiles were found to increase with β while the radial velocity profiles decreased with β. The linearisation method was found to be accurate and rapidly convergent to the numerical results.

ACKNOWLEDGMENT

The authors wish to acknowledge financial support from the National Research Foundation (NRF).

REFERENCES

Adomian, G., "Nonlinear stochastic differential equations," *J Math. Anal. Appl.* **55**, 441 - 52 (1976).

Arikoglu, A. and I. Ozkol, "On the MHD and slip flow over a rotating disk with heat transfer," *Int. Num. J. Heat & Fluid Flow*, **16**, 172-184 (2006).

Attia, H.A., "Ion slip effect on the flow due to a rotating disk," *The Arab. J. Sci. and Eng.*, **29**, 165 - 172 (2004).

Attia, H.A., "Unsteady flow and heat transfer of viscous incompressible fluid with temperature-dependent viscosity due to a rotating disc in a porous medium," *J. Phys. A: Math. Gen.*, **39**, 979 - 991 (2006).

Attia, H.A., "Rotating disk flow and heat transfer of a conducting non-Newtonian fluid with suction-injection and ohmic heating," *J. Braz. Soc. Mech. Sci. and Eng.*, **19**, 168 - 173 (2007).

Attia, H.A., "Rotating disk flow and heat transfer through a porous medium of a non-Newtonian fluid with suction and injection," *Comm. Nonlinear Sc. Num. Simul.*, **13**, 1571 - 1580 (2008).

Canuto, C., M.Y. Hussaini, A. Quarteroni, and T.A. Zang, *Spectral Methods in Fluid Dynamics*, Springer-Verlag, Berlin (1988).

He, J.H., "A coupling method for homotopy technique and perturbation technique for non-linear problem," *Int. J. Non-Linear. Mech.*, **35**, 37 - 43 (2000).

He, J.H. and X.H. Hu, "Variational iteration method: New development and applications," *Computers and Mathematics with Applications*, **54**, 115 - 123 (2007).

Liao, S.J., *Beyond perturbation: Introduction to homotopy analysis method.* CRC Press (2003).

Makukula, Z.G., P. Sibanda and S.S. Motsa, "On a new solution for the viscoelastic squeezing flow between two parallel plates," *Journal of Advanced Research in Applied Mathematics*, **2**, 31 - 38 (2010a).

Makukula, Z.G., P. Sibanda and S.S. Motsa, "A note on the solution of the von Kármán equations using series and Chebyshev spectral methods," *Mathematical Problems in Engineering*, doi:10.1155/2010/528956 (2010b).

Makukula, Z.G., P. Sibanda, S.S. Motsa, "A novel numerical technique for two-dimensional laminar flow between two moving porous walls," *Mathematical Problems in Engineering*, doi:10.1155/2010/528956 (2010c).

Makukula, Z.G., P. Sibanda, S.S. Motsa, "A note on the solution of the von Krmn equations using series and Chebyshev spectral methods," *Boundary Value Problems*, doi:10.1155/2010/471793 (2010d).

Makukula, Z.G., P. Sibanda, S.S. Motsa, "On new solutions for heat transfer in a visco-elastic fluid between parallel plates," *International Journal of Mathematical Models and Methods in Applied Sciences*, **4**, 221 - 230 (2010e).

Motsa, S.S. and S. Shateyi, "A new approach for the solution of three-dimensional magneto-hydrodynamic rotating flow over a shrinking sheet," *Mathematical Problems in Engineering*, doi:10.1155/2010/586340 (2010).

Motsa, S.S., P. Sibanda and S. Shateyi, "A new spectral-homotopy analysis method for solving a nonlinear second order BVP," *Commun. Nonlinear Sci. Numer. Simul.*, **15**, 2293 - 2302 (2010).

Shateyi, S. and S.S. Motsa, "Variable viscosity on magnetohydrodynamic fluid flow and heat transfer over an unsteady stretching surface with Hall effect," *Boundary Value Problems*, doi:10.1155/2010/257568 (2010).

Schlichting, H., *Boundary layer theory*, McGraw Hill, NY (1979).

Shevchuk, I.V. and M.H. Buschmann, "Rotating disk heat transfer in a fluid swirling as a forced vortex," *Heat Mass Transfer*, **41**, 1112 - 1121 (2005).

Sibanda, P. and O.D. Makinde, "On MHD flow and heat transfer past a rotating disk in a porous medium with ohmic heating and viscous dissipation," *International Journal of Numerical Methods for Heat & Fluid Flow*, **20**, 269 - 285 (2010).

Takhar, H.S., A.K. Sing and G. Nath, "Unsteady MHD flow and heat transfer on a rotating disk in an ambient fluid," *Int. J. Therm. Sci.*, **41**, 147 - 155 (2002).

Trefethen, L.N., *Spectral Methods in MATLAB*, SIAM (2000).

Turkyilmazoglu, M., "Unsteady mhd flow with variable viscosity: Applications of spectral scheme," *Int. J. Therm. Sci.*, **49**, 563 - 570 (2010).

von Kármán, T., "Uberlaminare und turbulence reibung," *ZAMM*, **1**, 233 - 252 (1921).

4.4. Summary

In Section 4.1, the spectral homotopy analysis method together with the improved spectral homotopy analysis methods were used to find solutions of a Reiner-Rivlin swirling flow problem. The ISHAM was shown to be an improvement of the SHAM as it generated converging results at lower orders of approximation than the SHAM. Comparison with existing results in the literature showed a good agreement. The von Kàrmàn equations were solved in Section 4.2 using the SLM and the SHAM. Compared with results obtained using the HAM and HAM Padè techniques, the SHAM proved to give better convergence rates than the two methods. The SLM also showed to be efficient in generating fast converging solutions. In Section 4.3, the SLM was used to solve the von Kàrmàn problem with heat transfer.

5

Fluid flow through porous medium

Darcy (1937) pioneered the mathematical study of fluid flows through porous media. For steady state flow he assumed that the viscous forces are in equilibrium with external forces due to the pressure difference and the body forces (Sharma et al., 2007). Modifications of Darcy's law have since been documented in the literature for example, by Brinkman (1947). Porous media occur naturally while some are man-made and occur in various systems in industry. Flows with heat transfer through porous media have received attention because of their wide applications in different fields of science and engineering. Such fields include biomedical, civil, chemical and mechanical engineering (Vafai, 2005; Sharma et al., 2007; Nield and Bejan, 2006).

In this Chapter we investigated two fluid flow problems in porous media. The steady two-dimensional flow of a viscous incompressible fluid in a rectangular domain bounded by two permeable surfaces was investigated using the spectral-homotopy analysis and the successive linearisation methods in Section 5.1. The results were compared with those in the literature obtained using the homotopy analysis method and the homotopy perturbation method. Both the spectral-homotopy analysis method and the successive linearisation method proved to be computationally efficient and accurate compared to the other methods.

The SHAM, ISHAM and SLM were used to solve the problem of MHD viscous flow due to a shrinking sheet with a chemical reaction in Section 5.2. A comparison was made of the convergence rates, ease of use, and expensiveness of the three techniques. The results were validated using the bvp4c algorithm and with results in the literature. The ISHAM converged at second order for all simulations and the size of the parameter values used did not affect its performance. However, the ISHAM is expensive in terms of the size of the code and computer time. It took about three times as long as the SLM to compute the same result and about double the time taken using the SHAM. The SLM is easy to implement and converged at third order with good stability levels. The SHAM gave good convergence under the same conditions but convergence rates were retarded for highly nonlinear problems. It is easier to implement compared to the ISHAM but not as easy as the SLM. The results obtained were in excellent agreement with results from the bvp4c. In this study it was indicated that the ISHAM performs better than the SHAM and SLM in terms of the accuracy of the results and speed of convergence. A parametric study of the effects of different parameters was done and results were found to be in good agreement with those in the literature.

5.1. A novel numerical technique for two-dimensional laminar flow between two moving porous walls [1]

Corrigendum

Please note the addition of the geometry of the flow below;

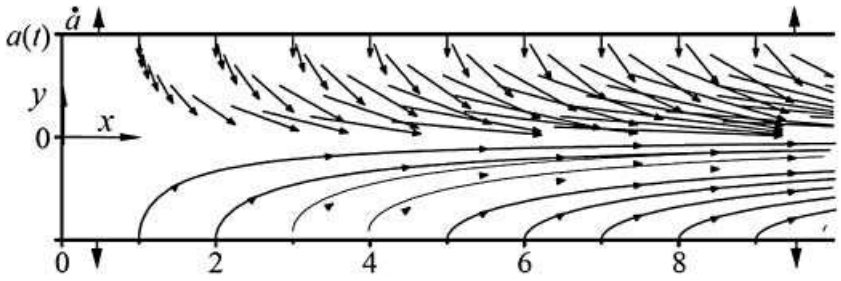

Figure 5.1: *Two-dimensional domain with expanding or contracting porous walls.*

Further explanations

(i) On page 4 the initial solution $F_0(y)$ in equation (3.1) was chosen to satisfy the boundary conditions, (2.7) and (2.8) of the problem.

(ii) The bvp4c was used to generate the numerical results in Tables $1-4$ on pages $10-11$.

(iii) The SHAM results on Table 5, page 12 were generated using $N = 60$.

(iv) All SHAM results were generated using the default value $\hbar = -1$, $\hbar$-curves were not used in this work.

[1] Z. G. Makukula, S. S. Motsa and P. Sibanda (2010). *Mathematical Problems in Engineering* Volume 2010, Article ID 528956, 15 pages doi:10.1155/2010/528956 (Impact factor; 0.689).

Hindawi Publishing Corporation
Mathematical Problems in Engineering
Volume 2010, Article ID 528956, 15 pages
doi:10.1155/2010/528956

Research Article

A Novel Numerical Technique for Two-Dimensional Laminar Flow between Two Moving Porous Walls

Zodwa G. Makukula,[1] Precious Sibanda,[1] and Sandile S. Motsa[2]

[1] *School of Mathematical Sciences, University of KwaZulu-Natal, Private Bag X01, Scottsville, Pietermaritzburg 3209, South Africa*
[2] *Department of Mathematics, University of Swaziland, Private Bag 4, M201 Kwaluseni, Swaziland*

Correspondence should be addressed to Precious Sibanda, sibandap@ukzn.ac.za

Received 16 February 2010; Revised 6 July 2010; Accepted 5 August 2010

Academic Editor: K. Vajravelu

We investigate the steady two-dimensional flow of a viscous incompressible fluid in a rectangular domain that is bounded by two permeable surfaces. The governing fourth-order nonlinear differential equation is solved by applying the spectral-homotopy analysis method and a novel successive linearisation method. Semianalytical results are obtained and the convergence rate of the solution series was compared with numerical approximations and with earlier results where the homotopy analysis and homotopy perturbation methods were used. We show that both the spectral-homotopy analysis method and successive linearisation method are computationally efficient and accurate in finding solutions of nonlinear boundary value problems.

1. Introduction

Laminar viscous flow in tubes that allow seepage across contracting or expanding permeable walls is encountered in the transport of biological fluids such as blood and filtration in kidneys and lungs. Such flows have many other practical applications such as in binary gas diffusion, chromatography, ion exchange, and ground water movement [1–6]. In addition, flow in channels with permeable walls provides a good starting point for the study of flow in multichannel filtration systems such as the wall flow monolith filter used to reduce emissions from diesel engines introduced by Oxarango et al. in [7]. Consequently, in the past four decades a considerable amount of research effort has been expended in the study of laminar flows in rectangular domains that are bounded by permeable walls [8–15].

The equations governing such flows are generally nonlinear and in the past asymptotic techniques, and numerical methods have been used to analyze such flows and to solve the equations; for example, in the pioneering study by Berman [8] asymptotic methods were used

to solve the steady flow problem for small suction. In the study by Uchida and Aoki [16], numerical methods were used to solve the governing nonlinear equations and to explain the flow characteristics. Majdalani and Roh [4] and Majdalani [3] studied the oscillatory channel flow with wall injection, and the resulting governing equations were solved using asymptotic formulations (WKB and multiple-scale techniques). The multiple-scale solution was found to be advantageous over the others in that its leading-order term is simpler and more accurate than other formulations, and it displayed clearly the relationship between the physical parameters that control the final motion. It also provided means of quantifying important flow features such as corresponding vortical wave amplitude, rotational depth of penetration, and near wall velocity overshoot to mention a few. Jankowski and Majdalani [12] used the same approach and drew similar conclusions about the multiple-scale solution for oscillatory channel flow with arbitrary suction. An analytical solution by means of the Liouville-Green transformation was developed for laminar flow in a porous channel with large wall suction and a weakly oscillatory pressure by Jankowski and Majdalani [13]. The scope of the problem had many limitations, for example, the study did not consider variations in thermostatic properties and the oscillatory pressure amplitude was taken to be small in comparison with the stagnation pressure. Zhou and Majdalani [17] investigated the mean-flow for slab rocket motors with regressing walls. The transformed governing equation was solved numerically, using finite differences, and asymptotically, using variation of parameters and small parameter perturbations in the blowing Reynolds number. The results from the two methods were compared for different Reynolds numbers Re and the wall regression rate α, and it was observed that accuracy of the analytical solution deteriorates for small Re and large α. A good agreement between the solutions was observed for large values of Re. A similar analysis was done by Majdalani and Zhou [6] for moderate-to-large injection and suction driven channel flows with expanding or contracting walls.

In recent years, the use of nonperturbation techniques such as the Adomian decomposition method [18, 19]. He's homotopy perturbation method [20, 21], and the homotopy analysis method [22, 23] has been increasingly preferred to solve nonlinear differential equations that arise in science and engineering. Dinarvand et al. [2] solved Berman's model of two-dimensional viscous flow in porous channels with wall suction or injection using both the HAM and the homotopy perturbation method (HPM). They concluded that the HPM solution is not valid for large Reynolds numbers, a weakness earlier observed in the case of other perturbation techniques. Using the homotopy analysis method, Xu et al. [24] developed highly accurate series approximations for two-dimensional viscous flow between two moving porous walls and obtained multiple solutions associated with this problem. The multiple solutions associated with this problem were also reported by Zarturska et al. [25]. Although the homotopy analysis method is a reliable and efficient semi-analytical technique, it however suffers from a number of limiting assumptions such as the requirements that the solution ought to conform to the so-called rule of solution expression and the rule of coefficient ergodicity. A modification of the homotopy analysis method, see Motsa et al. [26, 27], seeks to produce a more efficient method while also addressing the limitations of the HAM. In this paper, we use the spectral homotopy analysis method to solve the nonlinear differential equation that governs the flow of a viscous incompressible fluid in a rectangular domain bounded by two permeable walls. The problem is also solved using a new and highly efficient technique, the successive linearisation method (see [28, 29]) so as to independently corroborate and validate the SHAM results. The results are also compared with numerical approximations and the recent results reported in Xu et al. [24] and Dinarvand and Rashidi [30].

2. Governing Equations

Consider two-dimensional laminar, isothermal, and incompressible viscous fluid flow in a rectangular domain bounded by two permeable surfaces that enable the fluid to enter or exit during successive expansions or contractions. The walls are placed at a separation $2a$ and contract or expand uniformly at a time-dependent rate $\dot{a}(t)$. The governing Navier-Stokes equations are given in Majdalani et al. [31] as

$$\frac{\partial \hat{u}}{\partial \hat{x}} + \frac{\partial \hat{v}}{\partial \hat{y}} = 0, \tag{2.1}$$

$$\frac{\partial \hat{u}}{\partial t} + \hat{u}\frac{\partial \hat{u}}{\partial \hat{x}} + \hat{v}\frac{\partial \hat{u}}{\partial \hat{y}} = -\frac{1}{\rho}\frac{\partial \hat{p}}{\partial \hat{x}} + \nu\nabla^2\hat{u}, \tag{2.2}$$

$$\frac{\partial \hat{v}}{\partial t} + \hat{u}\frac{\partial \hat{v}}{\partial \hat{x}} + \hat{v}\frac{\partial \hat{v}}{\partial \hat{y}} = -\frac{1}{\rho}\frac{\partial \hat{p}}{\partial \hat{y}} + \nu\nabla^2\hat{v}, \tag{2.3}$$

where $\hat{u}$ and $\hat{v}$ are the velocity components in the $\hat{x}$ and $\hat{y}$ directions, respectively, $\hat{p}$, ρ, ν and t are the dimensional pressure, density, kinematic viscosity, and time, respectively. Assuming that inflow or outflow velocity is v_w, then the boundary conditions are

$$\begin{aligned} &\hat{u}(\hat{x}, a) = 0, \qquad \hat{v}(a) = -v_w = -\dot{a}/c, \\ &\frac{\partial \hat{u}}{\partial \hat{y}}(\hat{x}, 0) = 0, \qquad \hat{v}(0) = 0, \qquad \hat{u}(0, \hat{y}) = 0, \end{aligned} \tag{2.4}$$

where $c(= \dot{a}/v_w)$ is the injection or suction coefficient. Introducing the stream function $\hat{\varphi} = \nu\hat{x}\hat{F}(y,t)/a$ and the transformations

$$\varphi = \frac{\hat{\varphi}}{a\dot{a}}, \qquad u = \frac{\hat{u}}{\dot{a}}, \qquad v = \frac{\hat{v}}{\dot{a}}, \qquad x = \frac{\hat{x}}{a}, \qquad y = \frac{\hat{y}}{a}, \qquad F = \frac{\hat{F}}{\mathrm{Re}}, \tag{2.5}$$

Majdalani et al. [31] and Dinarvand and Rashidi [30] showed that (2.1)–(2.3) reduce to the normalized nonlinear differential equation

$$F^{IV} + \alpha(yF''' + 3F'') + \mathrm{Re}(FF''' - F'F'') = 0, \tag{2.6}$$

subject to the boundary conditions

$$F = 0, \quad F'' = 0, \quad \text{at } y = 0, \tag{2.7}$$

$$F = 1, \quad F' = 0, \quad \text{at } y = 1, \tag{2.8}$$

where $\alpha(t) = \dot{a}a/\nu$ is the nondimensional wall dilation rate defined to be positive for expansion and negative for contraction, and $\mathrm{Re} = av_w/\nu$ is the filtration Reynolds number defined positive for injection and negative for suction through the walls. Equation (2.6) is strongly nonlinear and not easy to solve analytically, and most researchers have studied

the classic Berman formula [8]; that is, when $\alpha = 0$. In this paper, we seek to solve (2.6) subject to the boundary conditions (2.7) and (2.8) using a novel spectral modification of the homotopy analysis method and the successive linearisation method. By comparison with the numerical approximations and previously obtained results, we show that these new techniques are accurate and more efficient than the standard homotopy analysis method.

3. Spectral Homotopy Analysis Method Solution

In applying the spectral-homotopy analysis method, it is convenient to first transform the domain of the problem from $[0,1]$ to $[-1,1]$ and make the governing boundary conditions homogeneous by using the transformations

$$y = \frac{\xi + 1}{2}, \quad U(\xi) = F(y) - F_0(y), \quad F_0(y) = \frac{3}{2}y - \frac{1}{2}y^3. \tag{3.1}$$

Substituting (3.1) in the governing equation and boundary conditions (2.6)–(2.8) gives

$$16U^{1V} + 8a_1U''' + 4a_2U'' + 2a_3U' - 3\,\mathrm{Re}\,U + 8\,\mathrm{Re}(UU''' - U'U'') = \phi(y), \tag{3.2}$$

subject to

$$\begin{aligned} U = 0, \quad U'' = 0, \quad \xi = -1, \\ U = 0, \quad U' = 0, \quad \xi = 1, \end{aligned} \tag{3.3}$$

where the primes denote differentiation with respect to ξ and

$$\begin{aligned} a_1 = \alpha y + \mathrm{Re}\left(\frac{3}{2}y - \frac{1}{2}y^3\right), \qquad a_2 = 3\alpha - \frac{3}{2}\mathrm{Re}\left(1 - y^2\right), \\ a_3 = 3y\mathrm{Re}, \qquad \phi(y) = 12\alpha y + 3\,\mathrm{Re}\,y^3. \end{aligned} \tag{3.4}$$

The initial approximation is taken to be the solution of the nonhomogeneous linear part of the governing equations (3.2) given by

$$16U_0^{1V} + 8a_1U_0''' + 4a_2U_0'' + 2a_3U_0' - 3\,\mathrm{Re}\,U_0 = \phi(y), \tag{3.5}$$

subject to

$$\begin{aligned} U_0 = 0, \quad U_0'' = 0, \quad \xi = -1, \\ U_0 = 0, \quad U_0' = 0, \quad \xi = 1. \end{aligned} \tag{3.6}$$

We use the Chebyshev pseudospectral method to solve (3.5)–(3.6). The unknown function $U_0(\xi)$ is approximated as a truncated series of Chebyshev polynomials of the form

$$U_0(\xi) \approx \mathrm{U}_0^N(\xi_j) = \sum_{k=0}^{N} \widehat{U}_k T_k(\xi_j), \quad j = 0, 1, \ldots, N, \tag{3.7}$$

where T_k is the kth Chebyshev polynomial, $\widehat{U}_k$, are coefficients and $\xi_0, \xi_1, \ldots, \xi_N$ are Gauss-Lobatto collocation points (see [32]) defined by

$$\xi_j = \cos\frac{\pi j}{N}, \quad j = 0, 1, \ldots, N. \tag{3.8}$$

Derivatives of the functions $U_0(\xi)$ at the collocation points are represented as

$$\frac{d^r U_0}{d\xi^r} = \sum_{k=0}^{N} \mathfrak{D}_{kj}^r U_0(\xi_j), \tag{3.9}$$

where r is the order of differentiation and $\mathfrak{D}$ is the Chebyshev spectral differentiation matrix ([32, 33]). Substituting (3.7)–(3.9) in (3.5)–(3.6) yields

$$\mathbf{A}\mathbf{U}_0 = \mathbf{\Phi}, \tag{3.10}$$

subject to the boundary conditions

$$U_0(\xi_0) = 0, \qquad U_0(\xi_N) = 0, \tag{3.11}$$

$$\sum_{k=0}^{N} \mathfrak{D}_{Nk}^2 U_0(\xi_k) = 0, \qquad \sum_{k=0}^{N} \mathfrak{D}_{0k} U_0(\xi_k) = 0, \tag{3.12}$$

where

$$A = 16\mathfrak{D}^4 + 8\mathbf{a}_1\mathfrak{D}^3 + 4\mathbf{a}_2\mathfrak{D}^2 + 2\mathbf{a}_3\mathfrak{D} - 3\,\mathrm{Re}\,\mathbf{I},$$

$$\mathbf{U}_0 = [U_0(\xi_0), U_0(\xi_1), \ldots, U_0(\xi_N)]^T, \tag{3.13}$$

$$\mathbf{\Phi} = [\phi(y_0), \phi(y_1), \ldots, \phi(y_N)]^T,$$

$$\mathbf{a}_s = \mathrm{diag}([a_s(y_0), a_s(y_1), \ldots, a_s(y_{N-1}), a_s(y_N)]), \quad s = 1, 2, 3. \tag{3.14}$$

In the above definitions, the superscript T denotes transpose, diag is a diagonal matrix and $\mathbf{I}$ is an identity matrix of size $(N + 1) \times (N + 1)$.

To implement the boundary conditions (3.11), we delete the first and the last rows and columns of A and delete the first and last rows of $\mathbf{U}_0$ and $\mathbf{\Phi}$. The boundary conditions (3.12) are imposed on the resulting first and last rows of the modified matrix $\mathbf{A}$ and

setting the resulting first and last rows of the modified matrix $\mathbf{\Phi}$ to be zero. The values of $[U_0(\xi_1), U_0(\xi_2), \ldots, U_0(\xi_{N-1})]$ are then determined from

$$\mathbf{U}_0 = \mathbf{A}^{-1}\mathbf{\Phi}. \tag{3.15}$$

To find the SHAM solutions of (3.2) we begin by defining the following linear operator:

$$\mathcal{L}\left[\tilde{U}(\xi;q)\right] = 16\frac{\partial^4\tilde{U}}{\partial\xi^4} + 8a_1\frac{\partial^3\tilde{U}}{\partial\xi^3} + 4a_2\frac{\partial^2\tilde{U}}{\partial\xi^2} + 2a_3\frac{\partial\tilde{U}}{\partial\xi} - 3\,\mathrm{Re}\,\tilde{U}, \tag{3.16}$$

where $q \in [0,1]$ is the embedding parameter, and $\tilde{U}(\xi;q)$ is an unknown function.

The zeroth order deformation equation is given by

$$(1-q)\mathcal{L}\left[\tilde{U}(\xi;q) - U_0(\xi)\right] = q\hbar\left\{\mathcal{N}\left[\tilde{U}(\xi;q)\right] - \mathbf{\Phi}\right\}, \tag{3.17}$$

where $\hbar$ is the nonzero convergence controlling auxiliary parameter and $\mathcal{N}$ is a nonlinear operator given by

$$\mathcal{N}\left[\tilde{U}(\xi;q)\right] = 16\frac{\partial^4\tilde{U}}{\partial\xi^4} + 8a_1\frac{\partial^3\tilde{U}}{\partial\xi^3} + 4a_2\frac{\partial^2\tilde{U}}{\partial\xi^2} + 2a_3\frac{\partial\tilde{U}}{\partial\xi} - 3\,\mathrm{Re}\,\tilde{U} + 8\,\mathrm{Re}\left(U\frac{\partial^3\tilde{U}}{\partial\xi^3} - \frac{\partial\tilde{U}}{\partial\xi}\frac{\partial^2\tilde{U}}{\partial\xi^2}\right). \tag{3.18}$$

Differentiating (3.17) m times with respect to q and then setting $q = 0$ and finally dividing the resulting equations by $m!$ yields the mth order deformation equations

$$\mathcal{L}[U_m(\xi) - \chi_m U_{m-1}(\xi)] = \hbar R_m, \tag{3.19}$$

subject to the boundary conditions

$$U_m(-1) = U_m(1) = U_m''(-1) = U_m'(1) = 0, \tag{3.20}$$

where

$$\begin{aligned} R_m(\xi) = {} & 16U_{m-1}^{IV} + 8a_1U_{m-1}''' + 4a_2U_{m-1}'' + 2a_3U_{m-1}' - 3\,\mathrm{Re}\,U_{m-1} \\ & + 8\,\mathrm{Re}\sum_{n=0}^{m-1}\left(U_nU_{m-1-n}''' - U_n'U_{m-1-n}''\right) - \phi(y)(1-\chi_m), \end{aligned} \tag{3.21}$$

$$\chi_m = \begin{cases} 0, & m \le 1 \\ 1, & m > 1. \end{cases} \tag{3.22}$$

Applying the Chebyshev pseudospectral transformation on (3.19)–(3.21) gives

$$\mathbf{A}\mathbf{U}_m = (\chi_m + \hbar)\mathbf{A}\mathbf{U}_{m-1} - \hbar(1-\chi_m)\mathbf{\Phi} + \hbar P_{m-1} \tag{3.23}$$

subject to the boundary conditions

$$U_m(\xi_0) = 0, \qquad U_m(\xi_N) = 0, \tag{3.24}$$

$$\sum_{k=0}^{N} \mathfrak{D}_{Nk}^2 U_m(\xi_k) = 0, \qquad \sum_{k=0}^{N} \mathfrak{D}_{0k} U_m(\xi_k) = 0, \tag{3.25}$$

where A and $\mathbf{\Phi}$, are as defined in (3.13) and

$$\begin{aligned} \mathbf{U}_m &= [U_m(\xi_0), U_m(\xi_1), \ldots, U_m(\xi_N)]^T, \\ P_{m-1} &= 8\,\mathrm{Re} \sum_{n=0}^{m-1} \left[U_n \left(\mathfrak{D}^3 U_{m-1-n} \right) - (\mathfrak{D} U_n) \left(\mathfrak{D}^2 U_{m-1-n} \right) \right]. \end{aligned} \tag{3.26}$$

To implement the boundary conditions (3.24) we delete the first and last rows of P_{m-1} and $\mathbf{\Phi}$ and delete the first and last rows and first and last columns of $\mathbf{A}$ in (3.23). The boundary conditions (3.25) are imposed on the first and last row of the modified $\mathbf{A}$ matrix on the left side of the equal sign in (3.23). The first and last rows of the modified $\mathbf{A}$ matrix on the right of the equal sign in (3.23) are the set to be zero. This results in the following recursive formula for $m \geq 1$:

$$\mathbf{U}_m = (\chi_m + \hbar)\mathbf{A}^{-1}\tilde{\mathbf{A}}\mathbf{U}_{m-1} + \hbar\mathbf{A}^{-1}\left[\mathbf{P}_{m-1} - (1 - \chi_m)\mathbf{\Phi}\right]. \tag{3.27}$$

Thus, starting from the initial approximation, which is obtained from (3.15), higher-order approximations $U_m(\xi)$ for $m \geq 1$ can be obtained through the recursive formula (3.27).

4. Successive Linearisation Method

In this section, we solve (2.6) using the successive linearisation method. The main assumptions underpinning the use of the successive linearisation method are the following.

(i) The unknown function $F(y)$ maybe expanded as

$$F(y) = F_i(y) + \sum_{m=0}^{i-1} F_m(y), \quad i = 1, 2, 3, \ldots, \tag{4.1}$$

where F_i are unknown functions and F_m $(m \geq 1)$ are approximations which are obtained by recursively solving the linear part of the equation that results from substituting (4.1) in the governing equation (2.6).

(ii) F_i becomes progressively smaller as i becomes large, that is,

$$\lim_{i \to \infty} F_i = 0. \tag{4.2}$$

Substituting (4.1) in the governing equation gives

$$F_i^{(iv)} + a_{1,i-1}F_i''' + a_{2,i-1}F_i'' + a_{3,i-1}F_i' + a_{4,i-1}F_i + \mathrm{Re}(F_iF_i''' - F_i'F_i'') = r_{i-1}, \tag{4.3}$$

where the coefficient parameters $a_{k,i-1}$, $(k = 1,2,3,4)$, and r_{i-1} are defined as

$$\begin{aligned} a_{1,i-1} &= \mathrm{Re}\sum_{m=0}^{i-1} F_m + \alpha y, \qquad a_{2,i-1} = -\mathrm{Re}\sum_{m=0}^{i-1} F_m' + 3\alpha, \\ a_{3,i-1} &= -\mathrm{Re}\sum_{m=0}^{i-1} F_m'', \qquad a_{4,i-1} = \mathrm{Re}\sum_{m=0}^{i-1} F_m''', \\ r_{i-1} &= -\left(\sum_{m=0}^{i-1} F_m^{(iv)} + \alpha y\sum_{m=0}^{i-1} F_m''' + 3\alpha\sum_{m=0}^{i-1} F_m''\right) - \mathrm{Re}\left(\sum_{m=0}^{i-1} F_m\sum_{m=0}^{i-1} F_m''' - \sum_{m=0}^{i-1} F_m'\sum_{m=0}^{i-1} F_m''\right). \end{aligned} \tag{4.4}$$

The SLM algorithm starts from the initial approximation

$$F_0(y) = \frac{1}{2}(3+\beta)y - \frac{1}{2}(1+3\beta)y^3 + \beta y^4, \tag{4.5}$$

which is chosen to satisfy the boundary conditions (2.7)–(2.8). The parameter β in (4.5) is an arbitrary constant which when varied results in multiple solutions. The subsequent solutions for F_m, $m \geq 1$ are obtained by successively solving the linearized form of (4.3) and which is given as

$$F_i^{(iv)} + a_{1,i-1}F_i''' + a_{2,i-1}F_i'' + a_{3,i-1}F_i' + a_{4,i-1}F_i = r_{i-1}, \tag{4.6}$$

subject to the boundary conditions

$$F_i(0) = 0, \quad F_i''(0) = 0, \quad F_i(1) = 1, \quad F_i'(1) = 0. \tag{4.7}$$

Once each solution for F_i, $(i \geq 1)$ has been found from iteratively solving (4.6) for each i, the approximate solution for $F(y)$ is obtained as

$$F(y) \approx \sum_{m=0}^{M} F_m(y), \tag{4.8}$$

where M is the order of SLM approximation. Since the coefficient parameters and the right hand side of (4.6), for $i = 1,2,3,\ldots$, are known from previous iterations, (4.6) can easily be solved using analytical means or any numerical methods such as finite differences, finite elements, Runge-Kutta-based shooting methods, or collocation methods. In this paper, (4.6) is integrated using the Chebyshev spectral collocation method [32, 33] as described in the previous section.

Applying the Chebyshev spectral method to (4.6) leads to the matrix equation

$$\mathbf{A}_{i-1}\mathbf{F}_i = \mathbf{R}_{i-1}, \tag{4.9}$$

in which $\mathbf{A}$ is an $(N+1)\times(N+1)$ square matrix and $\mathbf{Y}$ and $\mathbf{R}$ are $(N+1)\times 1$ column vectors defined by

$$\begin{aligned} \mathbf{A} &= \mathbf{D}^4 + \mathbf{a}_{1,i-1}\mathbf{D}^3 + \mathbf{a}_{2,i-1}\mathbf{D}^2 + \mathbf{a}_{3,i-1}\mathbf{D} + \mathbf{a}_{4,i-1}, \\ \mathbf{R}_{i-1} &= \mathbf{r}_{i-1}, \end{aligned} \tag{4.10}$$

with

$$\begin{aligned} \mathbf{F}_i &= [F_i(x_0), F_i(x_1), \ldots, F_i(x_{N-1}), F_i(x_N)]^T, \\ \mathbf{r}_{i-1} &= [r_{i-1}(x_0), r_{i-1}(x_1), \ldots, r_{i-1}(x_{N-1}), r_{i-1}(x_N)]^T. \end{aligned} \tag{4.11}$$

In the above definitions, N is the number of collocation points, $x = 2y-1$, $\mathbf{a}_{k,i-1}$, $(k = 1,2,3,4)$ are diagonal matrices of size $(N+1)\times(N+1)$, and $\mathbf{D} = 2\mathfrak{D}$. After modifying the matrix system (4.9) to incorporate boundary conditions, the solution is obtained as

$$\tilde{\mathbf{Y}}_i = \mathbf{A}_{i-1}^{-1}\mathbf{R}_{i-1}. \tag{4.12}$$

5. Results and Discussion

In this section, we compare the results obtained using the various methods: the SHAM, the SLM, and the numerical approximations with those obtained using the HAM in Dinarvand and Rashidi [30] and the homotopy-Páde method in Xu et al. [24]. The solution obtained using most numerical solutions depends on the initial approximation. Using different initial guesses can give rise to multiple solutions. Multiple solutions were obtained if the initial guess in (4.5) is used in the SHAM method in place of $F_0(y)$ in (3.1). In this paper, it was observed that using different values of β results in multiple solutions. For the multiple solutions comparison was made against the HAM results of [24].

An optimal $\hbar$ value can easily be sought that can considerably improve the convergence rate of the results. However, for comparison purposes we used $\hbar = -1$. It is however worth noting, as pointed out in Dinarvand et al. [2], that when $\hbar = -1$, the solution series obtained by the HAM is the same solution series obtained by means of the homotopy perturbation method.

In Table 1 we compare the values of $F(y)$ when $\alpha = -1$ and Re $= -2, 0$ and 2 with the numerical and the HAM results reported in Dinarvand and Rashidi [30]. In [30], convergence up to six decimal places was achieved at the sixth order of the HAM approximation for Re $= 0$ and 2. In this study, the same level of convergence and accuracy was achieved at the first order approximation for the same values of Re. For Re $= -2$ the convergence of the homotopy analysis method series solution was achieved at the eighth order of approximation while with the spectral homotopy analysis method series solution gives the same level of convergence at the second order.

Table 1: Comparison of the numerical results against the SHAM approximate solutions for $F(y)$ when $\alpha = -1$ with $N = 60$ and $\hbar = -1$.

Re	y	0th order	1st order	2nd order	3rd order	Numerical	Ref. [30]
−2	0.2	0.273828	0.273831	0.273832	0.273832	0.273832	0.273832
	0.4	0.532827	0.532839	0.532839	0.532839	0.532839	0.532839
	0.6	0.759442	0.759467	0.759468	0.759468	0.759468	0.759468
	0.8	0.928967	0.928990	0.928990	0.928990	0.928990	0.928990
0	0.2	0.279449	0.279449	0.279449	0.279449	0.279449	0.279449
	0.4	0.542243	0.542243	0.542243	0.542243	0.542243	0.542243
	0.6	0.768950	0.768950	0.768950	0.768950	0.768950	0.768950
	0.8	0.933889	0.933889	0.933889	0.933889	0.933889	0.933889
2	0.2	0.283996	0.283983	0.283983	0.283983	0.283983	0.283983
	0.4	0.549759	0.549738	0.549738	0.549738	0.549738	0.549738
	0.6	0.776328	0.776306	0.776306	0.776306	0.776306	0.776306
	0.8	0.937518	0.937507	0.937507	0.937507	0.937507	0.937507

Table 2: Comparison of the numerical results against the SHAM approximate solutions for $F''(1)$ when $\alpha = -1$ with $N = 60$ and $\hbar = -1$ for different values of Re.

Re	0th order	1st order	2nd order	3rd order	4th order	Numerical
0	−3.8213722	−3.8213723	−3.8213723	−3.8213723	−3.8213723	−3.8213723
5	−3.1725373	−3.1731774	−3.1731800	−3.1731800	−3.1731800	−3.1731800
10	−2.9069253	−2.9069653	−2.9069654	−2.9069654	−2.9069654	−2.9069654
15	−2.7783086	−2.7784366	−2.7784369	−2.7784369	−2.7784369	−2.7784369
20	−2.7056150	−2.7060556	−2.7060557	−2.7060557	−2.7060557	−2.7060557
25	−2.6596223	−2.6603920	−2.6603907	−2.6603907	−2.6603907	−2.6603907
30	−2.6281102	−2.6291718	−2.6291682	−2.6291682	−2.6291682	−2.6291682
40	−2.5879160	−2.5894333	−2.5894247	−2.5894247	−2.5894247	−2.5894247
50	−2.5634446	−2.5652868	−2.5652732	−2.5652733	−2.5652733	−2.5652733
100	−2.5139141	−2.5165255	−2.5164964	−2.5164967	−2.5164967	−2.5164967
150	−2.4972813	−2.5001845	−2.5001479	−2.5001484	−2.5001484	−2.5001484

In Table 2, we demonstrate the computational efficiency of the SHAM solution for large values of Re. As has been noted in the introduction, some semi-analytical methods fail to converge at large values of Re, for example, Dinarvand et al. [2] have shown that for $|\mathrm{Re}| > 9.5$ the HPM fails to converge. However, in using the SHAM convergence up seven decimal places is achieved at the third order of approximation for values of Re as large as $\mathrm{Re} = 150$. For $5 \leq \mathrm{Re} < 100$ convergence up six decimal places is achieved at the second order. In Table 3, $\mathrm{Re} = 2$ is fixed and $F''(1)$ evaluated for $-2.5 \leq \alpha \leq 2.5$. Convergence up to seven digits is achieved at the first order for $\alpha = 0$, at the second order for $-2 \leq \alpha \leq -0.5$, and at the third-order approximation for $\alpha = -2.5$. Clearly the SHAM gives faster convergence than the HAM under the same conditions.

Table 3 also gives a comparison of the SHAM approximate results with the numerical results generated using different values of N. It is evident however that for small values of N (say less than $N = 20$) the SHAM results are not very accurate. Accuracy however improves with an increase in N.

Table 4 gives a comparison of the numerical and the SHAM results of $F''(1)$ when $-2.5 \leq \alpha \leq 2.5$. Convergence is generally achieved at either the third- or the fourth-order

Table 3: Comparison of the numerical results against the SHAM approximate solutions for $F''(1)$ when $\alpha = -1$ with Re = 10 and $\hbar = -1$ for different values of N.

N	0th order	1st order	2nd order	3rd order	4th order	Numerical
10	−2.7059921	−2.7064302	−2.7064302	−2.7064302	−2.7064302	−2.7060557
15	−2.7056141	−2.7060549	−2.7060550	−2.7060549	−2.7060549	−2.7060557
20	−2.7056150	−2.7060556	−2.7060557	−2.7060557	−2.7060557	−2.7060557
30	−2.7056150	−2.7060556	−2.7060557	−2.7060557	−2.7060557	−2.7060557
40	−2.7056150	−2.7060556	−2.7060557	−2.7060557	−2.7060557	−2.7060557
60	−2.7056150	−2.7060556	−2.7060557	−2.7060557	−2.7060557	−2.7060557

Table 4: Comparison of the numerical results against the SHAM approximate solutions for $F''(1)$ when Re = 2 with $N = 60$ and $\hbar = -1$ for different values of α.

α	1st order	2nd order	3rd order	4th order	Numerical
−2.5	−4.5258487	−4.5258506	−4.5258505	−4.5258505	−4.5258505
−2.0	−4.1673848	−4.1673892	−4.1673892	−4.1673892	−4.1673892
−1.5	−3.8209704	−3.8209740	−3.8209740	−3.8209740	−3.8209740
−1.0	−3.4873966	−3.4873982	−3.4873982	−3.4873982	−3.4873982
−0.5	−3.1674332	−3.1674334	−3.1674334	−3.1674334	−3.1674334
0.0	−2.8618116	−2.8618116	−2.8618116	−2.8618116	−2.8618116
0.5	−2.5712067	−2.5712055	−2.5712055	−2.5712055	−2.5712056
1.0	−2.2962176	−2.2962075	−2.2962076	−2.2962076	−2.2962076
1.5	−2.0373492	−2.0373088	−2.0373092	−2.0373092	−2.0373092
2.0	−1.7949940	−1.7948795	−1.7948810	−1.7948810	−1.7948810
2.5	−1.5694172	−1.5691503	−1.5691557	−1.5691556	−1.5691556

of the SHAM approximation. Figures 1 and 2 give a comparison of the numerical and the SHAM solutions for the characteristic mean-flow function $F(y) = -v/c$ and $F'(y) = \mu c/x$ at different Reynolds numbers and α. The mean-flow function $F(y)$, increases with increasing (positive) values of Re and α while $F'(y)$ decreases, which makes sense since $F(y)$ is inversely proportional to the injection or suction coefficient $c = \alpha/\text{Re}$ while $F'(y)$ is directly proportional. Figure 1 further illustrates the efficiency of the solution method with excellent agreement for Re as large as 200.

Using the initial approximation $F_0(y)$ in (4.5) with different values of β in place of (3.1) in the SHAM implementation leads to multiple solutions. When $\beta = 0$ and -5, the SHAM gives the multiple solutions observed in Xu et al. [24]. A comparison of the SHAM results against the HAM results reported in [24] is presented in Table 5. It is evident that the SHAM results converge much more rapidly than the HAM results of [24] for both branches of the solution.

Tables 6 and 7 give, first, the analytical approximations of $F'(0)/\text{Re}$ and $F'''(0)/\text{Re}$ for the two solutions obtained using the successive linearisation method. Secondly, the tables give a direct comparison of the convergence rates of the SLM and the $[m, m]$ homotopy-Padé method used by Xu et al. [24]. The fourth-order SLM approximation gives the same level of accuracy as the twenty-fourth-order of the $[m, m]$ homotopy-Páde approximation, which suggests that the successive linearisation method is much more computationally efficient and accurate compared to the $[m, m]$ homotopy-Páde approximation (although it is not clear at this stage whether this could be attributed to the use of a more efficient initial guess).

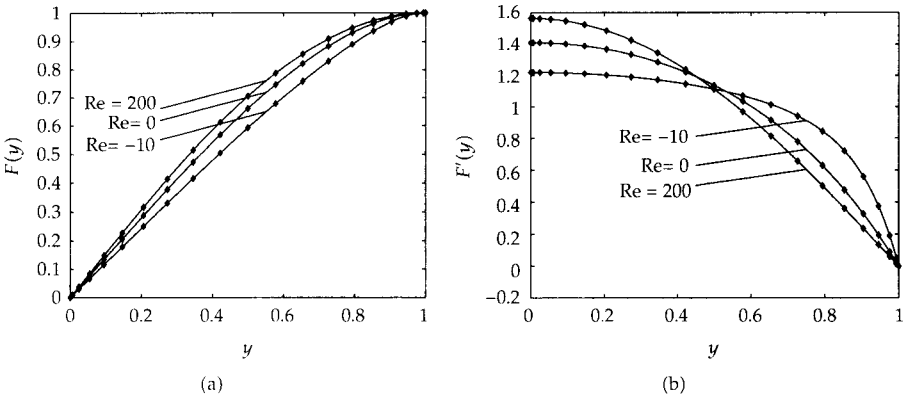

Figure 1: Comparison between numerical and SHAM approximate solution of $F(y)$ and $F'(y)$ for different values of Re when $\alpha = -1$ when $\hbar = -1.14$ (for Re $= -10$) and $\hbar = -1$ (for Re $= 0, 200$).

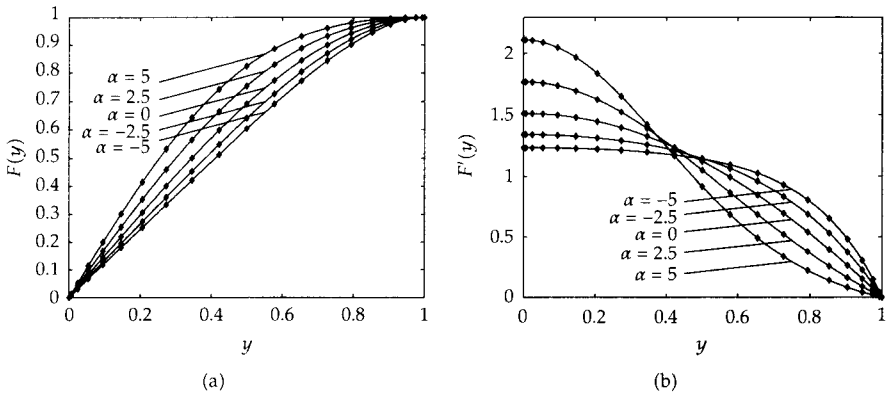

Figure 2: Comparison between numerical and SHAM approximate solution of $F(y)$ and $F'(y)$ for different values of α when Re $= 2$ when $\hbar = -1$ (for $\alpha = -5, -2.5, 0, 2.5$) and $\hbar = -0.94$ (for $\alpha = 5$).

Table 5: Comparison between the multiple solutions of HAM results (see [24]) and the present SHAM results in the case of Re $= -10$ and $\alpha = 4$.

	HAM solution [24]			SHAM solution		
	Order of approx.	$F'(0)$	$F''''(0)$	Order of approx.	$F'(0)$	$F''''(0)$
First solution	10	0.624 161	8.267 56	5	0.625549	8.24662
	20	0.624 967	8.256 03	10	0.625016	8.25532
	30	0.625 005	8.255 48	15	0.625008	8.25544
	40	0.625 007	8.255 45	20	0.625007	8.25545
	50	0.625 007	8.255 45	25	0.625007	8.25545
Second solution	10	−1.189 95	35.8984	5	−1.190529	35.85647
	20	−1.190 03	35.8474	10	−1.190322	35.85414
	30	−1.190 41	35.8555	15	−1.190323	35.85416
	40	−1.190 31	35.8539	20	−1.190323	35.85416
	50	−1.190 33	35.8542	25	−1.190323	35.85416

Table 6: Comparison of $F'(0)/\mathrm{Re}$ and $F'''(0)/\mathrm{Re}$ obtained at different orders for the SLM, and the $[m, m]$ homotopy-Páde approximation when Re = −10 and $\alpha = 4$. For the SLM first solution, $\beta = -1$, and $N = 25$, and for the SLM second solution, $\beta = -5$, and $N = 25$.

	$[m, m]$ homotopy-Padé [24]			SLM		
	order	$F'(0)/\mathrm{Re}$	$F'''(0)/\mathrm{Re}$	order	$F'(0)$	$F'''(0)$
First solution	4	0.624478732	8.265444222	2	0.624485895	8.26283765
	8	0.625005336	8.255477422	3	0.625007516	8.25544430
	16	0.625007395	8.255446127	4	0.625007396	8.25544612
	20	0.625007396	8.255446125	6	0.625007396	8.25544612
	24	0.625007396	8.255446124	8	0.625007396	8.25544612
Second solution	4	−1.219891	36.01091	2	−1.190934	35.86042
	8	−1.178465	35.17878	3	−1.190323	35.85416
	16	−1.190319	35.85409	4	−1.190323	35.85416
	20	−1.190323	35.85415	6	−1.190323	35.85416
	24	−1.190323	35.85416	8	−1.190323	35.85416

Table 7: Comparison of $F'(0)/\mathrm{Re}$ and $F'''(0)/\mathrm{Re}$ obtained at different orders for the SLM, and the $[m, m]$ homotopy-Páde approximation when Re = −11 and $\alpha = 3/4$. For the SLM first solution, $\beta = -5$, and $N = 25$, $\beta = 1$, and $N = 25$ for the SLM second solution, and for the SLM third solution $\beta = 3$, and $N = 25$.

	$[m, m]$ homotopy-Páde [24]			SLM		
	order	$F'(0)/\mathrm{Re}$	$F'''(0)/\mathrm{Re}$	order	$F'(0)$	$F'''(0)$
First solution	4	−1.0231621	24.2925851	2	−1.3250168	27.8640486
	8	−1.0237700	24.2863797	3	−1.0765777	24.9095006
	16	−1.0237712	24.2863088	4	−1.0259527	24.3119987
	20	−1.0237712	24.2863088	6	−1.0237712	24.2863088
	24	−1.0237712	24.2863088	8	−1.0237712	24.2863088
Second solution	4	0.1668590	10.282860	2	0.2134950	9.682581
	8	0.1679980	10.239451	3	0.1718420	10.216566
	16	0.1693518	10.245026	4	0.1693573	10.245102
	20	0.1693532	10.245150	6	0.1693531	10.245151
	24	0.1693532	10.245151	8	0.1693531	10.245151
Third solution	4	...	...	2	2.76262	−15.5266
	8	2.81591	−15.8950	3	2.76111	−15.5123
	16	2.76154	−15.5157	4	2.76111	−15.5122
	20	2.76113	−15.5123	6	2.76111	−15.5122
	24	2.76111	−15.5123	8	2.76111	−15.5122

6. Conclusion

In this paper, we have used the spectral homotopy analysis method (SHAM) and the successive linearisation method (SLM) to solve a fourth-order nonlinear boundary value problem that governs the two-dimensional Laminar flow between two moving porous walls. Multiple solutions recently reported in Xu et al. [24] have been obtained, depending on the initial approximation used. Comparison of the computational efficiency and accuracy of the results between the current methods and the previous homotopy analysis method results described in Dinarvand and Rashidi [30] and Xu et al. [24] has been made. Our simulations show that the convergence of the SHAM solution series to the numerical solution (up to six

decimal place accuracy) is achieved at the second order (for Re = −2) and first order for $R = 0, 2$. In contrast to the standard homotopy analysis method (c.f. Dinarvand and Rashidi [30]) convergence was achieved at the eighth order (for Re = −2) and sixth order for Re = 0, 2. The SHAM is apparently more efficient because it offers more flexibility in choosing linear operators compared to the standard HAM. It is however important to note that if the same initial guess and linear operators were to be used, the two methods would give the same solution.

We have further shown that notwithstanding the acceleration of the convergence ratio of the homotopy series by means of the homotopy-Padé technique, the successive linearisation techniques is more computationally efficient (although this again could be due, in part, to the use of a different initial guess) and gives accurate results.

Acknowledgments

The authors wish to acknowledge financial support from the University of KwaZulu-Natal and the National Research Foundation (NRF). The authers also thank the anonymous reviewers whose helpful comments have contributed to the improvement of our work.

References

[1] E. C. Dauenhauer and J. Majdalani, "Exact self-similarity solution of the Navier-Stokes equations for a porous channel with orthogonally moving walls," *Physics of Fluids*, vol. 15, no. 6, pp. 1485–1495, 2003.

[2] S. Dinarvand, A. Doosthoseini, E. Doosthoseini, and M. M. Rashidi, "Comparison of HAM and HPM methods for Berman's model of two-dimensional viscous flow in porous channel with wall suction or injection," *Advances in Theoretical and Applied Mechanics*, vol. 1, no. 7, pp. 337–347, 2008.

[3] J. Majdalani, "The oscillatory channel flow with arbitrary wall injection," *Zeitschrift für Angewandte Mathematik und Physik*, vol. 52, no. 1, pp. 33–61, 2001.

[4] J. Majdalani and T.-S. Roh, "The oscillatory channel flow with large wall injection," *Proceedings of the Royal Society of London. Series A*, vol. 456, no. 1999, pp. 1625–1657, 2000.

[5] J. Majdalani and W. K. van Moorhem, "Multiple-scales solution to the acoustic boundary layer in solid rocket motors," *Journal of Propulsion and Power*, vol. 13, no. 2, pp. 186–193, 1997.

[6] J. Majdalani and C. Zhou, "Moderate-to-large injection and suction driven channel flows with expanding or contracting walls," *Zeitschrift für Angewandte Mathematik und Mechanik*, vol. 83, no. 3, pp. 181–196, 2003.

[7] L. Oxarango, P. Schmitz, and M. Quintard, "Laminar flow in channels with wall suction or injection: a new model to study multi-channel filtration systems," *Chemical Engineering Science*, vol. 59, no. 5, pp. 1039–1051, 2004.

[8] A. S. Berman, "Laminar flow in channels with porous walls," *Journal of Applied Physics*, vol. 24, pp. 1232–1235, 1953.

[9] J. F. Brady, "Flow development in a porous channel and tube," *Physics of Fluids*, vol. 27, no. 5, pp. 1061–1076, 1984.

[10] S. M. Cox, "Two-dimensional flow of a viscous fluid in a channel with porous walls," *Journal of Fluid Mechanics*, vol. 227, pp. 1–33, 1991.

[11] S. P. Hastings, C. Lu, and A. D. MacGillivray, "A boundary value problem with multiple solutions from the theory of laminar flow," *SIAM Journal on Mathematical Analysis*, vol. 23, no. 1, pp. 201–208, 1992.

[12] T. A. Jankowski and J. Majdalani, "Symmetric solutions for the oscillatory channel flow with arbitrary suction," *Journal of Sound and Vibration*, vol. 294, no. 4, pp. 880–893, 2006.

[13] T. A. Jankowski and J. Majdalani, "Laminar flow in a porous channel with large wall suction and a weakly oscillatory pressure," *Physics of Fluids*, vol. 14, no. 3, pp. 1101–1110, 2002.

[14] C. Lu, "On the asymptotic solution of laminar channel flow with large suction," *SIAM Journal on Mathematical Analysis*, vol. 28, no. 5, pp. 1113–1134, 1997.

[15] R. M. Terrill, "Laminar flow in a uniformly porous channel," *The Aeronautical Quarterly*, vol. 15, pp. 299–310, 1964.
[16] S. Uchida and H. Aoki, "Unsteady flows in a semi-infinite contracting or expanding pipe," *Journal of Fluid Mechanics*, vol. 82, no. 2, pp. 371–387, 1977.
[17] C. Zhou and J. Majdalani, "Improved mean-flow solution for slab rocket motors with regressing walls," *Journal of Propulsion and Power*, vol. 18, no. 3, pp. 703–711, 2002.
[18] G. Adomian, "Nonlinear stochastic differential equations," *Journal of Mathematical Analysis and Applications*, vol. 55, no. 2, pp. 441–452, 1976.
[19] G. Adomian, "A review of the decomposition method and some recent results for nonlinear equations," *Computers & Mathematics with Applications*, vol. 21, no. 5, pp. 101–127, 1991.
[20] J.-H. He, "A coupling method of a homotopy technique and a perturbation technique for non-linear problems," *International Journal of Non-Linear Mechanics*, vol. 35, no. 1, pp. 37–43, 2000.
[21] J.-H. He, "Homotopy perturbation method for solving boundary value problems," *Physics Letters A*, vol. 350, no. 1-2, pp. 87–88, 2006.
[22] S. J. Liao, *The proposed homotopy analysis technique for the solution of nonlinear problems*, Ph.D. thesis, Shanghai Jiao Tong University, 1992.
[23] S. Liao, *Beyond Perturbation: Introduction to Homotopy Analysis Method*, vol. 2 of *CRC Series: Modern Mechanics and Mathematics*, Chapman & Hall/CRC, Boca Raton, Fla, USA, 2004.
[24] H. Xu, Z. L. Lin, S. J. Liao, J. Z. Wu, and J. Majdalani, "Homotopy based solutions of the Navier–Stokes equations for a porous channel with orthogonally moving walls," *Physics of Fluids*, vol. 22, Article ID 053601, 18 pages, 2010.
[25] M. B. Zaturska, P. G. Drazin, and W. H. H. Banks, "On the flow of a viscous fluid driven along a channel by suction at porous walls," *Fluid Dynamics Research*, vol. 4, no. 3, pp. 151–178, 1988.
[26] S. S. Motsa, P. Sibanda, and S. Shateyi, "A new spectral-homotopy analysis method for solving a nonlinear second order BVP," *Communications in Nonlinear Science and Numerical Simulation*, vol. 15, no. 9, pp. 2293–2302, 2010.
[27] S. S. Motsa, P. Sibanda, F. G. Awad, and S. Shateyi, "A new spectral-homotopy analysis method for the MHD Jeffery-Hamel problem," *Computers and Fluids*, vol. 39, no. 7, pp. 1219–1225, 2010.
[28] Z. Makukula, S. S. Motsa, and P. Sibanda, "On a new solution for the viscoelastic squeezing flow between two parallel plates," *Journal of Advanced Research in Applied Mathematics*, vol. 2, no. 4, pp. 31–38, 2010.
[29] S. S. Motsa and P. Sibanda, "A new algorithm for solving singular IVPs of Lane-Emden type," in *Proceedings of the 4th International Conference on Applied Mathematics, Simulation, Modelling*, WSEAS International Conferences, pp. 176–180, Corfu Island, Greece, July 2010.
[30] S. Dinarvand and M. M. Rashidi, "A reliable treatment of a homotopy analysis method for two-dimensional viscous flow in a rectangular domain bounded by two moving porous walls," *Nonlinear Analysis: Real World Applications*, vol. 11, no. 3, pp. 1502–1512, 2010.
[31] J. Majdalani, C. Zhou, and C. A. Dawson, "Two-dimensional viscous flow between slowly expanding or contracting walls with weak permeability," *Journal of Biomechanics*, vol. 35, no. 10, pp. 1399–1403, 2002.
[32] C. Canuto, M. Y. Hussaini, A. Quarteroni, and T. A. Zang, *Spectral Methods in Fluid Dynamics*, Springer Series in Computational Physics, Springer, New York, NY, USA, 1988.
[33] L. N. Trefethen, *Spectral Methods in MATLAB*, vol. 10 of *Software, Environments, and Tools*, SIAM, Philadelphia, Pa, USA, 2000.

5.2. On new numerical techniques for the MHD flow past a shrinking sheet with heat and mass transfer in the presence of a chemical reaction [2]

Corrigenda

(i) Problem geometry

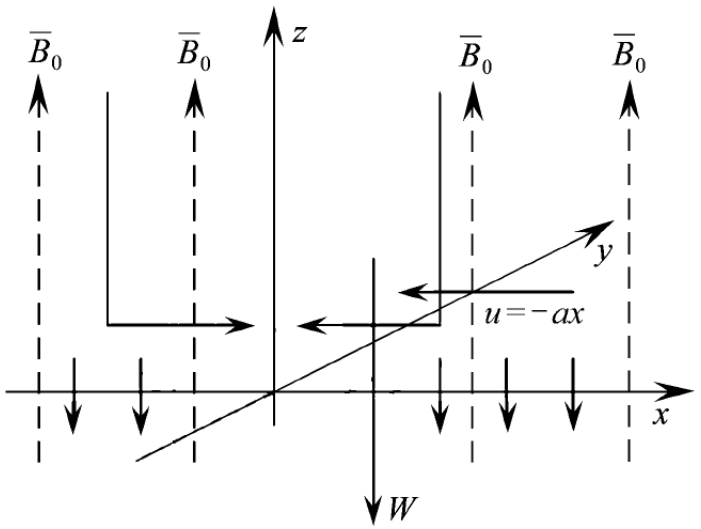

Figure 5.2: *Flow analysis on a shrinking surface*

(ii) In equation (2.3), the correct similarity transformation for η is

$$\eta = \sqrt{\frac{a}{\nu}}y$$

and the variable F should be replaced by f.

[2] Z. G. Makukula, P. Sibanda, S. S. Motsa and S. Shateyi (2011). *Mathematical Problems in Engineering* Volume 2011, Article ID 489217, 19 pages doi:10.1155/2011/489217 (Impact factor; 0.689).

Hindawi Publishing Corporation
Mathematical Problems in Engineering
Volume 2011, Article ID 489217, 19 pages
doi:10.1155/2011/489217

Research Article

On New Numerical Techniques for the MHD Flow Past a Shrinking Sheet with Heat and Mass Transfer in the Presence of a Chemical Reaction

Z. G. Makukula,[1] P. Sibanda,[1] S. S. Motsa,[1] and S. Shateyi[2]

[1] *School of Mathematical Sciences, University of KwaZulu-Natal, Private Bag X01, Scottsville, Pietermaritzburg 3209, South Africa*
[2] *Department of Mathematics and Applied Mathematics, University of Venda, Private Bag X5050, Thohoyandou 0950, South Africa*

Correspondence should be addressed to S. Shateyi, stanford.shateyi@univen.ac.za

Received 29 July 2011; Revised 22 August 2011; Accepted 23 August 2011

Academic Editor: Oleg V. Gendelman

We use recent innovative solution techniques to investigate the problem of MHD viscous flow due to a shrinking sheet with a chemical reaction. A comparison is made of the convergence rates, ease of use, and expensiveness (the number of iterations required to give convergent results) of three seminumerical techniques in solving systems of nonlinear boundary value problems. The results were validated using a multistep, multimethod approach comprising the use of the shooting method, the Matlab bvp4c numerical routine, and with results in the literature.

1. Introduction

Boundary layer flow over a stretching surface occurs in several engineering processes such as hot rolling, wire drawing, and glass-fibre production. Materials that are manufactured by extrusion processes and heat-treated substances proceeding between a feed roll and a wind-up roll can be classified as a continuously stretching surface [1–3]. A shrinking film is useful in the packaging of bulk products since it can be unwrapped easily with adequate heat [4–7]. Shrinking problems can also be applied to the study of capillary effects in small pores and the hydraulic properties of agricultural clay soils [8]. Studies of flow due to a shrinking sheet with heat transfer and/or mass transfer have been considered by, among others, [7, 9].

In recent years, several analytical or semianalytical methods have been proposed and used to find solutions to most nonlinear equations. These methods include the Adomian decomposition method (ADM) [10, 11], differential transform method (DTM) [12],

variational iteration method (VIM) [13], homotopy analysis method (HAM) [14–17], and Homotopy perturbation method (HPM) [18–23].

Motsa and Shateyi [24] obtained a numerical solution of magnetohydrodynamic (MHD) and rotating flow over a porous shrinking sheet by the new approach known as spectral homotopy analysis method (SHAM). Muhaimin et al. [5] studied magnetohydrodynamic viscous flow due to a shrinking sheet in the presence of suction. The study found out that the shrinking of the sheet has a substantial effect on the flow field and, thus, on the heat and mass transfer rate from the sheet to the fluid.

In this paper we provide a qualitative assessment of key features of three recent seminumerical techniques, namely, the successive linearisation method (SLM), the spectral-homotopy analysis method (SHAM), and the improved spectral-homotopy analysis method (ISHAM). The two methods were introduced and used by Motsa and his coworkers (see Motsa et al. [25, 26] and Makukula et al. [27–30]) to solve nonlinear boundary value problems. In Motsa et al. [25, 26, 29] the SHAM approach was tested on simple one-dimensional nonlinear boundary value problems. Later, Makukula et al. [28, 30, 31] extended the application of the SHAM to a system of two coupled nonlinear equations that model the von Kármán fluid flow problem. The SLM method was applied on one-dimensional nonlinear differential equations in Makukula et al. [27]. In this study we solve the nonlinear equations that govern the shrinking sheet problem for purposes of evaluating the efficiency of each method with regards to speed of convergence, ease of use, and expensiveness (in terms of the number of iterations required to give convergent results). We introduce the ISHAM as a method that is meant to improve the accuracy of the standard SHAM approach. The governing equations for the problem are a rather formidable system of three nonlinear differential equations in three unknowns. Parametric study of the effect of different parameters is made and the results compared with previous findings in the literature (see Noor et al. [6], Mohd and Hashim [7], and Muhaimin et al. [5]). The solutions are further compared with results obtained using the shooting method and the bvp4c solver, which is based on Runge-Kutta fourth-order schemes.

2. Mathematical Formulation

We investigate the effect of chemical reaction, heat and mass transfer on nonlinear MHD boundary layer past a porous shrinking sheet with suction. The governing boundary layer equations of momentum, energy, and mass diffusion in terms of the velocity components u, v, and w are (see Muhaimin et al. [5])

$$\frac{\partial u}{\partial x}+\frac{\partial v}{\partial y}+\frac{\partial w}{\partial z}=0,$$

$$u\frac{\partial u}{\partial x}+v\frac{\partial u}{\partial y}+w\frac{\partial u}{\partial z}=\frac{1}{\rho}\frac{\partial p}{\partial x}+\nu\left\{\frac{\partial^2 u}{\partial x^2}+\frac{\partial^2 u}{\partial y^2}+\frac{\partial^2 u}{\partial z^2}\right\}-u\frac{\sigma B_0^2}{\rho}-u\frac{\nu}{K},$$

$$u\frac{\partial v}{\partial x}+v\frac{\partial v}{\partial y}+w\frac{\partial v}{\partial z}=\frac{1}{\rho}\frac{\partial p}{\partial y}+\nu\left\{\frac{\partial^2 v}{\partial x^2}+\frac{\partial^2 v}{\partial y}+\frac{\partial^2 v}{\partial z^2}\right\}-v\frac{\sigma B_0^2}{\rho}-v\frac{\nu}{K},$$

$$u\frac{\partial w}{\partial x}+v\frac{\partial w}{\partial y}+w\frac{\partial w}{\partial z}=\frac{1}{\rho}\frac{\partial p}{\partial z}+\nu\left\{\frac{\partial^2 w}{\partial x^2}+\frac{\partial^2 w}{\partial y^2}+\frac{\partial^2 w}{\partial z^2}\right\},$$

$$u\frac{\partial T}{\partial x}+v\frac{\partial T}{\partial y}+w\frac{\partial T}{\partial z}=\alpha\left\{\frac{\partial^2 T}{\partial x^2}+\frac{\partial^2 T}{\partial y^2}+\frac{\partial^2 T}{\partial z^2}\right\},$$
$$u\frac{\partial C}{\partial x}+v\frac{\partial C}{\partial y}+w\frac{\partial C}{\partial z}=D\left\{\frac{\partial^2 C}{\partial x^2}+\frac{\partial^2 C}{\partial y^2}+\frac{\partial^2 C}{\partial z^2}\right\}-k_1 C, \tag{2.1}$$

where α is the thermal conductivity of the fluid, B_0 is the magnetic field, κ is the thermal viscosity, K is the permeability of the porous medium, k_1 is the rate of chemical reaction, $\nu=\mu/\rho$ is the kinetic viscosity, μ is the dynamic viscosity, and σ is the electrical conductivity.

The applicable boundary conditions are

$$\begin{gathered}u=-ax,\quad v=-a(m-1)y,\quad w=-W,\quad T=T_w,\quad C=C_w,\quad \text{at } y=0,\\ u\longrightarrow 0,\quad C\longrightarrow C_\infty,\quad T\longrightarrow T_\infty \quad \text{as } y\longrightarrow\infty,\end{gathered} \tag{2.2}$$

where $a>0$ is the shrinking constant and W is the suction velocity. The cases $m=1$ and $m=2$ correspond to shrinking sheets in the x- and y-directions, respectively.

Using the similarity transformations (see Sajid and Hayat [32]):

$$\begin{gathered}u=axF'(\eta),\qquad v=a(m-1)yF'(\eta),\qquad w=-\sqrt{a\nu}mF(\eta),\qquad \eta=\sqrt{\frac{a}{\nu}}z,\\ \theta(\eta)=\frac{(T-T_\infty)}{(T_w-T_\infty)},\qquad \phi(\eta)=\frac{(C-C_\infty)}{(C_w-C_\infty)},\end{gathered} \tag{2.3}$$

(2.1) are transformed to the system of nonlinear equations

$$f'''-\left(M^2+\lambda Pr\right)f'-f'^2+mff''=0, \tag{2.4}$$
$$\theta''-Prf'\theta+mPrf\theta'=0, \tag{2.5}$$
$$\phi''-Scf'\phi+mScf\phi'-Sc\gamma\phi=0, \tag{2.6}$$

subject to

$$\begin{gathered}f(0)=s,\qquad f'(0)=-1,\qquad f'(\infty)=0,\qquad \theta(0)=1,\qquad \theta(\infty)=0,\\ \phi(0)=1,\qquad \phi(\infty)=0,\end{gathered} \tag{2.7}$$

where $Pr=\nu/\kappa$ is the Prandtl number, $Sc=\nu/D$ is the Schmidt number, $\lambda=\kappa/Ka$ is the porosity, and γ is the chemical reaction parameter. We remark that (2.4) can be solved independently of equations of (2.5)-(2.6) for f, but the solutions for θ and ϕ directly depend on the solution for f. To demonstrate how robust the proposed methods of solution are, the system of (2.4)-(2.5) is solved simultaneously in the next section. Solving the equations simultaneously is also important when conducting the parametric study because some of the governing parameters such as Pr and m affect all three unknown variables.

3. Solution Methods

We solve (2.4)–(2.6) using three recent innovative semi-numerical methods. Validation of the results is done by further solving the equations numerically using a shooting method and the Matlab bvp4c solver. For the last two methods we used a tolerance of 10^{-6}.

We begin by transforming the domain $[0,\infty)$ to $[-1,1]$, using the domain truncation method, the domain $[0,\infty)$ is first approximated by the computational domain $[0,L]$, where L is a fixed length that is taken to be larger than the thickness of the boundary layer. The domain $[0,L]$ is then transformed to $[-1,1]$ using the algebraic mapping

$$\xi = \frac{2\eta}{L} - 1, \quad \xi \in [-1,1]. \tag{3.1}$$

3.1. The Successive Linearisation Method (SLM)

The successive linearisation method (see Makukula et al. [27, 28]) is used to solve (2.4)–(2.7). The starting point is to assume that the independent variables $f(\eta)$, $\theta(\eta)$, and $\phi(\eta)$ may be expanded as

$$\begin{aligned} f(\eta) &= f_i(\eta) + \sum_{m=0}^{i-1} F_m(\eta), \qquad \theta(\eta) = \theta_i(\eta) + \sum_{m=0}^{i-1} \Theta_m(\eta), \\ \phi(\eta) &= \phi_i(\eta) + \sum_{m=0}^{i-1} \Phi_m(\eta), \quad i = 1,2,3,\ldots, \end{aligned} \tag{3.2}$$

where f_i, θ_i and ϕ_i, are unknown functions and F_m, Θ_m, and $\Phi_m (m \geq 1)$ are approximations that are obtained by recursively solving the linear part of the equation that results from substituting (3.2) in the governing equations (2.4)–(2.7). Substituting (3.2) in the governing equations (2.4)–(2.7) gives

$$\begin{aligned} f_i''' + a_{1,i-1} f_i'' + a_{2,i-1} f_i' + a_{3,i-1} f_i + m f f'' - f'^2 &= r_{1,i-1}, \\ \theta_i'' + b_{1,i-1}\theta_i' + b_{2,i-1}\theta_i + b_{3,i-1} f_i' + b_{4,i-1} f_i - Pr f'\theta + mPr f\theta' &= r_{2,i-1}, \\ \phi_i'' + c_{1,i-1}\phi_i' + c_{2,i-1}\phi_i + c_{3,i-1} f_i' + c_{4,i-1} f_i - Sc f'\phi + mSc f\phi' &= r_{3,i-1}, \end{aligned} \tag{3.3}$$

where the coefficient parameters $a_{k,i-1}$, $b_{k,i-1}$, $c_{k,i-1}$ $(k = 1,\ldots,4)$, $r_{1,i-1}$, $r_{2,i-1}$, and $r_{3,i-1}$ are defined as

$$\begin{aligned} a_{1,i-1} &= m\sum_{m=0}^{i-1} F_m, \qquad a_{2,i-1} = -\left(2\sum_{m=0}^{i-1} F_m' + M^2 + \lambda Pr\right), \qquad a_{3,i-1} = m\sum_{m=0}^{i-1} F_m'', \\ b_{1,i-1} &= mPr\sum_{m=0}^{i-1} F_m, \qquad b_{2,i-1} = -Pr\sum_{m=0}^{i-1} F_m', \qquad b_{3,i-1} = -Pr\sum_{m=0}^{i-1} \Theta_m, \\ b_{4,i-1} &= mPr\sum_{m=0}^{i-1} \Theta_m', \qquad c_{1,i-1} = mSc\sum_{m=0}^{i-1} F_m, \qquad c_{2,i-1} = -Sc\sum_{m=0}^{i-1} F_m' - Sc\gamma, \end{aligned}$$

$$c_{3,i-1} = -Sc\sum_{m=0}^{i-1}\Phi_m, \qquad c_{4,i-1} = mSc\sum_{m=0}^{i-1}\Phi'_m,$$

$$r_{1,i-1} = -\left[\sum_{m=0}^{i-1}F'''_m - \sum_{m=0}^{i-1}F'_m\sum_{m=0}^{i-1}F'_m + m\sum_{m=0}^{i-1}F''_m\sum_{m=0}^{i-1}F_m - \left(M^2 + \lambda Pr\right)\sum_{m=0}^{i-1}F'_m\right],$$

$$r_{2,i-1} = -\left[\sum_{m=0}^{i-1}\Theta''_m - Pr\sum_{m=0}^{i-1}F'_m\sum_{m=0}^{i-1}\Theta_m + mPr\sum_{m=0}^{i-1}F_m\sum_{m=0}^{i-1}\Theta'_m\right],$$

$$r_{3,i-1} = -\left[\sum_{m=0}^{i-1}\Phi''_m - Sc\sum_{m=0}^{i-1}F'_m\sum_{m=0}^{i-1}\Phi_m + mSc\sum_{m=0}^{i-1}F_m\sum_{m=0}^{i-1}\Phi'_m - Sc\gamma\sum_{m=0}^{i-1}\Phi\right]. \tag{3.4}$$

Starting from the initial approximations

$$F_0(\eta) = s + e^{-2\eta} - e^{-\eta}, \qquad \Theta_0(\eta) = e^{-\eta}, \qquad \Phi_0(\eta) = e^{-\eta}, \tag{3.5}$$

which are chosen to satisfy the boundary conditions (2.7), the subsequent solutions for F_m, Θ_m, and Φ_m, $m \geq 1$, are obtained by successively solving the linearized form of (3.3) which are

$$\begin{aligned} F'''_i + a_{1,i-1}F''_i + a_{2,i-1}F'_i + a_{3,i-1}F_i &= r_{1,i-1}, \\ \Theta''_i + b_{1,i-1}\Theta'_i + b_{2,i-1}\Theta_i + b_{3,i-1}F'_i + b_{4,i-1}F_i &= r_{2,i-1}, \\ \Phi''_i + c_{1,i-1}\Phi'_i + c_{2,i-1}\Phi_i + c_{3,i-1}F'_i + c_{4,i-1}F_i &= r_{3,i-1}, \end{aligned} \tag{3.6}$$

subject to the boundary conditions

$$F_i(0) = F'_i(0) = F'_i(\infty) = 0, \qquad \Theta_i(0) = 0, \qquad \Phi_i(0) = 0. \tag{3.7}$$

Once each solution for F_i, Θ_i, and Φ_i $(i \geq 1)$ has been found from iteratively solving (3.6)-(3.7) for each i, the approximate solutions for $f(\eta)$, $\theta(\eta)$, and $\phi(\eta)$ are obtained as

$$f(\eta) \approx \sum_{m=0}^{M}F_m(\eta), \qquad \theta(\eta) \approx \sum_{m=0}^{M}\Theta_m(\eta), \qquad \phi(\eta) \approx \sum_{m=0}^{M}\Phi_m(\eta). \tag{3.8}$$

In coming up with (3.8), we have assumed that

$$\lim_{i\to\infty} f_i = 0, \qquad \lim_{i\to\infty} \theta_i = 0, \qquad \lim_{i\to\infty} \phi_i = 0. \tag{3.9}$$

Equations (3.6)-(3.7) are integrated using the Chebyshev spectral collocation method (Canuto et al. [33] and Trefethen [34]). The unknown functions are defined by the Chebyshev interpolating polynomials with the Gauss-Lobatto points defined as

$$y_j = \cos\frac{\pi j}{N}, \quad j = 0, 1, \ldots, N, \tag{3.10}$$

where N is the number of collocation points used. The unknown functions F_i, Θ_i, and Φ_i are approximated at the collocation points by

$$\begin{aligned} F_i(\xi) &\approx \sum_{k=0}^{N} F_i(\xi_k) T_k(\xi_j), \qquad \Theta_i(\xi) \approx \sum_{k=0}^{N} \Theta_i(\xi_k) T_k(\xi_j), \\ \Phi_i(\xi) &\approx \sum_{k=0}^{N} \Phi_i(\xi_k) T_k(\xi_j), \qquad j = 0, 1, \ldots, N, \end{aligned} \tag{3.11}$$

where T_k is the kth Chebyshev polynomial defined as

$$T_k(\xi) = \cos\left[k \cos^{-1}(\xi)\right]. \tag{3.12}$$

The derivatives at the collocation points are represented as

$$\begin{aligned} \frac{d^a F_i}{d\eta^a} &= \sum_{k=0}^{N} \mathbf{D}_{kj}^a F_i(\xi_k), \qquad \frac{d^a \Theta_i}{d\eta^a} = \sum_{k=0}^{N} \mathbf{D}_{kj}^a \Theta_i(\xi_k), \\ \frac{d^a \Phi_i}{d\eta^a} &= \sum_{k=0}^{N} \mathbf{D}_{kj}^a \Phi_i(\xi_k), \quad j = 0, 1, \ldots, N, \end{aligned} \tag{3.13}$$

where a is the order of differentiation and $\mathbf{D} = (2/L)\mathfrak{D}$ with $\mathfrak{D}$ being the Chebyshev spectral differentiation matrix. Substituting (3.13) in (3.6)-(3.7) leads to the matrix equation

$$\mathbf{A}_{i-1}\mathbf{X}_i = \mathbf{R}_{i-1}, \tag{3.14}$$

where $\mathbf{B}_{i-1}$ is a $3(N+1) \times 3(N+1)$ square matrix and $\mathbf{X}_i$ and $\mathbf{P}_{i-1}$ are $3(N+1) \times 1$ column vectors defined by

$$\mathbf{A}_{i-1} = \begin{pmatrix} \mathbf{D}^3 + \mathbf{a}_1\mathbf{D}^2 + \mathbf{a}_2\mathbf{D} + \mathbf{a}_3\mathbf{I} & 0\mathbf{I} & 0\mathbf{I} \\ \mathbf{b}_3\mathbf{D} + \mathbf{b}_4\mathbf{I} & \mathbf{D}^2 + \mathbf{b}_1\mathbf{D} + \mathbf{b}_2\mathbf{I} & 0\mathbf{I} \\ \mathbf{c}_3\mathbf{D} + \mathbf{c}_4\mathbf{I} & 0\mathbf{I} & \mathbf{D}^2 + \mathbf{c}_1\mathbf{D} + \mathbf{c}_2\mathbf{I} \end{pmatrix},$$

$$\begin{aligned} \mathbf{X}_i = [&F_m(\xi_0), F_m(\xi_1), \ldots, F_m(\xi_N), \Theta_m(\xi_0), \Theta_m(\xi_1), \ldots, \Theta_m(\xi_N), \\ &\Phi_m(\xi_0), \Phi_m(\xi_1), \ldots, \Phi_m(\xi_N)]^T, \end{aligned}$$

$$\mathbf{R}_{i-1} = [r_{1,i-1}(\eta_0), r_{1,i-1}(\eta_1), \ldots, r_{1,i-1}(\eta_N), r_{2,i-1}(\eta_0), r_{2,i-1}(\eta_1), \ldots, r_{2,i-1}(\eta_N), r_{3,i-1}(\eta_0), r_{3,i-1}(\eta_1), \ldots, r_{3,i-1}(\eta_N)]^T. \tag{3.15}$$

In the above definitions, $\mathbf{a}_{k,i-1}$, and $\mathbf{b}_{k,i-1}$, $\mathbf{c}_{k,i-1}$ $(k = 1, \ldots, 4)$ are diagonal matrices of size $(N + 1) \times (N + 1)$. After modifying the matrix system (3.14) to incorporate the boundary conditions, the solution is obtained as

$$\mathbf{X}_i = \mathbf{A}_{i-1}^{-1}\mathbf{R}_{i-1}. \tag{3.16}$$

3.2. *Spectral-Homotopy Analysis Method (SHAM)*

The spectral-homotopy analysis method (SHAM) has been used by Motsa et al. [25, 26]. It is also convenient to first ensure that the boundary conditions are made homogeneous by using the transformations

$$f(\eta) = F(\xi) + f_0(\eta), \qquad \theta(\eta) = \Theta(\xi) + \theta_0(\eta), \qquad \phi(\eta) = \Phi(\xi) + \phi_0(\eta), \tag{3.17}$$

where $f_0(\eta)$, and $\theta_0(\eta)$, $\phi_0(\eta)$ are chosen to satisfy the boundary conditions (2.7) of the governing equations (2.4)–(2.6). From (3.1) and the chain rule, we have that

$$\begin{aligned} f'(\eta) &= \frac{2}{L}F'(\xi) + f_0'(\eta), \qquad f''(\eta) = \frac{4}{L^2}F''(\xi) + f_0''(\eta), \\ f'''(\eta) &= \frac{8}{L^3}F'''(\xi) + f_0'''(\eta), \\ \theta'(\eta) &= \frac{2}{L}\Theta'(\xi) + \theta_0'(\eta), \qquad \theta''(\eta) = \frac{4}{L^2}\Theta''(\xi) + \theta_0''(\eta), \\ \phi'(\eta) &= \frac{2}{L}\Phi'(\xi) + \phi_0'(\eta), \qquad \phi''(\eta) = \frac{4}{L^2}\Phi''(\xi) + \phi_0''(\eta). \end{aligned} \tag{3.18}$$

Substituting (3.1) and (3.17)-(3.18) in the governing equations and boundary conditions gives

$$\begin{aligned} &a_0F''' + a_1F'' + a_2F' + a_3F + \frac{4}{L^2}mF''F - \frac{4}{L^2}F'F' = r_1(\eta), \\ &b_0\Theta'' + b_1\Theta' + b_2\Theta + b_3F' + b_4F - \frac{2}{L}PrF'\Theta + \frac{2}{L}mPrF\Theta' = r_2(\eta), \\ &c_0\Phi'' + c_1\Phi' + c_2\Phi + c_3F' + c_4F - \frac{2}{L}ScF'\Phi + \frac{2}{L}mScF\Phi' = r_3(\eta), \end{aligned} \tag{3.19}$$

where prime now denotes derivative with respect to ξ and

$$a_0 = \frac{8}{L^3}, \quad a_1 = \frac{4}{L^2}mf_0, \quad a_2 = -\left(\frac{2}{L}\left(M^2 + \lambda Pr\right) + \frac{4}{L}f_0'\right), \quad a_3 = mf_0'',$$

$$r_1(\eta) = -\left(f_0''' + mf_0f_0'' - f_0'f_0' - \left(M^2 + \lambda Pr\right)f_0'\right),$$

$$b_0 = \frac{4}{L^2}, \quad b_1 = \frac{2}{L}mPrf_0, \quad b_2 = -Prf_0', \quad b_3 = -\frac{2}{L}Pr\theta_0, \quad b_4 = mPr\theta_0',$$

$$r_2(\eta) = -(\theta'' - Prf_0'\theta_0 + mPrf_0\theta_0),$$

$$c_0 = \frac{4}{L^2}, \quad c_1 = \frac{2}{L}mScf_0, \quad c_2 = -Sc(f_0' + \gamma), \quad c_3 = -\frac{2}{L}Sc\phi_0, \quad c_4 = mSc\phi_0',$$

$$r_3(\eta) = -(\phi'' - Scf_0'\phi_0 + mScf_0\phi_0' - Sc\gamma\phi). \tag{3.20}$$

The initial guesses used are

$$f_0(\eta) = s + e^{-2\eta} - \eta e^{-\eta}, \quad \theta_0(\eta) = e^{-\eta}, \quad \phi_0(\eta) = e^{-\eta}. \tag{3.21}$$

Solving the linear part of the equation system (3.19), that is,

$$\begin{aligned} a_0F_0''' + a_1F_0'' + a_2F_0' + a_3F_0 &= r_1(\eta), \\ b_0\Theta_0'' + b_1\Theta_0' + b_2\Theta_0 + b_3F_0' + b_4F_0 &= r_2(\eta), \\ c_0\Phi_0'' + c_1\Phi_0' + c_2\Phi_0 + c_3F_0' + c_4F_0 &= r_3(\eta), \end{aligned} \tag{3.22}$$

subject to

$$F_0(-1) = \frac{2}{L}F_0'(-1) = \frac{2}{L}F_0'(1) = 0, \quad \Theta_0(-1) = \Theta_0(1) = 0, \quad \Phi_0(-1) = \Phi_0(1) = 0, \tag{3.23}$$

will yield the initial SHAM approximate solution. Applying the Chebyshev pseudospectral method on equations (3.22)-(3.23) yields the matrix form

$$\mathbf{BY}_0 = \mathbf{R}, \tag{3.24}$$

where

$$\mathbf{B} = \begin{pmatrix} \mathbf{a}_0\mathfrak{D}^3 + \mathbf{a}_1\mathfrak{D}^2 + \mathbf{a}_2\mathfrak{D} + \mathbf{a}_3\mathbf{I} & 0\mathbf{I} & 0\mathbf{I} \\ \mathbf{b}_3\mathfrak{D} + \mathbf{b}_4\mathbf{I} & \mathbf{b}_0\mathfrak{D}^2 + \mathbf{b}_1\mathfrak{D} + \mathbf{b}_2\mathbf{I} & 0\mathbf{I} \\ \mathbf{c}_3\mathfrak{D} + \mathbf{c}_4\mathbf{I} & 0\mathbf{I} & \mathbf{c}_0\mathfrak{D}^2 + \mathbf{c}_1\mathfrak{D} + \mathbf{c}_2\mathbf{I} \end{pmatrix}, \tag{3.25}$$

$$\begin{aligned} \mathbf{R} &= [r_1(\eta_0), r_1(\eta_1), \ldots, r_1(\eta_N), r_2(\eta_0), r_2(\eta_1), \ldots, r_2(\eta_N), r_3(\eta_0), r_3(\eta_1), \ldots, r_3(\eta_N)]^T, \\ \mathbf{Y}_0 &= [F_0(\xi_0), F_0(\xi_1), \ldots, F_0(\xi_N), \Theta_0(\xi_0), \Theta_0(\xi_1), \ldots, \Theta_0(\xi_N), \Phi_0(\xi_0), \Phi_0(\xi_1), \ldots, \Phi_0(\xi_N)]^T, \\ \mathbf{a}_i &= \operatorname{diag}([a_i(\eta_0), \ldots, a_i(\eta_{N-1}), a_i(\eta_N)]), \qquad \mathbf{b}_i = \operatorname{diag}([b_i(\eta_0), \ldots, b_i(\eta_{N-1}), b_i(\eta_N)]), \\ \mathbf{c}_i &= \operatorname{diag}([c_i(\eta_0), \ldots, c_i(\eta_{N-1}), c_i(\eta_N)]), \quad i = 0, 1, 2, 3, 4. \end{aligned} \tag{3.26}$$

The superscript T denotes the transpose, diag is a diagonal matrix, and $\mathbf{I}$ is an identity matrix of size $(N+1) \times (N+1)$. The boundary conditions (3.23) are implemented in matrix $\mathbf{B}$ and vector $\mathbf{R}$ of equation (3.24). The values of $[Y_0(\xi_1), Y_0(\xi_2), \ldots, Y_0(\xi_{N-1})]$ are then determined from the following equation:

$$\mathbf{Y}_0 = \mathbf{B}^{-1}\mathbf{R}, \tag{3.27}$$

which provides us with the initial approximation for the solution of the governing equations (3.19). With the initial approximate solution, we then find approximate solutions for the nonlinear equations (3.19). We start by defining the following linear operators:

$$\begin{aligned} \mathcal{L}_F\left[\tilde{F}(\xi;q)\right] &= a_0\frac{\partial^3\tilde{F}}{\partial\xi^3} + a_1\frac{\partial^2\tilde{F}}{\partial\xi^2} + a_2\frac{\partial\tilde{F}}{\partial\xi} + a_3\tilde{F}, \\ \mathcal{L}_\Theta\left[\tilde{F}(\xi;q), \tilde{\Theta}(\xi;q)\right] &= b_0\frac{\partial^2\tilde{\Theta}}{\partial\xi^2} + b_1\frac{\partial\tilde{\Theta}}{\partial\xi} + b_2\tilde{\Theta} + b_3\frac{\partial\tilde{F}}{\partial\xi} + b_4\tilde{F}, \\ \mathcal{L}_\Phi\left[\tilde{F}(\xi;q), \tilde{\Phi}(\xi;q)\right] &= c_0\frac{\partial^2\tilde{\Phi}}{\partial\xi^2} + c_1\frac{\partial\tilde{\Phi}}{\partial\xi} + c_2\tilde{\Phi} + c_3\frac{\partial\tilde{F}}{\partial\xi} + c_4\tilde{F}, \end{aligned} \tag{3.28}$$

where $q \in [0,1]$ is the embedding parameter and $\tilde{F}(\xi;q)$, $\tilde{\Theta}(\xi;q)$, and $\tilde{\Phi}(\xi;q)$ are unknown functions. The *zeroth*-order deformation equations are given by

$$\begin{aligned} (1-q)\mathcal{L}_F\left[\tilde{F}(\xi;q) - F_0(\xi)\right] &= q\hbar\left\{\mathcal{N}_F\left[\tilde{F}(\xi;q)\right] - r_1\right\}, \\ (1-q)\mathcal{L}_\Theta\left[\tilde{\Theta}(\xi;q) - \Theta_0(\xi)\right] &= q\hbar\left\{\mathcal{N}_\Theta\left[\tilde{F}(\xi;q), \tilde{\Theta}(\xi;q)\right] - r_2\right\}, \\ (1-q)\mathcal{L}_\Phi\left[\tilde{\Phi}(\xi;q) - \Phi_0(\xi)\right] &= q\hbar\left\{\mathcal{N}_\Phi\left[\tilde{F}(\xi;q), \tilde{\Phi}(\xi;q)\right] - r_3\right\}, \end{aligned} \tag{3.29}$$

where $\hbar$ is the nonzero convergence controlling auxiliary parameter and $\mathcal{N}_F$, $\mathcal{N}_\Theta$, and $\mathcal{N}_\Phi$ are nonlinear operators given by

$$\begin{aligned}
\mathcal{N}_F\left[\tilde{F}(\xi;q)\right] &= a_0\frac{\partial^3\tilde{F}}{\partial\xi^3} + a_1\frac{\partial^2\tilde{F}}{\partial\xi^2} + a_2\frac{\partial\tilde{F}}{\partial\xi} + a_3\tilde{F} + \frac{4}{L^2}m\tilde{F}\frac{\partial^2\tilde{F}}{\partial\xi^2} - \frac{4}{L^2}\frac{\partial\tilde{F}}{\partial\xi}\frac{\partial\tilde{F}}{\partial\xi},\\
\mathcal{N}_\Theta\left[\tilde{F}(\xi;q),\tilde{\Theta}(\xi;q)\right] &= b_0\frac{\partial^2\tilde{\Theta}}{\partial\xi^2} + b_1\frac{\partial\tilde{\Theta}}{\partial\xi} + b_2\tilde{\Theta} + b_3\frac{\partial\tilde{F}}{\partial\xi} + b_4\tilde{F}\\
&\quad + \frac{2}{L}Pr\left(-\tilde{\Theta}\frac{\partial\tilde{F}}{\partial\xi} + m\tilde{F}\frac{\partial\tilde{\Theta}}{\partial\xi}\right),\\
\mathcal{N}_\Phi\left[\tilde{F}(\xi;q),\tilde{\Phi}(\xi;q)\right] &= c_0\frac{\partial^2\tilde{\Phi}}{\partial\xi^2} + c_1\frac{\partial\tilde{\Phi}}{\partial\xi} + c_2\tilde{\Phi} + c_3\frac{\partial\tilde{F}}{\partial\xi} + c_4\tilde{F}\\
&\quad + \frac{2}{L}Sc\left(-\tilde{\Phi}\frac{\partial\tilde{F}}{\partial\xi} + m\tilde{F}\frac{\partial\tilde{\Phi}}{\partial\xi}\right).
\end{aligned} \tag{3.30}$$

The m-th order deformation equations are given by

$$\begin{aligned}
\mathcal{L}_F\left[F_m(\xi) - \chi_m F_{m-1}(\xi)\right] &= \hbar R_m^F,\\
\mathcal{L}_\Theta\left[\Theta_m(\xi) - \chi_m \Theta_{m-1}(\xi)\right] &= \hbar R_m^\Theta,\\
\mathcal{L}_\Phi\left[\Phi_m(\xi) - \chi_m \Phi_{m-1}(\xi)\right] &= \hbar R_m^\Phi,
\end{aligned} \tag{3.31}$$

subject to the boundary conditions

$$F_m(-1) = F_m'(-1) = F_m'(1) = 0, \qquad \Theta_m(-1) = \Theta_m(1) = 0, \qquad \Phi_m(-1) = \Phi_m(1) = 0, \tag{3.32}$$

where

$$\begin{aligned}
R_m^F(\xi) &= a_0F_{m-1}''' + a_1F_{m-1}'' + a_2F_{m-1}' + a_3F_{m-1}\\
&\quad + \frac{4}{L^2}\sum_{n=0}^{m-1}\left(-F_n'F_{m-1-n}' + mF_nF_{m-1-n}''\right) - r_1(\eta)(1-\chi_m),\\
R_m^\Theta(\xi) &= b_0\Theta_{m-1}'' + b_1\Theta_{m-1}' + b_2\Theta_{m-1} + b_3F_{m-1}' + b_4F_{m-1}\\
&\quad + \frac{2}{L}Pr\sum_{n=0}^{m-1}\left(-F_n'\Theta_{m-1-n} + m\Theta_n'F_{m-1-n}\right) - r_2(\eta)(1-\chi_m),
\end{aligned}$$

$$R_m^{\Phi}(\xi) = c_0\Phi''_{m-1} + c_1\Phi'_{m-1} + c_2\Phi_{m-1} + c_3F'_{m-1} + c_4F_{m-1} + \frac{2}{L}Sc\sum_{n=0}^{m-1}\left(-F'_n\Phi_{m-1-n} + m\Phi'_nF_{m-1-n}\right) - r_3(\eta)(1-\chi_m), \tag{3.33}$$

$$\chi_m = \begin{cases} 0, & m \le 1 \\ 1, & m > 1. \end{cases} \tag{3.34}$$

Applying the Chebyshev pseudospectral transformation to equations (3.31)–(3.33) gives rise to the matrix equation

$$\mathbf{B}\mathbf{Y}_m = (\chi_m + \hbar)\mathbf{B}\mathbf{Y}_{m-1} - \hbar(1-\chi_m)\mathbf{R} + \hbar\mathbf{Q}_{m-1}, \tag{3.35}$$

subject to the boundary conditions

$$\sum_{k=0}^{N}\mathfrak{D}_{0k}F_m(\xi_k) = 0, \quad \sum_{k=0}^{N}\mathfrak{D}_{Nk}F_m(\xi_k) = 0, \quad F_m(\xi_N) = 0,$$
$$\Theta_m(\xi_0) = 0, \quad \Theta_m(\xi_N) = 0, \quad \Phi_m(\xi_0) = 0, \quad \Phi_m(\xi_N) = 0, \tag{3.36}$$

where $\mathbf{B}$ and $\mathbf{R}$ are as defined in (3.25) and

$$\mathbf{Y}_m = [F_m(\xi_0), F_m(\xi_1), \ldots, F_m(\xi_N), \Theta_m(\xi_0), \Theta_m(\xi_1), \ldots, \Theta_m(\xi_N), \Phi_m(\xi_0), \Phi_m(\xi_1), \ldots, \Phi_m(\xi_N)]^T,$$
$$\mathbf{Q}_{m-1} = \begin{pmatrix} \sum_{n=0}^{m-1}\left[-\frac{4}{L^2}(\mathfrak{D}F_n)(\mathfrak{D}F_{m-1-n}) + \frac{4}{L^2}mF_n(\mathfrak{D}^2F_{m-1-n})\right] \\ \frac{2}{L}Pr\sum_{n=0}^{m-1}\left[-(\mathfrak{D}F_n)\Theta_{m-1-n} + m(\mathfrak{D}\Theta_n)F_{m-1-n}\right] \\ \frac{2}{L}Sc\sum_{n=0}^{m-1}\left[-(\mathfrak{D}F_n)\Phi_{m-1-n} + m(\mathfrak{D}\Phi_n)F_{m-1-n}\right] \end{pmatrix}. \tag{3.37}$$

Applying the boundary conditions (3.32) on the right-hand side of (3.35) yields the following recursive formula for higher-order approximations $Y_m(\xi)$ for $m \ge 1$:

$$\mathbf{Y}_m = (\chi_m + \hbar)\mathbf{B}^{-1}\tilde{\mathbf{B}}\mathbf{Y}_{m-1} + \hbar\mathbf{B}^{-1}\left[\mathbf{Q}_{m-1} - (1-\chi_m)\mathbf{R}\right]. \tag{3.38}$$

3.3. *Improved Spectral-Homotopy Analysis Method (ISHAM)*

Details of the improved spectral-homotopy analysis method (ISHAM) can be found in Makukula et al. [30]. The main objective is to improve the convergence rate of the spectral-homotopy analysis method by using an optimal initial approximation. Hence, instead of a random solution choice a systematic approach is employed to find the optimal initial approximation. This is achieved by first assuming that the solutions $f(\eta)$, $\theta(\eta)$, and $\phi(\eta)$ can be expanded into

$$\begin{aligned} f(\eta) &= F_i(\eta) + \sum_{m=0}^{i-1} F_m(\eta), \qquad \theta(\eta) = \Theta_i(\eta) + \sum_{m=0}^{i-1} \Theta_m(\eta), \\ \phi(\eta) &= \Phi_i(\eta) + \sum_{m=0}^{i-1} \Phi_m(\eta), \quad i = 1, 2, 3, \ldots, \end{aligned} \tag{3.39}$$

where F_i, Θ_i, and Φ_i are unknown functions whose solutions are obtained using the SHAM approach at the ith iteration and F_m, Θ_m, and Φ_m ($m \geq 1$) are known from previous iterations. We use the same initial guesses as with the SHAM solution in Sections 3.1 and 3.2. Substituting (3.39) into the governing equations gives

$$\begin{aligned} &F_i''' + a_{1,i-1}F_i'' + a_{2,i-1}F_i' + a_{3,i-1}F_i + mF_i''F_i - F_i'F_i' = r_{1,i-1}(\eta), \\ &\Theta_i'' + b_1\Theta_i' + b_2\Theta_i + b_3F_i' + b_4F_i - PrF_i'\Theta_i + mPrF_i\Theta_i' = r_{2,i-1}(\eta), \\ &\Phi_i'' + c_1\Phi_i' + c_2\Phi_i + c_3F_i' + c_4F_i - ScF_i'\Phi_i + mScF_i\Phi_i' = r_{3,i-1}(\eta), \end{aligned} \tag{3.40}$$

subject to the boundary conditions

$$F_i(0) = 0, \quad F_i'(0) = F_i'(\infty) = 0, \quad \Theta_i(0) = 0, \quad \Theta_i(\infty) = 0, \quad \Phi_i(0) = 0, \quad \Phi_i(\infty) = 0. \tag{3.41}$$

The coefficient parameters $a_{k,i-1}$, $b_{k,i-1}$, $c_{k,i-1}$ ($k = 0, \ldots, 4$), $r_{1,i-1}$, $r_{2,i-1}$, and $r_{3,i-1}$ are as defined in equation (3.4). Starting from the initial guesses (3.5), the subsequent solutions F_i, Θ_i, and Φ_i ($i \geq 1$) are obtained by recursively solving (3.40) using the SHAM approach. To find the SHAM solutions of (3.40), we start by defining the following linear operators:

$$\begin{aligned} \mathcal{L}_F\left[\tilde{F}_i(\eta;q)\right] &= \frac{\partial^3\tilde{F}_i}{\partial\eta^3} + a_{1,i-1}\frac{\partial^2\tilde{F}_i}{\partial\eta^2} + a_{2,i-1}\frac{\partial\tilde{F}_i}{\partial\eta} + a_{3,i-1}\tilde{F}_i, \\ \mathcal{L}_\Theta\left[\tilde{F}_i(\eta;q), \tilde{\Theta}_i(\eta;q)\right] &= \frac{\partial^2\tilde{\Theta}_i}{\partial\eta^2} + b_{1,i-1}\frac{\partial\tilde{\Theta}_i}{\partial\eta} + b_{2,i-1}\tilde{\Theta}_i + b_{3,i-1}\frac{\partial\tilde{F}_i}{\partial\eta} + b_{4,i-1}\tilde{F}_i, \\ \mathcal{L}_\Phi\left[\tilde{F}_i(\eta;q), \tilde{\Phi}_i(\eta;q)\right] &= \frac{\partial^2\tilde{\Phi}_i}{\partial\eta^2} + c_{1,i-1}\frac{\partial\tilde{\Phi}_i}{\partial\eta} + c_{2,i-1}\tilde{\Phi}_i + c_{3,i-1}\frac{\partial\tilde{F}_i}{\partial\eta} + c_{4,i-1}\tilde{F}_i. \end{aligned} \tag{3.42}$$

The zeroth-order deformation equations are given by

$$\begin{aligned}
(1-q)\mathcal{L}_F\left[\tilde{F}_i(\eta;q)-F_{i,0}(\eta)\right] &= q\hbar\left\{\mathcal{N}_F\left[\tilde{F}_i(\eta;q)\right]-r_{1,i-1}\right\},\\
(1-q)\mathcal{L}_\Theta\left[\tilde{\Theta}_i(\eta;q)-\Theta_{i,0}(\eta)\right] &= q\hbar\left\{\mathcal{N}_\Theta\left[\tilde{F}_i(\eta;q),\tilde{\Theta}_i(\eta;q)\right]-r_{2,i-1}\right\},\\
(1-q)\mathcal{L}_\Phi\left[\tilde{\Phi}_i(\eta;q)-\Phi_{i,0}(\eta)\right] &= q\hbar\left\{\mathcal{N}_\Phi\left[\tilde{F}_i(\eta;q),\tilde{\Phi}_i(\eta;q)\right]-r_{3,i-1}\right\},
\end{aligned} \tag{3.43}$$

$\mathcal{N}_F$, $\mathcal{N}_\Theta$, and $\mathcal{N}_\Phi$ are nonlinear operators given by

$$\begin{aligned}
\mathcal{N}_F\left[\tilde{F}_i(\eta;q)\right] &= \frac{\partial^3\tilde{F}_i}{\partial\eta^3}+a_{1,i-1}\frac{\partial^2\tilde{F}_i}{\partial\eta^2}+a_{2,i-1}\frac{\partial\tilde{F}_i}{\partial\eta}+a_{3,i-1}\tilde{F}_i\\
&\quad+m\tilde{F}_i\frac{\partial^2\tilde{F}_i}{\partial\eta^2}-\frac{\partial\tilde{F}_i}{\partial\eta}\frac{\partial\tilde{F}_i}{\partial\eta},\\
\mathcal{N}_\Theta\left[\tilde{F}_i(\eta;q),\tilde{\Theta}_i(\eta;q)\right] &= \frac{\partial^2\tilde{\Theta}_i}{\partial\eta^2}+b_{1,i-1}\frac{\partial\tilde{\Theta}_i}{\partial\eta}+b_{2,i-1}\tilde{\Theta}_i+b_{3,i-1}\frac{\partial\tilde{F}_i}{\partial\eta}+b_{4,i-1}\tilde{F}_i\\
&\quad+Pr\left(-\tilde{\Theta}_i\frac{\partial\tilde{F}_i}{\partial\eta}+m\tilde{F}_i\frac{\partial\tilde{\Theta}_i}{\partial\eta}\right),\\
\mathcal{N}_\Phi\left[\tilde{F}_i(\eta;q),\tilde{\Phi}_i(\eta;q)\right] &= \frac{\partial^2\tilde{\Phi}_i}{\partial\eta^2}+c_{1,i-1}\frac{\partial\tilde{\Phi}_i}{\partial\eta}+c_{2,i-1}\tilde{\Phi}_i+c_{3,i-1}\frac{\partial\tilde{F}_i}{\partial\eta}+c_{4,i-1}\tilde{F}_i\\
&\quad+Sc\left(-\tilde{\Phi}_i\frac{\partial\tilde{F}_i}{\partial\eta}+m\tilde{F}_i\frac{\partial\tilde{\Phi}_i}{\partial\eta}\right).
\end{aligned} \tag{3.44}$$

The mth order deformation equations are

$$\begin{aligned}
\mathcal{L}_F\left[F_{i,m}(\eta)-\chi_m F_{i,m-1}(\eta)\right] &= \hbar R^F_{i,m},\\
\mathcal{L}_\Theta\left[\Theta_{i,m}(\eta)-\chi_m\Theta_{i,m-1}(\eta)\right] &= \hbar R^\Theta_{i,m},\\
\mathcal{L}_\Phi\left[\Phi_{i,m}(\eta)-\chi_m\Phi_{i,m-1}(\eta)\right] &= \hbar R^\Phi_{i,m},
\end{aligned} \tag{3.45}$$

subject to the boundary conditions

$$F_{i,m}(0)=F'_{i,m}(0)=F'_{i,m}(\infty)=0,\qquad \Theta_{i,m}(0)=\Theta_{i,m}(\infty)=0,\qquad \Phi_{i,m}(0)=\Phi_{i,m}(\infty)=0, \tag{3.46}$$

where

$$
\begin{aligned}
R_{i,m}^{F}(\eta) &= F_{i,m-1}''' + a_{1,i-1}F_{i,m-1}'' + a_{2,i-1}F_{i,m-1}' + a_{3,i-1}F_{i,m-1} \\
&\quad + \sum_{n=0}^{m-1}\left(-F_{i,n}'F_{i,m-1-n}' + mF_{i,n}F_{i,m-1-n}''\right) - r_{1,i-1}(\eta)(1-\chi_m), \\
R_{i,m}^{\Theta}(\eta) &= \Theta_{i,m-1}'' + b_{1,i-1}\Theta_{i,m-1}' + b_{2,i-1}\Theta_{i,m-1} + b_{3,i-1}F_{i,m-1}' + b_{4,i-1}F_{i,m-1} \\
&\quad + Pr\sum_{n=0}^{m-1}\left(-F_{i,n}'\Theta_{i,m-1-n} + m\Theta_{i,n}'F_{i,m-1-n}\right) - r_{2,i-1}(\eta)(1-\chi_m), \\
R_{i,m}^{\Phi}(\eta) &= \Phi_{i,m-1}'' + c_{1,i-1}\Phi_{i,m-1}' + c_{2,i-1}\Phi_{i,m-1} + c_{3,i-1}F_{i,m-1}' + c_{4,i-1}F_{i,m-1} \\
&\quad + Sc\sum_{n=0}^{m-1}\left(-F_{i,n}'\Phi_{i,m-1-n} + m\Phi_{i,n}'F_{i,m-1-n}\right) - r_{3,i-1}(\eta)(1-\chi_m).
\end{aligned}
\tag{3.47}
$$

The initial approximations $F_{i,0}$, $\Theta_{i,0}$, and $\Phi_{i,0}$ that are used in the higher-order equations (3.45)–(3.47) are obtained by solving the linear part of (3.40) given by

$$
\begin{aligned}
F_{i,0}''' + a_{1,i-1}F_{i,0}'' + a_{2,i-1}F_{i,0}' + a_{3,i-1}F_{i,0} &= r_{1,i-1}, \\
\Theta_{i,0}'' + b_{1,i-1}\Theta_{i,0}' + b_{2,i-1}\Theta_{i,0} + b_{3,i-1}F_{i,0}' + b_{4,i-1}F_{i,0} &= r_{2,i-1}, \\
\Phi_{i,0}'' + c_{1,i-1}\Phi_{i,0}' + c_{2,i-1}\Phi_{i,0} + c_{3,i-1}F_{i,0}' + c_{4,i-1}F_{i,0} &= r_{3,i-1},
\end{aligned}
\tag{3.48}
$$

with the boundary conditions

$$
\begin{aligned}
&F_{i,0}(0) = F_{i,0}'(0) = F_{i,0}'(\infty) = 0, \quad \Theta_{i,0}(0) = 0, \quad \Theta_{i,0}(\infty) = 0, \quad \Phi_{i,0}(0) = 0, \\
&\qquad\qquad \Phi_{i,0}(\infty) = 0.
\end{aligned}
\tag{3.49}
$$

In a similar manner, we apply the spectral methods to solve for the initial approximate solutions $F_{i,0}$, $\Theta_{i,0}$, and $\Phi_{i,0}$, and the higher-order deformation equations (3.45)–(3.47) for higher order approximate solutions $F_{i,m}$, $\Theta_{i,m}$, and $\Phi_{i,m}$ for $m \geq 1$. The solutions for F_i, Θ_i, and Φ_i are then generated using the solutions for $F_{i,m}$, $\Theta_{i,m}$, and $\Phi_{i,m}$ as follows:

$$
\begin{aligned}
F_i &= F_{i,0} + F_{i,1} + F_{i,2} + F_{i,3} + \cdots + F_{i,m}, \\
\Theta_i &= \Theta_{i,0} + \Theta_{i,1} + \Theta_{i,2} + \Theta_{i,3} + \cdots + \Theta_{i,m}, \\
\Phi_i &= \Phi_{i,0} + \Phi_{i,1} + \Phi_{i,2} + \Phi_{i,3} + \cdots + \Phi_{i,m}.
\end{aligned}
\tag{3.50}
$$

The $[i, m]$ approximate solutions for $f(\eta)$, $\theta(\eta)$, and $\phi(\eta)$ are then obtained by substituting F_i, Θ_i, and Φ_i from (3.50) into (3.39), where i is the ith iteration of the higher-order deformation equation and m is the mth iteration of the initial approximation.

Table 1: Comparison of the approximate solutions of $f''(0)$ at different orders of the SLM, SHAM, and ISHAM against the numerical solutions at different values of λ when $s = 3$, $M = 1$, m=1, $Sc = 0.62$, γ =3, $Pr = 1$, $\lambda = 0$, $\hbar$=−1, $L = 30$, and $N = 150$.

	SLM		SHAM		ISHAM		Shooting	bvp4c	Ref. [9]
λ	order	$f''(0)$	order	$f''(0)$	order	$f''(0)$	$f''(0)$	$f''(0)$	$f''(0)$
1	1	3.32068	1	3.30709	[1,1]	3.33858	3.30278	3.30278	3.302776
	2	3.30283	2	3.30338	[2,2]	3.30278			
	3	3.30278	4	3.30279	[3,3]	3.30278			
	4	3.30278	6	3.30278	[4,4]	3.30278			
2	1	3.57292	1	3.56643	[1,1]	3.59883	2.30278	2.30278	3.561553
	2	3.56157	2	3.56225	[2,2]	2.30278			
	3	3.56155	4	3.56157	[3,3]	2.30278			
	4	3.56155	6	3.56155	[4,4]	2.30278			
4	1	4.00770	1	4.00549	[1,1]	4.03789	4.00000	4.00000	4.000000
	2	4.00000	2	4.00084	[2,2]	4.00000			
	3	4.00000	4	4.00002	[3,3]	4.00000			
	4	4.00000	6	4.00000	[4,4]	4.00000			

Table 2: Comparison of the approximate solutions of $-\theta'(0)$ at different orders of the SLM, SHAM, and ISHAM against the numerical solutions at different values of λ when $s = 3$, $M = 1$, $m = 1$, $Sc = 0.62$, $\gamma = 3$, $Pr = 1$, $\lambda = 0$, $\hbar = -1$, $L = 30$, and $N = 150$.

	SLM		SHAM		ISHAM		Shooting	bvp4c	Ref. [9]
λ	order	$-\theta'(0)$	order	$-\theta'(0)$	order	$-\theta'(0)$	$-\theta'(0)$	$-\theta'(0)$	$-\theta'(0)$
1	1	2.56783	1	2.67511	[1,1]	2.80912	2.66554	2.66554	2.665537
	2	2.66485	2	2.66656	[2,2]	2.66554			
	3	2.66554	4	2.66556	[3,3]	2.66554			
	4	2.66554	6	2.66554	[4,4]	2.66554			
2	1	2.59198	1	2.69041	[1,1]	2.84009	2.68032	2.68032	2.680315
	2	2.67987	2	2.68132	[2,2]	2.68032			
	3	2.68032	4	2.68034	[3,3]	2.68032			
	4	2.68032	6	2.68032	[4,4]	2.68032			
4	1	2.62914	1	2.71316	[1,1]	2.88452	2.70240	2.70240	2.702455
	2	2.70215	2	2.70336	[2,2]	2.70240			
	3	2.70240	4	2.70241	[3,3]	2.70240			
	4	2.70240	6	2.70240	[4,4]	2.70240			

4. Results and Discussion

Equations (2.4)-(2.6) subject to boundary conditions (2.7) have been solved using three recent semi-numerical techniques as described above. To validate our results, we have compared the skin friction coefficient, the Nusselt number, and the Sherwood number with the theoretical results of Muhaimin et al. [9]. We have further compared our results with the full numerical solutions obtained using the shooting method and the Matlab bvp4c routine. The comparison is given in Tables 1–3.

Tables 1–3 give values of the skin friction, heat transfer rate, and the mass transfer rate, respectively, for different porosity values. The convergence to the two numerical results of the SLM is achieved at the third order of approximation, at the sixth order for the SHAM, and at

Table 3: Comparison of the approximate solutions of $-\phi'(0)$ at different orders of the SLM, SHAM, and ISHAM against the numerical solutions at different values of λ when $s = 3$, $M = 1$, $m = 1$, $Sc = 0.62$, $\gamma = 3$, $Pr = 1$, $\lambda = 0$, $\hbar = -1$, $L = 30$, and $N = 150$.

	SLM		SHAM		ISHAM		Shooting	bvp4c	Ref. [9]
λ	order	$-\phi'(0)$	order	$-\phi'(0)$	order	$-\phi'(0)$	$-\phi'(0)$	$-\phi'(0)$	$-\phi'(0)$
1	1	2.39294	1	2.41413	[1,1]	2.43976	2.41029	2.41029	2.410283
	2	2.41026	2	2.41085	[2,2]	2.41029			
	3	2.41029	4	2.41030	[3,3]	2.41029			
	4	2.41029	6	2.41029	[4,4]	2.41029			
2	1	2.40181	1	2.42137	[1,1]	2.44981	2.41700	2.41700	2.417000
	2	2.41698	2	2.41764	[2,2]	2.41700			
	3	2.41700	4	2.41702	[3,3]	2.41700			
	4	2.41700	6	2.41700	[4,4]	2.41700			
4	1	2.41559	1	2.43236	[1,1]	2.46460	2.42722	2.42722	2.427225
	2	2.42721	2	2.42797	[2,2]	2.42722			
	3	2.42722	4	2.42724	[3,3]	2.42722			
	4	2.42722	6	2.42722	[4,4]	2.42722			

second order for the ISHAM. Comparison with results reported in Muhaimin et al. [9] shows an excellent agreement.

Table 1 shows an increase in the surface shear stress $f''(0)$ with an increase in the porosity parameter λ. The increase in the skin friction with the porosity may be accounted for by the fact that the velocity gradient increases with porosity (Takhar et al. [35]). Tables 2 and 3 show an increase in the surface heat transfer rate $-\theta'(0)$ and the mass transfer rate $-\theta'(0)$ with the porosity parameter for large suction values ($s = 3$), suggesting an increase in temperature and concentration gradients with increasing porosity.

Figure 1 serves two purposes: (a) to give sense of the accuracy of the improved spectral homotopy analysis (ISHAM) by means of a comparison between the numerical results and the second-order improved spectral-homotopy analysis results and (b) to demonstrate the effects of the suction parameter s and the Hartmann number M on the velocity profiles $f'(\eta)$.

Firstly we observe an excellent agreement between the second-order ISHAM and the numerical bvp4c results for all parameter values used. Secondly we note that these results are qualitatively similar to those reported in Noor et al. [6] for the case of one-direction shrinking ($m = 1$) and show that increasing the suction parameter s and the Hartmann number M leads to an increase in the velocity. This in turn leads to a decrease in the boundary layer thickness as fluid is sucked out of the flow region.

5. Conclusions

We have successfully solved the nonlinear system of equations governing MHD boundary layer past a porous shrinking sheet with a chemical reaction and suction. We demonstrated three recent innovative methods, namely, the successive linearisation method (SLM), the spectral-homotopy analysis method (SHAM), and the improved spectral-homotopy analysis method (ISHAM), and compared the performance of the three methods with regard to the speed of convergence of the solution (the number of iterations required), computational efficiency, and the ease of application of the method. The results were compared with those obtained using the well-known shooting method and the Matlab bvp4c solver. We found that

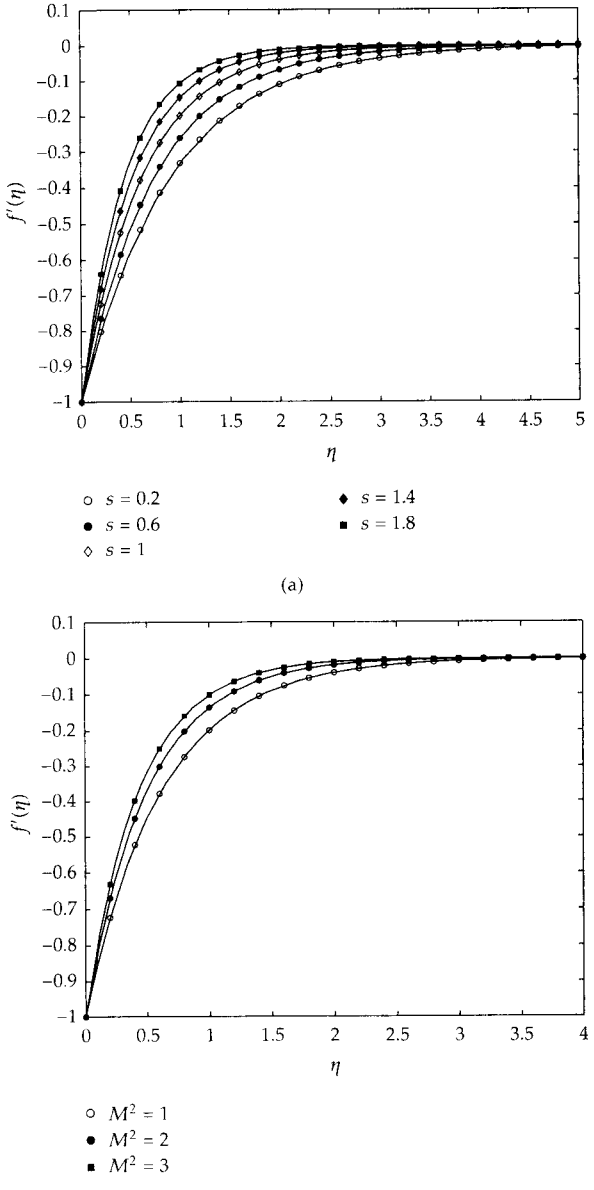

Figure 1: On the comparison between the 2nd-order ISHAM solution (figures) and the bvp4c numerical solution (solid line) for $f(\eta)$ and $\theta(\eta)$ at different values of λ when $M = 1$, $m = 1$, $Pr = 3$, $\lambda_1 = 2$, $s = 1$, $L = 30$, and $N = 150$.

the ISHAM converged at second order. The magnitude of the parameter values used did not affect its performance under the same conditions with the SLM and SHAM. Nevertheless, the ISHAM does not come cheap in terms of the size of the code and computer time, taking about three times as long as the SLM to compute the same result and about double the time taken with the SHAM. The SLM converged at third order, is easy to implement, and has

shown a good level of stability when solving highly nonlinear problems. The SHAM gives good convergence under the same conditions but poor convergence with highly nonlinear problems. It is easy to implement but not as easy as with the SLM.

Results from simulations revealed an excellent agreement between results from the shooting method and the bvp4c. Our findings indicate that the ISHAM is the best approach of the three methods in terms of the accuracy of the results and speed of convergence. Parametric studies for effects of different parameter values in the problems agreed with results present in the literature.

Acknowledgments

The authors wish to acknowledge financial support from the University of KwaZulu-Natal, University of Venda, and the National Research Foundation (NRF).

References

[1] N. Bachok, A. Ishak, and I. Pop, "Unsteady three-dimensional boundary layer flow due to a permeable shrinking sheet," *Applied Mathematics and Mechanics*, vol. 31, no. 11, pp. 1421–1428, 2010.

[2] T.-G. Fang, J. Zhang, and S. S. Yao, "Slip magnetohydrodynamic viscous flow over a permeable shrinking sheet," *Chinese Physics Letters*, vol. 27, no. 12, article 124702, 2010.

[3] T. Fang, S. Yao, J. Zhang, and A. Aziz, "Viscous flow over a shrinking sheet with a second order slip flow model," *Communications in Nonlinear Science and Numerical Simulation*, vol. 15, no. 7, pp. 1831–1842, 2010.

[4] T. Fang and J. Zhang, "Closed-form exact solutions of MHD viscous flow over a shrinking sheet," *Communications in Nonlinear Science and Numerical Simulation*, vol. 14, no. 7, pp. 2853–2857, 2009.

[5] Muhaimin, R. Kandasamy, and A. B. Khamis, "Effects of heat and mass transfer on nonlinear MHD boundary layer flow over a shrinking sheet in the presence of suction," *Applied Mathematics and Mechanics*, vol. 29, no. 10, pp. 1309–1317, 2008.

[6] N. F. M. Noor, S. Awang Kechil, and I. Hashim, "Simple non-perturbative solution for MHD viscous flow due to a shrinking sheet," *Communications in Nonlinear Science and Numerical Simulation*, vol. 15, no. 2, pp. 144–148, 2010.

[7] N. F. Mohd and I. Hashim, "MHD flow and heat transfer adjacent to a permeable shrinking sheet embedded in a porous medium," *Sains Malaysiana*, vol. 38, no. 4, pp. 559–565, 2009.

[8] S. Nadeem and A. Hussain, "MHD flow of a viscous fluid on a nonlinear porous shrinking sheet with homotopy analysis method," *Applied Mathematics and Mechanics*, vol. 30, no. 12, pp. 1569–1578, 2009.

[9] Muhaimin, R. Kandasamy, I. Hashim, and A. B. Khamis, "On the effect of chemical reaction, heat and mass transfer on nonlinear MHD boundary layer past a porous shrinking sheet with suction," *Theoretical and Applied Mechanics*, vol. 36, no. 2, pp. 101–117, 2009.

[10] S. Abbasbandy, "A numerical solution of Blasius equation by Adomian's decomposition method and comparison with homotopy perturbation method," *Chaos, Solitons and Fractals*, vol. 31, no. 1, pp. 257–260, 2007.

[11] N. S. Elgazery, "Numerical solution for the Falkner-Skan equation," *Chaos, Solitons and Fractals*, vol. 35, no. 4, pp. 738–746, 2008.

[12] B. L. Kuo, "Heat transfer analysis for the Falkner-Skan wedge flow by the differential transformation method," *International Journal of Heat and Mass Transfer*, vol. 48, no. 23-24, pp. 5036–5046, 2005.

[13] A. Wazwaz, "The variational iteration method for solving two forms of Blasius equation on a half-infinite domain," *Applied Mathematics and Computation*, vol. 188, no. 1, pp. 485–491, 2007.

[14] S. J. Liao, *Beyond Perturbation*, Introduction to Homotopy Analysis Method, Chapman & Hall, Boca Raton, Fla, USA, 2003.

[15] B. Yao and J. Chen, "A new analytical solution branch for the Blasius equation with a shrinking sheet," *Applied Mathematics and Computation*, vol. 215, no. 3, pp. 1146–1153, 2009.

[16] B. Yao and J. Chen, "Series solution to the Falkner-Skan equation with stretching boundary," *Applied Mathematics and Computation*, vol. 208, no. 1, pp. 156–164, 2009.

[17] A. A. Joneidi, G. Domairry, M. Babaelahi, and M. Mozaffari, "Analytical treatment on magnetohydrodynamic (MHD) flow and heat transfer due to a stretching hollow cylinder," *International Journal for Numerical Methods in Fluids*, vol. 63, no. 5, pp. 548–563, 2010.

[18] A. R. Noiey, N. Haghparast, M. Miansari, and D. D. Ganji, "Application of homotopy perturbation method to the MHD pipe flow of a fourth grade fluid," *Journal of Physics*, vol. 96, no. 1, 2008.

[19] M. Jalaal and D. D. Ganji, "An analytical study on motion of a sphere rolling down an inclined plane submerged in a Newtonian fluid," *Powder Technology*, vol. 198, no. 1, pp. 82–92, 2010.

[20] M. Jalaal, D. D. Ganji, and G. Ahmadi, "An analytical study on settling of non-spherical particles," *Asia-Pacific Journal of Chemical Engineering*, 2010.

[21] M. Jalaal, D. D. Ganji, and G. Ahmadi, "Analytical investigation on acceleration motion of a vertically falling spherical particle in incompressible Newtonian media," *Advanced Powder Technology*, vol. 21, no. 3, pp. 298–304, 2010.

[22] M. Jalaal and D. D. Ganji, "On unsteady rolling motion of spheres in inclined tubes filled with incompressible Newtonian fluids," *Advanced Powder Technology*, vol. 22, pp. 58–67, 2011.

[23] S. M. Moghimi, D. D. Ganji, H. Bararnia, M. Hosseini, and M. Jalaal, "Homotopy perturbation method for nonlinear MHD Jeffery-Hamel problem," *Computers & Mathematics with Applications*, vol. 61, no. 8, pp. 2213–2216, 2011.

[24] S. S. Motsa and S. Shateyi, "A new approach for the solution of three-dimensional magnetohydrodynamic rotating flow over a shrinking sheet," *Mathematical Problems in Engineering*, vol. 2010, Article ID 586340, 15 pages, 2010.

[25] S. S. Motsa, P. Sibanda, and S. Shateyi, "A new spectral-homotopy analysis method for solving a nonlinear second order BVP," *Communications in Nonlinear Science and Numerical Simulation*, vol. 15, no. 9, pp. 2293–2302, 2010.

[26] S. S. Motsa, P. Sibanda, F. G. Awad, and S. Shateyi, "A new spectral-homotopy analysis method for the MHD Jeffery-Hamel problem," *Computers & Fluids*, vol. 39, no. 7, pp. 1219–1225, 2010.

[27] Z. G. Makukula, P. Sibanda, and S. Motsa, "On a new solution for the viscoelastic squeezing flow between two parallel plates," *Journal of Advanced Research in Applied Mathematics*, vol. 2, no. 4, pp. 31–38, 2010.

[28] Z. G. Makukula, P. Sibanda, and S. S. Motsa, "A note on the solution of the von Kármán equations using series and Chebyshev spectral methods," *Boundary Value Problems*, vol. 2010, Article ID 471793, 17 pages, 2010.

[29] Zodwa G. Makukula, Precious Sibanda, and Sandile S. Motsa, "A novel numerical technique for two-dimensional laminar flow between two moving porous walls," *Mathematical Problems in Engineering*, vol. 2010, Article ID 528956, 15 pages, 2010.

[30] Z. G. Makukula, P. Sibanda, and S. Motsa, "On a new quasi-linearisation method for heat transfer in a visco-elastic fluid between parallel plates," in *New Aspects of Fluid Mechanics, Heat Transfer and Environment*, N. Mastorakis, V. Mladenov, and Z. Bojkovic, Eds., 8th iasme/wseas international conference on fluid mechanics & Aerodynamics (FMA '10), pp. 178–186, Tapei, Taiwan, August 2010.

[31] Z. G. Makukula, P. Sibanda, and S. S. Motsa, "On new solutions for heat transfer in a visco-elastic fluid between parallel plates," *International Journal of Mathematical Models and Methods in Applied Sciences*, vol. 4, no. 4, pp. 221–230, 2010.

[32] M. Sajid and T. Hayat, "The application of homotopy analysis method for MHD viscous flow due to a shrinking sheet," *Chaos, Solitons and Fractals*, vol. 39, no. 3, pp. 1317–1323, 2009.

[33] C. Canuto, M. Y. Hussaini, A. Quarteroni, and T. A. Zang, *Spectral Methods in Fluid Dynamics*, Springer, Berlin, Germany, 1988.

[34] L. N. Trefethen, *Spectral Methods in MATLAB*, vol. 10, Society for Industrial and Applied Mathematics, Philadelphia, Pa, USA, 2000.

[35] H. S. Takhar, A. J. Chamkha, and G. Nath, "Natural convection on a thin vertical cylinder moving in a high-porosity ambient medium," *International Journal of Engineering Science*, vol. 41, no. 16, pp. 1935–1950, 2003.

5.3. Summary

In Section 5.1 the spectral homotopy analysis method together with the successive linearisation method were used to find solutions of a fourth-order nonlinear boundary value problem for the two dimensional Laminar flow between two moving porous walls. The results were compared with those available in the literature computed using the homotopy analysis method. The SHAM proved to be more flexible while producing convergent results at low orders of approximation. In Section 5.2, the performances of the SHAM, SLM and ISHAM were compared for a shrinking sheet problem with heat and mass transfer. Comparison was made in terms of computer run times and convergence rates. The ISHAM proved faster convergence than the SLM and SHAM but was more expensive in terms of computer time. It took longer to generate results than both the SLM and SHAM. The SLM has shown to be the easiest to use with shorter CPU run times than the SHAM and also gave faster convergence than the SHAM. However comparison with some existing numerical methods still proves that all three methods are still viable and improved tools to be used in the science and engineering fields.

6

Conclusions

In this thesis we have introduced new semi-numerical methods for solving nonlinear equations in fluid dynamics. The methods have been used to solve different fluid flow problems. A summary of the findings for each problem solved is given below.

In Chapter 3, we solved two parallel plate fluid flow problems. In Section 3.1, we considered the steady laminar flow of a third grade fluid with heat transfer through a channel using the successive linearisation method and the improved spectral homotopy analysis method. The convergence rates of the methods were compared against the exact results. It was observed that both methods converged rapidly with the improved spectral homotopy analysis method performing better for large parameter values. The study showed the accuracy and efficiency of the method for a third grade fluid problem. In this study, my contribution was to find solutions of the equations using the improved spectral homotopy analysis method and to write a draft version of this article.

In Section 3.2 the third grade fluid flow equations were solved using the standard homotopy analysis method and the spectral homotopy analysis method. Comparing the solutions showed that the spectral homotopy analysis method is computationally more efficient compared to

the homotopy analysis method. In this paper both the SHAM and the MSHAM were used and my contribution was to solve the equations using the both methods.

In Section 3.3, the nonlinear differential equation that describes squeezing flow between two infinite plates was successfully solved using the successive linearisation method. A comparison of the successive linearisation method results against those previously obtained using the HAM (Ran et al., 2009) and the bvp4c solver was made. The comparison showed that the successive linearisation method converges faster than the HAM and its efficiency is not affected by the magnitude of the parameters innate to the problem.

In Chapter 4, solutions of rotating disk flows were sought using the new methods. In Section 4.1, a strongly nonlinear system of differential equations governing the Reiner-Rivlin fluid with Joule heating and viscous dissipation was solved using the improved spectral homotopy analysis method. A comparison with the original spectral homotopy analysis method was made. The improved spectral homotopy analysis method converged to the numerical solutions at the second orders for all flow parameters while the spectral homotopy analysis method converged at the eighth order for some of the flow parameters. This shows that the improved spectral homotopy analysis method is more accurate than the spectral homotopy analysis method. In this study, my input was to solve the problem using the improved spectral homotopy analysis method, and to write a draft version of the paper.

In Section 4.2, we used the spectral homotopy analysis method and the successive linearisation method to solve the von Kármán nonlinear equations for swirling flow with suction/injection across the disk walls and an applied magnetic field. The results were benchmarked against those obtained using the bvp4c, the HAM and the homotopy Padé methods. The comparison showed a better performance in terms of convergence rates and accuracy of the spectral ho-

motopy analysis method and successive linearisation method compared to both the HAM and HAM-Padé. Comparison with results in the literature (Turkyilmazoglu, 2010), showed that the successive linearisation solutions had no oscillations compared to the HAM solutions. The successive linearisation method also gave converging results at lower orders than the spectral homotopy analysis method. In this article, my contribution was to use both the spectral homotopy analysis method and successive linearisation method to find solutions of the classical von Kármán equations.

In Section 4.3, the successive linearisation method was used to find the solution of the laminar heat transfer problem of a rotating disk in a forced vortex. The velocity components were computed and the study showed the rapid convergence of the successive linearisation method solutions to the numerical results.

In Chapter 5, we solved fluid flow problems in porous media. In Section 5.1, a fourth-order nonlinear boundary value problem for two-dimensional laminar flow between two moving porous walls was investigated using the spectral homotopy analysis method and the successive linearisation method. The problem has been studied by Xu et al. (2010) and Dinarvand et al. (2008). Again the successive linearisation method and spectral homotopy analysis method were shown to be efficient and flexible in solving a fourth-order nonlinear equation.

In Section 5.2, a comparison of the performances of the successive linearisation method, spectral homotopy analysis method and improved spectral homotopy analysis method in solving the MHD flow problem past a shrinking sheet with heat and mass transfer in the presence of a chemical reaction was made. The comparison made was with regard to the speed of convergence of the solution (the number of iterations required), computational efficiency and the ease of application of the method. The results were benchmarked against those obtained

using the shooting method and the bvp4c.

The improved spectral homotopy analysis method solutions converged at second order and its performance was not affected by the magnitude of the parameter values under the same conditions as the successive linearisation method and spectral homotopy analysis method. However, the improved spectral homotopy analysis method required more computational work in terms of the size of the code. The successive linearisation method showed stability and ease of application when solving highly nonlinear problems. The spectral homotopy analysis method's convergence was quite good also but shown to be less robust for highly nonlinear problems. It is easier to implement than the improved spectral homotopy analysis method, but not as easy as with the successive linearisation method. An excellent agreement was observed with results from the shooting method and the bvp4c. From this investigation, the improved spectral homotopy analysis method performed better than the spectral homotopy analysis method and successive linearisation method in terms of the accuracy of the results and speed of convergence.

From this study we may conclude that in comparison to some existing methods, the successive linearisation method, spectral homotopy analysis method, and improved spectral homotopy analysis method are efficient, accurate and robust. The equations solved ranged from linear to strongly nonlinear and to systems of equations. The methods generated accurate results at low orders, such as with two terms for the improved spectral homotopy analysis method and with three terms for the successive linearisation method.

However, the methods need to be extended to other types of equations such as, time-dependent evolution equations, partial differential equations and difference equations. Also, except in the case of the spectral homotopy analysis method and improved spectral homotopy analysis

method, a strong mathematical motivation for the successive linearisation method needs to be further developed.

Bibliography

Abassy, T. A. (2010a). Improved Adomian decomposition method. *Computers and Mathematics with Applications 59*, 42–54.

Abassy, T. A. (2010b). Modified variational iteration method (nonlinear homogeneous initial value problem). *Computers and Mathematics with Applications 59*, 912–918.

Abassy, T. A., M. A. El-Tawil, and H. K. Saleh (2007). The solution of Burgers' and good Boussinesq equations using ADM-Padé technique. *Chaos, Solitons & Fractals 32*, 1008–1026.

Abassy, T. A., M. A. El-Tawil, and H. E. Zoheiry (2007a). Exact solutions of some nonlinear partial differential equations using the variational iteration method linked with Laplace transforms and the Padé technique. *Computers and Mathematics with Applications 54*, 940–954.

Abassy, T. A., M. A. El-Tawil, and H. E. Zoheiry (2007b). Modified variational iteration method for Boussinesq equation. *Computers and Mathematics with Applications 54*, 955–965.

Abassy, T. A., M. A. El-Tawil, and H. E. Zoheiry (2007c). Solving nonlinear partial differential

equations using the modified variational iteration Padé technique. *Journal of Computational and Applied Mathematics 207*, 73–91.

Abassy, T. A., M. A. El-Tawil, and H. E. Zoheiry (2007d). Toward a modified variational iteration method. *Journal of Computational and Applied Mathematics 207*, 137–147.

Abbasbandy, S. (2006a). The application of the homotopy analysis method to nonlinear equations arising in heat transfer. *Physics Letters A 360*, 109–113.

Abbasbandy, S. (2006b). Homotopy perturbation method for quadratic Riccati differential equation and comparison with Adomian's decomposition method. *Applied Mathematics and Computation 172*, 485–490.

Abbasbandy, S. (2007a). The application of the homotopy analysis method to solve a generalized Hirota-Satsuma coupled KdV equation. *Physics Letters A 361*, 478–483.

Abbasbandy, S. (2007b). Homotopy analysis method for heat radiation equations. *International Communications in Heat and Mass Transfer 34*, 380–387.

Abbasbandy, S. (2008). Soliton solutions for the 5th-order KdV equation with the homotopy analysis method. *Nonlinear Dynamics 51*, 83–87.

Abedini, A. A. and R. Ghiassi (2010). A three-dimensional finite volume model for shallow water flow simulation. *Australian Journal of Basic and Applied Sciences 4*(8), 3208–3215.

Abia, L. M. and J. C. López-Marcos (1995). Runge-Kutta methods for age-structured population models. *Applied Numerical Mathematics 17*, 1–17.

Aboiyar, T., E. H. Georgoulis, and A. Iske (2006). High order WENO finite volume schemes

using polyharmonic spline reconstruction. In *Proceedings of the international conference on numerical analysis and approximation theory: NAAT2006, CLUJ-NAPOCA (Romania).*

Adomian, G. (1976). Nonlinear stochastic differential equations. *Journal of Mathematical Analysis and Applications 55*, 441–452.

Adomian, G. (1991). A review of the decomposition method and some recent results for nonlinear equations. *Computers and Mathematics with Applications 21*, 101–127.

Adomian, G. (1994). *Solving frontier problems of physics: The decomposition method*. Kluwer Academic Publishers, Boston.

Al-Mdallal, Q. M., M. I. Syam, and M. N. Anwar (2010). A collocation-shooting method for solving fractional boundary value problems. *Communications in Nonlinear Science and Numerical Simulation 15*, 3814–3822.

Alharbi, A. and E. S. Fahmy (2010). ADM-Padé solutions for generalized Burgers and Burgers-Huxley systems with two coupled equations. *Journal of Computational and Applied Mathematics 233*, 2071–2080.

Ali, J., S. Islam, S. Islam, and G. Zaman (2010). The solution of multipoint boundary value problems by the optimal homotopy asymptotic method. *Computers and Mathematics with Applications 59*, 2000–2006.

Alizadeh, E., M. Farhadi, K. Sedighi, H. R. Ebrahimi-Kebria, and A. Ghafourian (2009). Solution of the Falkner - Skan equation for wedge by Adomian decomposition method. *Communications in Nonlinear Science and Numerical Simulation 14*, 724–733.

Allan, F. M. (2007). Derivation of the adomian decomposition method using the homotopy analysis method. *Applied Mathematics and Computation 190*, 6–14.

Alvarez, J. and J. Rojo (2003). An improved class of generalized Runge-Kutta methods for stiff problems. Part II: The separated system case. *Journal of Computational and Applied Mathematics 159*, 717–758.

Alvarez, J. and J. Rojo (2004). An improved class of generalized Runge-Kutta-Nyström methods for special second-order differential equations. *Communications in Nonlinear Science and Numerical Simulation 9*, 217–227.

Aminataei, A. and S. S. Hosseini (2007). The comparison of the stability of Adomian decomposition method with numerical methods of equation solution. *Applied Mathematics and Computation 186*, 665–669.

Ampadu, E. (2007). Implementation of some finite difference methods for the pricing of derivatives using C++ programming. MSc Thesis, Worcester Polytechnic Institute.

Ariel, P. D. (2007a). Axisymmetric flow due to a stretching sheet with partial slip. *Computers and Mathematics with Applications 54*, 1169–1183.

Ariel, P. D. (2007b). The three-dimensional flow past a stretching sheet and the homotopy perturbation method. *Computers and Mathematics with Applications 54*, 920–925.

Ariel, P. D. (2009). Extended homotopy perturbation method and computation of flow past a stretching sheet. *Computers and Mathematics with Applications 58*, 2402–2409.

Ariel, P. D., T. Hayat, and S. Asghar (2006). Homotopy perturbation method and axisymmet-

ric flow over a stretching sheet. *International Journal of Nonlinear Sciences and Numerical Simulation 7*, 399–406.

Arikoglu, A. and I. Ozkol (2005). Inner-outer matching solution of Blasius equation by DTM. *Aircraft Engineering and Aerospace Technology: An International Journal 77*(4), 298–301.

Arikoglu, A. and I. Ozkol (2006). Solution of difference equations by using differential transform method. *Applied Mathematics and Computation 174*, 1216–1228.

Arslanturk, C. (2005). A decomposition method for fins efficiency of convective straight fins with temperature-dependent thermal conductivity. *International Communications in Heat and Mass Transfer 32*, 831–841.

Asai, A. (2006). A shooting method for nonlinear heat transfer using automatic differentiation. *Journal of Computational and Applied Mathematics 180*, 264–269.

Ashgriz, N. and J. Mostaghimi (2001). An introduction to computational fluid dynamics. http://mussl.mie.utoronto.ca, (5 August 2011).

Attia, H. A. (2005). The effect of suction and injection on the unsteady flow between two parallel plates with variable properties. *Tamkang Journal of Science and Engineering 8*(1), 17–22.

Ayaz, F. (2003). On the two-dimensional differential transform method. *Journal of Computational and Applied Mathematics 143*, 361–374.

Babolian, E., M. Bromilow, R. England, and M. Saravi (2007). A modification of pseudo-spectral method for solving a linear ODE with singularity. *Applied Mathematics and Computation 188*, 1260–1266.

Balsara, D. S. (2009). Divergence-free reconstruction of magnetic fields and WENO schemes for magnetohydrodynamics. *Journal of Computational Physics 228*, 5040–5056.

Barth, T. and M. Ohlberger (2004). *Finite volume methods: Foundation and analysis*. John Wiley & Sons, Ltd.

Basak, K. C., P. C. Ray, and R. K. Bera (2009). Solution of nonlinear Klein-Gordon equation with a quadratic nonlinear term by Adomian decomposition method. *Communications in Nonlinear Science and Numerical Simulation 14*, 718–723.

Bashier, E. B. M. and K. C. Patidar (2011). A novel fitted operator finite difference method for a singularly perturbed delay parabolic partial differential equation. *Applied Mathematics and Computation 217*, 4728–4739.

Bataineh, A. S., M. S. M. Noorani, and I. Hashim (2009). On a new reliable modification of homotopy analysis method. *Communications in Nonlinear Science and Numerical Simulation 14*, 409–423.

Belgacem, F. B. and M. Grundmann (1998). Approximation of the wave and electromagnetic diffusion equations by spectral methods. *The SIAM Journal on Scientific Computing 20*, 13–32.

Bellman, R. (1966). *Perturbation techniques in mathematics, physics and engineering*. Holt, Rinehart and Winston, Inc., New York.

Bender, C. M., K. A. Milton, S. S. Pinsky, and L. M. Simmons (1989). A new perturbative approach to nonlinear problems. *Journal of Mathematical Physics 30*, 1447–1455.

Benton, E. R. (1966). On the flow due to a rotating disk. *Journal of Fluid Mechanics 24*, 781 – 800.

Biazar, J. and H. Aminikhah (2009). A new technique for solving nonlinear integral-differential equations. *Computers and Mathematics with Applications 58*, 2084–2090.

Biazar, J., B. Ghanbari, and M. G. Porshokouhi (2011). He's homotopy perturbation method: A strongly promising method for solving nonlinear systems of the mixed Volterra-Fredholm integral equations. *Computers and Mathematics with Applications 61*, 1016–1023.

Boyd, J. P. (2000). *Chebyshev and Fourier spectral methods*. Dover Publications Inc., New York.

Bratsos, A., M. Ehrhardt, and I. T. Famelis (2008). A discrete Adomian decomposition method for discrete nonlinear Schrödinger equations. *Applied Mathematics and Computation 197*, 190–205.

Brinkman, H. C. (1947). A calculation of the viscous force exerted by a flowing fluid on a dense swarm of particles. *Applied Scientific Research A 1*, 27–34.

Budd, C., O. Koch, and E. Weinmüller (2006). From nonlinear PDEs to singular ODEs. *Applied Numerical Mathematics 56*, 413–422.

Butcher, J. C. (1987). *The numerical analysis of ordinary differential equations*. John Wiley & Sons, Great Britain.

Canuto, C., M. Y. Hussaini, A. Quarteroni, and T. A. Zang (1988). *Spectral methods in fluid dynamics*. Springer-Verlag, Berlin.

Canuto, C., M. Y. Hussaini, A. Quarteroni, and T. A. Zang (2007). *Spectral methods: Evolution to complex geometries and applications to fluid dynamics*. Springer-Verlag, Berlin.

Capdeville, G. (2008). A Hermite upwind WENO scheme for solving hyperbolic conservation laws. *Journal of Computational Physics 227*, 2430–2454.

Cash, J. R. (1996). Runge-Kutta methods for the solution of stiff two-point boundary value problems. *Applied Numerical Mathematics 22*, 165–177.

Catal, S. (2008). Solution of free vibration equations of beam on elastic soil by using differential transform method. *Applied Mathematical Modelling 32*, 1744–1757.

Cebeci, T. and J. P. Shao (2003). A non-iterative method for boundary-layer equations - part II: Two-dimensional laminar and turbulent flows. *International Journal for Numerical Methods in Fluids 43*, 1139–1148.

Chen, W. and Z. Lu (2004). An algorithm for Adomian decomposition method. *Applied Mathematics and Computation 159*, 221–235.

Cheng, T. S. and K. S. Lee (2005). Numerical simulations of underexpanded supersonic jet and free shear layer using WENO schemes. *International Journal of Heat and Fluid Flow 26*, 755–770.

Chih-Wen, C., C. Jiang-Ren, and L. Chein-Shan (2006). The lie-group shooting method for boundary layer equations in fluid mechanics. *Journal of Hydrodynamics, Series B 18*(3), 103–108.

Chowdhury, M. S. H. and I. Hashim (2009a). Application of homotopy-perturbation method to Klein-Gordon and sine-Gordon equations. *Chaos, Solitons & Fractals 39*, 1928–1935.

Chowdhury, M. S. H. and I. Hashim (2009b). Application of multistage homotopy-perturbation method for the solutions of the Chen system. *Nonlinear Analysis: Real World Applications 10*, 381–391.

Chowdhury, M. S. H., T. H. Hassan, and S. Mawa (2010). A new application of homotopy perturbation method to the reaction-diffusion Brusselator model. *Procedia Social and Behavioral Sciences 8*, 648–653.

Chun, C., H. Jafari, and Y. I. Kim (2009). Numerical method for the wave and nonlinear diffusion equations with the homotopy perturbation method. *Computers and Mathematics with Applications 57*, 1226–1231.

Cochran, W. G. (1934). The flow due to a rotating disk. *Mathematical Proceedings of the Cambridge Philosophical Society 30*, 365 – 375.

Collin, M. and A. Schett (1983). OSIRIS : A Runge-Kutta solver of systems of ordinary differential equations. Technical report INDC(FR) 61/L, Center Etudes of Bruyères-le-Châtel.

Cueto-Felgueroso, L. and R. Juanes (2009). Adaptive rational spectral methods for the linear stability analysis of nonlinear fourth-order problems. *Journal of Computational Physics 28*(17), 6536–6552.

Darcy, H. (1937). *The flow of fluids through porous media*. McGraw-Hill, New York.

Dargush, G. F. and M. M. Grigoriev (2000). A poly-region boundary element method for two-dimensional Boussinesq flows. *Computational Methods in Applied Mechanics and Engineering 190*, 1261–1287.

de Weck, O. and I. Y. Kim (2004). Finite element method. http://web.mit.edu, (17 July 2011).

Dehghan, M., A. Hamidi, and M. Shakourifar (2007). The solution of coupled Burgers' equations using Adomian-Padé technique. *Applied Mathematics and Computation 189*, 1034–1047.

Dehghan, M. and R. Salehi (2010). Solution of a nonlinear time-delay model in biology via semi-analytical approaches. *Computer Physics Communications 181*, 1255–1265.

Dehghan, M. and F. Shakeri (2008a). Application of He's variational iteration method for solving the Cauchy reaction-diffusion problem. *Journal of Computational and Applied Mathematics 214*, 435–446.

Dehghan, M. and F. Shakeri (2008b). Approximate solution of a differential equation arising in astrophysics using the variational iteration method. *New Astronomy 13*, 53–59.

Dehghan, M., M. Shakourifar, and A. Hamidi (2009). The solution of linear and nonlinear systems of Volterra functional equations using Adomian-Padé technique. *Chaos, Solitons & Fractals 39*, 2509–2521.

Devi, S. P. A. and R. U. Devi (2011). On hydromagnetic flow due to a rotating disk with radiation effects. *Nonlinear Analysis: Modelling and Control 16*(1), 17–29.

Dinarvand, S., A. Doosthoseini, E. Doosthoseini, and M. M. Rashidi (2008). Comparison of HAM and HPM methods for Berman's model of two-dimensional viscous flow in porous channel with wall suction or injection. *Advances in Theoretical and Applied Mechanics 1*(7), 337–347.

Domairry, G. and N. Nadim (2008). Assessment of homotopy analysis method and homotopy perturbation method in nonlinear heat transfer equation. *International Communications in Heat and Mass Transfer 35*, 93–103.

Duffy, D. J. (2004). A critique of the Crank Nicolson scheme: Strengths and weaknesses for financial instrument pricing. http://www.datasim-component.com, (19 July 2011).

Ebaid, A. E. (2010). Approximate periodic solutions for the nonlinear relativistic harmonic oscillator via differential transformation method. *Communications in Nonlinear Science and Numerical Simulation 15*, 1921–1927.

Ebaid, A. E. (2011). A reliable aftertreatment for improving the differential transformation method and its application to nonlinear oscillators with fractional nonlinearities. *Communications in Nonlinear Science and Numerical Simulation 16*, 528–536.

Ekström, E., P. Lötstedt, and J. Tysk (2009). Boundary values and finite difference methods for the single factor term structure equation. *Applied Mathematical Finance 16*(3), 253–259.

El-Bashir, T. (2006). *Fluid flow at small Reynolds number: Numerical applications*. Hikari Ltd, Bulgaria.

El-Gebeily, M. A. and B. S. Attil (2003). An iterative shooting method for a certain class of singular two-point boundary value problems. *Computers and Mathematics with Applications 45*, 69–76.

El-Hawary, H. M. (2001). A deficient spline function approximation for boundary layer flow. *International Journal of Numerical Methods for Heat & Fluid Flow, 11*, 227–236.

Eldho, T. I. and D.-L. Young (2001). Solution of stokes flow problem using dual reciprocity boundary element method. *Journal of the Chinese Institute of Engineers 24*(2), 141–150.

Elishakoff, I. and Y. Ren (2003). *Finite elements methods for structures with large stochastic variations*. Oxford University Press Inc., New York.

Engmann, J., C. Servais, and A. S. Burbidge (2005). Squeeze flow theory and applications to rheometry: A review. *Journal of Non-Newtonian Fluid Mechanics 132*, 1–27.

Esmaeilpour, M. and D. D. Ganji (2010). Solution of the Jeffery-Hamel flow problem by optimal homotopy asymptotic method. *Computers and Mathematics with Applications 59*, 3405–3411.

Ferracina, L. (2005). *Monotonicity and boundedness in general Runge-Kutta methods*. PhD Thesis, Thomas Stieltjes Institute for Mathematics.

Ferzinger, J. H. and M. Perić (2002). *Computational methods for fluid dynamics*. Springer, New York.

Fletcher, C. A. J. (1988). *Computational techniques for fluid dynamics*, Volume 1. Springer-Verlag, New York.

Florez, W., H. Power, and F. Chejne (2003). Multi-domain DRM boundary element method for non-isothermal non-Newtonian Stokes flow with viscous dissipation. *International Journal of Numerical Methods for Heat & Fluid Flow 13*(6), 736–768.

Frusteri, F. and E. Osalusi (2007). On MHD and slip flow over a rotating porous disk with variable properties. *International Communications in Heat and Mass Transfer 34*, 492–501.

Ganji, D. D. (2006). The application of He's homotopy perturbation method to nonlinear equations arising in heat transfer. *Physics Letter A 355*, 337–341.

Ganji, Z. Z., D. D. Ganji, and M. Esmaeilpour (2009). Study on nonlinear Jeffery-Hamel flow by He's semi-analytical methods and comparison with numerical results. *Computers and Mathematics with Applications 58*, 2107–2116.

Geiser, J. (2005). Introduction to the finite difference and finite element methods, convergence theory, applications. http://www.mathematik.hu-berlin.de, (19 July 2011).

Geng, F. (2010). A modified variational iteration method for solving Riccati differential equations. *Computers and Mathematics with Applications 60*, 1868–1872.

Ghasemi, M., M. T. Kajani, and E. Babolian (2007). Application of He's homotopy perturbation method to nonlinear integro-differential equations. *Applied Mathematics and Computation 188*, 538–548.

Gheorghiu, C. I. (2007). Spectral methods for differential problems. http://www.ictp.acad.ro, (17 July 2011).

Ghorbani, A. and S. Momani (2010). An effective variational iteration algorithm for solving Riccati differential equations. *Applied Mathematics Letters 23*, 922–927.

Ghorbani, A. and J. Saberi-Nadjafi (2008). Exact solutions for nonlinear integral equations by a modified homotopy perturbation method. *Computers and Mathematics with Applications 56*, 1032–1039.

Ghorbani, A. and J. Saberi-Nadjafi (2009). An effective modification of He's variational iteration method. *Nonlinear Analysis: Real World Applications 10*, 2828–2833.

Gökdoğan, A., M. Merdan, and A. Yildirim (2011). The modified algorithm for the differential transform method to solution of Genesio systems. *Communications in Nonlinear Science and Numerical Simulation* (doi:10.1016/j.cnsns.2011.03.039).

Golbabai, A. and M. Javidi (2007). Application of He's homotopy perturbation method for nth-order integro-differential equations. *Applied Mathematics and Computation 190*, 1409–1416.

Grandclément, P. and J. Novak (2009). Spectral methods for numerical relativity. *Living Reviews in Relativity 12*(1), 107 pages.

Grecu, L., G. Demian, and M. Demian (2009). Two boundary element approaches for the compressible fluid flow around a non-lifting body. *Buletin Ştiinţific, Universitatea Politehnica din Bucureşti: Series A 71*(1), 73–83.

Grosan, T. and I. Pop (2011). Axisymmetric mixed convection boundary layer flow past a vertical cylinder in a nanofluid. *International Journal of Heat and Mass Transfer 54*, 3139–3145.

Ha, S. N. (2001). A nonlinear shooting method for two-point boundary value problems. *Computers and Mathematics with Applications 42*, 1411–1420.

Ha, Y., Y. J. Kim, and T. G. Myers (2008). On the numerical solution of a driven thin film equation. *Journal of Computational Physics 227*, 7246–7263.

Haelterman, R., J. Vierendeels, and D. V. Heule (2009). A generalization of the Runge-Kutta iteration. *Journal of Computational and Applied Mathematics 224*, 152–167.

Hale, N. (2006). A sixth-order extension to the MATLAB package bvp4c of J. Kierzenka and L. Shampine. MSc Thesis, Imperial College London.

Hale, N. and D. R. Moore (2008). A sixth-order extension to the MATLAB package bvp4c of J. Kierzenka and L. Shampine. Technical report NA 08/04, Oxford University Computing Laboratory, UK.

Harley, C. and E. Momoniat (2008). First integrals and bifurcations of a Lane-Emden equation of the second kind. *Journal of Mathematical Analysis and Applications 344*, 757–764.

Hashim, I. (2006a). Adomian decomposition method for solving BVPs for fourth-order integro-differential equations. *Journal of Computational and Applied Mathematics 193*, 658–664.

Hashim, I. (2006b). Comparing numerical methods for the solutions of two-dimensional diffusion with an integral condition. *Applied Mathematics and Computation 181*, 880–885.

Hashim, I., M. S. H. Chowdhury, and S. Mawa (2008). On multistage homotopy-perturbation method applied to nonlinear biochemical reaction model. *Chaos, Solitons & Fractals 36*, 823–827.

Hashim, I., M. S. M. Noorani, R. Ahmad, S. A. Bakar, E. S. Ismail, and A. M. Zakaria (2006). Accuracy of the Adomian decomposition method applied to the Lorenz system. *Chaos, Solitons & Fractals 28*, 1149–1158.

Hassan, S. M. and N. M. Alotaibi (2010). Solitary wave solutions of the improved KdV equation by VIM. *Applied Mathematics and Computation 217*, 2397–2403.

Hayat, T., Z. Abbas, M. Sajid, and S. Asghar (2007). The influence of thermal radiation

on MHD flow of a second grade fluid. *International Journal of Heat Mass Transfer 50*, 931–941.

Hayat, T., Q. Hussain, and T. Javed (2009). The modified decomposition method and Padé approximants for the MHD flow over a nonlinear stretching sheet. *Nonlinear Analysis: Real World Applications 10*, 966–973.

Hayat, T., M. Khan, M. Sajid, and S. Asghar (2007). Rotating flow of a third grade fluid in a porous space with hall current. *Nonlinear Dynamics 49*, 83–91.

Hayat, T. and M. Sajid (2007a). Analytic solution for axisymmetric flow and heat transfer of a second grade fluid past a stretching sheet. *International Journal of Heat Mass Transfer 50*, 75–84.

Hayat, T. and M. Sajid (2007b). On analytic solution for thin film flow of a forth grade fluid down a vertical cylinder. *Physics Letters A 361*, 316–322.

He, J. H. (1997). A new approach to nonlinear partial differential equations. *Communications in Nonlinear Science and Numerical Simulation 2*, 230–235.

He, J. H. (1998a). An approximation solution technique depending upon an artificial parameter. *Communications in Nonlinear Science and Numerical Simulation 3*, 92–97.

He, J. H. (1998b). Newton-like method for solving algebraic equations. *Communications in Nonlinear Science and Numerical Simulation 3*, 106–109.

He, J. H. (1999a). Approximate analytical solution of Blasius' equation. *Communications in Nonlinear Science and Numerical Simulation 4*(1), 75–78.

He, J. H. (1999b). Homotopy perturbation technique. *Computer Methods in Applied Mechanics 178*, 257–262.

He, J. H. (1999c). Variational iteration method - A kind of nonlinear analytical technique: Some examples. *International Journal of Non-Linear Mechanics 34*(4), 699–708.

He, J. H. (2003). Homotopy perturbation method: A new nonlinear analytical technique. *Applied Mathematics and Computation 135*, 73–79.

He, J. H. (2004). Comparison of homotopy perturbation and homotopy analysis method. *Journal of Computational and Applied Mathematics 156*, 527–539.

He, J. H. (2005a). Application of homotopy perturbation method to nonlinear wave equations. *Chaos Solitons & Fractals 26*, 695–700.

He, J. H. (2005b). Homotopy perturbation method for bifurcation of nonlinear problems. *International Journal of Communications in Nonlinear Science and Numerical Simulation 6*, 2007–208.

He, J. H. (2006). Homotopy perturbation method for solving boundary value problems. *Physics Letters A 350*, 87–88.

Hesthaven, J. S., S. Gottlieb, and D. Gottlieb (2007). *Spectral methods for time-dependent problems*. Cambridge University Press, United Kingdom.

Hollborn, S. (2011). Reconstructions from backscatter data in electric impedance tomography. *Inverse Problems 27*(4), doi:10.1088/0266–5611/27/4/045007.

Holmes, M. H. (1995). *Introduction to perturbation methods*. Springer-Verlag, New York.

Hosseini, M. M. (2006). Adomian decomposition method with Chebyshev polynomials. *Applied Mathematics and Computation 175*, 1685–1693.

Hussaini, M. Y. and T. A. Zang (1987). Spectral methods in fluid dynamics. *Annual Review of Fluid Mechanics 19*, 339–367.

Idrees, M., S. Islam, S. Haqa, and S. Islam (2010). Application of the optimal homotopy asymptotic method to squeezing flow. *Computers and Mathematics with Applications 59*, 3858–3866.

Inc, M. (2008). The approximate and exact solutions of the space- and time-fractional Burgers equations with initial conditions by variational iteration method. *Journal of Mathematical Analysis and Applications 345*, 476–484.

Iqbal, S., M. Idrees, A. M. Siddiqui, and A. R. Ansari (2010). Some solutions of the linear and nonlinear Klein-Gordon equations using the optimal homotopy asymptotic method. *Applied Mathematics and Computation 216*, 2898–2909.

Iqbal, S. and A. Javed (2011). Application of optimal homotopy asymptotic method for the analytic solution of singular Lane-Emden type equation. *Applied Mathematics and Computation 217*, 7753–7761.

Iqbal, S., A. Zeb, A. M. Siddiqui, and T. Haroon (2011). A numerical study of the flow with heat transfer of a pseudoplastic fluid between parallel plates. *Journal of Quantum Information Science 1*, 18–25.

Jafari, H. and V. Daftardar-Gejji (2006). Positive solutions of nonlinear fractional boundary value problems using Adomian decomposition method. *Applied Mathematics and Computation 180*, 700–706.

Jang, B. (2010). Solving linear and nonlinear initial value problems by the projected differential transform method. *Computer Physics Communications 181*, 848–854.

Javidi, M. and A. Golbabai (2007). A numerical solution for solving system of Fredholm integral equations by using homotopy perturbation method. *Applied Mathematics and Computation 189*, 1921–1928.

Joneidi, A. A., D. D. Ganji, and M. Babaelahi (2009). Differential transformation method to determine fin efficiency of convective straight fins with temperature dependent thermal conductivity. *International Communications in Heat and Mass Transfer 36*, 757–762.

Juang, H. M. H. and M. Kanamitsu (1994). The NMC regional spectral model. *Monthly Weather Review 122*, 3–26.

Kadalbajoo, M. K. and K. C. Patidar (2001). Variable mesh spline approximation method for solving singularly perturbed turning point problems having boundary layer(s). *Computers and Mathematics with Applications 42*, 1439–1453.

Kadalbajoo, M. K. and K. C. Patidar (2002). Numerical solution of singularly perturbed two-point boundary value problems by spline in tension. *Applied Mathematics and Computation 131*, 299–320.

Kadalbajoo, M. K. and K. C. Patidar (2006). ε-Uniformly convergent fitted mesh finite difference methods for general singular perturbation problems. *Applied Mathematics and Computation 179*, 248–266.

Kafoussias, N., A. Karabis, and M. Xenos (1999). Numerical study of two dimensional laminar boundary layer compressible flow with pressure gradient and heat and mass transfer. *International Journal of Engineering Science 37*, 1795–1812.

Kanth, A. S. V. R. and K. K. Aruna (2008). Solution of singular two-point boundary value problems using differential transformation method. *Physics Letters A 372*, 4671–4673.

Karim, M. M., M. M. Rahman, and M. A. Alim (2011). Comparative study between flows around sphere and pod using finite volume method. *Journal of Naval Architecture and Marine Engineering 8*, 49–58.

Katsikadelis, J. T. (2002). *Boundary elements: Theory and applications*. Elsevier science Ltd, United Kingdom.

Kevorkian, J. and J. D. Cole (1981). *Perturbation methods in applied mathematics*. Springer-Verlag, New York.

Khan, Y. and Q. Wu (2011). Homotopy perturbation transform method for nonlinear equations using He's polynomials. *Computers and Mathematics with Applications 61*, 1963–1967.

Kierzenka, J. and L. F. Shampine (2001). A BVP solver based on residual control and the MATLAB PSE. *ACM Transactions on Mathematical Software 27*(3), 299–316.

Kierzenka, J. and L. F. Shampine (2008). A BVP solver that controls residual and error. *Journal of Numerical Analysis, Industrial and Applied Mathematics 3*(1-2), 27–41.

Kikani, J. (1989). *Application of boundary element method to streamline generation and pressure transient testing*. PhD Thesis, Stanford University.

Korostyshevskiy, V. R. and T. Wanner (2007). A hermite spectral method for the computation of homoclinic orbits and associated functionals. *Journal of Computational and Applied Mathematics 206*, 986–1006.

Kurulay, M. and M. Bayram (2010). Approximate analytical solution for the fractional modified KdV by differential transform method. *Communications in Nonlinear Science and Numerical Simulation 15*, 1777–1782.

Lebedev, K. A. and E. G. Lovtsov (2002). Mathematical simulation of a stationary electrodiffusion kinetics in multilayer ion-exchange membrane systems with the help of the numerical shooting parallel method continued by parameters. *Desalination 147*, 393–398.

Lee, J. and D. H. Kim (2005). An improved shooting method for computation of effectiveness factors in porous catalysts. *Chemical Engineering Science 60*, 5569–5573.

Liang, S. and H. Chen (1999). Numerical simulation of underwater blast-wave focusing using a high-order scheme. *The American Institute of Aeronautics and Astronautics 37*, 1010–1013.

Liao, S. J. (1992). *The proposed homotopy analysis technique for the solution of nonlinear problems*. PhD Thesis, Shanghai Jiao Tong University.

Liao, S. J. (2003a). An analytic approximate technique for free oscillations of positively damped systems with algebraically decaying amplitude. *International Journal of Non-Linear Mechanics 38*, 1173–1183.

Liao, S. J. (2003b). *Beyond perturbation: Introduction to homotopy analysis method.* Chapman & Hall/CRC Press.

Liao, S. J. (2009). Notes on the homotopy analysis method: Some definitions and theorems. *Communications in Nonlinear Science and Numerical Simulation 14*, 983–997.

Liao, S. J. (2010). An optimal homotopy-analysis approach for strongly nonlinear differential equations. *Communications in Nonlinear Science and Numerical Simulation 15*, 2003–2016.

Liu, C. S. (2001). Cone of nonlinear dynamical system and group preserving schemes. *International Journal of Non-Linear Mechanics 36*, 1047–1068.

Liu, C. S. and J. R. Chang (2008). The lie-group shooting method for multiple-solutions of Falkner-Skan equation under suction-injection conditions. *International Journal of Non-Linear Mechanics 43*, 844–851.

Liu, Y. (2009). Adomian decomposition method with orthogonal polynomials: Legendre polynomials. *Mathematical and Computer Modelling 49*, 1268–1273.

Lough, M. F., S. H. Lee, and J. Kamath (1998). An efficient boundary integral formulation for flow through fractured porous media. *Journal of Computational Physics 143*, 462–483.

Lubuma, J. M. S. and K. C. Patidar (2006). Uniformly convergent non-standard finite difference methods for self-adjoint singular perturbation problems. *Journal of Computational and Applied Mathematics 191*, 228 238.

Ludwig, M., J. Koch, and B. Fischer (2008). An application of the finite volume method to the bio-heat-transfer-equation in premature infants. *Electric Transactions on Numerical Analysis 28*, 136–148.

Lyapunov, A. M. (1992). *General problem on stability of motion*. Taylor & Francis, London, (English translation).

Makinde, O. D. (2007). Adomian decomposition approach to a SIR epidemic model with constant vaccination strategy. *Applied Mathematics and Computation 184*, 842–848.

Makinde, O. D. (2009a). On MHD boundary-layer flow and mass transfer past a vertical plate

in a porous medium with constant heat flux. *International Journal of Numerical Methods for Heat & Fluid Flow 34*(3-4), 546–554.

Makinde, O. D. (2009b). On thermal stability of a reactive third-grade fluid in a channel with convective cooling the walls. *Applied Mathematics and Computation 213*, 170–176.

Makinde, O. D. and W. M. Charles (2010). Computational dynamics of hydromagnetic stagnation flow towards a stretching sheet. *Applied and Computational Mathematics 9*(2), 243–251.

Makukula, Z. G., P. Sibanda, and S. Motsa (2010a). On a new solution for the viscoelastic squeezing flow between two parallel plates. *Journal of Advanced Research in Applied Mathematics 2*, 31–38.

Makukula, Z. G., P. Sibanda, and S. S. Motsa (2010b). A note on the solution of the von Kármán equations using series and Chebyshev spectral methods. *Boundary Value Problems Volume 2010*(Article ID 471793, doi:10.1155/2010/471793), 17 pages.

Makukula, Z. G., P. Sibanda, and S. S. Motsa (2010c). A novel numerical technique for two-dimensional laminar flow between two moving porous walls. *Mathematical Problems in Engineering Volume 2010*(Article ID 528956, doi:10.1155/2010/528956), 15 pages.

Makukula, Z. G., P. Sibanda, and S. S. Motsa (2010d). On new solutions for heat transfer in a visco-elastic fluid between parallel plates. *International Journal of Mathematical Models and Methods in Applied Sciences 4*(4), 221–230.

Makukula, Z. G., P. Sibanda, and S. S. Motsa (2011a). On a quasi-linearisation method for the von Kármán flow problem with heat transfer. Accepted, *Latin American Applied Research*, http://www.laar.uns.edu.ar/.

Makukula, Z. G., P. Sibanda, and S. S. Motsa (2011b). On new numerical techniques for the MHD flow past a shrinking sheet with heat and mass transfer in the presence of a chemical reaction. *Mathematical Problems in Engineering Volume 2011* (Article ID 489217, doi:10.1155/2011/489217), 19 pages.

Maleque, K. A. (2009). Magnetohydrodynamic convective heat and mass transfer flow due to a rotating disk with thermal diffusion effect. *Journal of Heat Transfer 131*, 082001–1–8.

Mantzaris, N. V., P. Daoutidis, and F. Srienc (2001). Numerical solution of multi-variable cell population balance models. II. Spectral methods. *Computers and Chemical Engineering 25*, 1441–1462.

Marinca, V., N. Herisanu, and I. Nemes (2008). Optimal homotopy asymptotic method with application to thin film flow. *The Central European Journal of Physics 6*, 648–653.

Meek, P. C. and J. Norbury (1984). Nonlinear moving boundary problems and a Keller box scheme. *SIAM Journal on Numerical Analysis 21*(5), 883–893.

Moczo, P., J. Kristek, and L. Halada (2004). The finite-difference method for seismologists: An introduction. ftp://www.nuquake.eu, (17 July 2011).

Moghimi, M. and F. S. A. Hejazi (2007). Variational iteration method for solving generalized BurgerFisher and Burger equations. *Chaos, Solitons & Fractals 33*, 1756–1761.

Momani, S. and V. S. Ertürk (2008). Solutions of nonlinear oscillators by the modified differential transform method. *Computers and Mathematics with Applications 55*, 833–842.

Motsa, S., P. Sibanda, and Z. G. Makukula (2010). On a linearisation method for Reiner-

Rivlin swirling flow. Accepted, *Journal of Computational and Applied Mathematics*, http://www.journals.elsevier.com/journal-of-computational-and-applied-mathematics/.

Motsa, S., P. Sibanda, and S. Shateyi (2010). A new spectral-homotopy analysis method for solving a nonlinear second order BVP. *Communications in Nonlinear Science and Numerical Simulation 15*, 2293–2302.

Motsa, S. S. and S. Shateyi (2010). A new approach for the solution of three-dimensional magnetohydrodynamic rotating flow over a shrinking sheet. *Mathematical Problems in Engineering Volume 2010*(Article ID 586340, doi:10.1155/2010/586340), 15 pages.

Motsa, S. S. and P. Sibanda (2011). On the solution of MHD flow over a nonlinear stretching sheet by an efficient semi-analytical technique. *International Journal for Numerical Methods in Fluids* (doi: 10.1002/fld.2541).

Motsa, S. S., P. Sibanda, F. G. Awad, and S. Shateyi (2010). A new spectral-homotopy analysis method for the MHD Jeffery-Hamel problem. *Computers & Fluids 39*, 1219–1225.

Muhammad, G., N. A. Shah, and M. Mushtaq (2009). Merits and demerits of boundary element methods for incompressible fluid flow problems. *Journal of American Science 5*(6), 57–61.

Mushtaq, M., N. A. Shah, and G. Muhammad (2010). A brief description of developments and applications of direct boundary element method for compressible fluid flow problems. *Kragujevac Journal of Science 32*, 25–30.

Nayfeh, A. H. (1973). *Perturbation methods*. John Wiley & Sons, New York.

Nield, D. A. and A. Bejan (2006). *Convection in porous media*. Springer.

Niu, Z. and C. Wang (2010). A one-step optimal homotopy analysis method for nonlinear differential equations. *Communications in Nonlinear Science and Numerical Simulation 15*, 2026–2036.

Noelle, S. (2000). The MoT-ICE: A new high-resolution wave-propagation algorithm for multidimensional systems of conservation laws based on Fey's method of transport. *Journal of Computational Physics 164*, 283–334.

Odibat, Z. and S. Momani (2008). A generalized differential transform method for linear partial differential equations of fractional order. *Applied Mathematics Letters 21*, 194–199.

Odibat, Z. M. (2007). A new modification of the homotopy perturbation method for linear and nonlinear operators. *Applied Mathematics and Computation 189*, 746–753.

Odibat, Z. M., C. Bertelle, M. A. Aziz-Alaoui, and G. H. E. Duchamp (2010). A multi-step differential transform method and application to non-chaotic or chaotic systems. *Computers and Mathematics with Applications 59*, 1462–1472.

Pamuk, S. (2005). Solution of the porous media equation by Adomians decomposition method. *Physics Letters A 344*, 184–8.

Patera, A. T. (1984). A spectral element method for fluid dynamics: Laminar flow in a channel expansion. *Journal of Computational Physics 54*, 468–488.

Perot, J. B. and V. Subramanian (2007). A discrete calculus analysis of the Keller box scheme and a generalization of the method to arbitrary meshes. *Journal of Computational Physics 226*, 494–508.

Pinho, F. T. (2001). The finite-volume method applied to computational rheology: II- fundamentals for stress-explicit fluids. *Journal of the Portuguese Society of Rheology 1*, 63–100.

Prokopakls, G. J. and W. D. Selder (1981). Adaptive semi-implicit Runge-Kutta method for solution of stiff ordinary differential equations. *Industrial and Engineering Chemistry Fundamentals 20*, 255–266.

Qiu, J. (2007). WENO schemes with Lax-Wendroff type time discretizations for Hamilton-Jacobi equations. *Journal of Computational and Applied Mathematics 200*, 591–605.

Qiu, J. and C. W. Shu (2005). Hermite WENO schemes for Hamilton-Jacobi equations. *Journal of Computational Physics 204*, 82–99.

Ran, X. J., Q. Y. Zhu, and Y. Li (2009). An explicit series solution of the squeezing flow between two infinite plates by means of the homotopy analysis method. *Communications in Nonlinear Science and Numerical Simulations 14*, 119–132.

Rashidi, M. M. (2009). The modified differential transform method for solving MHD boundary-layer equations. *Computer Physics Communications 180*, 2210–2217.

Rashidi, M. M., N. Laraqi, and S. M. Sadri (2010). A novel analytical solution of mixed convection about an inclined flat plate embedded in a porous medium using the DTM-Padé. *International Journal of Thermal Sciences 49*, 2405–2412.

Raspo, I. (2003). A direct spectral domain decomposition method for the computation of rotating flows in a T-shape geometry. *Computers & Fluids 32*, 431–456.

Reddy, J. N. and D. K. Gartling (1994). *The finite element method in heat transfer and fluid dynamics*. CRC Press Inc., Tokyo.

Ribeiro, P. (2004). Non-linear forced vibrations of thin/thick beams and plates by the finite element and shooting methods. *Computers and Structures 82*, 1413–1423.

Rinehart, A. (2011). An Introduction to the application of the finite difference method in seismology. http://www.ees.nmt.edu, (17 July 2011).

Sahoo, B. (2009). Effects of partial slip, viscous dissipation and joule heating on von Kármán flow and heat transfer of an electrically conducting non-Newtonian fluid. *Communications in Nonlinear Science and Numerical Simulation 14*, 2982 – 2998.

Sajid, M. and T. Hayat (2008). Comparison of HAM and HPM methods for nonlinear heat conduction and convection equations. *Nonlinear Analysis: Real World Applications 9*, 2296–2301.

Salleh, M. Z., R. Nazar, A. Zaharim, and K. Sopian (2009). Free convection boundary layer flow near the lower stagnation point of a sphere with newtonian heating in a micropolar fluid. In *Proceedings of the 4th IASME/WSEAS International Conference on Continuum Mechanics (CM'09)*.

Sato, K. (1992). *Accelerated perturbation boundary element model for flow problems in heterogeneous reservoirs*. PhD Thesis, Stanford University.

Schuberth, B. (2003). *The spectral element method for seismic wave propagation*. PhD Thesis, Ludwig-Maximilians-Universität.

Segawa, H. (2011). *A Family of higher-order implicit time integration methods for unsteady compressible flows*. PhD Thesis, North Carolina State University.

Shampine, L. F. (2003). Singular boundary value problems for ODEs. *Applied Mathematics and Computation 138*, 99–112.

Shampine, L. F., I. Gladwell, and S. Thompson (2003). *Solving ODEs with MATLAB*. Cambridge University Press.

Shampine, L. F., R. Ketzscher, and S. A. Forth (2005). Using AD to solve BVPs in Matlab. *ACM Transactions on Mathematical Software 31*(1), 1–16.

Shan, X. W. (1994). Magnetohydrodynamic stabilization through rotation. *Physical Review Letters 73*, 1623–1627.

Shan, X. W., D. Montgomery, and H. D. Chen (1991). Nonlinear magnetohydrodynamics by Galerkin-method computation. *Physical Review A 44*, 6800–6818.

Shanbghazani, M., V. Heidarpour, and I. Mirzaee (2009). Computer-aided analysis of flow in a rotating single disk. *World Academy of Science, Engineering and Technology 58*, 160–163.

Sharma, B. K., A. K. Jha, and R. C. Chaudhary (2007). Forced flow of a conducting viscous fluid through a porous medium induced by a rotating disk with applied magnetic field. *Ukrainian Journal of Physics 52*(7), 639–635.

Shi, J., C. Hu, and C. W. Shu (2002). A technique of treating negative weights in WENO schemes. *Journal of Computational Physics 175*, 108–127.

Shu, C. W. (1997). Essentially non-oscillatory and weighted essentially non-oscillatory schemes for hyperbolic conservation laws. ICASE Technical report 97-65, Brown University.

Shu, C. W. (2001). Recent development and applications of WENO schemes. Technical report ADA412801, Brown University.

Shu, J. J. and G. Wilks (1995). An accurate numerical method for systems of differentio-integral equations associated with multiphase flow. *Compurers & Fluids 24*(6), 625–652.

Shu, J. J. and G. Wilks (2009). Heat transfer in the flow of a cold, two-dimensional draining sheet over a hot, horizontal cylinder. *European Journal of Mechanics B/Fluids 28*, 185–190.

Sibanda, P., S. S. Motsa, and Z. G. Makukula (2012). A spectral-homotopy analysis method for heat transfer flow of a third grade fluid between parallel plates. *International Journal of Numerical Methods for Heat & Fluid Flow 22*(1), 4–23.

Siddiqui, A. M., T. Haroon, and S. Irum (2009). Torsional flow of third grade fluid using modified homotopy perturbation method. *Computers and Mathematics with Applications 58*, 2274–2285.

Soltani, L. A. and A. Shirzadi (2010). A new modification of the variational iteration method. *Computers and Mathematics with Applications 59*, 2528–2535.

Song, L. and H. Q. Zhang (2007). Application of homotopy analysis method to fractional KdV-Burgers-Kuramoto equation. *Physics Letters A 367*, 88–94.

Steinhauser, M. O. (2008). *Computational multiscale modeling of fluids and solids*. Springer-Verlag, New York.

Sweilam, N. H. and M. M. Khader (2009). Exact solutions of some coupled nonlinear partial differential equations using the homotopy perturbation method. *Computers and Mathematics with Applications 58*, 2134–2141.

Tandjiria, V. (1999). Development of finite difference method applied to consolidation analysis of embankments. *Dimensi Teknik Sipil 1*(2), 73–80.

Thomé, R. C. A., H. M. Yang, and L. Esteva (2010). Optimal control of *aedes aegypti* mosquitoes by the sterile insect technique and insecticide. *Mathematical Biosciences 223*, 12–23.

Thomée, V. (1984). The finite difference versus the finite element method for the solution of boundary value problems. *Bulletin of the Australian Mathematical Society 29*, 267–288.

Toro, E. F. (1999). *Riemann solvers and numerical methods for fluid dynamics: A practical introduction*. Springer, Heidelberg.

Trefethen, L. N. (2000). *Spectral methods in MATLAB*. SIAM.

Trefethen, L. N. and M. R. Trummer (1987). An instability phenomenon in spectral methods. *SIAM Journal on Numerical Analysis 24*(5), 1008–1023.

Tu, J., G. H. Yeoh, and C. Liu (2008). *Computational fluid dynamics: A practical approach*. Butterworth-Heinemann, USA.

Turkyilmazoglu, M. (2010). Purely analytic solutions of magnetohydrodynamic swirling boundary layer flow over a porous rotating disk. *Computers & Fluids 39*(5), 793–799.

Urzay, J., V. Nayagam, and F. A. Williams (2011). Theory of the propagation dynamics of spiral edges of diffusion flames in von Kármán swirling flows. *Combustion and Flame 158*, 255–272.

Vafai, K. (2005). *Handbook of pourous media* (second ed.). Taylor & Francis Group, LLC, Boca Raton.

van de Vosse, F. N. and P. D. Minev (2002). Spectral element methods: Theory and applications. http://www.mate.tue.nl, (17 July 2011).

van Gorder, R. A. and K. Vajravelu (2009). On the selection of auxiliary functions, operators, and convergence control parameters in the application of the homotopy analysis method to nonlinear differential equations: A general approach. *Communications in Nonlinear Science and Numerical Simulation 14*, 4078–4089.

von Dyke, M. (1975). *Perturbation methods in fluid mechanics*. The Parabolic Press, Stanford, Carlifonia.

Wang, X. (2001). Solving optimal control problems with MATLAB - Indirect methods. http://www4.ncsu.edu, (12 July 2011).

Wang, Z., L. Zou, and Z. Zong (2011). Adomian decomposition and Padé approximate for solving differential-difference equation. *Applied Mathematics and Computation* (doi:10.1016/j.amc.2011.06.019).

Watson, J. O. (2003). Boundary elements from 1960 to the present day. *Electronic Journal of Boundary Elements 1*(1), 34–46.

Wazwaz, A. M. (1999a). The modified decomposition method and Padé approximants for solving the Thomas-Fermi equation. *Applied Mathematics and Computation 105*, 11–19.

Wazwaz, A. M. (1999b). A reliable modification of Adomian decomposition method. *Applied Mathematics and Computation 102*, 77–86.

Wazwaz, A. M. (2001a). Analytic treatment for variable coefficient fourth-order parabolic partial differential equations. *Applied Mathematics and Computation 123*, 219–227.

Wazwaz, A. M. (2001b). A new algorithm for solving differential equations of Lane-Emden type. *Applied Mathematics and Computation 118*, 287–310.

Wazwaz, A. M. (2001c). The numerical solution of sixth-order boundary value problems by the modified decomposition method. *Applied Mathematics and Computation 118*, 311–325.

Wazwaz, A. M. (2001d). A reliable algorithm for solving boundary value problems for higher-order integro-differential equations. *Applied Mathematics and Computation 118*, 327–342.

Wazwaz, A. M. (2002a). A new method for solving singular initial value problems in the second-order ordinary differential equations. *Applied Mathematics and Computation 128*, 45–57.

Wazwaz, A. M. (2002b). A reliable treatment for mixed Volterra- Fredholm integral equations. *Applied Mathematics and Computation 127*, 405–414.

Wazwaz, A. M. (2003). An analytic study on the third-order dispersive partial differential equations. *Applied Mathematics and Computation 142*, 511–520.

Wazwaz, A. M. (2006). The modified decomposition method and Padé approximants for a boundary layer equation in unbounded domain. *Applied Mathematics and Computation 177*, 737–744.

Wazwaz, A. M. (2007). The variational iteration method for rational solutions for KdV, $K(2,2)$, Burgers, and cubic Boussinesq equations. *Journal of Computational and Applied Mathematics 207*, 18–23.

Wazwaz, A. M. (2008). A study on linear and nonlinear Schrödinger equations by the variational iteration method. *Chaos, Solitons & Fractals 37*, 1136–1142.

Wazwaz, A. M. and S. A. Khuri (1996). A reliable technique for solving the weakly singular

second-kind Volterra-type integral equations. *Applied Mathematics and Computation 80*, 287–299.

Wolke, R. and O. Knoth (2000). Implicit-explicit Runge-Kutta methods applied to atmospheric chemistry-transport modelling. *Environmental Modelling & Software 15*, 711–719.

Xie, D. (2011). An improved approximate Newton method for implicit Runge-Kutta formulas. *Journal of Computational and Applied Mathematics 235*, 5249–5258.

Xu, H., Z. L. Lin, S. J. Liao, J. Z.Wu, and J. Majdalani (2010). Homotopy based solutions of the Navier-Stokes equations for a porous channel with orthogonally moving walls. *Physics of Fluids 22*, Article ID 053601, 18 pages.

Yabushita, K., M. Yamashita, and K. Tsuboi (2007). An analytic solution of projectile motion with the quadratic resistance law using the homotopy analysis method. *Journal of Physics A 40*, 8403–16.

Yang, J., S. Yang, Y. Chen, and C. Hsu (1998). Implicit weighted ENO schemes for the three-dimensional incompressible Navier-Stokes equations. *Journal of Computational Physics 146*, 464–487.

Yang, S. D. (2006). Shooting methods for numerical solutions of exact controllability problems constrained by linear and semi-linear wave equations with local distributed controls. *Applied Mathematics and Computation 177*, 128–148.

Yıldırım, A. and T. Öziş (2009). Solutions of singular IVPs of Lane-Emden type by the variational iteration method. *Nonlinear Analysis 70*, 2480–2484.

Yusufoğlu, E. (2009). An improvement to homotopy perturbation method for solving system of linear equations. *Computers and Mathematics with Applications 58*, 2231–2235.

Zahran, Y. H. (2009). An efficient WENO scheme for solving hyperbolic conservation laws. *Applied Mathematics and Computation 212*, 37–50.

Zandbergen, P. J. and D. Dijkstra (1987). von Kármán swirling flows. *Annual Reviews: Fluid Mechanics 19*, 465–491.

Zhang, B. Q., Q. B. Wu, and X. G. Luo (2006). Experimentation with two-step Adomian decomposition method to solve evolution models. *Applied Mathematics and Computation 175*, 1495–1502.

Zhang, S. and J. Li (2011). Explicit numerical methods for solving stiff dynamical systems. *Journal of Computational and Nonlinear Dynamics 6*, 041008–1–3.

Zhang, Y. T., J. Shi, and Y. Zhou (2003). Numerical viscosity and resolution of high-order weighted essentially nonoscillatory schemes for compressible flows with high reynolds numbers. *Physical Review E 68*, 046709–1–16.

Zhao, J. (2011). A unified theory for cavity expansion in cohesive-frictional micromorphic media. *International Journal of Solids and Structures 48*, 1370–1381.

Zhmayev, E., H. Zhou, and Y. L. Joo (2008). Modeling of non-isothermal polymer jets in melt electrospinning. *Journal of Non-Newtonian Fluid Mechanics 153*, 95–108.

Zou, L., Z. Wang, and Z. Zong (2009). Generalized differential transform method to differential-difference equation. *Physics Letters A 373*, 4142–4151.